UNIVERSIDADE ESTADUAL DE CAMPINAS
FACULDADE DE ENGENHARIA DE ALIMENTOS

MARIA PAULA GIULIANETTI DE ALMEIDA

ECOLOGICAL ENGINEERING OF ACIDOGENIC FERMENTATION AND MICROALGAE PHOTOTROPHIC COUPLED PROCESSES FOR CHEESE WHEY VALORIZATION

ENGENHARIA ECOLÓGICA DE FERMENTAÇÃO ACIDOGÊNICA ACOPLADOS A PROCESSOS FOTOTRÓFICOS DE MICROALGAS PARA A VALORIZAÇÃO DO SORO DE QUEIJO

CAMPINAS
2023

MARIA PAULA GIULIANETTI DE ALMEIDA

ECOLOGICAL ENGINEERING OF ACIDOGENIC FERMENTATION AND MICROALGAE PHOTOTROPHIC COUPLED PROCESSES FOR CHEESE WHEY VALORIZATION

ENGENHARIA ECOLÓGICA DE FERMENTAÇÃO ACIDOGÊNICA ACOPLADOS A PROCESSOS FOTOTRÓFICOS DE MICROALGAS PARA A VALORIZAÇÃO DO SORO DE QUEIJO

Thesis presented to the Faculty of Food Engineering of the University of Campinas in partial fulfillment of the requirements for the degree of Doctor in Science.

Tese apresentada à Faculdade de Engenharia de Alimentos da Universidade Estadual de Campinas como parte dos requisitos exigidos para a obtenção do título de Doutora em Ciências.

Supervisor/Orientador: Prof. Dr. Gustavo Mockaitis
Co-supervisor/Coorientador: Prof. Dr. David Gregory Weissbrodt

ESTE TRABALHO CORRESPONDE À VERSÃO FINAL DA TESE DEFENDIDA PELA ALUNA MARIA PAULA GIULIANETTI DE ALMEIDA, E ORIENTADA PELO PROF. DR. GUSTAVO MOCKAITIS

CAMPINAS

2023

Ficha catalográfica
Universidade Estadual de Campinas
Biblioteca da Faculdade de Engenharia de Alimentos
Claudia Aparecida Romano - CRB 8/5816

G448e

Giulianetti de Almeida, Maria Paula, 1981-
Ecological engineering of acidogenic fermentation and microalgae phototrophic coupled processes for cheese whey valorization / Maria Paula Giulianetti de Almeida. – Campinas, SP : [s.n.], 2023.

Orientador: Gustavo Mockaitis.
Coorientador: David Gregory Weissbrodt.
Tese (doutorado) – Universidade Estadual de Campinas, Faculdade de Engenharia de Alimentos.

1. Biorecuperação de resíduos. 2. Fermentação acidogênica. 3. Fotoheterotrofia. 4. Microalgas. 5. Soro de queijo. 6. Economia circular. I. Mockaitis, Gustavo. II. Weissbrodt, David Gregory. III. Universidade Estadual de Campinas. Faculdade de Engenharia de Alimentos. IV. Título.

Informações Complementares

Título em outro idioma: Engenharia ecológica de fermentação acidogênica acoplados a processos fototróficos de microalgas para a valorização do soro de queijo
Palavras-chave em inglês:
Resource biorecovery
Acidogenic fermentation
Photoheterotrophy
Microalgae
Cheese whey
Circular economy
Área de concentração: Bioenergia
Titulação: Doutora em Ciências
Banca examinadora:
Gustavo Mockaitis [Orientador]
Rosana Goldbeck Coelho
Ariovaldo Jose da Silva
Serge Roger Guiot
Wendong Tao
Data de defesa: 07-07-2023
Programa de Pós-Graduação: Bioenergia

Identificação e informações acadêmicas do(a) aluno(a)
- ORCID do autor: https://orcid.org/0000-0001-7113-7766
- Currículo Lattes do autor: http://lattes.cnpq.br/7405931996056750

Comissão Examinadora

Prof. Dr. Gustavo Mockaitis
Presidente Comissão Examinadora

Prof. (a) Dr(a). Rosana Goldbeck Coelho
Membro Titular
Universidade Estadual de Campinas

Prof. Dr. Ariovaldo José da Silva
Membro Titular
Universidade Estadual de Campinas

Prof. Dr. Serge Roger Guiot
Membro Titular
Université de Montréal

Prof. Dr. Wendong Tao
Membro Titular
The State University of New York

A Ata de Defesa com as respectivas assinaturas dos membros encontra-se no SIGA/Sistema de Fluxo de Dissertações/Teses e na Secretaria do Programa de Pós-Graduação.

To my sister Magda, thank you for the love and support from day one.

Acknowledgments

One cannot accomplish this section without avoiding clichés. As any great athlete, a Ph.D. candidate also goes out there and gives 110%. Most times, even more. Also, as any good sportsperson, I know there is not an I in TEAM. So, I would like to give credit when credit is due.

I would like to thank my supervisor Prof. Dr. Gustavo Mockaitis for all the guidance and support during my Ph.D. Thank you Prof. Dr. David G. Weissbrodt for being my co-supervisor and welcoming me as part of your group. I am very grateful for all opportunities you have provided me while in TU Delft and back home.

I am very fortunate to soon call Unicamp my *alma mater*. Throughout my Ph.D., the university was a place of knowledge gathering, friendship forging, nutrition, health checking, and just plain nature contemplation. Thanks to all staff that made life so much easier on campus.

I would like to thank FEAGRI for making me feel so at ease and in awe at the view in every sunset. Thanks to the staff and professors, always very friendly and helpful. I am going to miss the avocados. A big shout out to my dear friends Nilsa, Laísa, Ju Massari, Ju Fontenelli, and Nicolás for the friendship and great times spent together. A special thanks to Rosa, Ritinha, Seu Devis and Seu Luís, and the guys in the computer center for all the help. At FEA, I would like to thank Camila and Andrea for all the bureaucratic help throughout these years.

During my Ph.D., LMAS was my home. I spent most of my time there and had the pleasure to work with wonderful people. Ju Martins and Hugo, thank you for the friendship, help, knowledge sharing, and window shopping. You are very special to me. I also was fortunate to work with Izabela, always willing to help and a pleasure to be around. Brenno, with his contagious great mood, thank you for always finding time to help us around. Thanks to Maria Lídia for the talks, and laughs. I am grateful for having Vítor as my Padawan. We have learned a lot from each other and “have great success you will.” Thank you Cecília, a.k.a. roomie and friend. I appreciate the talks, the help, and the times you let me crash in when I needed to go back to Campinas.

Thanks to my PIBIC Jr. students, Júllia, and Huryel, for letting me share a bit of my passion for science and for your eagerness to learn, and perform experiments. I want to express my gratitude to Giovani, who taught me a lot about the lab, its equipment, and how to run experiments with safety. Prof. Dr. Bruna Moraes and Prof. Dr. Ariovaldo Silva, and fellow members of LMAS, thank you for reinforcing that together we can go farther.

In 2019, I was awarded a PSDE Capes scholarship to do part of my Ph.D. in The Netherlands. So, thank you Capes for the opportunity given to refine my laboratory skills and learn new things. Thanks to Guilherme Brandini, who motivated me to go for the PDSE scholarship.

A big thank you to Miranda, who was ever so nice and efficient. She makes all bureaucracy less complicated. Thank you Kawieta for such a warm welcome. All staff in Applied Sciences were helpful and accommodating which made the quality of life at work excellent. A special thank you to Marcel Langeveld, Johan Knoll, Cor Ras, Rob Kerste, Dirk Geerts, Armand Middeldorp, and Max Zomerdijk for your help with the experiments and equipment.

All my colleagues in EBT were super nice and I felt immediately included. Many thanks to Mark van Loosdrecht for welcoming me to the department. Robbert Kleerebezem, I appreciate your availability to clear my thermodynamic doubts even though it is still Greek to me. Yuemei Lin, I appreciated our talks during lunch and the Chinese balm for pain. You are very thoughtful!

Viktor, I appreciate your help getting me some sludge for my experiments. Jure, master of Origin, many thanks for teaching me how to navigate this software most easily. I sure miss our conversations. Dimitry, I am grateful for all your help in the lab. Sirous, thanks for helping me understand a bit more about reactors and for helping me with solving some equations. I cannot express my gratitude enough to Zita. I reckon that without her help I would have spent the triple amount of time assembling my reactor. Also, thank you for helping us build the prototype enclosure for the reactor, for all the tips, the help with Dutch, and overall friendliness. Ben Abbas, thank you for all your help during my time in Delft.

I am very happy and grateful to have collaborators like Guillaume Bruant and Julien Tremblay who elevated our work with their expertise. A special thanks to Prof. Dr. Juliano Bicas, Prof. Dr. Merle de Kreuk, and Prof. Dr. Ralph Lindeboom for the feedback regarding this work.

A huge thank you to Marta, Michele, and Jules for making office life great. Michele, thank you for our conversations careerwise and Jules, thank you for the banana tree. I hope you are taking good care of it for me. Camille and Saman: it was a pleasure being your daily supervisor. I hope I was able to share a bit of my knowledge and I am grateful to have learned from you. The same goes for Sofie.

To my friends Marta, David, Ale, Ingrid, Sergio, Cansel, Dana, Flo, Daniel, Fabio, Georg, Danny, Simon, Vojtěch, Alberte, Dana, and Chris, thank you for making my life in Delft so much more enjoyable! I am very lucky to have met you. David, Marta, Ale, and Ingrid: thank you for all the extra help! Botanische Tuin TU Delft will always have a special place in my heart.

A special thanks to my family and friends. It is comforting to know that we are not alone. Thank you, Magda, for all the love and support. Thank you Cissa, Cícero, Lis, and Weder for the friendship, laughs, and support. Thanks for lending me your house, your shoulders, and your ears. Thank you Délcio for listening and helping me throughout the years. Thank you Moacir, Rodney, and Amaury for being the sunshine in my life and for allowing me to know what unconditional love is. The type of love that only pets can give. I am positive that, these acknowledgments although extensive, are not complete. For that, I would like to thank all the people that played a part in this Ph.D. yet somehow are not mentioned by name.

Finally, I would like to make Snoop Dogg's words mine:

"Last but not least, I wanna thank me
I wanna thank me for believing in me
I wanna thank me for doing all this hard work
I wanna thank me for having no days off
I wanna thank me for, for never quitting".

A Ph.D. program is not for the faint-hearted and despite all the hurdles, which were plenty, I did complete it. Happy days!

Agradeço ao Conselho Nacional do Desenvolvimento Cientifico e Tecnológico - CNPq, pela concessão de bolsa durante o período de desenvolvimento deste doutorado.

'O presente trabalho foi realizado com o apoio do Conselho Nacional do Desenvolvimento Cientifico e Tecnológico - CNPq.' 'This study was financed in part by the Conselho Nacional do Desenvolvimento Cientifico e Tecnológico – CNPq.'

'O presente trabalho foi realizado com o apoio da Coordenação de Aperfeiçoamento de Pessoal de Nível Superior – Brasil (CAPES) – Código de financiamento 001.' 'This study was financed in part by the Coordenação de Aperfeiçoamento de Pessoal de Nível Superior – Brasil (CAPES) – Finance code 001.'

Somewhere, something incredible is waiting to be known. (Carl Sagan)

Resumo

Esta tese visa demonstrar a eficiência de interações entre bactérias e microalgas em processos conjugados como fermentação acidogênica e processos fototróficos para a valorização do soro de queijo, um co-produto da indústria de laticínios com grande potencial industrial.

No **Capítulo 2**, foi realizada uma revisão sobre o soro de queijo desde a sua descoberta até sua utilização atual. Os impactos ambientais gerados pelos 66.5 Mm^3 ano^{-1} de soro de queijo não absorvidos pela indústria foram abordados ao enfatizar alternativas para a biorecuperação e valorização do soro de queijo.

O principal objetivo deste trabalho foi estudar a eficácia de processos conjugados como fermentação acidogênica e processo fototrófico para a valorização do soro de queijo. O **Capítulo 2**, explorou os diversos usos do soro de queijo, bem como os impactos ambientais causados pelos 66,5 Mm^3 ano^{-1} de soro de queijo atualmente não absorvidos pela indústria. O capítulo de revisão enfatizou processos de biorecuperação do soro de queijo, como a produção de ácidos graxos voláteis (AVGs) de cadeia curta e média através da fermentação acidogênica, seguida pela produção de biomassa fotoorganoheterotrófica de microalgas com recuperação de nitrogênio e fósforo. A partir de um modelo de biorefinaria de ciclo fechado, a biomassa das microalgas pode ser processada em produtos de valor agregado de interesse industrial valorizando o soro de queijo.

Para isso, as partes interessadas como por exemplo, o setor lácteo, governo, academia e setores privados devem ser reunidas para forjar parcerias, reduzir as lacunas de conhecimento e tecnologia entre países, oferecer subsídios e implementar legislação para valorizar o soro de queijo, preservando ao mesmo tempo, o meio ambiente.

O **Capítulo 3** visou a implementação da fermentação acidogênica do soro de queijo para a produção de AGVs. Os pré-tratamentos alcalino e térmico do inóculo combinados com ensaios de headspace pressurizado e não pressurizado foram realizados em batelada com o objetivo de interromper a metanogênese e melhorar a produção de AGVs. Em geral, o pré-tratamento térmico combinado com headspace não pressurizado e uma relação F/M de 0,5 gCOD gVS^{-1} levou a uma maior produção de AGVs. Além disso, o pré-tratamento térmico suspendeu a metanogênese.

No **Capítulo 4**, observou-se o crescimento fotolitoautotrófico de microalgas de aproximadamente 650 mg SSV L^{-1}. Como demonstrado no **Capítulo 3**, o acetato foi o AGV mais produzido durante a fermentação acidogênica do soro de queijo. Este AGV, provou ser a melhor fonte de carbono orgânico para o cultivo mixotrófico de microalgas com um rendimento de 1,15 mg SSV mg C^{-1} (i.e., carbono) em condições anaeróbias sendo sua absorção considerada através do ciclo de glioxilato.

O aumento de escala em um reator quimiostato usando acetato como fonte de carbono orgânico e com uma taxa de diluição de 0,17 d^{-1} foi bem-sucedido, evitando a lavagem (washout) das microalgas fotoorganoheterotroficas. Estas descobertas corroboraram a proposta do **Capítulo 2** de fermentação acidogênica e processos fototróficos para a valorização do soro de queijo.

Um modelo matemático foi proposto no Capítulo 5 para prever o crescimento da biomassa microalgal e a produção de lipídios sob diferentes regimes tróficos. O modelo levou em conta parâmetros como intensidade e disponibilidade de luz, e disponibilidade de nutrientes. O **Capítulo 6**, abordou as conclusões deste trabalho, assim como suas contribuições e limitações. Uma perspectiva para trabalhos futuros foi sugerida.

Palavras-chave: biorecuperação de resíduos, economia circular, fermentação acidogênica, fotoheterotrofia, microalgas, soro de queijo

Abstract

The effectiveness of microalgal-bacterial coupling via acidogenic fermentation and phototrophic process for valorizing cheese whey was the main goal of this work. **Chapter 2**, explored the various uses of cheese whey as well as the environmental impacts caused by the 66.5 Mm^3 $year^{-1}$ of cheese whey currently not absorbed by the industry. The review emphasized biorecovery processes such as the production of short and mid-chain volatile fatty acids (VFAs) through the acidogenic fermentation of cheese whey followed by the photoorganoheterotrophic microalgae biomass production with nitrogen and phosphorus recovery as a closed-loop alternative to valorizing cheese whey. Microalgae biomass can be processed into added-value products of industrial interest.

For that, stakeholders (e.g., the dairy sector, government, academia, and private sectors) should be brought together to forge partnerships, reduce the knowledge and technology gaps among countries, offer subsidies, and implement legislation implementation to valorize cheese whey while preserving the environment.

Chapter 3 aims at the implementation of cheese whey acidogenic fermentation for VFAs production. Inoculum alkaline and thermal pre-treatments, combined with pressurized and non-pressurized headspace assays were performed in batches to halt methanogenesis and enhance VFAs production. Overall, thermal pre-treatment combined with non-pressurized headspace and an F/M ratio of 0.5 g_{COD} g_{VS}^{-1} led to higher VFAs production. Additionally, thermal pre-treatment efficiently halted methanogenesis.

In **Chapter 4**, photolitoautotrophic microalgal mixed-culture growth was successful presenting a biomass concentration of about 650 mg VSS L^{-1}. Acetate, the VFA most produced in cheese whey acidogenic fermentation as demonstrated in **Chapter 3**, proved to be the best organic carbon source for microalgae mixed-culture growth with a yield of 1.15 mg VSS mg C^{-1} (i.e., carbon) in anaerobic conditions with its uptake thought to be via glyoxylate cycle.

The scale-up in a chemostat reactor using acetate as an organic carbon source was successful with a dilution rate of 0.17 d^{-1} avoiding the wash-out of photoorganoheterotrophic microalgae. These findings corroborated **Chapter 1**

proposal of acidogenic fermentation and phototrophic processes for the valorization of cheese whey.

A mathematical model was proposed in **Chapter 5** to predict microalgal biomass growth and lipid production under different trophic regimes. The model considered parameters such as light intensity and availability, and nutrients' availability. The final chapter of this thesis, **Chapter 6**, addresses the conclusions of this work, as well as its contributions and limitations. An outlook with perspectives for future work is then given.

Keywords: acidogenic fermentation, circular economy, cheese whey, microalgae, photoheterotrophy, resource biorecovery

Summary

Chapter 1	Introduction	15
Chapter 2	*Got whey?* The significance of cheese whey at the confluence of dairying, environmental impacts, energy, and resource biorecovery	21
Chapter 3	Thermal and alkaline pre-treatments of inoculum halt methanogenesis and enables cheese whey valorization by batch acidogenic fermentation	68
Chapter 4	Beyond phycoremediation: Ecological engineering of photoorganoheterotrophic microalgal mixed cultures for cheese whey valorization	111
Chapter 5	Green microalgae mixotrophy: A mathematical model for triacylglycerol production and cheese whey valorization	149
	Appendices	232
Chapter 6	Discussion	249
Chapter 7	Conclusions and Outlook	258
Chapter 8	References	263
Chapter 9	Annex	269

1.Introduction

1 Background

In the dairy industry, whey is considered the remaining portion of the milk after cheese or casein production. Its characteristics depend on the animal that provided the milk, their feed, the time of the year, and just as importantly, the livestock stage of lactation (Tsakali et al., 2010).

Technological advances in the food, pharmaceutical, and nutrition industries led to the production of several value-added products, thus recognizing the economic potential of cheese whey. However, cheese whey is not repurposed in its totality. Depending on the location, cheese whey is still used as low-added-value products such as fertilizer, animal feed, and in worst-case scenarios, discarded in water bodies, leading to eutrophication processes (Lammifyad, 2020; Smithers, 2008).

In this process, due to cheese whey's tendency to quickly acidify and high organic load – 50 to 80 g O_2 L^{-1} in terms of chemical organic demand (COD) (Lappa et al., 2019), leading to hypoxic zones, nuisance, loss of fauna and flora, algal bloom, and an increase in GHG emissions (Wurtsbaugh et al., 2019).

Anaerobic digestion (AD) is a sustainable option to treat and reuse organic residues, reducing their organic loading and at the same time converting them into volatile fatty acids (VFAs), alcohols, hydrogen, and methane (González Siso, 1996).

In acidogenic fermentation (AF), methanogenesis can be suppressed in favor of acidogenesis, thus accumulating hydrogen and volatile fatty acids (VFAs) (Lagoa-Costa et al., 2020), making it a viable solution for the treatment and valorization of cheese whey given its tendency to acidify (Gameiro et al., 2020).

The products of AD processes can be used to produce various added-value products with industrial interests such as VFAs (Pais-Chanfrau et al., 2020), polyhydroxyalkanoates (PHAs) (Kucera et al., 2018), bioplastics (Yadav et al., 2020), electricity (Rabaey & Rozendal, 2010), biofuels (Christensen et al., 2011; Davila-Vazquez et al., 2011; Kushwaha et al., 2019), and nitrogen and phosphorus recovery from wastewaters. (Lee 2014). Environmental stress is an important tool to select microorganisms that can tolerate anaerobic digestion conditions, while being able to follow certain metabolic pathways, producing specific interest products (Nam et al., 2011).

Microalgae present great photosynthetic efficiency and their biomass can be processed into products with high economic and industrial interest. Their metabolic versatility, enables them to be cultivated in different trophic regimes (i.e.,

photoautotrophic, heterotrophic, photoheterotrophic, and mixotrophic) (Crane & Grover, 2010), and to use different carbon sources, including high-strength wastewater (Gonzalez-Fernandez et al., 2015).

Considering the 160.67 $Mm^3 year^{-1}$ of cheese whey produced and the fact that only 58.6% of its annual production is absorbed by industry (Tsakali et al., 2010; USDA, 2022), we can envision a different end-use for this by-product: the photoorganoheterotrophic production of microalgal biomass using a carbon source derived of cheese whey acidogenic fermentation.

Coupling AD processes, more specifically anaerobic fermentation (AF) processes and photobioprocesses enables the reduction of the organic and inorganic loads of wastewater, the production of added-value products, guaranteeing the full valorization of cheese whey, and a smooth transition of the dairy sector to the circular economy

2 Knowledge Gaps

Although technological advancements have allowed the dairy industry to produce several value-added products from cheese whey, its annual production is not absorbed by the industry. A staggering amount of 66.5 Mm^{-3} $year^{-1}$ is transformed into low-added-value products or discarded (Tsakali et al., 2010; USDA, 2022). This surplus can be directed to the production of a commodity that has more aggregated value: microalgal biomass.

AD is widely employed for the treatment of wastewater, reducing its organic load by breaking them down into VFAs, alcohols, H_2, and CH_4 (van Lier et al., 2001). Given the composition of cheese whey, AF is a suitable alternative to produce VFAs (Kleerebezem et al., 2015), that can serve as an organic carbon source for mixotrophic microalgae cultivation.

Microalgae biomass can be down streamed into a plethora of products with industrial, environmental, commercial, fine chemicals, drug screening, and biofuel applications (Abo et al., 2019; Caporgno & Mathys, 2018; Rizwan et al., 2018). Although microalgae have been studied for the phycoremediation of wastewater (Gonzalez-Fernandez et al., 2015), and the production of biofuels and other added-value products (e.g., pigments, supplements, antimicrobial agents)(Abo et al., 2019; Caporgno & Mathys, 2018; Rizwan et al., 2018), studies on non-axenic mixotrophic microalgal cultivation and microalgae-bacteria symbiotic relationships are still scarce (Riaño et al., 2016).

Hence, it is necessary to study microalgae biology, and their ecological relationships in a microbial community, while attempting to optimize acidogenic fermentation and photoroganoheterotrophic processes for cheese whey valorization. Consequently, the discharge of whey into hydric bodies will be minimized, decreasing the environmental impacts caused by the dairy industry (Kim et al., 2014). These can guarantee a full and smooth transition of the sector to the circular economy (Uvarova et al., 2020), in special small and medium-sized producers located in remote areas and in developing and least developing countries.

Therefore, considering the potential of cheese whey as nutrient media for a biotechnological process for biofuels and VFAs obtention and the recent advances in both microalgal and anaerobic processes, this work will provide an important link to the application of these two biotechnologies concomitantly. This work proposes the clarification of how microalgal and bacterial symbiosis can contribute to the coupling of anaerobic fermentation for organic carbon production and photoorganoheterotrophic processes for microalgae mixotrophic biomass production, thus valorizing cheese whey.

3 Research question

The main research question of this thesis focused on the microalgae and bacteria symbiotic relationships in the context of resource (i.e., cheese whey) valorization. The question is as follows:

"What is the microalgal and bacterial symbiotic role on acidogenic fermentation and photoorganoheterotrophic processes for volatile fatty acids and microalgae biomass production, and cheese whey valorization?"

The thesis was then centered around the following questions:

1. What is the total valorization potential of cheese whey? **(Chapter 2)**
2. How can selective pressure influence the product spectra of cheese whey acidogenic fermentation? **(Chapter 3)**

3. Which selective pressure parameters (i.e., inoculum pre-treatment, headspace pressure, and initial pH) enhance the production of VFAs (i.e., acetate) for the photoorganoheterotrophic production of microalgae biomass? **(Chapter 3)**
4. What are the best parameters (i.e., reactor regime, dilution rate, and retention time) for the selection of green photoorganoheterotrophic microorganisms? **(Chapter 4)**
5. How can a mathematical model optimize the microalgae-bacteria symbiotic relationships for the upscaling process of microalgae biomass and lipid production **(Chapter 5)**?

4 Chapters outline

A thorough review of cheese whey was performed in **Chapter 2**, where its valorization potential was addressed as well as the aspects that hinder this valorization (e.g., R&D, regulations and governance, and information access). We also discussed how anaerobic processes, such as the acidogenic fermentation of cheese whey can be coupled with photobioprocesses to produce microalgal biomass, closing the loop on cheese whey valorization. The review finally discussed how we can decrease the gap between countries regarding cheese whey valorization.

In **Chapter 3**, we studied how selective pressure can affect the metabolic pathways of a microbial Community using 40% demineralized cheese whey as a substrate. We identified these stressors (i.e., pH, inoculum pre-treatment, headspace pressure, and F/M ratio) influenced the product spectra of cheese whey acidogenic fermentation in batch reactors under the mesophilic temperature of 35°C. Inoculum pre-treatments (i.e., alkaline and thermal) can select microorganisms that can thrive in these conditions. So, we aimed to validate the efficiency of thermal pre-treatment in halting methanogenesis by replicating the experiment using a different inoculum. The results were analyzed to identify the selective pressures that increased the alcohol and VFAs production such as acetate, which can be a precursor in different bioprocesses (e.g., microalgal photoorganoheterotrophic biomass production).

The main goal of **Chapter 4** was to understand the ecological engineering of green photoorganoheterotrophic microorganisms regarding the uptake of organic carbon. We also attempted to understand microalgae-bacteria symbiosis for upscaling the production of microalgal biomass. Firstly, we enriched a photolithoautotrophic microalga mixed culture that was sampled from the surface of a channel in Delft, The

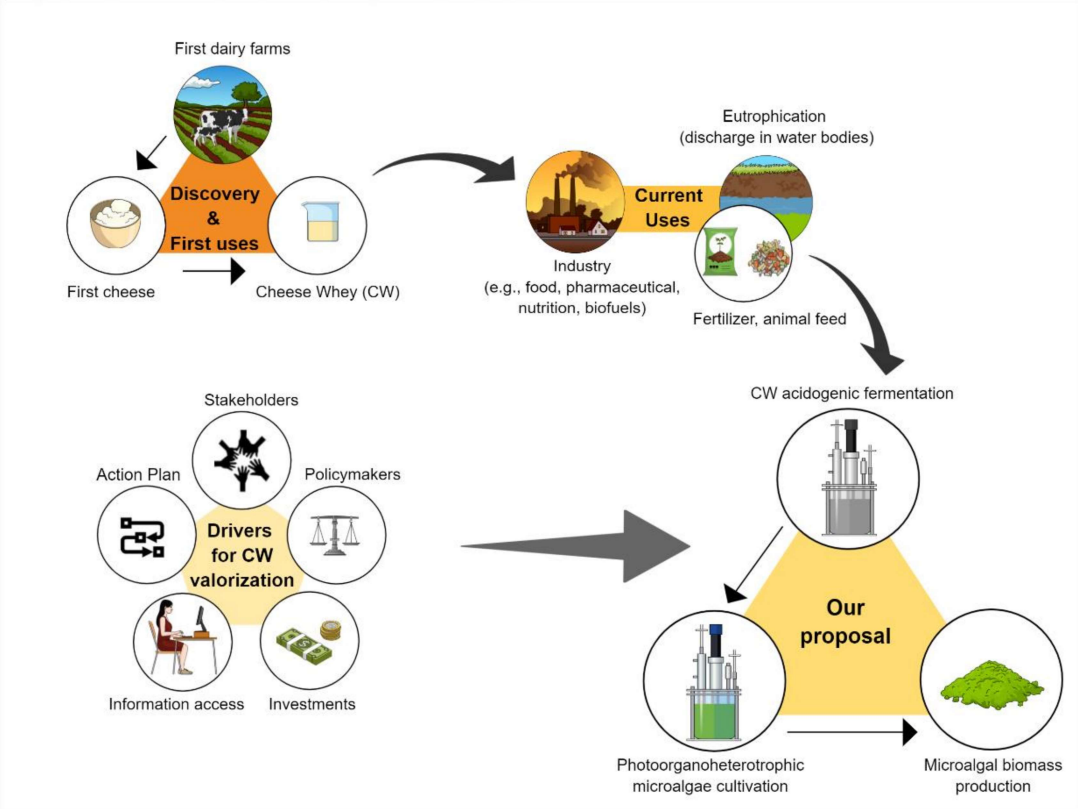
Netherlands, that served as the inoculum for our experiments. We initially monitored the photolithoautotrophic growth of the microalgae mixed culture using different nitrogen sources (i.e., ammonium and nitrate) and gas exchange conditions. Afterward, we selected those photoorganoheterotrophic microorganisms using different carbon sources derived from cheese whey such as (*i*) 40% demineralized cheese, which is most similar to raw cheese whey, (*ii*) lactose, cheese whey's main component, and (*iii*) acetate, a by-product of cheese whey acidogenic fermentation. Lastly, we monitored the photoorganoheterotrophic growth of microalgae in a continuous-flow reactor thus selecting the best reactor regime and parameters (i.e., dilution rate and hydraulic retention time) for microalgae selection.

In **Chapter 5**, we proposed a mathematical model based on ASM1 to predict microalgal biomass growth and lipid production under different trophic regimes. Parameters such as light intensity and availability and nutrients' availability were modeled. The focus was given to microalgae mixed cultures under mixotrophic conditions using raw cheese whey, whey powder, and .an optimized version of cheese whey as substrates, thus valorizing this dairy by-product. Lastly, **Chapter 6** presents the general conclusions of this work as well as the outlook on the use of anaerobic fermentation and photobioprocesses for the valorization of cheese whey.

2. *Got whey?* The significance of cheese whey at the confluence of dairying, environmental impacts, energy, and resource biorecovery

This chapter is deposited in a modified version as a preprint on *The Evolving Scholar*, the institutional open-access repository of the TU Delft. https://doi.org/10.24404/5fdd3c22eaf7860008874c47 , and will be submitted to *Chemical Society Reviews.*

Graphical abstract



Abstract

Milk discovery and processing enabled humans to settle and thrive in various settings. The discovery of cheese led to the production of whey as a dairy by-product. Although whey finds application in food, beverages, personal care products, pharmaceuticals, and medical sectors, it remains a massive dairying residue worldwide (160.7 million m^3 $year^{-1}$) with high organic and nutrient loads. About 42% is used as low-value products such as animal feed and fertilizers or even directly discharged into water streams, leading to ecosystem damage by eutrophication. We reviewed the uses and applications of cheese whey, along with associated environmental impacts and innovative ways to mitigate them in affordable and scalable technologies. Recycling and repurposing whey remains a challenge for remote locations and poor communities with limited access to expensive technology. We proposed a closed-loop biorefinery strategy to simultaneously mitigate environmental impacts and valorize whey resources. Anaerobic digestion utilizes whey to produce biogas and/or carboxylates. Alternative processes combining anaerobic digestion and low-cost open photobioprocesses can valorize whey and capture organic, nitrogenous, and phosphorous nutrients into microalgal biomass as food and crop supply or processed into biofuels, pigments, and antioxidants, among other value-added products. The complete valorization of cheese whey also depends on (*i*) facilitating access to relevant information on whey production, (*ii)* identifying stakeholders, *(iii)* decreasing technology gaps among countries, *(iv)* enforcing legislation and compliance, and *(v)* creating subsidies and foments partnerships with industries and between countries.

Keywords: cheese whey, food waste, anaerobic processes, microalgae, circular economy.

1 Introduction

Milk has been in our daily lives for centuries. Humans, unlike other mammals, make further use of this food past the lactation period. Although lactose tolerance is not inherent to most humans (Gross, 2018), the availability of dairy products continues to increase. Yogurts, cheese, and spreads, among other products, fill up our shelves.

Besides the direct consumption of milk, the production of cheese is another way to deal with milk surplus. In the dairy industry, liquid whey is the remaining portion of milk after cheese or casein production (Božanić et al., 2014) presenting a yellow/green color with a blueish tinge depending on the type and quality of the milk used (Smithers, 2008). Sweet whey results from the manufacturing of hard cheeses such as cheddar or Swiss cheese and is achieved by the rennet, a set of ruminant enzymes used in the coagulation process. The acidification of milk by *Lactobacillus* or the addition of mineral acid (HCl or H_2SO_4 acid) in cheese-making results in acid whey. Salty whey accounts for 2 to 5% of salted cheese production (Early, 1997; Tsakali et al., 2010).

Generally, whey consists of water (90%), proteins (6.0 g L^{-1}), lactose (46- 52 g L^{-1}), dissolved salts, lactic acid, lipids, minor components (*e.g.* citric acid, urea, and uric acid) and B-complex vitamins (Hammam et al., 2017). Its main characteristics depend on its type (acid, sweet or salty), source of milk (*e.g.,* bovine, caprine, sheep, and camel), animal feed, livestock stage of lactation, time of the year, and cheese-making processes. Variations in the milk casein and fat ratio can lead to cheese yield and quality fluctuation between seasons and locations influencing the quality of cheese whey produced (Tsakali et al., 2010).

Every 100 L of milk utilized in cheese production yields about 12 kg of cheese or 3 kg of casein (Archer, 1998). We can estimate the production of 87 L of whey per 100 L of milk. Large cheese-making plants can generate over a million liters of whey per day (Božanić et al., 2014). Cheese production is believed to increase by up to 14% by 2029 (N. Kim et al., 2022) and consequently, the volume of whey will also rise.

Amidst the covid-19 pandemic, the dairy industry underwent major market adaptations to survive (Munien & Telukdarie, 2021; Weersink et al., 2021) as dairy products are highly perishable and reliant on complex distribution logistics that are time-critical (Mishra & Shekhar, 2012). The dairy sector suffered direct consequences from the regulations that enforced the lockdown of education facilities and eating establishments for a certain period. Additionally, the fear that ruminants could carry the

coronavirus contributed to a decrease in the demand for dairy products (Huffstutter, 2020).

In many countries, milk had to be dumped (Holden & Goodling, 2021; Weersink et al., 2021). Some of the environmental, societal, and economic consequences of milk dumping can be translated into the contamination of soil and water bodies, eutrophication processes (Agustin et al., 2021), and farmer's bankruptcy (Roubík et al., 2022), as well as loss of jobs (Muhammad & Bhojiya, 2021). Producing cheese as an alternative to dumping milk still generates a surplus of whey that must be addressed.

Life cycle assessment (LCA) is a methodology used to identify the factors and measure the impacts generated by a product or process from concept to end-use (ISO, 2006). Implementation of LCAs in the dairy sector is recent and most consider cheese production (Soares et al., 2021). Although there are some LCA studies considering the use of cheese whey in the production of polyhydroxyalkanoates (PHA) (Asunis et al., 2021), lactic acid (Mediboyina et al., 2022), and bioplastics (Chalermthai et al., 2021), these studies still fail to address the complete environmental impacts of cheese whey during the production of cheese from milk collection to final consumption or discharge (Bacenetti et al., 2018; B. Yadav et al., 2019). The environmental impact assessment is oftentimes dependent on the chosen system boundaries (e.g., cradle-to-gate, gate-to-gate, cradle-to-grave) and the given allocations for the studies (Soares et al., 2021).

Thus, the complete valorization of cheese whey is necessary to guarantee the full transition of the dairy sector into the circular economy as well as to develop strategies to overcome unforeseen situations such as the coronavirus pandemic (Panghal et al., 2018; Uvarova et al., 2020). Circular economy (CE) aims to implement cascading processes that can further transform materials and their by-products into new added-value products (Carus & Dammer, 2018; Mohan et al., 2019; Uvarova et al., 2020), making use of renewable energy and moving toward zero waste production during processes (B. Yadav et al., 2020).

The European Commission has introduced a purposeful agenda to foster the transition to the circular economy and sustainable development in all European Union (EU) member countries (Asunis et al., 2021; Uvarova et al., 2020) with initiatives such as the Circular Economy Action Plan which is part of the Green Deal (European

Commission, 2020). Other examples of countries that are investing in CE are Japan with the Circular Economy Vision, South Korea, and the Framework Act on Resource Circulation (FARC), and China with the Circular Economy Promotion Law of the People's Republic of China (Cramer, 2022; Feng & Lam, 2021; Herrador et al., 2022).

Considering the amount of generated whey in cheese making (Archer, 1998), the whey global utilization balance (Tsakali et al., 2010), and the USDA Dairy World Market and Trade report (2022) the 2021 world cheese effective production was 160 million m^3 $year^{-1}$. In 2022, the cheese production forecast was approximately 160.1 million m^3 $year^{-1}$ (USDA, 2022). However, according to the USDA (2022), this forecast was surpassed in the first semester with a production of 160.7 million m^3 $year^{-1}$. This figure represents an excellent opportunity for fully valorizing cheese whey in the circular economy. **Figure 1** depicts the global utilization of cheese whey for the year 2022 (Archer, 1998; Tsakali et al., 2010; USDA, 2022) and the growing world cheese production in tonnes from 1960 to 2020 (FAO, n.d.).

Such valorization takes place after initial spray drying when both acid and sweet whey can be transformed into precursors for value-added products in the food, nutrition, and pharmaceutical industries. Salty whey has limited use in the industry due to its high salinity (Chandrapala, 2018). As seen in Figure 1, about 42% of whey is used as animal feed, and fertilizer or simply discarded (Tsakali et al., 2010).

Additionally, whey cannot be used as the sole source of animal feed due to ruminants' dietary needs (Pires et al., 2021). The same is valid for liquid whey, which is temperature-dependent, becoming unsafe for consumption once warm (Tsiouris et al., 2020). Soil application of whey or its direct discharge in water bodies is also not the best option as they result in severe environmental burdens. When used as a fertilizer, whey acidifies the soil pH drastically and stabilization reaches as low as 2 units on the pH scale (Ketterings et al., 2017). Its discharge into water bodies can unfavorably lead to eutrophication processes (Tsakali et al., 2010).

This review attempted to critically review and address cheese whey from its generation, discovery and first uses, characteristics, and valorization potential. We highlighted the issues that can still portray cheese whey as a burden rather than an opportunity, such as production location, highway network systems, regulations and governance, and information access. We outlined the technologies on cheese whey down streaming currently used by different industries (e.g., food, medical, nutrition).

We presented solutions to the surplus of whey with the implementation of anaerobic digestion or acidogenic fermentation of cheese whey followed by photobioprocesses for microalgal biomass production, thus providing a closed-loop system for cheese whey valorization. Finally, we call attention to (*i*) the need to bridge stakeholders together to tackle the problem of cheese whey residues, (*ii*) the importance of decreasing technology availability and affordability gaps among countries, as well as (*iii)* the necessity of legislation enforcement and fomenting partnerships between countries and industries to help in the full valorization of cheese whey.

Considering the increasing demand for cheese and that the most relevant type of whey regarding production volume and economic value comes from cow milk processing, we primarily focused on cheese whey derived from cow milk. Linking to the "***Got Milk?***" initiative, because of the need to safeguard natural ecosystems and since the potential of cheese whey to produce value-added products is undeniable, we advocate: "***Got Whey?***"

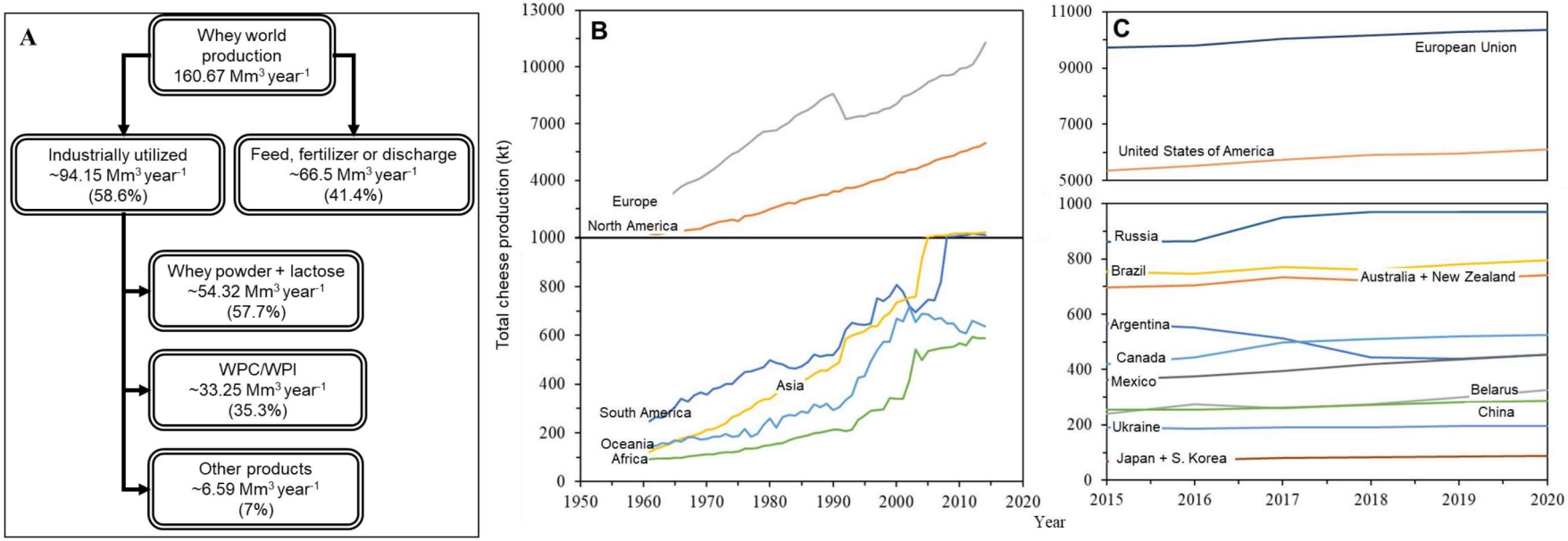


Figure 1 A) Global utilization of cheese whey for the year 2022. Estimative was based on the amount of whey generated per kilogram of cheese, the percentages of whey repurposed by industry and their remaining usage, and the forecast of cheese production for 2022 (Archer, 1998; Tsakali et al., 2010; USDA, 2022). **B)** Cheese production from 1960 to 2014 by continents. Geo-political changes were accounted for throughout the decades (FAO, n.d.). **C)** Cheese production was among the world's biggest producers from 2015 to 2020 according to the (USDA, 2019). Values for the year 2020 were forecasted. Given recent changes in the main world cheese producers, the year 2021 was not accounted in for the graph.

2 From dairying discovery to the importance of cheese and the benefits of cheese whey

2.1 Historical evolution of milk processing

Archaeozoology has long speculated about the history of cheese. Neolithization was the transition from a semi-nomadic lifestyle to sedentary habits substituting a hunter-gathering culture for an agricultural and livestock one (Leonardi et al., 2012; Mlekuž, 2015). This transition dates back to around 12,000 years before the present (BP) in the Near East and Anatolia, spreading to the Middle East, the Caucasus, Europe, and finally reaching Africa (Leonardi et al., 2012).

Dairying in South-Eastern and Near East Anatolia was intrinsically connected to the first domestication of animals dating from approximately 10,500 BP (Leonardi et al., 2012). Dunne et al. (2012), found similarities between the lifestyles of the Holocene Sahara and North Africa and Neolithic Europe and Eurasia as they both relied upon ruminants as livestock before domesticating plants or setup in farming communities.

The dairying profile required the culling of animals while they were babies to exploit the remaining milk (Leonardi et al., 2012; Stojanovski et al., 2020). Also, the production of meat would require harvesting the animal when it reached its maximum weight, demonstrating that the exploitation of livestock was compatible with milk production from the early Neolithic onwards (Leonardi et al., 2012).

In most mammals, the production of lactase gets down-regulated when the offspring is no longer dependent on milk for its survival. Once the levels of lactase have decreased, continuous consumption of milk caused lactose intolerance (Bayless et al., 2017). The Neolithic population minimized this disorder by processing the milk into cheese, yogurt, butter, and other dairy products (Leonardi et al., 2012). Genetic mutation of about 7,000 to 8,000 BP in Europe and North Africa allowed the digestion of lactose by adults (Callaway, 2012).

Dairying processing presented not only a measure to store and transport any milk surplus throughout the year but provided an alternative for lactose-intolerant people to consume milk by-products. By producing cheese and yogurt, most lactose was released with whey (Evershed et al., 2008).

2.2 The use of whey

Dairying was a cornerstone for human settling during the Neolithic. The discovery of cheese, yogurt, and derivatives resulted in whey as a by-product although its early use during the Neolithic is not well documented. Whey therapeutic purposes first began in 2410 BP with Hippocrates, continuing through the Middle Ages (Tunick, 2008). In Ancient Greece, whey was used as a skin balm or as a medicine (Ramos et al., 2016). Whey baths were famous from the nineteenth century until World War II (Tunick, 2008).

The first clinic to use cheese whey as medicine was opened in Switzerland by Hoffman in 1760, where its diuretic and laxative properties were recognized and used as medicine. Soon, other whey therapy clinics opened across Europe. Spas in central Europe served around 1.5 kg of whey per day to patients treating several different illnesses, from gout to arthritis and liver diseases (Pien, 1943).

Cheese whey became a fashionable drink in the mid-seventeenth century, including whey-borse (a broth), whey-butter, whey-porridge, and whey-whig, a drink made with herbs (Ayto, 1993). The Scandinavian medieval population from the Norse made use of sour whey to pickle meats and also produced a Scandinavian whey cheese with high lactose content (30%-35%) (Grek et al., 2020).

In the early centuries, all the surplus whey was used as animal feed. However, research on the nutritional aspects of whey started in the nineteenth century (Tunick, 2008). Currently, whey is still used as animal feed. Depending on the location, the excess whey can also be used as a fertilizer, irrigation water, or dumped into water bodies (Božanić et al., 2014; Smithers, 2008; Tsakali et al., 2010; Tunick, 2008).

The nuisance caused by whey's foul smell and its high salinity does not make whey the best fertilizer available. Cheese whey disposal on land or in the municipal sewage system is not allowed in numerous locations. The high costs associated with whey collection, treatment, and disposal by local governments leave small dairy farms in financial struggle and with no other choice but to dispose of whey in hydric bodies (Montecchio et al., 2018).

The illegal disposal of whey in hydric bodies can lead to catastrophic consequences. It leads to eutrophication processes that can directly affect the local ecosystem, water quality, and water resource availability. The environmental burdens of cheese whey and how to manage them are discussed in the following section.

Milk processing was a driving force for human settlement allowing the discovery of dairy and livestock management. However, despite its many uses throughout the centuries (Smithers, 2015) whey production and handling still need to be addressed toward circular practices in the dairying sector.

3 Environmental impacts and management of cheese whey residues

Whey is the highest organic pollutant comprised of the wastewater of the dairy industry. It presents an organic concentration as high as 50 to 80 g COD L^{-1} (in terms of chemical oxygen demand – COD) or 40 to 60 g BOD L^{-1} (expressed as biochemical oxygen demand – BOD) (Lappa et al., 2019).

Once in the water stream, cheese whey can lead to eutrophication. Besides organic matter, cheese whey is composed of organic nitrogen (0.2- 1.8 kg N m^{-3}) and inorganic phosphorus (0.12-0.54 kg P m^{-3}) that drive algal bloom (Prazeres et al., 2012). Whey treatment and recovery are paramount to valorize it and mitigate its environmental burden.

3.1 Environmental burden and elevated costs of treatment of whey residues

The treatment of whey surplus is fundamental to preventing environmental impacts. As previously mentioned, the high organic and nutrient concentrations of whey render its utilization as fertilizer unfavorable. Whey acidifies and degrades quickly, leading to a decrease in soil quality and productivity (Caballero et al., 2020).

Additionally, whey has little microbial stability and lactose has low water solubility, crystallizing at low temperatures (Miracco et al., 1981). Transportation of whey must be performed in temperature-controlled vehicles, and the farther the distance from production to use the site, the higher the transportation costs. Most often cheese producers must bear the costs of whey transportation, making its use as a fertilizer economically unfeasible (Robbins & Lehrsch, 1998). Still, depending on the location, the use of whey as a fertilizer is common.

The difficulty in establishing costs for treating cheese whey and dairy wastewater is not a recent issue. Procedures depend on the plant size, quality of the whey, and geological and climatic factors (Belloin, 1988). Hughes et al. (2018) stated that small

cheese producers in the USA must only give proper treatment and disposal of whey for production over 5,000 kg per year with an average cost of 105.00 USD per ton disposed of. This led to a substantial decrease in their profit margins.

Another matter in question is that logistics and regulations can be decisive in how whey and dairy wastewater are treated. This is oftentimes related to the producers' location (Lammifyad, 2020). Regarding cheese whey disposal, treatment, and valorization, big dairy cooperatives are in most cases responsible for further processing cheese whey into other products (Tsakali et al., 2010).

Whey must be collected by an industrial and/or municipal sewer system. In developed countries, due to strict environmental regulations such as the EU Landfill Directive 1999/31/EC (Papademas & Kotsaki, 2019), and great road networks, whey, and dairy wastewater usually receive a centralized treatment at the wastewater treatment plant (Marwaha & Kennedy, 1988; Smithers, 2008).

In developing countries and remote locations, whey, and dairy wastewater treatment are mostly decentralized (Marwaha & Kennedy, 1988; Smithers, 2008). Micro-, small- and medium producers have limitations due to the lack of infrastructure connecting them to the industry, the little sector research and development (R&D) investments, the high cost *vs.* benefits of processing cheese whey into value-added products, and the few markets available to sell the recovered products. These factors are closely related to the location of production (Alves et al., 2014). Additionally, if regulations are not enforced, small and medium dairy producers may be encouraged to discharge their whey residues directly into a water stream (Marwaha & Kennedy, 1988; Smithers, 2008).

Small and medium-sized dairy farms can benefit from centralized treatment facilities where alternatives to whey valorization are combined with existing whey processing technology (*i.e.*, spray drying), significantly reducing the disposal of whey in water bodies (M. Guo & Wang, 2019). The greatest obstacles to small-scale whey processing remain health and safety issues, especially due to its contamination and low shelf life (Lustrato et al., 2013; Wang et al., 2020).

Brazil illustrates an example of the importance of an efficient road network and a centralized whey treatment to increase whey valorization. Modern and artisanal cheese producers are scattered around the country and about 40% of produced cheese whey is not exploited (Trindade et al., 2019). Small dairy farms have to deal

with higher costs to process whey, and therefore use whey as animal feed or fertilizer or discharge it into the environment (Trindade et al., 2019; Tsakali et al., 2010).

The COVID-19 pandemic affected the dairy supply chain unprecedentedly. It disrupted the supply chains worldwide. Consequently, the environmental burdens caused by milk dumping will persist for many years. The relaxation of the rules and regulations on dumping milk was a measure many countries implemented to keep dairy producers afloat during the unanticipated COVID-19 pandemic. Nevertheless, environmental regulations are crucial to guarantee a smooth transition to a circular economy with the full valorization of cheese whey.

3.2 Paving the way for an ecologically balanced, circular, and participative dairying economy

Successful implementation of change stems from engaging different stakeholders involved in the whey problem towards a common goal for its sustainable use, treatment, and disposal (Ellen MacArthur Foundation, 2015). In a circular economy, the full valorization of cheese whey can be achieved by implementing a closed-loop approach, with cascading processes aiming to recover high-added value compounds with industrial applications (e.g., nutraceuticals, biofuels, food formulas) while producing minimum to zero waste (Asunis et al., 2020; Lappa et al., 2019; J. S. S. Yadav et al., 2015).

Environmental laws and policies started in the 1970s with the establishment of the US Environmental Protection Agency and the first European environmental policy (Gunningham, 2009). Community pressure led to changes in legislation, either banning or restricting the disposal of untreated whey, improving its waste management (Božanić et al., 2014; Ramos et al., 2016; Smithers, 2008).

The European Green Deal, an ambitious initiative that covers all the different aspects of the economy, aims to mitigate climate change by fully transitioning to a circular economy making the best use of the resources available while minimizing pollution and biodiversity loss (European Commission, 2020).

Among other legislation and frameworks, the Circular Economy Package (*Circular Economy Package (COM (2015) 614 Final*, 2015), comprises regulations regarding waste management and recycling. Such laws and regulations were paramount to the development of alternatives on how to deal with the surplus of cheese whey. **Table 1**

shows the legislation pertinent to hydric resources and agroindustrial residues among the world's biggest cheese producers, considering the authors' best knowledge.

However, the Environment Rule of Law of the United Nations (2019) divulged that, although most countries comprise environmental conservation regulations, only a few comply with them. This is often due to incomplete, irregular, or ineffective enforcement. In countries that embrace the polluter-pay principle model, industries often fail to comply with effective mitigation solutions beyond 'polluter pays'. Non-compliance can also originate from the difficulty in interpreting regulations due to an overload of information, jargon, and amendments. It also results from the misconception that environmental regulations hinder economic growth and competitiveness (Spence, 2001).

Oftentimes, the implementation of environmental management and resource recovery plans by companies mostly relies on economic viability and/or business opportunities. The management of cheese whey residues is an excellent illustration of it. Economical support programs should be implemented for small producers to collect, dispose of, treat, and possibly valorize cheese whey. At a higher scale, market niches should be identified for the recovered products, if not directly re-used as resources or energy on the industrial site.

In the Basque region of Spain, an action plan has been implemented for recovering whey over territory, in close connection to the industry (VALORLACT, 2016). It resulted in the development of whey processing plants and the production of 15 different value-added products for food and fodder. Another successful example is AgriChemWhey (ACW), in Ireland. ACW is an integrating biorefinery that produces lactic acid and other added-value chemicals from whey permeate (WP) and de-lactose whey permeate (DlWP). This project counts on a consortium of 11 partners across 5 different countries (Austria, Belgium, Germany, Ireland, and The Netherlands). The project was also funded by the Bio-Based Industries Joint Undertaking under the EU's Horizon 2020 Framework (AgriChemWhey, n.d.).

Industries are already processing cheese whey into added-value products. Glanbia, Fonterra, and its joint ventures, FrieslandCampina Ingredients, Saputo, Carbery, Milk Specialties Global, Arla, and Lactalis Global are some of the companies that are already repurposing their cheese whey into added-value products such as whey powder concentrate (WPC), isolate (WPI) and hydrolysate (WPH),

galactooligosaccharides (GOS), caseins and caseinates, probiotics, and prebiotics, which are employed in pharmaceutical, nutraceutical, food, and animal feed industries (Arla Food Ingredients, n.d.; Carbery, n.d.; Clover Fonterra, n.d.; FrieslandCampina Ingredients, n.d.; Glanbia, n.d.; Lactalis Global, n.d.; Milk Specialties Global, n.d.; Saputo, n.d.).

Governance, regulations, and law enforcement are of utmost importance to implement environmental changes and boost the circular economy. Policymakers, industry, dairy producers, and other stakeholders must join interests to implement regulations and R&D for integrating cheese whey valorization into a bio-based economy. This can be achieved by stakeholders and decision analyses (Brugha & Varvasovszky, 2000; Kiker et al., 2005) and the following implementation of progressive policies favoring renewable energies and material resource recovery from used streams rather than focusing only on prices and the understanding that low-income countries' transition can only be effective with financial and technological investments from high-income countries (Kemp-Benedict, 2015).

Table 1. Available legislation on (waste)water management in countries with higher cheese whey production.

World's biggest cheese producers	Water management legislations	Reference
Argentina	National constitution ART 121 civil code	(The Law Library of Congress & Rodriguez - Ferrand,2013)
Australia	Environmental Protection Act, 1993 The National Waste Policy, 2009	(Government of South Australia, n.d.)
Belarus	Water Code of the Republic of Belarus, 2014	(Cis Legislation, 2014)
Brazil	Water code, 1934 National Policy of Hydric Resources (Federal Law 9,433), 1997 National Solid Waste Policy, PNRS, 2010	(Ministry of the Environment, n.d.)
Canada	Canada Water Act, 1985 Wastewater Systems Effluent Regulations 2015	(Government of Canada, n.d.)
China	The Water Law of the People's Republic of China, 1988	(Zhifang, 1991)
European Union	Waste Framework Directive (2006/12/EC) Urban Wastewater Directive (91/271/ EEC) Renewable Energy Directive (2009/28/EC) Circular Economy package (COM (2015) 614 final	(European Union, n.d.)
Japan	Water pollution control law, 1970	(Japan - Ministry of The Environment, 1970)
Mexico	National Water Law	(Mexican Official Standard NOM-001-ECOL-1996,n.d.)
New Zealand	National Policy Statement for Freshwater Management - under the Resource Management Act 1991	(New Zealand - Ministry for the Environment,2014)
Russia	Water Code of the Russian Federation, 2006	(Cis Legislation, 2006)
South Korea	Water Quality and Ecosystem Conservation Act, 2009	(Water Quality and Ecosystem Conservation 2005)
Ukraine	The Water Code of Ukraine, 1995	(Legal Services Online, n.d.)
United States of America	Clean Water Act, 1972	(United States of America, 1972)

3.3 Information access to drive mitigation, whey valorization, and development engineering

Information access is crucial to any research field. Scientific work is only made possible when we can find information that can either support or refute our initial hypothesis so we can tailor our work, achieve results and publish them reaching the scientific community. The handling of cheese whey by practitioners and local communities across the globe is hampered by the failure of information access. Some known barriers to accessing information consist of but are not limited to *(i)* lack of critical thinking; (*ii)* language; (*iii)* library facilities; *(iv)* search engines and web hosts; *(v)* economic restraints and *(vi)* commercial sensitivity. Most times these barriers are interconnected and interdependent (di Bitetti & Ferreras, 2017; Fell & Lukianova, 2015; A. Hussain, 2015; Kralisch & Mandl, 2006; Landa, 2006; Meneghini & Packer, 2007; Ugah, 2007).

The lack of incentive to provide information on stakeholders' interests hinders them from perfecting important skills in R&D and everyday life situations. Language barriers can also limit access to information for speakers of other languages than English. This can be a great obstacle when doing research (Kralisch & Mandl, 2006) since significant information can become unknown or even obsolete because of a lack of English fluency (Landa, 2006; Meneghini & Packer, 2007).

English is the *lingua franca* of Science. However, most science is not made by native English speakers (Meneghini & Packer, 2007). This fact leads to various assumptions and limitations. The lack of critical thinking due to language and cultural barriers is one of the main made assumptions (Fell & Lukianova, 2015). Non-native English speakers and countries with research in dominant *lingua mater* are often the dark horses of the publishing race (di Bitetti & Ferreras, 2017) regardless of the quality of their work. Scientists are encouraged to publish in English to make their research relevant, cited, and known (Meneghini & Packer, 2007).

Some solutions to minimize language barriers issues are free, accurate online translations tools to engage readers, inclusive language texts reducing the 'digital divide' (Kralisch & Mandl, 2006), hosting exchange programs between different institutions, access to international conferences and articles written in both *lingua*

mater and *lingua franca* as offered by electronic libraries like Scientific Electronic Library Online - SciELO and PLOs One (Landa, 2006; Meneghini & Packer, 2007).

Most people have libraries as primary places to study and research. In specific, undergraduates do not have any practical research activities. According to Ugah et al.(2007), a lot of facilities have obsolete, scarce, and difficultly located sources of materials that can be unavailable for either consultation or lending. Libraries also face budget cuts to invest in their facilities, materials, and staff (Savova & Price, 2019). Digital libraries can be an alternative to existing ones but they still present issues around web hosts and domain names (Kralisch & Mandl, 2006; Ugah, 2007).

Another issue is the cost of subscriptions to academic journals. Some institutions especially in low-income countries cannot afford them, limiting their research scope (*e.g.*, Research Information Network (2009)). Search engines can be useful tools to search and retrieve documents from the internet (A. Hussain, 2015). However, it is important to improve and update their scientific content (Lawrence & Giles, 1998; Ugah, 2007). The internet offers great features such as databases with open-access material such as OCLC's Cooperative Online Resource Catalog, The Research Libraries Group (RLG), INFOMINE (Byrum), and other repositories. Other platforms like arXiv, ChemRxiv, BioRxiv, and many alike functions provide direct access to the latest research via pre-prints.

Institutional repositories and open access mega journals like The Evolving Scholar lately launched by the Delft University of Technology in the Netherlands are important ways to convey information in open access. Still, digital access relies on internet access, which remains a challenge for remote and marginalized areas and communities. In the present digitalization era, key challenges need to be solved to promote effective information access and solutions for development engineering.

4 Clearing the whey: product, resource, and energy recovery

About 66.5 million m^3 $year^{-1}$ of whey is currently not absorbed by industry (Tsakali et al., 2010). The potential of valorization with the manufacturing of value-added products can improve the sustainability of cheese processing (Božanić et al., 2014). Until recently, whey by-products were seen as low-value products. The lack of understanding of whey characteristics and functionality, together with its inconsistent

performance in food systems (*i.e.,* water and flavor binding, solubility, and emulsification properties) and soy protein consolidated market limited the use of whey regardless of available processing technology. This scenario has changed considerably since the initial process development of lactose down-streaming and its related value-added products (Onwulata & Huth, 2008; Smithers, 2008).

The high concentrations of organic matter, nitrogen, and phosphorus in whey (Tsitouras et al., 2020) make this residue an interesting feedstock for resource and energy recovery. Alternatives for valorization comprise of production of health and other industrial value-added products (Božanić et al., 2014; Smithers, 2008), phosphorus and nitrogen recovery (Marazzi et al., 2020), carbon capture (Imtiaz-Ul-Islam et al., 2011), transformation by anaerobic digestion and fermentation processes (Singh, 2016), as well as other biotechnological processes for the valorization of biomass, biofuel, and biomaterials (Dinika & Utama, 2019). The following sections discourse these alternatives as well as our proposal to couple anaerobic digestion or acidogenic fermentation of cheese whey with photobioprocesses to biorecover energy and resources on top of safeguarding the natural environment.

4.1 Technological processes employed to recover whey

The first attempts to concentrate dry whey started in the 1920s. Technologies involved conventional hot roller milk driers, heating whey until a concentrated liquid was obtained, cooling whey until it solidified following a tunnel extrusion, and combining spray drying and rotary drum drying (Gillies, 1974). Due to the hygroscopic nature of lactose to this day, some processes are still rather costly, especially for small and medium-sized cheese producers (Miracco et al., 1981). Despite this, the hot drum drying process is still one of the most used processes for whey powder production (Tunick, 2008). **Table 2** depicts the different techniques currently used in whey processing and its added-value products, and applications.

Whey by-products (*e.g.,* whey powder concentrate or isolate) became commodities of interest for nutritional, pharmaceutical, and medical industries given that its proteins and peptides components present nutritional value and antimicrobial, anti-viral, anticarcinogenic, and antioxidant properties (Onwulata & Huth, 2008; Smithers, 2008; Tsakali et al., 2010).

D-tagatose, a low-calorie sweetener can be produced from whey. It presents prebiotic properties and antihyperglycemic activities (Zheng et al., 2019). It is also used in the food, cosmetic, and pharmaceutical industries as a bulking agent, and acts as an additive in detergents or as an intermediate component for the synthesis of other substances (Ibrahim, 2018).

Table 2 Cheese whey downstream processes, available technologies, product spectra, and current applications. Adapted from (Božanić et al., 2014; Dinika & Utama, 2019; Gillies, 1974; Ibrahim, 2018; Ko & Kwak, 2009; Lappa et al., 2019; Onwulata & Huth, 2008; Zheng et al., 2019).

Cheese whey processing and applications in pharma, nutrition, & personal care, food, and feed		
Physical separation	**Protein separation**	**Protein modification**
Membrane separation (PF, MF, RO, NF) High hydrostatic pressure Pulse electric field Microwave Ultrasound	Spray drying Extrusion texturization Carbon dioxide precipitation	Enzymatic modification Chemical modification
Products obtained	**Products obtained**	**Products obtained**
Whey powder Dry whey powder (DWP) Whey powder concentrate (WPC) 35% Whey permeate α-, β-lactoalbumin Lactose Casein	Whey powder concentrate 80% Lactose pharma grade Whey protein blends (WPI + WPC) Pure whey isolate Minerals	Lactic acid, lactulose Bovine serum albumin (BSA) D-Tagatose Galactooligosaccharides (GOS) Other bioactive compounds (immunoglobulins, l lactoferrins, glycomacropeptides, transferrins, lactoperoxidase, lysozymes, albutensin A, -lactorphin, β-lactotensin, β-lactorphin, serorphin)

Galactooligosaccharides (GOS) are a by-product of cheese whey known for their prebiotic functions and high market value. GOS are usually present in infant formulas but are also used as sweeteners and bulking agents, and are present in beverages, meal replacers, and sweets. Lactulose, another prebiotic derived from lactose, is mainly used in food formulas for medical purposes (Lappa et al., 2019).

As the technology evolved, protein separation and modification enabled the discovery of new uses for whey such as isolates and other bioactive compounds (Onwulata & Huth, 2008). Current technologies for cheese whey processing therefore notably consist of physical separations and bioengineering for protein recovery and modification.

4.2 Anaerobic digestion and acidogenic fermentation of cheese whey

Anaerobic digestion of cheese whey has been studied regardless of its trend to acidify (Gameiro et al., 2020). The high biodegradability (~99%) of cheese whey, pH

reduction (below 5), and low bicarbonate alkalinity (50 meq L^{-1}) can lead to operational difficulties (Charalambous et al., 2020; Malaspina et al., 1996). However, the high organic content of cheese whey makes it suitable for energy recovery via biogas production by anaerobic digestion (González Siso, 1996). The efficiency of the bioprocess relates to parameters like the substrate feed, temperature, pH, and hydraulic retention time (Patel et al., 1995).

Acidogenic fermentation of cheese whey is an interesting alternative to anaerobic digestion (Bengtsson et al., 2008; Kleerebezem et al., 2015). Methanogenesis can be stopped after the conversion of whey by fermentative microorganisms to accumulate hydrogen and volatile fatty acids (VFAs) (Lagoa-Costa et al., 2020). Anaerobic digestion without the production of biogas is an opportunity for the valorization of VFAs via the carboxylate platform (Agler et al., 2011; Cadavid-Rodríguez & Horan, 2014; Rombouts et al., 2019).

The acidogenic fermentation of cheese whey can be driven by inoculum pre-treatment (*e.g.,* physical, biological) (Gioannis et al., 2014; Girotto et al., 2017), lowering the hydraulic retention times (*i.e.,* between 2 to 5 days) (Sultana et al., 2015), and controlling pH (*i.e.,* below 7.0 to 3.3) (Venetsaneas et al., 2009), thus selecting acidogens to outcompete methanogens. Other fermentation processes can also valorize cheese whey. These processes can be performed either in axenic pure-culture systems or via mixed-culture fermentation in non-sterile open systems (X. Guo et al., 2010; Roukas & Kotzekidou, 1998).

Some of the products obtained from cheese whey valorization are short-, mid-, and long-chain organic acids (Angenent et al., 2016; Calero et al., 2018; Pais-Chanfrau et al., 2020), intracellular storage products (*i.e.,* polyhydroxyalkanoates, PHAs) (Colombo et al., 2016; Kucera et al., 2018; Mulders et al., 2020), bioplastics (Ryan & Walsh, 2016; B. Yadav et al., 2019), biohydrogen (Davila-Vazquez et al., 2008), bioethanol (Christensen et al., 2011; Zhou et al., 2019) and biobutanol (Kushwaha et al., 2019; Raganati et al., 2013). Other innovative bioprocesses involve the conversion of VFAs into electricity or other value-added products using bioelectrochemical systems (*i.e.*, microbial fuel cells and microbial electrosynthesis cells) (Rabaey & Rozendal, 2010).

4.3 Co-digestion of whey

Anaerobic co-digestion is a process where different substrates from agricultural farming, manure, municipal, food, and industrial wastes are combined in anaerobic digestion to optimize parameters such as temperature (30-50°C), pH (5-7), organic matter concentration, nutrients availability, alkalinity, and C: N (25 to 35:1) ratio. Consequently, the overall biogas yield is increased and resource recovery is facilitated, diverging from waste disposal in landfills and leading to environmental and financial benefits (Hagos et al., 2016; Nghiem et al., 2017).

The synergy between substrates is paramount for higher biogas production. The anaerobic co-digestion process with proteins can increase biogas production and halt inhibition by an excess of ammonia, although this synergy is yet to be proved in full-scale reactors (Castro-Molano et al., 2018).

The co-digestion of cheese whey has been studied by combining it with other substrates such as animal manure (Gelegenis et al., 2007), food waste (Jaimes-Estévez et al., 2020), and other wastes (Maragkaki et al., 2018), and microalgae (Markou & Georgakakis, 2011). Currently, some anaerobic digestion plants use cheese whey as the substrate for their processes (*e.g.*, Iona -Lemming Biogas)(Iona Capital, n.d.). The anaerobic digestion of cheese whey seems a sound bet for repurposing the current surplus of the whey.

4.4 Light-based valorization of cheese whey using photobioprocesses: harnessing eutrophication in bioprocess boundaries

We advocate for new biorecovery process alternatives coupling the acidogenic fermentation of cheese whey into short and mid-chain VFAs production before feeding into algal ponds, photo-activated sludge systems, or photobiotechnologies to produce a photoorganoheterotrophic microalgal biomass. This biomass can be processed into an outlet of products with an industrial interest (*e.g.,* pigments, antioxidants, vitamins, anticancer drugs) and of higher value than biogas.

Although most hydrogen production results from “dark fermentation” processes performed by chemoheterotrophic bacteria and microalgae (Davila-Vazquez et al., 2008), it can also occur in the presence of light. This process is known as biophotolysis, comprising direct and indirect biophotolysis and photofermentation (Yu & Takahashi,

2015). In direct biophotolysis, water is oxidized into hydrogen and oxygen in the presence of light during photosynthesis by photoautotrophic microalgae. In indirect photolysis, hydrogen is the product of the reduction of organic compounds by photosynthetic bacteria, cyanobacteria, and microalgae (Yu & Takahashi, 2015).

Photofermentation is a process where anoxygenic photosynthetic bacteria (*i.e.,* green sulfur bacteria, purple sulfur, and purple non-sulfur bacteria) (Chen et al., 2020; Warthmann et al., 1992) use alternative reduced compounds as electron donors (*e.g.,* hydrogen sulfide, organic acids, and carbon sources) nitrogenase and light as an energy source to synthesize hydrogen (Najafpour et al., 2016). The biological water-gas shift is performed by hydrogenogenic carboxydotrophic bacteria that oxidize carbon monoxide while catalyzing the water-gas shift reaction
(Alfano & Cavazza, 2018; Najafpour et al., 2016), producing hydrogen. The biological water-gas shift can be an alternative to the current chemical shift used for syngas production (Alfano & Cavazza, 2018).

Cheese whey has been used both in the dark (Pais-Chanfrau et al., 2020) and photofermentation (Pandey et al., 2019) processes. It also served as a substrate for microalgae cultivation. Given microalgae photosynthetic and lipid production efficiency, photofermentation processes using VFAs as carbon sources for biomass production can give a more profitable use for the 66.5 million m^3 $year^{-1}$ of cheese whey currently used as animal feed, fertilizer, or discharged in water streams.

4.5 Synergetic interactions between microalgal and bacterial processes to valorize whey

Compared to other feedstocks for biofuel production, microalgae are advantageous as they can be cultivated in arid land (Naeini et al., 2020) and brackish or high-strength waters (Hussain et al., 2021). They can remove nitrogen and phosphorus from wastewater simultaneously (Aslan & Kapdan, 2006) and mitigate carbon dioxide, given their photosynthetic efficiency (Jeong, 2003). Besides biofuels, **Table 3** shows the value-added products obtained from microalgae and their respective uses.

The carbon metabolism of microalgae can be photolithoautotrophic, photoorganoheterotrophic, and mixotrophic (Crane & Grover, 2010; S. Kim et al.,

2013). Heterotrophic microalgae are attractive for light-based processes designed to treat and capture organic matter and nutrients from municipal and agro-industrial wastewater (S. Kim et al., 2013; Pittman et al., 2011). Mixotrophic microalgae can display a combination of photolithoautotrophic and photo- and/or chemo-organoheterotrophic regimes. Due to respiratory metabolic propensities, mixotrophic microalgae exhibit lower photoinhibition, improved growth rate, and reduced losses of biomass by night (Cheirsilp & Torpee, 2012). Current industrial application dwells in the production of unsaturated fatty acids (*e.g.,* omega-3 fatty acids or arachidonic acid), antibiotics, and pigments, such as carotenoids (Perez-Garcia et al., 2011). However, the carbon assimilation and growth mechanisms of mixotrophic microalgae remain to get elucidated (Pang et al., 2019).

Microalgal mixed-culture bioprocesses have notably been studied in combination with anaerobic bacterial processes for, *e.g.*, digestion and methanization of microalgal biomass, nutrient polishing from anaerobic digester supernatants with microalgae, production of biomass from used water streams, or production of lipid-based biofuels and biopolymeric materials (Gonzalez-Fernandez et al., 2015; Posadas et al., 2014; Schnurr et al., 2013). Along with technological applications, microalgal-bacterial assemblies drive scientific interest in ecological relationships (Dao et al., 2018; Ramanan et al., 2016), and can foster mixed-culture photobiotechnologies.

Table 3 Microalgae biomass applications consider different uses and product spectra. Compiled from (Abo et al., 2019; Caporgno & Mathys, 2018; Khan et al., 2018; Rizwan et al., 2018; Spolaore et al., 2006).

Microalgal biomass applications			
Fine chemicals	Fatty acids Carotenoids Antioxidants Vitamins Other bioactive compounds	**Industrial**	Pharmaceutical Aquaculture Animal feed Biofertilizer
Drug screening	Antimicrobial agents Antiviral drugs Anticancer drugs	**Environmental**	Pollutants removal Wastewater co-digestion CO_2 mitigation Biochar
Commercial	Nutraceuticals Nutrition Cosmetics Pigments Recombinant proteins Stable isotopes Biochemicals	**Biofuels**	Biodiesel Bioethanol Biobutanol Biosyngas Biogas Electricity Heat

At a cellular level, the symbiotic relationships between microalgae and bacteria are important concerning the exchange of substrates (*e.g.,* CO_2-O_2 exchange between bacteria and microalgae, bacterial cobalamin supply to auxotrophic microalgae), signaling transduction (*e.g.,* quorum sensing, growth inhibition or stimulation by exudates release), or horizontal gene transfer (Kouzuma & Watanabe, 2015). Microbial ecology still presents various knowledge gaps regarding the study and comprehension of microalgal-bacterial symbiosis (Kim et al., 2014). The knowledge of bacto-microalgal chemical interactions is still scarce. The advent of 'multi-omics' (*e.g.* metagenomics, transcriptomics, proteomics, lipidomics, metabolomics) is now providing key analytical means to elucidate them.

Even though interactions between microalgal and anaerobic bacterial processes are increasingly studied (*e.g.,* biomass, biofuels, value-added products production, CO_2 mitigation, or wastewater treatment), studies addressing process scale-up are limited (Zhang et al., 2020). Bottlenecks of such mixed-culture process integration notably relate to the *(i)* costs and energy requirement of microalgae biomass harvesting, *(ii)* complex micro-ecosystems and their dynamics that can shift in a short period, and *(iii)* absorption of light across mixed liquors and biofilms beyond the photic zone (Zhang et al., 2020).

Microalgal growth on cheese whey (Markou & Georgakakis, 2011), cheese-whey-related products (*e.g.,* dairy waste, digested cheese whey, second cheese whey, permeate) (Tsolcha et al., 2016), and co-digestion processes (Pittman et al., 2011) have been studied. However, the bio-valorization of cheese whey has seldom been tailored so far via combined microalgal-bacterial mixed-culture biotechnologies (Riaño et al., 2016).

4.6 Phosphorus and nitrogen removal and recovery from cheese whey

The prevention of eutrophication usually goes via the biological or chemical removal of phosphorus and nitrogen from wastewater (Lee et al., 2014). Bioprocesses for removing nutrients from municipal and industrial wastewater have been studied and operated extensively worldwide (Jenkins & Wanner, 2014). Technologies using biofilms and granular sludge have enabled the intensification and integration of process units in wastewater treatment plants (Nicolella et al., 2000). Combining

anaerobic digestion and digestate polishing for nutrient removal is a standard operation for the treatment of high-loaded agro-industrial streams (Vaneeckhaute et al., 2017). Such process combination can be applied to the handling of cheese whey (Escalante et al., 2018). However, beyond nutrient removal, nutrient capture technologies would become more sustainable. Over the last decade, the environmental engineering sector went along a paradigm shift to transform wastewater treatment plants into water resource recovery facilities (Daigger, 2011; Guest et al., 2009; Weissbrodt et al., 2020).

The demand for fertilizers is constantly increasing. Phosphorus is a non-renewable resource that is currently extracted from geological deposits of phosphate rocks or phosphorites (Desmidt et al., 2015), while nitrogen resource is obtained by costly chemical reactions (van der Hoek et al., 2018). Hence, the anaerobic digestion of high-strength wastewater combined with nitrogen and phosphorus recovery processes is a feasible alternative.

Phosphorus can be removed and/or recovered from wastewater streams by sedimentation enhanced biological phosphorus removal (*i.e.,* by phosphorus-accumulating organisms), or chemical precipitation (*i.e.,* with aluminum or iron salts into insoluble phosphates compounds) (Parsons & Smith, 2008). Nitrogen recovery uses energy from ammonia producing atmospheric nitrogen, followed by the Haber-Bosch process reversing the previous reaction. Other technologies for nitrogen recovery are struvite precipitation, adsorption, ammonia stripping, the combination of air stripping and absorption, membrane distillation, and membrane gas separation (Beckinghausen et al., 2020).

Struvite ($NH_4MgPO_4 \cdot 6H_2O$) production is a well-established process to recover phosphorus and nitrogen by crystallization (Desmidt et al., 2015). The low water solubility of whey and its high N and P concentration is advantageous for struvite precipitation (Escalante et al., 2018). Most struvite recovery studies focus on municipal wastewater (le Corre et al., 2009) or source separated-urine (Wilsenach et al., 2007). However, struvite precipitation has its drawbacks. Phosphorus removal increases the amount of sludge and decreases digesters' pipeline diameters leading to operational problems. Notwithstanding, its recovery reduces the overall costs of anaerobic digestion processes as well as the costs of sludge handling, disposal, and scaling (Parsons & Smith, 2008).

Phosphorus can also be recovered as vivianite ($Fe_3(PO_4)\cdot 8H_2O$) (Prot et al., 2020) which is more thermodynamically favored than struvite precipitation and displays a high aggregated value. Since vivianite does not separate easily from sludge, technologies for vivianite recovery are currently studied by magnetic separation (Prot et al., 2020; Wu et al., 2019).

These active developments highlight the strong technological potential for the capture and recovery of organic matter and nutrients from used streams. The combination of biological and physical-chemical processes is efficient to capture and recover resources. The key will consist of developing economically-affordable, scalable, and implementable processes to valorize resources across regions. The photoorganoheterotrophic processes using microalgae or purple phototrophic bacteria form in combination with an anaerobic fermentation process an efficient bio-based solution for the capture and concentration of organics and nutrients at low cost into valuable biomass and associated bioproducts (Alloul et al., 2020; Cerruti et al., 2020; Zarezadeh et al., 2019) from waste feedstocks like cheese whey, such as for use in agriculture and food supply.

5 Conclusions and future perspectives

Cheese production and whey management are interdependent. The cheese demand increases yearly and therefore, whey management must be addressed. Since its discovery, cheese whey has been given different uses as food, feed, medicine, and fertilizer. Technological advances have enabled whey down-streaming, making an inexpensive dairy by-product into a sought commodity. However, about 42% of whey annual production is not absorbed by the industry, being regarded as a low-value (waste) product or even discarded in water bodies. Consequently, the early use of whey as animal feed and fertilizer continues to this day in various locations around the world.

To tackle this issue, we have conceived different scenarios for the valorization of the surplus of cheese whey residues as illustrated in **Figure 2,** *(i)* Anaerobic digestion of whey for either the production of biogas or VFAs combined with phosphorus and nitrogen recovery. Biogas production could generate heat and electricity and biofuels. The VFAs produced can be valorized in evolved mixed-culture processes by chain

elongation into biofuels or biopolymers; (ii) Combining acidogenic fermentation of cheese whey and green or purple photobioprocesses for biomass production which would not only capture the organic matter but also the nutrients contained in the whey pre-fermented stream.

Both processes allow struvite precipitation to recover phosphorus and nitrogen that together with anaerobic digestion and microalgae biomass digestate can be turned into fertilizers. This simple process integration can form an attractive scalable alternative for environmental resource biorecovery, leading to the development of a whey biorefinery besides mitigating eutrophication into bioprocess boundaries.

Besides producing valued biomass, future research should address process strategies to manage the selection and interaction of fermentative and photoorganoheterotrophic organisms, *e.g.*, via single-sludge or two-sludge systems, and to control the metabolic routes to form selected bioproducts such as triacylglycerides to produce biofuels.

Scalable solutions need to be developed for the handling of whey. Notwithstanding, we understand that there is no standard solution for whey's full valorization as each location has its limitations considering the local geography, economy, and politics.

These hindrances can be overcome with (*i*) more LCA studies on different cheese whey biorefinery scenarios, so the best decision can be taken by accounting for the environmental impacts resulting from chosen processes; (*ii*) identification of stakeholders (*e.g.*, farmers, dairy cooperatives, researchers, industry, government) so dialogue is built for knowledge transfer and utilization, solution design, and informed decisions; (*iii*) the crafting of an action plan that considers implementable and user-friendly technologies, the development level of countries and enforces regulations and policies in a way that benefits, especially small producers; (*iv*) revision and update of obsolete legislation so they reflect current needs towards water resources and agroindustrial waste; (*v)* enforcement of knowledge development, regulation, and technology for remote locations, (*vi*) and implementation of government incentive programs encouraging compliance, giving subsidies for whey repurposing and fomenting partnerships with industries or other countries that have the means and know-how to help this transition.

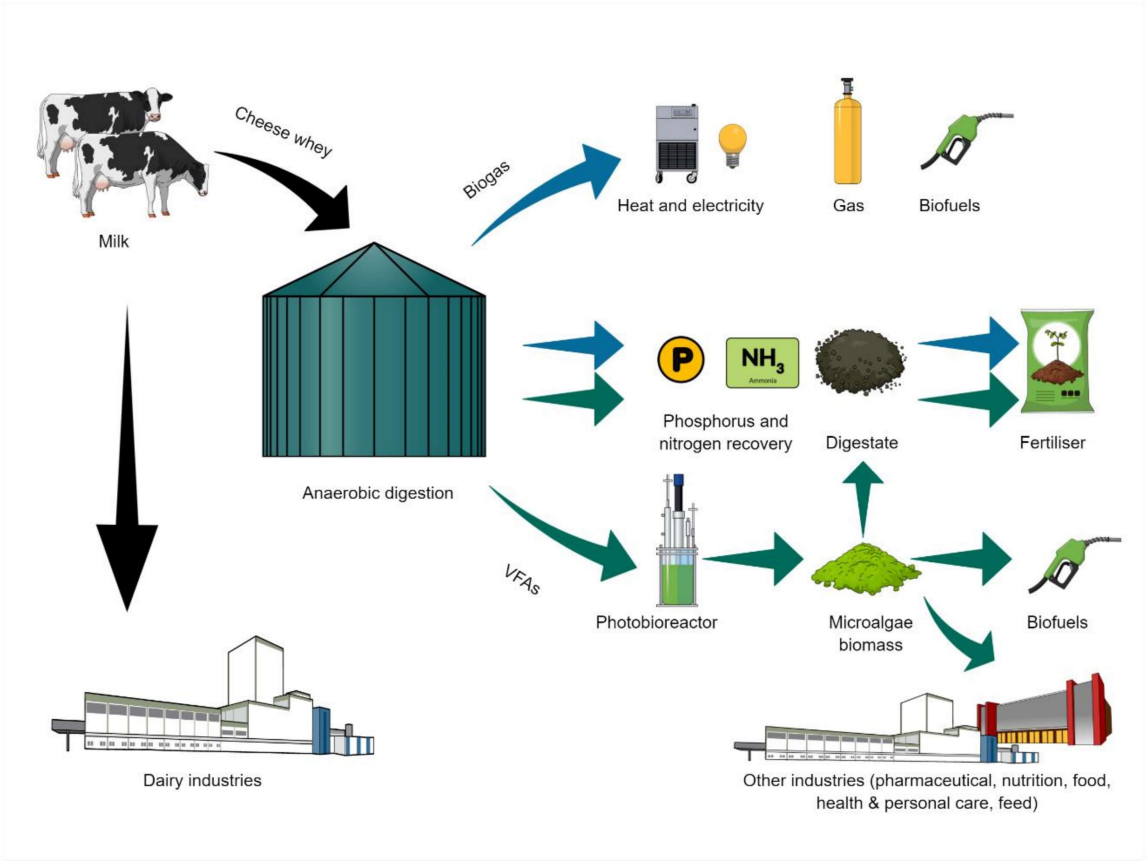


Figure 2 Scenarios for the full valorization of cheese whey. The surplus of whey can undergo (*i*) biogas production generating heat, electricity, gas, and biofuels, and (*ii*) VFAs production that would serve as a carbon source for photoorganoheterotrophic processes. Microalgae biomass could serve as raw material for the production of biofuels or be absorbed by the industry for the production of high-added-value products. Struvite precipitation is possible regardless of the chosen pathway. Anaerobic digestion and microalgal biomass harvesting digestates together with phosphorus and nitrogen recovery can be turned into fertilizers.

In this review, we addressed the importance of cheese whey from its discovery to current days at the confluence of dairying, environmental impacts, energy, and resource biorecovery. We pinned issues that hinder whey valorization and alternatives to promote it. Raising awareness about cheese whey global production and complete valorization is paramount to showcase the economic potential of transforming whey surplus into value-added products and safeguarding the environment worldwide.

6 Reference

Abo, B. O., Odey, E. A., Bakayoko, M., & Kalakodio, L. (2019). Microalgae to biofuels production: A review on cultivation, application and renewable energy. *Reviews on Environmental Health*, *34*(1), 91–99. https://doi.org/10.1515/reveh-2018-0052

Agler, M. T., Wrenn, B. A., Zinder, S. H., & Angenent, L. T. (2011). Waste to bioproduct conversion with undefined mixed cultures: The carboxylate platform. *Trends in Biotechnology*, *29*(2), 70–78. https://doi.org/10.1016/j.tibtech.2010.11.006

AgriChemWhey. (n.d.). *AgriChemWhey*. Retrieved March 22, 2022, from https://www.agrichemwhey.com/

Agustin, Y., Kurniawan, M., Astuti, R., & Rahman, M. A. (2021). Environmental Impact Evaluation of a Fresh Milk Production. *Industria: Jurnal Teknologi Dan Manajemen Agroindustri*, *10*(2), 149–161. https://doi.org/10.21776/ub.industria.2021.010.02.6

Alfano, M., & Cavazza, C. (2018). The biologically mediated water-gas shift reaction: Structure, function, and biosynthesis of monofunctional [NiFe]-carbon monoxide dehydrogenases. *Sustainable Energy and Fuels*, *2*(8), 1653–1670. https://doi.org/10.1039/c8se00085a

Alloul, A., Cerruti, M., Adamczyk, D., Weissbrodt, D. G., & Vlaeminck, S. E. (2020). Control tools to selectively produce purple bacteria for microbial protein in raceway reactors. *BioRxiv*, 2020.01.20.912980. https://doi.org/10.1101/2020.01.20.912980

Alves, M. P., Moreira, R. de O., Júnior, P. H. R., Martins, M. C. de F., & Ítalo Tuler Perrone, A. F. de C. (2014). Whey: technologies for co-products production. *Rev. Inst. Laticínios Cândido Tostes*, *69*(3), 212–226. https://doi.org/http://dx.doi.org/10.14295/2238-6416.v69i3.341

Angenent, L. T., Richter, H., Buckel, W., Spirito, C. M., Steinbusch, K. J., Strik, D. P. B. T. B., Grootscholten, T. I. M., Buisman, C. J. N., & Hamelers, H. V. M. (2016). Chain elongation with reactor microbiomes : open-culture biotechnology to produce biochemicals - Extensive review. *Environmental Science and Technology*, *50*(6), 2796–2810. https://doi.org/10.1021/acs.est.5b04847

Archer, R. H. (1998). *Whey products*. New Zealand Dairy Research Institute. https://nzic.org.nz/app/uploads/2017/10/3G.pdf

Arla Food Ingredients. (n.d.). *Discovering the wonders of whey*. Retrieved March 23, 2022, from https://www.arlafoodsingredients.com/

Aslan, S., & Kapdan, I. K. (2006). Batch kinetics of nitrogen and phosphorus removal from synthetic wastewater by algae. *Ecological Engineering*, *18*, 64–70. https://doi.org/10.1016/j.ecoleng.2006.04.003

Asunis, F., de Gioannis, G., Dessì, P., Isipato, M., Lens, P. N. L., Muntoni, A., Polettini, A., Pomi, R., Rossi, A., & Spiga, D. (2020). The dairy biorefinery: Integrating treatment processes for cheese whey valorization. *Journal of Environmental Management*, *276*, 111240. https://doi.org/10.1016/j.jenvman.2020.111240

Asunis, F., de Gioannis, G., Francini, G., Lombardi, L., Muntoni, A., Polettini, A., Pomi, R., Rossi, A., & Spiga, D. (2021). Environmental life cycle assessment of polyhydroxyalkanoates production from cheese whey. *Waste Management*, *132*, 31–43. https://doi.org/10.1016/j.wasman.2021.07.010

Ayto, J. (1993). *The diner's dictionary: word origins of food and drink* (University of Michigan, Ed.; 2nd ed.). Oxford University Press ; by arrangement with Routledge.

Bacenetti, J., Bava, L., Schievano, A., & Zucali, M. (2018). Whey protein concentrate (WPC) production: Environmental impact assessment. *Journal of Food Engineering*, *224*, 139–147. https://doi.org/10.1016/j.jfoodeng.2017.12.018

Bayless, T. M., Brown, E., & Paige, D. M. (2017). Lactase non-persistence and lactose intolerance. *Current Gastroenterology Reports*, *19*(5), 23. https://doi.org/10.1007/s11894-017-0558-9

Beckinghausen, A., Odlare, M., Thorin, E., & Schwede, S. (2020). From removal to recovery : An evaluation of nitrogen recovery techniques from wastewater. *Applied Energy*, *263*, 114616. https://doi.org/10.1016/j.apenergy.2020.114616

Belloin, J. C. (1988). *Milk and dairy products : Production and processing costs*. Food and Agriculture Organization of the United Nations.

Bengtsson, S., Hallquist, J., Werker, A., & Welander, T. (2008). Acidogenic fermentation of industrial wastewaters: Effects of chemostat retention time and pH on volatile fatty acids production. *Biochemical Engineering Journal*, *40*(3), 492–499. https://doi.org/10.1016/j.bej.2008.02.004

Božanić, R., Barukčić, I., Kl, J., & Tratnik, L. (2014). Possibilities of whey utilisation. *Austin J Nutri Food Sci*, *2*(7), 1036–1042.

Bruch, C., Schang, S., Pendergrass, J., Fulton, S., Moraga-Lewy, N., Wright, M., & Swanson, G. (2019). *Environmental Rule of Law - First global report*. United Nations Environment Programme. https://www.unenvironment.org/resources/assessment/environmental-rule-law-first-global-report

Brugha, R., & Varvasovszky, Z. (2000). Stakeholder analysis: a review. *Health Policy and Planning*, *15*(3), 239–246.

Caballero, P., Rodríguez-Morgado, B., Sandra, M., Manuel, T., & Juan, P. (2020). Obtaining plant and soil biostimulants by waste whey fermentation. *Waste and Biomass Valorization*, *11*, 3281–3292. https://doi.org/10.1007/s12649-019-00660-7

Cadavid-Rodríguez, L. S., & Horan, N. J. (2014). Production of volatile fatty

acids from wastewater screenings using a leach-bed reactor. *Water Research*, *60*, 242–249. https://doi.org/10.1016/j.watres.2014.05.001

Calero, R., Lagoa-Costa, B. C., Kennes, C., Fernandez-Feal, M. C., & Veiga, M. C. (2018). Volatile fatty acids production from cheese whey: Influence of pH, solid retention time and organic load rate. *Journal of Chemical Technology and Biotechnology*, *93*(6). https://doi.org/10.1017/CBO9781107415324.004

Callaway, E. (2012). Pottery shards put a date on Africa's dairying. *Nature*. https://doi.org/10.1038/nature.2012.10863

Caporgno, M. P., & Mathys, A. (2018). Trends in microalgae incorporation into innovative food products with potential health benefits. *Frontiers in Nutrition*, *5*(58), 58. https://doi.org/10.3389/fnut.2018.00058

Carbery. (n.d.). *Product range*. Retrieved March 22, 2022, from https://www.carbery.com/nutrition/product-range/

Carus, M., & Dammer, L. (2018). The Circular Bioeconomy—Concepts, opportunities, and limitations. *Industrial Biotechnology*, *14*(2), 83–91. https://doi.org/10.1089/ind.2018.29121.mca

Castro-Molano, L. del P., Escalante-Hernández, H., Lambis-Benítez, L. E., & Marín-Batista, J. D. (2018). Synergistic effects in anaerobic co-digestion of chicken manure with industrial wastes. *DYNA (Colombia)*, *85*(206), 135–141. https://doi.org/10.15446/dyna.v85n206.68167

Cerruti, M., Stevens, B., Ebrahimi, S., Alloul, A., Vlaeminck, S. E., & Weissbrodt, D. G. (2020). Enrichment and Aggregation of Purple Non-sulfur Bacteria in a Mixed-Culture Sequencing-Batch Photobioreactor for Biological Nutrient Removal From Wastewater. *Frontiers in Bioengineering and Biotechnology*, *8*, 557234. https://doi.org/10.3389/fbioe.2020.557234

Chalermthai, B., Giwa, A., Schmidt, J. E., & Taher, H. A. B. (2021). Life cycle assessment of bioplastic production from whey protein obtained from dairy residues. *Bioresource Technology Reports*, *15*. https://doi.org/10.1016/j.biteb.2021.100695

Chandrapala, J. (2018). Whey wastes and powders. In M. M. A.-R. El-Barky, A. Sanchez, & B. M. Mehta (Eds.), *Microstructure of Dairy Products* (1st ed., pp. 261–292). Wiley-Blackwell.

Charalambous, P., Shin, J., Shin, S. G., & Vyrides, I. (2020). Anaerobic digestion of industrial dairy wastewater and cheese whey : Performance of internal circulation bioreactor and laboratory batch test at pH 5-6. *Renewable Energy*, *147*, 1–10. https://doi.org/10.1016/j.renene.2019.08.091

Cheirsilp, B., & Torpee, S. (2012). Enhanced growth and lipid production of microalgae under mixotrophic culture condition : Effect of light intensity , glucose concentration and fed-batch cultivation. *Bioresource Technology*, *110*, 510–516.

https://doi.org/10.1016/j.biortech.2012.01.125

Chen, J., Wei, J., Ma, C., Yang, Z., Li, Z., Yang, X., Wang, M., Zhang, H., Hu, J., & Zhang, C. (2020). Photosynthetic bacteria-based technology is a potential alternative to meet sustainable wastewater treatment requirement ? *Environment International*, *137*(February), 1–19. https://doi.org/10.1016/j.envint.2019.105417

Christensen, A. D., Kádár, Z., Oleskowicz-Popiel, P., & Thomsen, M. H. (2011). Production of bioethanol from organic whey using *Kluyveromyces marxianus*. *Journal of Industrial Microbiology and Biotechnology*, *38*(2), 283–289. https://doi.org/10.1007/s10295-010-0771-0

Cis Legislation. (2006). *Water Code of the Russian Federation of June 3, 2006 No. 74-FZ*. https://cis-legislation.com/document.fwx?rgn=13410

Cis Legislation. (2014). *Water Code of the Republic of Belarus of April 30, 2014 No. 149-Z*. https://cis-legislation.com/document.fwx?rgn=68800

Clover Fonterra. (n.d.). *NZMP (ingredients by Fonterra)*. Retrieved March 23, 2022, from https://www.cloverfonterra.com/ingredients_category/nzmp/

Colombo, B., Sciarria, T. P., Reis, M., Scaglia, B., & Adani, F. (2016). Polyhydroxyalkanoates (PHAs) production from fermented cheese whey by using a mixed microbial culture. *Bioresource Technology*, *218*, 692–699. https://doi.org/10.1016/j.biortech.2016.07.024

Cramer, J. (2022). Effective governance of circular economies: An international comparison. *Journal of Cleaner Production*, *343*, 130874. https://doi.org/https://doi.org/10.1016/j.jclepro.2022.130874

Crane, K. W., & Grover, J. P. (2010). Coexistence of mixotrophs , autotrophs , and heterotrophs in planktonic microbial communities. *Journal of Theoretical Biology*, *262*(3), 517–527. https://doi.org/10.1016/j.jtbi.2009.10.027

Daigger, G. (2011). Changing Paradigms: From Wastewater Treatment to Resource Recovery. *Proceedings of the Water Environment Federation*, *2011*, 942–957. https://doi.org/10.2175/193864711802836742

Dao, G.-H., Wu, G.-X., Wang, X.-X., Zhang, T.-Y., Zhan, X.-M., & Hu, H.-Y. (2018). Enhanced microalgae growth through stimulated secretion of indole acetic acid by symbiotic bacteria. *Algal Research*, *33*, 345–351. https://doi.org/10.1016/j.algal.2018.06.006

Davila-Vazquez, G., Alatriste-Mondragón, F., de León-Rodríguez, A., & Razo-Flores, E. (2008). Fermentative hydrogen production in batch experiments using lactose, cheese whey and glucose: Influence of initial substrate concentration and pH. *International Journal of Hydrogen Energy*, *33*(19), 4989–4997. https://doi.org/10.1016/j.ijhydene.2008.06.065

Desmidt, E., Ghyselbrecht, K., Zhang, Y., Pinoy, L., van der Bruggen, B.,

Verstraete, W., Rabaey, K., & Meesschaert, B. (2015). Global phosphorus scarcity and full-scale P-recovery techniques: A review. *Critical Reviews in Environmental Science and Technology*, *45*(4), 336–384. https://doi.org/10.1080/10643389.2013.866531

Di Bitetti, M. S., & Ferreras, J. A. (2017). Publish (in English) or perish : The effect on citation rate of using languages other than English in scientific publications. *Ambio*, *46*, 121–127. https://doi.org/10.1007/s13280-016-0820-7

Dinika, I., & Utama, G. L. (2019). Cheese whey as potential resource for antimicrobial edible film and active packaging production. *Foods and Raw Materials*, *7*(2), 229–239.

Dunne, J., Evershed, R. P., Salque, M., Cramp, L., Bruni, S., Ryan, K., Biagetti, S., & di Lernia, S. (2012). First dairying in Green Saharan Africa in the fifth millennium BC. *Nature*, *486*(7403), 390–394. https://doi.org/10.1038/nature11186

Early, R. (1997). *Technology of dairy products* (2nd ed.). Springer US.

Ellen MacArthur Foundation. (2015). *Delivering the circular economy - A toolkit for policymakers*. https://www.ellenmacarthurfoundation.org/publications/delivering-the-circular-economy-a-toolkit-for-policymakers

Escalante, H., Castro, L., Amaya, M. P., Jaimes, L., & Jaimes-Estévez, J. (2018). Anaerobic digestion of cheese whey: energetic and nutritional potential for the dairy sector in developing countries. *Waste Management*, *71*, 711–718. https://doi.org/10.1016/j.wasman.2017.09.026

Circular Economy package (COM (2015) 614 final, (2015) (testimony of European Commission). https://eur-lex.europa.eu/resource.html?uri=cellar:8a8ef5e8-99a0-11e5-b3b7-01aa75ed71a1.0012.02/DOC_1&format=PDF

European Commission. (2020). *Circular Economy Action Plan - The European Green Deal*. https://doi.org/10.2775/458852

European Union. (n.d.). *EU law*. Retrieved April 24, 2020, from https://europa.eu/european-union/law_en

Evershed, R. P., Payne, S., Sherratt, A. G., Copley, M. S., Coolidge, J., Urem-Kotsu, D., Kotsakis, K., Özdoğan, M., Özdoğan, A. E., Nieuwenhuyse, O., Akkermans, P. M. M. G., Bailey, D., Andeescu, R. R., Campbell, S., Farid, S., Hodder, I., Yalman, N., Özbaşaran, M., Biçakci, E., … Burton, M. M. (2008). Earliest date for milk use in the Near East and Southeastern Europe linked to cattle herding. *Nature*, *455*(7212), 528–531. https://doi.org/10.1038/nature07180

FAO. (n.d.). *FAOSTAT - Livestock processed*. Food and Agriculture Organization of the United Nations. Retrieved June 20, 2020, from http://www.fao.org/faostat/en/?#data/QP

Fell, E. v, & Lukianova, N. A. (2015). British universities : International students ' alleged lack of critical thinking. *Procedia - Social and Behavioral Sciences*, *215*(June), 2–8. https://doi.org/10.1016/j.sbspro.2015.11.565

Feng, K. (Emma), & Lam, C.-Y. (Anson). (2021). An Overview of Circular Economy in China: How the Current Challenges Shape the Plans for the Future. *The Chinese Economy*, *54*(5), 355–371. https://doi.org/10.1080/10971475.2021.1875156

FrieslandCampina Ingredients. (n.d.). *Nutrition segments*. Retrieved March 22, 2022, from https://www.frieslandcampinaingredients.com/

Gameiro, T., Novais, R. M., Correia, C. L., Carvalheiras, J., Seabra, M. P., Labrincha, J. A., Duarte, A. C., & Capela, I. (2020). Red mud-based inorganic polymer spheres : Innovative and environmentally friendly anaerobic digestion enhancers. *Bioresource Technology*, *316*. https://doi.org/10.1016/j.biortech.2020.123904

Gelegenis, J., Georgakakis, D., Angelidaki, I., & Mavris, V. (2007). Optimization of biogas production by co-digesting whey with diluted poultry manure. *Renewable Energy*, *32*(13), 2147–2160. https://doi.org/10.1016/j.renene.2006.11.015

Gillies, M. T. (1974). *Whey processing and utilization : economic and technical aspects*. Noyes Data Corp.

Gioannis, G. de, Friargiu, M., Massi, E., Muntoni, A., & Polettini, A. (2014). Biohydrogen production from dark fermentation of cheese whey : Influence of pH. *International Journal of Hydrogen Energy*, *39*(36), 20930–20941. https://doi.org/10.1016/j.ijhydene.2014.10.046

Girotto, F., Lavagnolo, M. C., Pivato, A., & Cossu, R. (2017). Acidogenic fermentation of the organic fraction of municipal solid waste and cheese whey for bio-plastic precursors recovery – Effects of process conditions during batch tests. *Waste Management*, *70*, 71–80. https://doi.org/10.1016/j.wasman.2017.09.015

Glambia. (n.d.). *Specialised nutrition*. Retrieved March 17, 2022, from https://www.glanbiairelandingredients.com/applications/specialised-nutrition

González Siso, M. I. (1996). The biotechnological utilization of cheese whey: A review. In *Bioresource Technology* (Vol. 57, Issue 1, pp. 1–11). Elsevier Science Ltd. https://doi.org/10.1016/0960-8524(96)00036-3

Gonzalez-Fernandez, C., Sialve, B., & Molinuevo-Salces, B. (2015). Anaerobic digestion of microalgal biomass: Challenges, opportunities and research needs. *Bioresource Technology*, *198*, 896–906. https://doi.org/10.1016/j.biortech.2015.09.095

Government of Canada. (n.d.). *Justice laws website*. Retrieved April 24, 2020, from https://laws-lois.justice.gc.ca/eng/acts/

Government of South Australia. (n.d.). *South Australia legislation*. Retrieved April 24, 2020, from https://www.legislation.sa.gov.au/index.aspx

Grek, O., Ovsiienko, K., Tymchuk, A., Onopriichuk, O., & Kumar, A. (2020). Influence of wheat food fiber on the structure formation process of whey-

creamy cheeses. *Ukranian Food Journal*, *9*(2), 332–343.

Gross, M. (2018). On the origins of cheese. *Current Biology*, *28*, 1171–1189.

Guest, J. S., Skerlos, S. J., Barnard, J. L., Beck, M. B., Daigger, G. T., Hilger, H., Jackson, S. J., Karvazy, K., Kelly, L., Macpherson, L., Mihelcic, J. R., Pramanik, A., Raskin, L., van Loosdrecht, M. C. M., Yeh, D., & Love, N. G. (2009). A New Planning and Design Paradigm to Achieve Sustainable Resource Recovery from Wastewater. *Environmental Science & Technology*, *43*(16), 6126–6130. https://doi.org/10.1021/es9010515

Gunningham, N. (2009). Environment law, regulation and governance: shifting architectures. *Journal of Environmental Law*, *21*(2), 179–212. https://doi.org/10.1093/jel/eqp011

Guo, M., & Wang, G. (2019). History of whey production and whey protein manufacturing. In M. Guo (Ed.), *Whey Protein Production , Chemistry , Functionality , and Applications* (1st ed., pp. 1–12). Wiley & Sons Ltd.

Guo, X., Zhou, J., & Xiao, D. (2010). Improved ethanol production by mixed immobilized cells of *Kluyveromyces marxianus* and *Saccharomyces cerevisiae* from cheese whey powder solution fermentation. *Appl Biochem Biotechnol*, *160*, 532–538. https://doi.org/10.1007/s12010-008-8412-z

Hagos, K., Zong, J., Li, D., Liu, C., & Lu, X. (2016). Anaerobic co-digestion process for biogas production : Progress , challenges and perspectives. *Renewable and Sustainable Energy Reviews*, *76*, 1485–1496. https://doi.org/10.1016/j.rser.2016.11.184

Hammam, A., Tammam, A., Elderwy, Y., & Hassan, A. (2017). Functional peptides in milk whey: An overview. *Assiut Journal of Agricultural Sciences*, *48*(4), 77–91. https://doi.org/10.21608/ajas.2017.19875

Herrador, M., de Jong, W., Nasu, K., & Granrath, L. (2022). Circular economy and zero-carbon strategies between Japan and South Korea: A comparative study. *Science of the Total Environment*, *820*. https://doi.org/10.1016/j.scitotenv.2022.153274

Holden, L. A., & Goodling, R. C. (2021). Managing milk market disruptions at the dairy farm level in the USA. In P. Bórawski, A. Parzonko, & I. Żuchowski (Eds.), *Challenges in the milk market (investments, disruptions, logistics, competitiveness, prices, and policy)* (pp. 61–67). Wydawnictwo Ostrołęckiego Towarzystwa Naukowego im. Adama Chętnika.

Huffstutter, P. J. (2020, April 3). *U.S. dairy farmers dump milk as pandemic upends food markets*. Reuters. https://www.reuters.com/article/us-health-coronavirus-dairy-insight-idUSKBN21L1DW

Hughes, P., Risner, D., & Meunier-Goddik, L. (2018). Whey to vodka. In IntechOpen (Ed.), *Whey - Biological Properties and Alternative Uses* (1st ed., pp. 1–21). IntechOpen. https://doi.org/10.5772/intechopen.81679

Hussain, A. (2015). Search engines as an effective tool for library

professionals. *Journal of Library & Information Technology*, *35*(6), 389–397. https://doi.org/10.14429/djlit.35.6.8804

Hussain, F., Shah, S. Z., Ahmad, H., Abubshait, S. A., Abubshait, H. A., Laref, A., Manikandan, A., Kusuma, H. S., & Iqbal, M. (2021). Microalgae an ecofriendly and sustainable wastewater treatment option : Biomass application in biofuel and bio-fertilizer production . A review. *Renewable and Sustainable Energy Reviews*, *137*(December 2020), 110603. https://doi.org/10.1016/j.rser.2020.110603

Ibrahim, O. (2018). A new low calorie tagatose sweetner D-Tagatose from lactose in cheese whey as a nutraceutical value-added product. *Journal of Food Health & Technology Innovations*, *1*(1), 11–28.

Imtiaz-Ul-Islam, Md., Hong, L., & Langrish, T. (2011). CO2 capture using whey protein isolate. *Chemical Engineering Journal*, *171*(3), 1069–1081. https://doi.org/10.1016/j.cej.2011.05.003

Iona Capital. (n.d.). *Leeming Biogas*. Retrieved April 16, 2022, from https://ionacapital.co.uk/investments/leeming-biogas/

ISO. (2006). *ISO 14044:2006 Environmental Management — Life Cycle Assessment — Principles and frameworks*. https://www.iso.org/standard/37456.html

Jaimes-Estévez, J., Castro, L., Escalante, H., Carrillo, D., Portillo, S., Sotres, A., & Morán, A. (2020). Cheese whey co-digestion treatment in a tubular system : Microbiological behaviour along the axial axis. *Biomass Conv. Bioref.* https://doi.org/https://doi.org/10.1007/s13399-020-00988-4

Japan - Ministry of The Environment. (1970). *Water Pollution Control Law Law No. 138 of 197*. http://www.env.go.jp/en/laws/water/wlaw/index.html

Jenkins, D., & Wanner, J. (2014). *Activated sludge - 100 years and counting* (D. Jenkins & J. Wanner, Eds.; 1st ed.). IWA Publishing.

Jeong, M. (2003). Carbon dioxide mitigation by microalgal photosynthesis. *Bull. Korean Chem. Soc.*, *24*(12), 1763–1766. https://doi.org/10.5012/bkcs.2003.24.12.1763

Kemp-Benedict, E. (2015). *3 key steps to a more sustainable economy*. World Economic Forum - Future of Economic Progress Sustainable Development. https://www.weforum.org/agenda/2015/09/3-key-steps-to-a-more-sustainable-economy/

Ketterings, Q., Czymmek, K., Gami, S., Godwin, G., & Ganoe, K. (2017). Guidelines for land application of acid whey. In *Department of Animal Science Publication Series* (Issue 247). http://nmsp.cals.cornell.edu/publications/files/AcidWheyGuidelines2017.pdf

Khan, M. I., Shin, J. H., & Kim, J. D. (2018). The promising future of microalgae: current status, challenges, and optimization of a sustainable and renewable industry for biofuels, feed, and other products. *Microbial Cell Factories*, *17*(36), 36. https://doi.org/10.1186/s12934-018-0879-x

Kiker, G. A., Bridges, T. S., Varghese, A., Seager, P. T. P., & Linkov, I. (2005). Application of multicriteria decision analysis in environmental decision making. In *Integrated environmental assessment and management* (Vol. 1, Issue 2, pp. 95–108). https://doi.org/10.1897/IEAM_2004a-015.1

Kim, J., Jung, H., & Lee, C. (2014). Shifts in bacterial and archaeal community structures during the batch biomethanation of *Ulva* biomass under mesophilic conditions. *Bioresource Technology*, *169*, 502–509. https://doi.org/10.1016/j.biortech.2014.07.041

Kim, N., Jeon, J., Elbert, J., Kim, C., & Su, X. (2022). Redox-mediated electrochemical desalination for waste valorization in dairy production. *Chemical Engineering Journal*, *428*, 131082. https://doi.org/https://doi.org10.1016/j.cej.2021.131082

Kim, S., Park, J., Cho, Y., & Hwang, S. (2013). Growth rate , organic carbon and nutrient removal rates of Chlorella sorokiniana in autotrophic , heterotrophic and mixotrophic conditions. *Bioresource Technology*, *144*, 8–13. https://doi.org/10.1016/j.biortech.2013.06.068

Kleerebezem, R., Joosse, B., Rozendal, R., & van Loosdrecht, M. C. M. (2015). Anaerobic digestion without biogas? *Reviews in Environmental Science and Biotechnology*, *14*(4), 787–801. https://doi.org/10.1007/s11157-015-9374-6

Ko, S., & Kwak, H.-S. (2009). Bioactive components in whey products. In Y. W. Park (Ed.), *Bioactive Components in Milk and Dairy Products* (pp. 263–285). Wiley-Blackwell.

Kouzuma, A., & Watanabe, K. (2015). Exploring the potential of algae/bacteria interactions. *Current Opinion in Biotechnology*, *33*, 125–129. https://doi.org/10.1016/j.copbio.2015.02.007

Kralisch, A., & Mandl, T. (2006). Barriers to information access across languages on the internet: Network and language effects. *Proceedings of the 39th Hawaii International Conference on System Sciences*, 1–10. https://doi.org/10.1109/HICSS.2006.71

Kucera, D., Pernicová, I., Kovalcik, A., Koller, M., Mullerova, L., Sedlacek, P., Mravec, F., Nebesarova, J., Kalina, M., Marova, I., Krzyzanek, V., & Obruca, S. (2018). Characterization of the promising poly (3-hydroxybutyrate) producing halophilic bacterium Halomonas halophila. *Bioresource Technology*, *256*, 552–556. https://doi.org/10.1016/j.biortech.2018.02.062

Kushwaha, D., Srivastava, N., Mishra, I., Upadhyay, S. N., & Mishra, P. K. (2019). Recent trends in biobutanol production. *Rev Chem Eng*, *35*(4), 475–504. https://doi.org/10.1515/revce-2017-0041

Lactalis Global. (n.d.). *Lactalis Ingredients*. Retrieved March 22, 2022, from https://www.lactalisingredients.com/

Lagoa-Costa, B., Kennes, C., & Veiga, M. C. (2020). Cheese whey fermentation into volatile fatty acids in an anaerobic sequencing batch reactor.

Bioresource Technology, *308*. https://doi.org/10.1016/j.biortech.2020.123226

Lammifyad, C. (2020). Review on impacts of COVID-19 pandemic on life animals and dairy product processing industries of the world. *Insights in Veterinary Science*, *4*(1), 018–024. https://doi.org/10.29328/journal.ivs.1001022

Landa, L. G. G. (2006). Academic language barriers and solutions. *Current Issues in Language Planning*, *7*(1), 61–81. https://doi.org/https://doi.org/10.2167/cilp084.0

Lappa, I., Papadaki, A., Kachrimanidou, V., Terpou, A., Koulougliotis, D., Eriotou, E., & Kopsahelis, N. (2019). Cheese whey processing: Integrated biorefinery concepts and emerging food applications. *Foods*, *8*(8), 347. https://doi.org/10.3390/foods8080347

Lawrence, S., & Giles, C. L. (1998). Searching the World Wide Web. *Science New Series*, *280*(5360), 98–100.

le Corre, K. S., Valsami-Jones, E., Hobbs, P., & Parsons, S. A. (2009). Phosphorus recovery from waste by struvite crystallisation: A review. *Critical Reviews in Environmental Science and Technology*, *39*(6), 433–477. https://doi.org/https://doi.org/10.1080/10643380701640573

Lee, K., Eisterhold, M. L., Rindi, F., Palanisami, S., & Nam, P. K. (2014). Isolation and screening of microalgae from natural habitats in the midwestern United States of America for biomass and biodiesel sources. *Journal of Natural Science, Biology and Medicine*, *5*(2), 333–339. https://doi.org/10.4103/0976-9668.136178

Legal Services Online. (n.d.). *The Water Code of Ukraine*. http://yurist-online.com/en/kodeks/009.php

Leonardi, M., Gerbault, P., Thomas, M. G., & Burger, J. (2012). The evolution of lactase persistence in Europe. A synthesis of archaeological and genetic evidence. *International Dairy Journal*, *22*(2), 88–97. https://doi.org/10.1016/j.idairyj.2011.10.010

Lustrato, G., Salimei, E., Alfano, G., Belli, C., Fantuz, F., Grazia, L., & Ranalli, G. (2013). Cheese whey recycling in traditional dairy food chain: Effects of vinegar from whey in dairy cow nutrition. *Acetic Acid Bacteria*, *2*(1s), 8. https://doi.org/10.4081/aab.2013.s1.e8

Malaspina, F., Cellamare, C. M., Stante, L., & Tilche, A. (1996). Anaerobic treatment of cheese whey with a downflow-upflow hybrid reactor. *Bioresource Technology*, *55*, 131–139. https://doi.org/https://doi.org/10.1016/0960-8524(95)00187-5

Maragkaki, A. E., Vasileiadis, I., Fountoulakis, M., Kyriakou, A., Lasaridi, K., & Manios, T. (2018). Improving biogas production from anaerobic co-digestion of sewage sludge with a thermal dried mixture of food waste, cheese whey and olive mill wastewater. *Waste Management*, *71*, 644–651. https://doi.org/10.1016/j.wasman.2017.08.016

Marazzi, F., Bellucci, M., Fantasia, T., Ficara, E., & Mezzanotte, V. (2020). Interactions between microalgae and bacteria in the treatment of wastewater from milk whey processing. *Water*,

12(1), 1–13. https://doi.org/10.3390/w12010297

Markou, G., & Georgakakis, D. (2011). Cultivation of filamentous cyanobacteria (blue-green algae) in agro-industrial wastes and wastewaters: A review. *Applied Energy*, *88*(10), 3389–3401. https://doi.org/10.1016/j.apenergy.2010.12.042

Marwaha, S. S., & Kennedy, J. F. (1988). Whey—Pollution problem and potential utilization. *International Journal of Food Science & Technology*, *23*(4), 323–336. https://doi.org/10.1111/j.1365-2621.1988.tb00586.x

Mediboyina, M. K., Holden, N. H., O'Neill, S., Routledge, K., Morrissey, B., Lawless, F., & Murphy, F. (2022). Upscale fermenter design for lactic acid production from cheese whey permeate focusing on impeller selection and energy optimization. *J. Food Sci. Technol.*, *59*(6), 2263–2273. https://doi.org/https://doi.org/10.1007/s13197-021-05239-6

Meneghini, R., & Packer, A. L. (2007). Is there Science beyond English? *EMBO Reports*, *8*(2), 2–6. https://doi.org/https://dx.doi.org/10.1038%2Fsj.embor.7400906

Milk Specialties Global. (n.d.). *Products*. Retrieved March 22, 2022, from https://www.milkspecialties.com/

Ministry of the Environment. (n.d.). *Brazilian legislation platform*. https://www.gov.br/mma/pt-br

Miracco, J. L., Alzamora, S. M., Chirife, J., & Ferro Fontan, C. (1981). On the water activity of lactose solutions. *Journal of Food Science*, *46*(5), 1612–1613. https://doi.org/https://doi.org/10.1111/j.1365-2621.1981.tb04231.x

Mishra, P. K., & Shekhar, B. R. (2012). Evaluating supply chain risk in Indian dairy industry: A case study. *Int. J. Decision Sciences, Risk and Management*, *4*(1–2), 77–91.

Mlekuž, D. (2015). Archaeological culture, please meet yoghurt culture: towards a relational archaeology of milk. *Documenta Praehistorica*, *42*, 275–288. https://doi.org/10.4312/dp.42.19

Mohan, S. V., Chiranjeevi, P., Chandrasekhar, K., Babu, P. S., & Sarkar, O. (2019). Acidogenic biohydrogen production from wastewater. In A. Pandey, S. V. Mohan, J.-S. Chang, P. C. Hallenbeck, & C. Larroche (Eds.), *Biohydrogen* (2nd ed., pp. 279–320). Elsevier B.V. https://doi.org/10.1016/B978-0-444-64203-5.00011-3

Montecchio, D., Yuan, Y., & Malpei, F. (2018). Hydrogen production dynamic during cheese whey dark fermentation : New insights from modelization. *International Journal of Hydrogen Energy*, *43*(37), 17588–17601. https://doi.org/10.1016/j.ijhydene.2018.07.146

Muhammad, A. Y., & Bhojiya, A. A. (2021). Global impact of Covid-19. *Journal of Indian Research*, *9*(1–2), 82–87.

Mulders, M., Tamis, J., Abbas, B., Sousa, J., Dijkman, H., Rozendal, R., & Kleerebezem, R. (2020). Pilot-scale polyhydroxyalkanoate production from organic waste: Process characteristics at high pH and high ammonium concentration. *Journal of Environmental*

Engineering, *146*(7), 4020049. https://doi.org/10.1061/(ASCE)EE.1943-7870.0001719

Munien, I., & Telukdarie, A. (2021). COVID-19 supply chain resilience modelling for the dairy industry. *Procedia Computer Science*, *180*, 591–599. https://doi.org/10.1016/j.procs.2021.01.280

Naeini, M. A., Zandieh, M., Najafi, S. E., & Sajadi, S. M. (2020). Analyzing the development of the third-generation biodiesel production from microalgae by a novel hybrid decision-making method : The case of Iran. *Energy*, *195*. https://doi.org/10.1016/j.energy.2020.116895

Najafpour, G. D., Shahavi, M. H., & Neshat, S. A. (2016). Assessment of biological hydrogen production processes: A review. *IOP Conference Series: Earth and Environmental Science*, *36*(1). https://doi.org/10.1088/1755-1315/36/1/012068

New Zealand - Ministry for the Environment. (2014). *The National Policy Statement for Freshwater Management (Freshwater NPS) Provides Direction on How Local Authorities Should Carry Out Their Responsibilities Under the Resource Management Act 1991 for Managing Fresh Water*. http://www.mfe.govt.nz/fresh-water/regulations/national-policy-statement-freshwater-management

Nghiem, L. D., Koch, K., Bolzonella, D., & Drewes, J. E. (2017). Full scale co-digestion of wastewater sludge and food waste: bottlenecks and possibilities. *Renewable and Sustainable Energy Reviews*, *72*, 354–362. https://doi.org/10.1016/j.rser.2017.01.062

Nicolella, C., van Loosdrecht, M. C. M., & Heijnen, J. J. (2000). Wastewater treatment with particulate biofilm reactors. *Journal of Biotechnology*, *80*, 1–33. https://doi.org/https://doi.org/10.1016/s0168-1656(00)00229-7

Onwulata, C., & Huth, P. J. (2008). *Whey processing, functionality and health benefits*. Wiley-Blackwell.

Pais-Chanfrau, J. M., Núñez-Pérez, J., Espin-Valladares, R. del C., Lara-Fiallos, M. V., & Trujillo-Toledo, L. E. (2020). Bioconversion of lactose from cheese whey to organic acids. In N. Gutiérrez-Méndez (Ed.), *Lactose and lactose derivatives* (1st ed., p. 22). IntechOpen. https://doi.org/10.5772/intechopen.87477

Pandey, A., Srivastava, S., Rai, P., & Duke, M. (2019). Cheese whey to biohydrogen and useful organic acids: A non-pathogenic microbial treatment by L. acidophilus. *Nature Scientific Reports*, *9*(1), 1–9. https://doi.org/10.1038/s41598-019-42752-3

Pang, N., Gu, X., Kirchhoff, H., Lei, H., & Roje, S. (2019). Exploiting mixotrophic for improving productivities of biomass and co-products of microalgae. *Renewable and Sustainable Energy Reviews*, *112*, 450–460. https://doi.org/10.1016/j.rser.2019.06.001

Panghal, A., Patidar, R., Jaglan, S., Chhikara, N., Khatkar, S. K., Gat, Y., &

Sindhu, N. (2018). Whey valorization: current options and future scenario – a critical review. *Nutrition & Food Science*, *48*(3), 520–535. https://doi.org/10.1108/NFS-01-2018-0017

Papademas, P., & Kotsaki, P. (2019). Technological utilization of whey towards sustainable exploitation. *Advances in Dairy Research*, *7*(231). https://doi.org/10.35248/2329-888X.19.7.231

Parsons, S. A., & Smith, J. A. (2008). Phosphorus removal and recovery from municipal wastewaters. *Elements*, *4*(2), 109–112. https://doi.org/10.2113/GSELEMENTS.4.2.109

Patel, P., Desai, M., & Madamwar, D. (1995). Biomethanation of cheese whey using anaerobic upflow fixed film reactor. *Journal of Fermentation and Bioengineering*, *79*(4), 398–399. https://doi.org/10.1016/0922-338X(95)94006-D

Perez-Garcia, O., Escalante, F. M. E., De-Bashan, L. E., & Bashan, Y. (2011). Heterotrophic cultures of microalgae: Metabolism and potential products. *Water Research*, *45*(1), 11–36. https://doi.org/10.1016/j.watres.2010.08.037

Pien, J. (1943). Utilisation des sérum de fromagerie et des lacto- protéines dans l'alimentation. *Le Lait*, *227*, 228.

Pires, A. F., Marnotes, N. G., Rubio, O. D., Garcia, A. C., & Pereira, C. D. (2021). Dairy by-products: A review on the valorization of whey and second cheese whey. *Foods*, *10*(5), 1067. https://doi.org/10.3390/foods10051067

Pittman, J. K., Dean, A. P., & Osundeko, O. (2011). The potential of sustainable algal biofuel production using wastewater resources. *Bioresource Technology*, *102*(1), 17–25. https://doi.org/10.1016/j.biortech.2010.06.035

Posadas, E., Bochon, S., & M. C., García-González, M. C., García-Encina, P. A., & Muñoz, R. (2014). Microalgae-based agro-industrial wastewater treatment : a preliminary screening of biodegradability. *J. Appl. Phycol.*, *26*, 2335–2345. https://doi.org/10.1007/s10811-014-0263-0

Prazeres, A. R., Carvalho, F., & Rivas, J. (2012). Cheese whey management: A review. In *Journal of Environmental Management* (Vol. 110, pp. 48–68). https://doi.org/10.1016/j.jenvman.2012.05.018

Prot, T., Wijdeveld, W., Eshun, L. E., Dugulan, A. I., Goubitz, K., Korving, L., & van Loosdrecht, M. C. M. (2020). Full-scale increased iron dosage to stimulate the formation of vivianite and its recovery from digested sewage sludge. *Water Research*, *182*, 115911. https://doi.org/10.1016/j.watres.2020.115911

Rabaey, K., & Rozendal, R. A. (2010). Microbial electrosynthesis — revisiting the electrical route for microbial production. *Nature Reviews Microbiology*, *8*, 706–716. https://doi.org/10.1038/nrmicro2422

Raganati, F., Olivieri, G., Procentese, A., Russo, M. E., Salatino, P., & Marzocchella, A. (2013). Butanol production by bioconversion of cheese whey in a continuous packed bed

reactor. *Bioresource Technology*, *138*, 259–265. https://doi.org/10.1016/j.biortech.2013.03.180

Ramanan, R., Kim, B. H., Cho, D. H., Oh, H. M., & Kim, H. S. (2016). Algae-bacteria interactions: Evolution, ecology and emerging applications. *Biotechnology Advances*, *34*(1), 14–29. https://doi.org/10.1016/j.biotechadv.2015.12.003

Ramos, O. L., Pereira, R. N., Rodrigues, R. M., Teixeira, J. A., Vicente, A. A., & Malcata, F. X. (2016). Whey and whey powders: production and uses. *Encyclopedia of Food and Health*, 498–505. https://doi.org/10.1016/B978-0-12-384947-2.00747-9

Water Quality and Ecosystem Conservation Act, (2005) (testimony of Republic of Korea - Ministry of Environment).

Research Information Network. (2009). *Overcoming barriers: access to research information content*. www.rin.ac.uk

Riaño, B., Blanco, S., Becares, E., & García-González, M. C. (2016). Bioremediation and biomass harvesting of anaerobic digested cheese whey in microalgal-based systems for lipid production. *Ecological Engineering*, *97*, 40–45. https://doi.org/10.1016/j.ecoleng.2016.08.002

Rizwan, M., Mujtaba, G., Memon, S. A., Lee, K., & Rashid, N. (2018). Exploring the potential of microalgae for new biotechnology applications and beyond: A review. *Renewable and Sustainable Energy Reviews*, *92*, 394–404. https://doi.org/10.1016/j.rser.2018.04.034

Robbins, C. W., & Lehrsch, G. A. (1998). Cheese whey as a soil conditioner. In A. Wallace & R. E. Terry (Eds.), *Handbook of Soil Conditioners* (1st ed., pp. 167–186). Marcel Dekker Inc.

Rombouts, J. L., Mos, G., Weissbrodt, D. G., Kleerebezem, R., & van Loosdrecht, M. C. M. (2019). Diversity and metabolism of xylose and glucose fermenting microbial communities in sequencing batch or continuous culturing. *FEMS Microbiology Ecology*, *95*(2), 1–12. https://doi.org/10.1093/femsec/fiy233

Roubík, H., Lošťák, M., Ketuama, C. T., Procházka, P., Soukupová, J., Hakl, J., Karlík, P., & Hejcman, M. (2022). Current coronavirus crisis and past pandemics - What can happen in post-COVID-19 agriculture? In *Sustainable Production and Consumption* (Vol. 30, pp. 752–760). Elsevier B.V. https://doi.org/10.1016/j.spc.2022.01.007

Roukas, T., & Kotzekidou, P. (1998). Lactic acid production from deproteinized whey by mixed cultures of free and co-immobilized *Latobacillus casei* and *Latococcus lactis* cells using fedbatch culture. *Enzyme and Microbial Technology*, *22*, 199–204.

Ryan, M. P., & Walsh, G. (2016). The biotechnological potential of whey. *Reviews in Environmental Science and Biotechnology*, *15*(3), 479–498. https://doi.org/10.1007/s11157-016-9402-1

Saputo. (n.d.). *Functional ingredients*. Retrieved March 23, 2022, from

https://uk.saputo.com/brands/functional-ingredients/demineralised-whey/

Savova, M., & Price, J. S. (2019). Redesigning the academic library materials budget for the digital age : Applying the power of faceted classification to acquisitions fund management. *Library Resources & Technical Services*, *63*(2), 131–142.

Schnurr, P. J., Espie, G. S., & Allen, D. G. (2013). Algae biofilm growth and the potential to stimulate lipid accumulation through nutrient starvation. *Bioresource Technology*, *136*, 337–344. https://doi.org/10.1016/j.biortech.2013.03.036

Mexican Official Standard NOM-001-ECOL-1996, (testimony of Secretary of Environment Natural Resources and Fisheries). http://cepis.org.pe/mexican-official-standard-001ecol1996/

Singh, R. S. (2016). Biotechnological approaches for valorization of whey. In R. S. Singh, A. Pandey, & C. Larroche (Eds.), *Advances in Industrial Biotechnology* (pp. 443–478). IK International Publishing House Pvt. Ltd.

Smithers, G. W. (2008). Whey and whey proteins-From "Gutter-to-Gold." *International Dairy Journal*, *18*(7), 695–704. https://doi.org/10.1016/j.idairyj.2008.03.008

Smithers, G. W. (2015). Whey-ing up the options – Yesterday, today and tomorrow. *International Dairy Journal*, *v. 48*, 2-14–2015 v.48. https://doi.org/10.1016/j.idairyj.2015.01.011

Soares, B. B., Alves, E. C., de Almeida Neto, J. A., & Rodrigues, L. B. (2021). Environmental impact of cheese production. In *Environmental Impact of Agro-Food Industry and Food Consumption* (pp. 169–187). Elsevier. https://doi.org/10.1016/B978-0-12-821363-6.00009-6

Spence, D. B. (2001). The shadow of the rational polluter: rethinking the role of rational actor models in environmental law recommended citation. *California Law Review*, *89*(4), 83. https://doi.org/10.15779/Z388X38

Spolaore, P., Joannis-Cassan, C., Duran, E., & Isambert, A. (2006). Commercial applications of microalgae. *Journal of Bioscience and Bioengineering*, *101*(2), 87–96. https://doi.org/10.1263/jbb.101.87

Stojanovski, D., Živaljević, I., Dimitrijević, V., Dunne, J., Evershed, R. P., Balasse, M., Dowle, A., Hendy, J., McGrath, K., Fischer, R., Speller, C., Jovanović, J., Casanova, E., Knowles, T., Balj, L., Naumov, G., Putica, A., Starović, A., & Stefanović, S. (2020). Living off the land: Terrestrial-based diet and dairying in the farming communities of the Neolithic Balkans. *PLOS ONE*, *15*(8), e0237608. https://doi.org/10.1371/journal.pone.0237608

Sultana, M., Mourti, C., Tatoulis, T., Akratos, C. S., Tekerlekopoulou, G., & Vayenas, D. v. (2015). Effect of hydraulic retention time , temperature , and organic load on a horizontal subsurface flow constructed wetland treating cheese whey wastewater. *J. Chem. T Echnol. Biotechnol*. https://doi.org/10.1002/jctb.4637

The Law Library of Congress, & Rodriguez-Ferrand, G. (2013). *National constitution ART 121 civil code*. Legislation on Use of Water in

Agriculture: Argentina. https://www.loc.gov/law/help/water-law/argentina.php#Legal

Trindade, M. B., Soares, B. C. V., Scudino, H., Guimarães, J. T., Esmerino, E. A., Freitas, M. Q., Pimentel, T. C., Silva, M. C., Souza, S. L. Q., Almada, R. B., & Cruz, A. G. (2019). Cheese whey exploitation in Brazil: A questionnaire survey. *Food Science and Technology*, *39*(3), 788–791. https://doi.org/10.1590/fst.07419

Tsakali, E., Petrotos, K., d'Allessandro, A., & Goulas, P. (2010). A review on whey composition and the methods used for its utilization for food and pharmaceutical products. In C. R. Centre (Ed.), *6th International Conference on Simulation and Modelling in the Food and Bio-Industry* (pp. 195–201).

Tsiouris, V., Kontominas, M. G., Filioussis, G., Chalvatzi, S., Giannenas, I., Papadopoulos, G., Koutoulis, K., Fortomaris, P., & Georgopoulou, I. (2020). The effect of whey on performance , gut health and bone morphology parameters in broiler chicks. *Foods*, *9*(588), 588. https://doi.org/doi:10.3390/foods9050588

Tsitouras, A., Basu, O., Al-ghussain, N., & Delatolla, R. (2020). Kinetic effects of anaerobic staging and aeration rates on sequencing batch moving bed biofilm reactors: carbon, nitrogen, and phosphorus treatment of cheese production wastewater. *Chemosphere*, *252*, 126407. https://doi.org/10.1016/j.chemosphere.2020.126407

Tsolcha, O. N., Tekerlekopoulou, A. G., Akratos, C. S., Bellou, S., Aggelis, G., Katsiapi, M., Moustaka-Gouni, M., & Vayenas, D. v. (2016). Treatment of second cheese whey effluents using a *Choricystis*-based system with simultaneous lipid production. *Journal of Chemical Technology and Biotechnology*, *91*(8), 2349–2359. https://doi.org/10.1002/jctb.4829

Tunick, M. H. (2008). Whey protein production and utilization: A brief history. In Charles I. Onwulata Ph.D.; Peter J. Huth (Ed.), *Whey Processing, Functionality and Health Benefits* (1st ed., p. 400). Wiley-Blackwell. https://doi.org/10.1002/9780813803845

Ugah, A. D. (2007). Obstacles to information access and use in developing countries. *Library Philosophy and Practice (e-Journal)*, *160*.

United States of America. (1972). *Clean Water Act*. Senate and House of Representatives of the United States of America in Congress. https://www.epa.gov/laws-regulations/summary-clean-water-act

USDA. (2019). *Dairy: World markets and trade*. https://www.fas.usda.gov/data/dairy-world-markets-and-trade

USDA. (2022). *Dairy: World markets and trade*. https://apps.fas.usda.gov/psdonline/circulars/dairy.pdf

Uvarova, I., Atstaja, D., Grinbergs, U., Petersons, J., Gegere-Zetterstroma, A., & Kraze, S. (2020). Transition to the circular economy and new circular business models – an in-depth study of the whey recycling. *IOP Conference Series: Earth and Environmental Science*, *578*(1), 012019.

https://doi.org/10.1088/1755-1315/578/1/012019

VALORLACT. (2016). *Comprehensive use of the whey generated by the dairy industry in the Basque Country VALORLACT - After life communication plan*. http://valorlact.eu/

van der Hoek, J. P., Duijff, R., & Reinstra, O. (2018). Nitrogen recovery from wastewater : possibilities , competition with other resources , and adaptation pathways. *Sustainability*, *10*(4605), 18. https://doi.org/10.3390/su10124605

Vaneeckhaute, C., Lebuf, V., Michels, E., Belia, E., & Vanrolleghem, P. A. (2017). Nutrient recovery from digestate : Systematic technology review and product classification. *Waste and Biomass Valorization*, *8*, 21–40. https://doi.org/https://doi.org/10.1007/s12649-016-9642-x

Venetsaneas, N., Antonopoulou, G., Stamatelatou, K., Kornaros, M., & Lyberatos, G. (2009). Using cheese whey for hydrogen and methane generation in a two-stage continuous process with alternative pH controlling approaches. *Bioresource Technology*, *100*(15), 3713–3717. https://doi.org/10.1016/j.biortech.2009.01.025

Wang, Q., Liu, C., Zhao, Y., Kitsos, A., Cannella, M., Wang, S., & Han, L. (2020). Impacts of the COVID-19 pandemic on the dairy industry: Lessons from China and the United States and policy implications. *Journal of Integrative Agriculture*, *19*(12), 2903–2915. https://doi.org/10.1016/S2095-3119(20)63443-8

Warthmann, R., Cypionka, H., & Pfennig, N. (1992). Photoproduction of H2 from acetate by syntrophic cocultures of green sulfur bacteria and sulfur-reducing bacteria. *Archives of Microbiology*, *157*, 343–348. https://doi.org/https://doi.org/10.1007/BF00248679

Weersink, A., von Massow, M., McDougall, B., & Bannon, N. (2021). Re-examining the implications of COVID-19 on the Canadian dairy and poultry sectors. *Canadian Journal of Agricultural Economics*, *69*(2), 215–224. https://doi.org/10.1111/cjag.12284

Weissbrodt, D. G., Winkler, M. K. H., & Wells, G. F. (2020). Responsible Science, Engineering and Education for water resource recovery and circularity. *Environmental Science: Water Research & Technology*, *6*(8), 1952–1966. https://doi.org/10.1039/D0EW00402B

Wilsenach, J. A. Ã., Schuurbiers, C. A. H., & Loosdrecht, M. C. M. van. (2007). Phosphate and potassium recovery from source separated urine through struvite precipitation. *Water Research*, *41*, 458–466. https://doi.org/10.1016/j.watres.2006.10.014

Wu, Y., Luo, J., Zhang, Q., Aleem, M., Fang, F., Xue, Z., & Cao, J. (2019). Potentials and challenges of phosphorus recovery as vivianite from wastewater: A review. *Chemosphere*, *226*, 246–258. https://doi.org/10.1016/j.chemosphere.2019.03.138

Yadav, B., Chavan, S., Atmakuri, A., Tyagi, R. D., & Drogui, P. (2020). A review on recovery of proteins from industrial wastewaters with special

emphasis on PHA production process: Sustainable circular bioeconomy process development. *Bioresource Technology*, *317*, 124006. https://doi.org/10.1016/j.biortech.2020.124006

Yadav, B., Pandey, A., Kumar, L. R., & Tyagi, R. D. (2019). Bioconversion of waste (water) residues to bioplastics - A circular bioeconomy approach. *Bioresource Technology*, *298*. https://doi.org/10.1016/j.biortech.2019.122584

Yadav, J. S. S., Yan, S., Pilli, S., Kumar, L., Tyagi, R. D., & Surampalli, R. Y. (2015). Cheese whey: A potential resource to transform into bioprotein, functional/nutritional proteins and bioactive peptides. In *Biotechnology Advances* (Vol. 33, Issue 6, pp. 756–774). Elsevier Inc. https://doi.org/10.1016/j.biotechadv.2015.07.002

Yu, J., & Takahashi, P. (2015). Biophotolysis-based hydrogen production by cyanobacteria and green microalgae. In A. Méndez-Vilas (Ed.), *Communicating Current Research and Educational Topics and Trends in Applied Microbiology* (pp. 79–89).

Zarezadeh, S., Moheimani, N. R., Jenkins, S. N., Hülsen, T., Riahi, H., & Mickan, B. S. (2019). Microalgae and phototrophic purple bacteria for nutrient recovery from agri-industrial effluents: Influences on plant growth, rhizosphere bacteria, and putative carbon- and nitrogen-cycling genes. In *Frontiers in Plant Science* (Vol. 10, p. 1193). https://www.frontiersin.org/article/10.3389/fpls.2019.01193

Zhang, B., Li, W., Guo, Y., Zhang, Z., Shi, W., Cui, F., Lens, P. N. L., Tay, J. H., & A. (2020). Microalgal-bacterial consortia : From interspecies interactions to biotechnological applications. *Renewable and Sustainable Energy Reviews*, *118*, 109563. https://doi.org/10.1016/j.rser.2019.109563

Zheng, Z., Xie, J., Liu, P., Li, X., & Ouyang, J. (2019). Elegant and efficient biotransformation for dual production of d -tagatose and bioethanol from cheese whey powder. *Journal of Agricultural and Food Chemistry*, *67*(3), 829–835. https://doi.org/10.1021/acs.jafc.8b05150

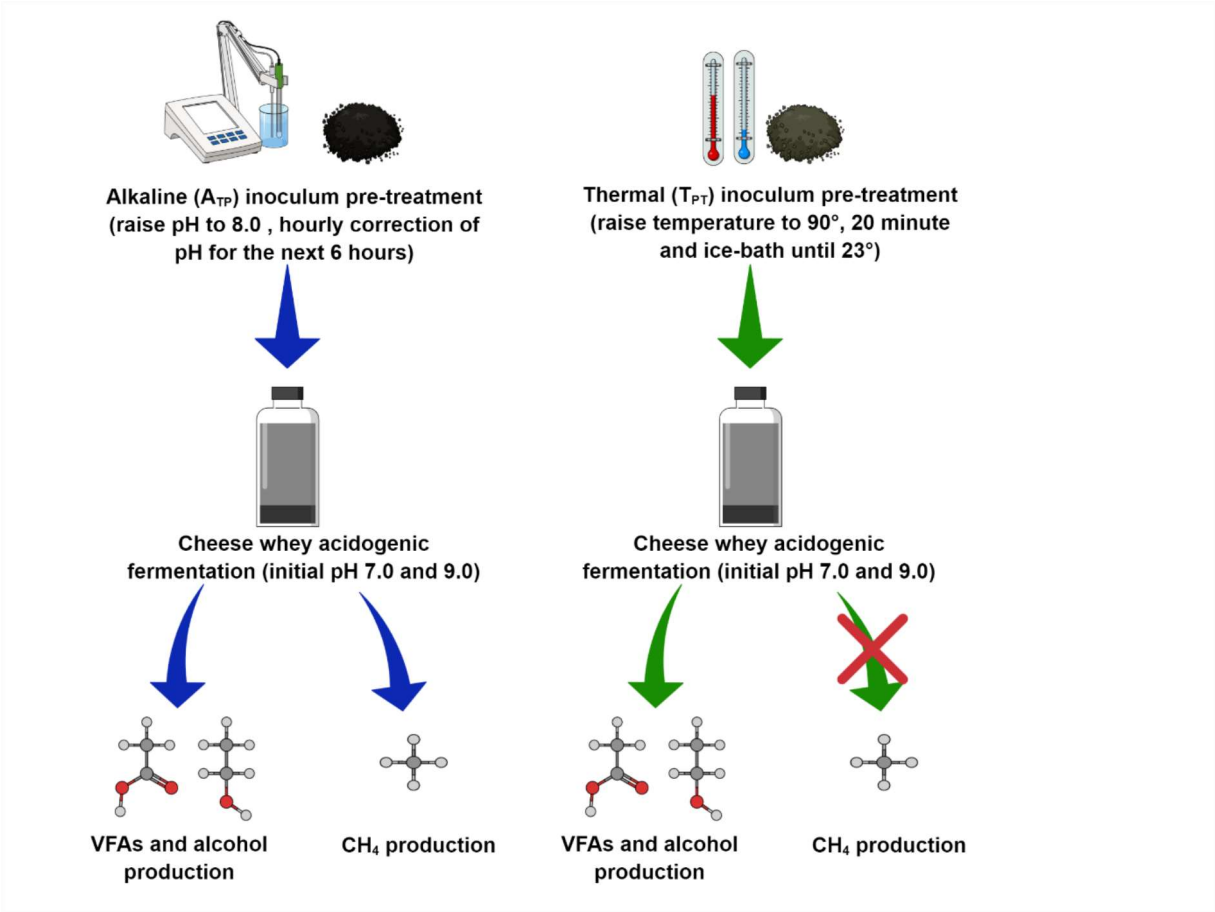
Zhifang, X. (1991). China's water law and environment. *Canadian Water Resources Journal*, *16*(3), 275–282. https://doi.org/10.4296/cwrj1603275

Zhou, X., Hua, X., Huang, L., & Xu, Y. (2019). Bio-utilization of cheese manufacturing wastes (cheese whey powder) for bioethanol and specific product (galactonic acid) production via a two-step bioprocess. *Bioresource Technology*, *272*, 70–76. https://doi.org/10.1016/j.biortech.2018.10.001

3.Thermal and alkaline pre-treatments of inoculum halt methanogenesis and enables cheese whey valorization by batch acidogenic fermentation

This chapter is deposited in a modified version as a preprint on bioRXiv, https://doi.org/10.1101/2023.02.22.529517, and submitted to *Bioresource Technology*.

Graphical Abstract



Abstract

Carboxylates like volatile fatty acids (VFAs) can be produced by acidogenic fermentation (AF) of dairy wastes like cheese whey, a massive residue produced at 160.67 million m^3 of which 42% are not valorized and impact the environment. In mixed-culture fermentations, selection pressures are needed to favor AF and halt methanogenesis. Inoculum pre-treatment was studied here as a selective pressure for AF demineralized cheese whey in batch processes. Alkaline (NaOH, pH 8.0, 6 h) and thermal (90°C for 5 min, ice-bath until 23°C) pre-treatments, were tested together with batch operations run at initial pH 7.0 and 9.0, food-to-microorganism (F/M) ratios of 0.5 to 4.0 g COD g^{-1} VS, and under pressurized and non-pressurized headspace, in experiments duplicated in two institutes. Acetic acid was highly produced (1.36 and 1.40 g COD_{AcOH} L^{-1}) at the expense of methanogenesis by combining a thermal pre-treatment of inoculum with a non-pressurized batch operation started at pH 9.0. Microbial communities comprised of VFAs and alcohol producers, such as *Clostridium*, *Fonticella*, and *Intestinimonas*, and fermenters such as *Longilinea* and *Leptolinea*. Communities also presented the lipid-accumulating and bulk and foaming *Candidatus Microthrix* and the metanogenic *Methanosaeta* regardless of no methane production. An F/M ratio of 0.5 g COD g^{-1} VS led to the best VFA production of 1,769.38 mg L^{-1}. Overall, inoculum thermal pre-treatment, initial pH 9.0, and non-pressurized headspace acted as a selective pressure for halting methanogen and producing VFAs, valorizing cheese whey via batch acidogenic fermentation.

Keywords: acidogenic fermentation, physicochemical pre-treatments, alkaline, thermal, volatile fatty acids, cheese whey

1 Introduction

Anaerobic digestion (AD) has been used from the 19th century onwards to obtain biogas as an energy carrier (Kigozi et al., 2014). Since then, AD processes are being constantly improved (Abbasi et al., 2012; van Lier et al., 2001) to process various waste streams (Ostrem et al., 2004) and address energy production, environmental burdens, and circular economy. The primary goal remains to reduce organic matter and remove nutrients from agro-industrial, food, and municipal solid wastes (Chen et al., 2008; Goud & Mohan, 2012; Wonglertarak & Wichitsathian, 2014).

Cheese whey (CW) is a by-product of the dairy industry with a high organic load (i.e., 50 to 80 g O_2 L^{-1}, in terms of chemical oxygen demand (COD))(Saddoud et al., 2007). It has an annual production of 160.67 million m^3 where 58% of the production is absorbed by various industries (e.g., food, nutrition, cosmetics, and pharmaceutical). However, a staggering amount of 66.5 million m^3 $year^{-1}$ of CW (FAO, n.d.; Tsakali et al., 2010; USDA, 2022) is currently transformed into low-added-value products such as animal feed, fertilizer, or being discharged into water bodies leading to eutrophication processes (Smithers, 2008; Tsakali et al., 2010). Hence, cheese whey can be an excellent substrate for AF processes.

Acidogenic fermentation focuses on the valorization of organic matter via the carboxylate platform, by combining the inhibition of methanogenesis and production of VFAs at high yields, which are of great economic interest due to their potential industrial applications (e.g., biofuels, biopolymers, and chemicals) (Angenent et al., 2016; Kleerebezem et al., 2015; Mulders et al., 2020; Rombouts et al., 2019).

Selective pressures (e.g., pH, physicochemical pre-treatments, reactor headspace pressure, and F/M ratio) can dictate microbial diversity and dynamics, interactions, energy requirements, and preferred metabolisms (Pretorius, 1987). Most studies in AD and AF processes focus on the pre-treatment of the substrate and waste-activated sludge (Sarkar et al., 2021). The present study focused on various selective pressure mechanisms for enhancing VFA production and halting methanogenesis in AF processes. We also investigated the effects of alkaline and thermal inoculum pre-

treatments, variations in the initial pH in headspace pressure, and different F/M ratios on the acidogenic fermentation of cheese whey.

Alkaline pre-treatments have been shown to improve AD processes by increasing sludge solubilization and enhancing methane production (Chen et al., 2007; H. Li et al., 2012; López-Torres & Llórens, 2016; Navia & Vidal, 2002; Wonglertarak & Wichitsathian, 2014), while thermal pre-treatments have been used to inhibit methanogenesis (Alibardi et al., 2012; Ramos-Suarez et al., 2021; Sarkar et al., 2017).

However, thermal pre-treatments, that can be performed at mesophilic or hyperthermophilic temperatures (i.e., 30°C to 180°C) are time-consuming (up to several hours), which would increase AF processes' overall costs (Corti & Lombardi, 2007). Contradictory results have also been observed regarding the effects of such pre-treatments on methanogenesis, with an inhibition observed after alkaline pre-treatment (Yuan et al., 2006) and an enhancement observed after thermal pre-treatment (S. Zhang et al., 2015). The lack of consensus on the best conditions for inoculum pre-treatment and their influence on AF processes still needs to be elucidated. To date, studies on thermal pre-treatments are mostly performed on waste-activated sludge. Their use as a selective pressure mechanism for VFA production remains scarce.

Variations in the initial pH can positively influence VFA production (Dareioti et al., 2014). In addition, uncontrolled pH approaches can reduce AF process costs since there is no further need for chemical utilization for stabilizing pH (Sarkar et al., 2021).

Headspace gas composition and pressure play a role in product formation and metabolic pathways preferentially used. However, most studies still focus on hydrogen production (Darvekar et al., 2019). According to Zhou (2018) and Sarkar (2017), low hydrogen pressure favors VFA formation. Finally, the F/M ratio, which is inoculum and substrate-dependent, is a parameter that impacts acidogenesis, with lower F/M ratios being beneficial to VFAs production (Pang et al., 2019; Shah et al., 2015).

In this work, we aimed at (*i*) identifying how abiotic factors (i.e., pH, inoculum pre-treatment, headspace pressure, and F/M ratio) influence the products spectra of cheese whey via AF, (*ii*) validating thermal pre-treatment efficiency for halting methanogenesis, and (*iii*) identifying the parameters that increase acetate level of

production for other biological processes (e.g., microalgal photoorganoheterotrophic biomass production).

2 Materials and Methods

Figure 1 depicts the overall methodology, involving experiments performed at the University of Campinas (UNICAMP, Brazil) and reproduced at Delft University of Technology (TU Delft, The Netherlands). Substrate and inoculum preparation and inoculum pre-treatment are common to all experiments apart from a few modifications described hereafter.

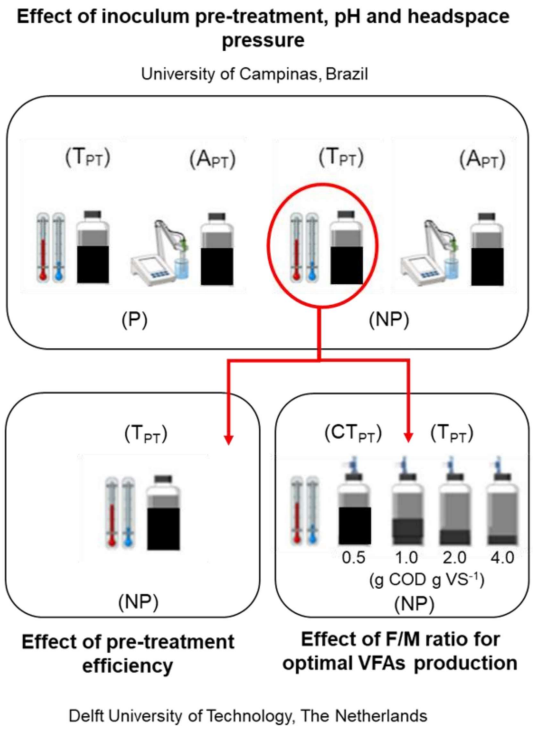


Figure 1 Overall experiment methodology. The inoculum went through alkaline (A_{PT}) and thermal (T_{PT}) pre-treatments. The initial pH at the start of the digestions was set at 7.0 and 9.0 and headspace assays were carried out in pressurized (P) and non-pressurized (NP) batches. Analyses encompassed gas and VFA profiles, total organic carbon (TOC), total nitrogen (TN), COD, solid series, carbohydrates, and amplicon sequencing (16S rRNA gene).

2.1 Demineralized cheese whey media

The chosen carbon source for all experiments consisted of 40% demineralized whey powder (WPC40), which was the closest substrate to raw cheese whey. The substrate medium for experiments held at UNICAMP was composed of (per L): WPC40 (Pic-Nic, Brazil) (4 g) (Mockaitis et al., 2006) and the following reagents: $NaHCO_3$ (1 g), NaCl (250 µg), $MgCl_2.6H_2O$ (7 µg) and $CaCl_2 \cdot 2H_2O$ (9.5 µg) (Torres, 1992). The medium was prepared fresh before experiments and its initial pH was approximately 7.0. No pH corrections were made after medium preparation. The sludge used as inoculum was obtained from a UASB reactor in Brazil (25°05'10.1" S 47°58'49.7" W). The National System for the Management of Genetic Heritage and Associated Traditional Knowledge (SisGen) register number is AE43468.

For the experiments held at TU Delft, the medium was composed of (per L): WPC40 (Subo International, The Netherlands) (4 g) amended with 0.3 mL of a micronutrients solution per g of substrate COD. The micronutrients solution was composed of $FeCl_3 \cdot 6H_2O$ (2 g L^{-1}), $CoCl_2 \cdot 6H_2O$ (2 g L^{-1}), $MnCl_2 \cdot 4H_2O$ (0.5 g L^{-1}), $CuCl_2 \cdot 2H_2O$ (32 mg L^{-1}), $ZnCl_2$ (50 mg L^{-1}), HBO3 (50 mg L^{-1}), $(NH_4)6Mo_7O_2 \cdot 4H_2O$ (90 mg L^{-1}), $Na_2SeO_3 \cdot 5H_20$ (100 mg L^{-1}), $NiCl_2 \cdot 6H_2O$ (6 mg L^{-1}), EDTA (1 g L^{-1}), HCl 36% (1 mL L^{-1}), Resazurine (0.5 g L^{-1}) and yeast extract (2 g L^{-1}). Sludge used as inoculum was obtained from an anaerobic digester at WWTP Harnashpolder in The Netherlands (52°00'48.8"N 4°19'02.5" E). It is valid to notice that 1 g L^{-1} of WPC40 corresponds to 1 g O_2 L^{-1} in COD terms.

2.2 Mechanical homogenization, thermal and alkaline pre-treatments of inocula

The anaerobic granular sludge used as inoculum at UNICAMP was mechanically disaggregated, consequently increasing their superficial area. The anaerobic granular sludge used as inoculum in TU Delft was used as is.

Thermal pre-treatment, which was performed both at UNICAMP and TU Delft, was adapted from Mockaitis et al. (2020). Briefly, the sludge was heated at 90°C in a water bath for 20 minutes under constant stirring. Heating was then halted by decreasing the sludge temperature to 23°C in an ice bath.

Alkaline pre-treatment consisted in increasing the sludge pH up to 8.0 using 1 M NaOH under continuous mixing, and controlling it for the next 6 hours, with a correction to 8.0 if needed. This pre-treatment was only performed at UNICAMP.

2.3 Effect of thermal and alkaline pre-treatments of inocula, initial batch pH, and headspace pressure on acidogenic fermentation

Batch experiments were conducted at UNICAMP. They assessed the effects of three factors evaluated at two levels in WPC40 acidogenic fermentation, namely: (*i*) inoculum pre-treatment (alkaline (A_{PT}) and thermal (T_{PT})) to enhance sludge biodegradability and select for alkaline-tolerant acetoclastic microorganisms, and to inactivate methanogenic microorganisms, respectively; (*ii*) variation in the initial pH of digestion process (7.0 and 9.0) to further select microorganisms adaptable to neutral and alkaline pH environments, and (*iii*) gas headspace pressure (pressurized (P) and non-pressurized (NP)) to investigate the influence on AF products spectra. **Table 1** shows the two-level factorial experimental design with 3 factors (2^3 designs) applied to this setup.

Experiments (**Figure 1**) were performed in 1 L Duran flasks (total volume of 1,130 mL) with an initial working volume of 730 mL and an initial headspace volume of 398 mL. Bottles were inoculated at a concentration of 6.6 g total volatile solids (TVS) L^{-1}, as depicted in Mockaitis et al. (2020). Batch reactors were continuously agitated at 50 rpm (Orbital Incubator Marconi – MA420) at a mesophilic temperature of 35°C for 30 days.

Table 1 The 23 experimental designs for phase one. The (±1) values indicate the upper and lower levels of the investigated factors. The design aimed at testing the main

effects (referred to as a, b, and c), the 2-factor interaction effects (ab, ac, and bc), and the 3- factors interaction effect (abc). Two control experiments were included.

Experiment	Factors		
	Pre-treatment (binomial)	**pH (continuous)**	**Headspace (continuous)**
A7P (*ac*)	Alkaline (+1)	7.0 (-1)	P (+1)
A9P (*abc*)	Alkaline (+1)	9.0 (+1)	P (+1)
A7NP (*a*)	Alkaline (+1)	7.0 (-1)	NP (-1)
A9NP (*ab*)	Alkaline (+1)	9.0 (+1)	NP (-1)
T7P (*c*)	Thermal (-1)	7.0 (-1)	P (+1)
T9P (*bc*)	Thermal (-1)	9.0 (+1)	P (+1)
T7NP (*1*)	Thermal (-1)	7.0 (-1)	NP (-1)
T9NP (*b*)	Thermal (-1)	9.0 (+1)	NP (-1)
Control (*P*)*	_____	8.25	P (+1)
Control (*NP*)*	_____	8.25	NP (-1)

2.3.1 Batches headspace pressure assays

The influence of headspace pressure (pressurized and non-pressurized batches) on VFAs production was investigated according to Peixoto et al., (2011). Manometric pressure was measured, then, 3 mL samples of gas were collected with a syringe containing a pressure lock (Thermo Fisher). Each sample corresponded to a batch condition.

In pressurized headspace assays, butyl rubber stoppers of each flask were covered with silicone sealant after manometric measurement and gas sample collection, allowing gas accumulation in the batch headspace.

In non-pressurized experiments, the headspace of each flask was punctured with a needle after pressure manometric reading and gas sampling, allowing the remaining gas to be released until reaching the atmospheric pressure value. After this step, butyl rubber stoppers were also covered with silicone sealant avoiding any gas release into the atmosphere.

Once collected, gas samples were analyzed with a gas chromatograph (GC) equipped with a thermal conductivity detector GC-TCD (Construmac, Brazil) with hydrogen as a carrier gas.

The volumetric production of biogas and its constituents were inferred through **equation 1** as a punctual function from sampling timestep t_0 = 0 to t for non-pressurized assays.

$$\Gamma_n = \frac{T^{STP}}{T \cdot P_{STP}} \cdot \sum_{i=1}^{n} V_{i-1}^{H} \left(P_i \cdot {}^{A}x_i - P_{atm} \cdot {}^{A}x_{i-1} \right) \quad \text{(Eq. 1)}$$

Where Γ_n is the volumetric production of a gas of interest (N_2, H_2, CH_4 or CO_2) in standard temperature and pressure (STP) equivalents (L), at a given time n; P_i is the measured pressure at sampling time (atm); V_{i-1}^{H} is the headspace volume before sampling (L); T is system's temperature (K), T^{STP} is the standard temperature (273 K), P^{STP} is standard pressure (1 atm), ${}^{A}x_i$ is the molar fraction of the gas of interest at sampling time and ${}^{A}x_{i-1}$ is the molar fraction of the gas of interest before sampling.

2.3.2 VFAs measurements

VFAs, alcohols, and carbohydrates were quantified by high-performance liquid chromatography (HPLC) based on Penteado et al.,(2012). The VFAs and alcohol profile consisted of the following: lactic acid, formic acid, acetic acid, propionic acid, butyric acid, iso-butyric acid, iso-valeric acid, and ethanol.

The chromatograph was equipped with two LC-20AD pumps, one DGU-20A3R degasser, a SIL-20AHT autosampler, a CTO-20A column oven, an SPD-20 UV detector with readings at 210 nm (Shimadzu, Japan), an Aminex HPX-87H 300 x 7.8 mm column (BioRad, USA), a RID-10A index refraction detector and a CBM-20A controller (Shimadzu, Japan).

Two mL of mixed liquors were centrifuged at 16,025 xg for 5 min.

Forty µL of H_2SO_4 (2M) was added to 1 mL of the supernatant to acidify the sample for ideal analyte separation. The samples were then filtered through regenerated

cellulose (RC) syringe filters (RC 0.20 µm) (GVS, Italy), and transferred to 1.5 mL pre-washed vials (H_2SO_4 at 2 mol L^{-1} to avoid any contamination) before HPLC analyses. The HPLC run time was 60 minutes per sample with a constant column oven temperature of 43°C and 0.005 M H_2SO_4 mobile phase at a flux rate of 0.5 mL min^{-1}.

2.4 Inoculum thermal pre-treatment and non-pressurized headspace efficiency

Inoculum thermal pre-treatment and non-pressurized headspace assays were reproduced to confirm the efficiency of such imposed conditions in halting methanogenesis while enhancing VFA production. Each factor was tested at one level, based on the effects identified at UNICAMP (section 2.3): inoculum thermal pre-treatment, initial pH of 9.0, and non-pressurized headspace. A batch with no inoculum pre-treatment, initial pH of 9.0, and non-pressurized headspace acted as a control. The experimental design with three factors applied to this set-up is shown in Table 2.

Similar to the first experiments conducted, the initial working volume of the 1 L Duran flasks was 750 mL with an initial headspace volume of 398 mL, for a total working volume of 1,148 mL. The inoculum concentration was identical at 6.6 g TVS L^{-1} as depicted in Mockaitis et al. (2020). Batch reactors were incubated for 10 days at a mesophilic temperature of 35°C in a Certomat® BS1 incubator (Sartorius Stedim Biotech, Germany) under continuous agitation (145 rpm). The headspace was released with the aid of Cole-Palmer stopcocks with Luer connection, a 1-way male lock (Cole-Parmer, USA). Experiments were performed in triplicate and lasted 12 days.

2.4.1 VFAs measurements

VFAs and carbohydrates were quantified by HPLC. One mL of mixed liquors was centrifuged at 5,073 x g for 5 minutes and supernatants were filtered using 0.45 µm syringe filters. Filtered samples were then transferred to 300 µL Waters total recovery vials, from which 10 µL were injected with a 2707 Waters HPLC autosampler at 15°C The chromatograph was equipped with a Waters M515 HPLC (Waters, USA) pump, a Waters 2414 refractive index (RI) detector, with 1,024 of sensitivity and a Waters 2489

UV/Visible detector at 210 nm. The column was a BioRad HPX-87H (300 x 7.8 mm) with a BioRad Cation-H refill cartridge (30 x 4.6 mm) guard column (BioRad, USA) and the column oven was built in-house. The flow rate of the pump was 0.6 mL min^{-1} and the temperature of the column was set at 59°C. The RI detector was operated at 30 °C. The mobile phase was 1.5 mmol L^{-1} phosphoric acid diluted in ultrapure water (MilliQ, Merck Millipore). The VFAs measured were acetic acid, butyric acid, formic acid, caproic acid, propionic acid, valeric acid, iso-butyric acid, iso-caproic acid, and iso-valeric acid.

2.5 Ideal F/M ratio for optimal VFAs production with thermally pre-treated inocula

The F/M ratio is a measurement used to determine the amount of substrate needed for the number of microorganisms present in a system. It is an important parameter to evaluate in an approach aiming at maximizing VFA production. To determine the best FM ratio for VFA production when working with a thermal pre-treated sludge at non-pressurized headspace, four different F/M ratios were tested: 0.5, 1.0, 2.0, and 4.0 $g_{COD}\ g_{VS}^{-1}$. These ratios were obtained by dividing the COD of the substrate by the VS of the sludge. The initial pH of all experiments was 9.0. In section 2.4, both control and thermal batches presented an F/M ratio of 0.5 $g_{COD}\ g_{VS}^{-1}$. $g_{COD}\ g_{VS}^{-1}$ acted as a control. Assays were conducted in duplicates for 14 days. The experimental design is depicted in **Table 2**.

Table 2 Experimental design for the F/M ratio experiments. All experiments were done in duplicate.

Experiment	Factors		
	Pre-treatment	F/M ratio (continuous)	Headspace (continuous)
FM0.5	Thermal	0.5	NP
FM0.5	Thermal	0.5	NP
FM1.0	Thermal	1.0	NP
FM1.0	Thermal	1.0	NP
FM2.0	Thermal	2.0	NP
FM2.0	Thermal	2.0	NP
FM4.0	Thermal	4.0	NP
FM4.0	Thermal	4.0	NP

2.5.1 Biogas measurements

The presence of CH_4 in the gas was detected by injecting 10 mL samples of gas from the headspace of the bottles in a GC (Agilenttech 7890 A, Agilent Technologies Inc., USA) equipped with an HP-PLOT Moleseive GC column (Agilent 19095P-MS6, Agilent Technologies Inc., USA) of 60 m x 0.53 mm x 200 µm and a thermal conductivity detector (TCD). The carrier gas was helium (14.8 psi, 23 mL min^{-1}) and the operating temperature was 200 ºC.

2.6 Physicochemical analyses

Mixed liquors and gas phases of the experimental flasks were sampled for physicochemical analyses in both original and replicated experiments. For the experiments held at UNICAMP, every 15 days, 150 mL of mixed liquors were collected and used in the following analyses and respective code methods: solid series (2540 B-F; 50 mL), COD (5220 B; 1 mL), sulfate (4500-SO_4^{2-} E; 1 mL), sulfide (4500-S^2 D, 1 mL), total organic carbon (5310-TOC; 15 mL) (APHA, 2005) and total nitrogen (TN, ASTM D8083; 15 mL) (ASTM International, 2016). Additional analyses were performed

consisting of pH measurements (4500 H) (Federation 2005), headspace assays (CH_4, N_2, and CO_2, 3 mL of gas phase), HPLC (2 mL) for VFAs, sugars and alcohols characterization, total carbohydrates measurements (Dubois et al., 1956) (1 mL), total alkalinity and VFAs measurements (Dilallo & Albertison, 1961; Ripley, L.E., Boyle, W.C. and Converse, 1986) (60 mL). The remainder sludge was discharged. On alternate days, these analyses were also performed.

For the replicated experiments performed at TU Delft, 100 mL of mixed liquors were collected on the first and last days of the process and were used in the following analyses in the same volume as mentioned above: solid series, COD, and TOC/TN. Other analyses were also performed, consisting of pH measurements, biogas composition determination, HPLC for VFAs and sugars characterization, and total carbohydrates measurements. In addition, on alternate days 12 mL of mixed liquors were sampled for pH, HPLC, COD, TOC, and TN measurements.

2.7 16S rRNA gene amplicon sequencing

2.7.1 Sequencing experiments

Microbial community analyses were performed through 16S rRNA gene amplicon sequencing on (*i*) the initial and final samples from inoculum thermal pre-treatment efficiency assays and (*ii*) the final samples of each F/M ratio experiment.

0.5 mL samples of mixed liquors were collected from each condition in 1.5 mL Eppendorf tubes completed with demineralized water for initial washing. Samples were centrifuged at 10,000 x g, 4 ºC for 3 minutes, and the supernatant was discarded. DNA was extracted using the Qiagen DNeasy® UltraClean® Microbial Kit (Qiagen, Germany) according to the manufacturer's instructions. The quality and concentrations of the DNA extracts were assessed using a Qubit fluorometer and the Qubit dsDNA HS assay kit (Thermo Fischer Scientific, USA) according to the manufacturer's instructions.

For each sample, a minimum of 20 µL of DNA extracts with concentrations ranging from 13.9 and 95 ng μL^{-1} were sent to Novogene (Beijing, China) for 16S rRNA gene amplicon sequencing. All sequencing experiments (i.e. 16S rRNA sequence amplifications, libraries preparations, and sequencing runs) were performed at

Novogene, according to their protocols. The targeted hypervariable regions V3-V4 of the 16S rRNA gene were amplified by PCR with the pair of barcoded primers 341F (CCTAYGGGRBGCASCAG) and 806R (GGACTACNNGGGTATCTAAT) (Yu et al., 2005). This set of primers is known to cover both bacteria and archaea with high specificity, except for *Planctomycetes* (Weissbrodt et al., 2020).

2.7.2 Sequences analyses

All sequencing data received from Novogene were analyzed using AmpliconTagger (Tremblay, 2019). Briefly, raw reads were scanned for sequencing adapters and PhiX spikes in sequences. The remaining paired-end reads were processed to remove primer sequences (pTrimmer v1.3.3 – (X. Zhang et al., 2019) and discard reads having average quality Phred score lower than 20. The remaining sequences were processed for generating Amplicon Sequence Variants (ASVs) (DADA2 v1.12.1) (Callahan 2016) using the following key parameters: filterAndTrim (maxEE =2; truncQ = 0; maxN = 0; minQ = 0) and learnErrors (nbases=1e8) functions for both forward and reverse filtered reads. Reads were then merged using the mergePairs (minOverlap = 10; maxMismatch = 0) function. Chimeras were removed with DADA2's internal removeBimeraDeNovo (method = 'consensus') method followed by UCHIME reference (Rognes et al., 2016). ASVs were assigned a taxonomic lineage with the RDP classifier (Q. Wang et al., 2007) using training sets containing the complete Silva release 138 database (Quast et al., 2013) supplemented with a customized set of mitochondria and plastid sequences. The RDP classifier gave a score of (0 to 1) to each taxonomic depth of each ASV. Any taxonomic depth having a score of ≥ 0.5 was kept reconstructing the final lineage. Taxonomic lineages were combined with the cluster abundance matrix obtained above to generate a raw ASV table from which the bacterial or fungi ASV tables were generated. Five hundred 1,000 reads rarefactions were then performed on these ASV tables and the average number of reads of each ASV of each sample was computed to obtain consensus rarefied ASV tables. Alpha diversity metrics (RTK v 0.93.2 – ((Saary et al., 2017) and taxonomic summaries microbiomeutils v 0.9.3 – (Tremblay, 2020)) were then computed using the consensus rarefied ASV tables. Figures were generated in R using the ggplot2 package.

3 Results and Discussion

3.1 Effects of inoculum thermal and alkaline pre-treatments and initial pH on the anaerobic digestion process

3.1.1 Inoculum thermal pre-treatment efficiently halted methanogenesis

As demonstrated in **Figure 2**, inoculum thermal pre-treatment successfully inhibited methanogenesis in all tested conditions (i.e., pressurized, and non-pressurized headspace assays with initial pH of 7.0 and 9.0).

Inoculum alkaline pre-treatment halted methanogenesis in both pressurized and non-pressurized assays but only with initial pH of 7.0, presenting negligible to no levels of total methane production of 0.0 and 0.54 mL, respectively. Initial pH 9.0 presented a total methane production of about 52.29 mL for pressurized assays and 0.67 mL for non-pressurized ones.

As a strategy to maximize VFA production, inoculum thermal pre-treatment appears to be the best selective pressure for impairing methanogens in batch processes. It is of utmost importance to confirm whether this selective pressure is also successful to halt methanogenesis considering different types of inoculum (e.g., waste-activated sludge and secondary sludge), reactors (e.g., sequence-batch reactors, and continuous-stirred tank reactors) and configurations (e.g., organic loading rate, hydraulic retention time, coupled reactors). If so, then inoculum thermal pre-treatment can be implemented in full-scale AF processes, decreasing their overall costs (Corti & Lombardi, 2007).

Some studies have used alkaline pre-treatment of inoculum to increase the biodegradability of waste-activated sludge (Wonglertarak & Wichitsathian, 2014), and to stabilize the sludge originated from aerobic processes while treating the mineralization of its remaining organic compounds (Navia & Vidal, 2002). Sludge alkaline pre-treatment increased the COD: COD_{Total} ratio (Navia & Vidal, 2002) VS while improving volatile solids (VS) reduction (Appels et al., 2011; J.-G. Lin et al., 1997). Hence, their methane production would also increase.

Noteworthily, the methane production levels observed in our experiments over 30 days (i.e., A_{PT}7NP, 0.54 mL; A_{PT}7P, 0.00 mL; A_{PT}9NP 0.67 mL, and A_{PT}9P, 52.29 mL),

did not agree with the findings of Wonglertarak and Wichitsathian (2014). Their methane production was about 2, 526.60 mL in a thermophilic reactor with alkaline pre-treated sludge and 2,173.8 mL in a mesophilic reactor with alkaline pre-treated sludge. Our findings also contradicted the ones found by Lin et al. (1997) which was an average CH_4 production rate of 222.25 L m^3 d^{-1}.

This could be explained using different methodologies in each work such as maintaining the reactor with a constant alkaline pH after treating the sludge, different reactors configurations (e.g., single-stage high-rate reactor and continuous stirred tank reactor and batch reactor), hydraulic retention times, organic loading rates as well as the type of inoculum used (i.e., WAS and UASB granular sludge).

For instance, we used 1 M NaOH to treat the inoculum, correcting the pH to 8.0 hourly for 6 hours. However, after pre-treating the inoculum, batch reactors were assembled with initial pH of 7.0 and 9.0, with the final pH from both pressurized and non-pressurized headspaces, ranging from 4.9 and 5.1, respectively. Lin et al. (1997), treated secondary sludge with NaOH ranging from 0.02 to 0.2 M, which pH increased from 7.21 to 13.2 in 24 h hydrolysis and 0.2 M NaOH. Alternatively, Wonglertarak and Wichitsathian's (2014) alkaline inoculum pre-treatment consisted of treating waste-activated sludge with pH varying from 8.0 to14.0 and varying NaOH concentration from 8 to 31,000 g m^{-3} wet sludge.

Another result of interest regarding inoculum alkaline pre-treatment was the correlation between acetate and methane production. While there was no methane production in inoculum alkaline treatment with initial pH 7.0 in both non-pressurized and pressurized headspace batches, acetate production differed 185.6% from non-pressurized headspace assay to pressurized headspace (i.e., A_{PT}7NP 1,056.04 mg COD_{AcOH} L^{-1} and A_{PT}7P 369.82 mg COD_{AcOH} L^{-1}). So, headspace pressure can favor acetate production in acetoclastic methanogens.

The detected levels of CO_2 in both A_{PT}7NP and A_{PT}7P (i.e., 1.84 mL and 60.78 mL, respectively) were low as was the average of the final pH for both conditions (i.e., 4.8). Hence, instead of methanogenesis being inhibited due to disturbance in the buffer system (Casallas-Ojeda et al., 2020), we can infer that most CO_2 was dissolved in the liquid phase, decreasing the pH (Deublein & Steinhauser, 2011). **Figure 2** shows the

methane and carbon dioxide production in alkaline and thermal batches with both pressurized and non-pressurized headspaces.

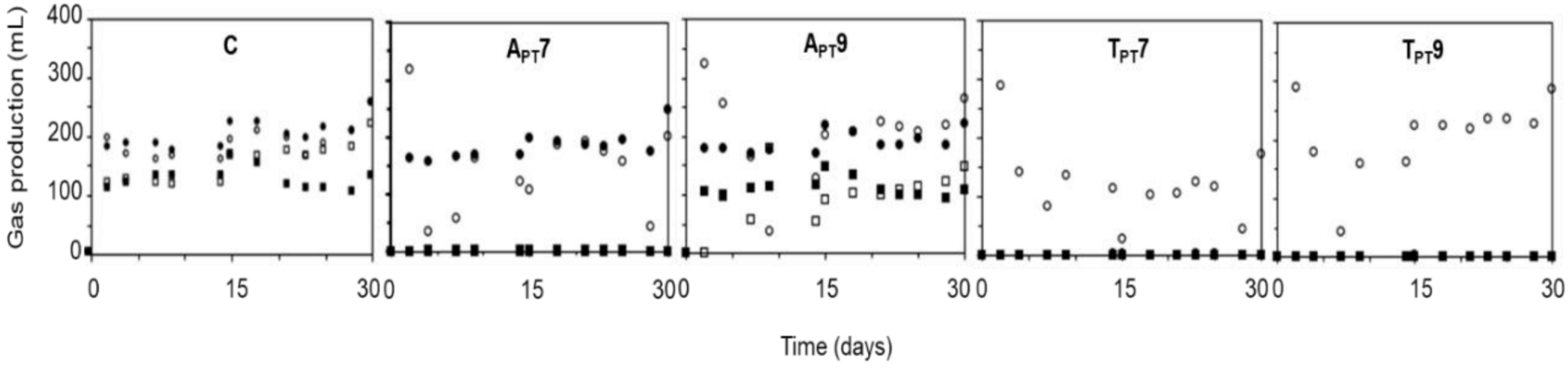
3.1.2 Initial pH, headspace pressure, and inoculum pre-treatments influenced VFAs product spectra.

Cheese whey has a natural tendency to acidify and since pH was not controlled during the experiments (pressurized and non-pressurized batches displayed an average pH of 4.96 and 5.26, respectively), likely, hydrolysis was not a limiting step in the AF process.

An additional hypothesis to justify the different production of VFAs and alcohol in all batches was that together with uncontrolled pH, the headspace internal pressure variation from pressurized and non-pressurized batches played a key role in the spectra and quantity of VFAs produced. In pressurized batches, the pressure would contribute to the gas phase being accumulated within the liquid phase, which influenced both gas and VFA spectra. In non-pressurized batches, due to headspace release, gas and VFAs production restarted daily, after each sampling.

Overall, non-pressurized batches produced more VFAs than pressurized ones. Special highlights can be given to $A_{PT}9$ NP (21,360.54 mg $COD_{compound}$ L^{-1}), $T_{PT}9$ NP (4,108.71 mg $COD_{compound}$ L^{-1}), and $T_{PT}7$ NP (3,414.15 mg $COD_{compound}$ L^{-1}) when compared to their counterparts ($A_{PT}9$ P 1,940.14 mg $COD_{compound}$ L^{-1}, $T_{PT}9$ P 2,151.99 mg $COD_{compound}$ L^{-1} and $T_{PT}7$ P 2,140.62 mg $COD_{compound}$ L^{-1}). Both pressurized and non-pressurized controls and $A_{PT}7$ did not present a substantial difference with an increase of approximately 2.9% in VFAs produced in non-pressurized batches compared to pressurized batches as seen in Table 3.

Figure 2 Methane and carbon dioxide gas production profiles for control (C), inoculum alkaline (A_{PT}), and thermal (T_{PT}) pre-treatment with initial pH of 7.0 and 9.0 during 30 days. Non-pressurized (NP) and Pressurized (P) headspace assays are also represented. In the figure: ■ CH_4NP, □ CH_4P, ● CO_2NP and ○ CO_2P



It is important to stress that although $A_{PT}9$ NP, $T_{PT}9$ NP, and $T_{PT}7$ NP produced greater quantities of metabolites, they did not produce a great variety of VFAs and alcohol. $A_{PT}9$ NP produced 7,677.30 mg COD_{IBA} L^{-1} of iso-butyric acid and 13,683.24 mg COD_{EtOH} L^{-1} of ethanol. These metabolites' production together with the absence of acetic acid production is a clear result of a metabolic shift that was favored due to the imposed selective pressures in this batch (i.e., alkaline inoculum pre-treatment, initial pH of 9.0, and non-pressurized headspace).

This was in opposition to all other conditions tested. It is likely that in such operational conditions, acetate served as the substrate for fermentative bacteria to form iso-butyric acid and ethanol, as already described by Thatikayala et al. (2021) and Liu et al. (2022). Both chemicals are of great industrial interest (i.e., pharmaceutical, feed, chemical, biofuels). Optimization of AF processes towards the production of either ethanol or iso-butyric acid or both can be an additional approach for cheese whey valorization.

$T_{PT}9$ NP and $T_{PT}7$ NP displayed a production of acetic acid of 1,479.13 and 1,558.17 mg COD_{AcOH} L^{-1}, respectively. As shown in Figure 2, there was no production of methane. Acetic acid was consumed in $A_{PT}9$NP, whereas in $A_{PT}7$NP its production was slightly lower than both $T_{PT}9$ NP and $T_{PT}7$ NP with 1,056.04 mg COD_{AcOH} L^{-1}.

Interestingly, CNP also presented a higher acetic acid production of 1,109.13 mg COD_{AcOH} L^{-1}, which shows that headspace pressure is a more suitable selective pressure parameter than inoculum pre-treatment for acetic acid production. The produced acetic acid can thus be utilized as an organic carbon source for higher added-value biological processes (i.e., microalgal photoorganoheterotrophic biomass production).

The imposed parameters (*i.e.*, inoculum pre-treatments, initial pH, and headspace pressure) also acted as selective pressures in the batch experiments modifying the microbial fermentation end-products. In general, thermal pre-treatment, non-pressurized headspace, and initial pH 9.0 displayed a trend for higher VFA production. Nevertheless, it is not possible to affirm what the best combination of parameters would be since there was not a pattern of production observed for all VFAs in this given setup.

However, the combination of parameters can be suitable for the production of specific volatile acids or ethanol, as seen in T_{PT}7NP and T_{PT}9NP for the production of acetic (1,479.13 and 1,558.17 mg COD_{AcOH} L^{-1}, respectively) and butyric acids (1,207.46 and 1,425.36 mg COD_{BTA} L^{-1}), and A_{PT}9NP for iso-butyric acid and ethanol (7,677.30 mg COD_{IBA} L^{-1} and 13,683.24 mg COD_{EtOH} L^{-1}).

Non-pressurized batches presented a global production of 3 times more VFAs than pressurized batches. Besides common VFAs, pressurized headspace batches produced formic and lactic acids but in negligible quantities as shown in **Table 3**.

Table 3 VFAs and alcohols product spectra of pressurized (P) and non-pressurized (NP) headspace batches with alkaline (A_{PT}) and thermal (T_{PT}) pre-treatments and initial pH of 7.0 and 9.0. Experiments lasted for 30 days.

		Batch operational conditions (mg COD compound L^{-1})									
	Time	Control		$A_{PT}7$		$A_{PT}9$		$T_{PT}7$		$T_{PT}9$	
		P	NP	P	NP	P	NP	P	NP	P	NP
Acetic acid	t0	53.88	154.34	97.50	0.00	0.00	180.11	183.94	314.61	154.56	308.26
	tf	267.62	1,109.13	369.82	1,056.04	280.22	0.00	377.39	1,479.13	417.91	1,558.17
Butyric acid	t0	0.00	0.00	0.00	0.00	0.00	0.00	0.00	0.00	0.00	0.00
	tf	929.83	317.63	662.53	177.73	773.31	0.00	881.05	1,207.46	821.59	1,425.36
Iso-butyric acid	t0	0.00	0.00	0.00	0.00	0.00	0.00	536.00	10.84	537.85	0.00
	tf	108.02	0.00	7.47	113.92	78.36	7,677.30	57.69	29.77	182.37	85.14
Ethanol	t0	0.00	0.00	0.00	0.00	0.00	0.00	0.00	0.00	0.00	0.00
	tf	494.93	0.00	489.74	0.00	598.57	13,683.24	621.32	302.99	479.02	303.51
Formic acid	t0	0.00	0.00	0.00	0.00	0.00	0.00	0.00	0.00	0.00	0.00
	tf	0.33	0.00	0.50	0.00	0.46	0.00	0.52	0.00	0.44	0.00
Lactic acid	t0	0.00	0.00	0.00	0.00	94.07	0.00	37.61	1,524.34	38.72	1,137.60
	tf	0.50	0.00	0.42	0.00	0.00	0.00	0.22	0.00	0.00	0.00
Propionic acid	t0	0.00	0.00	0.00	0.00	0.00	0.00	0.00	0.00	0.00	0.00
	tf	69.37	189.39	34.78	130.51	65.84	0.00	15.53	91.24	20.04	111.16
Valeric acid	t0	0.00	0.00	0.00	0.00	0.00	0.00	0.00	0.00	0.00	0.00
	tf	0.00	0.00	0.00	0.00	0.00	0.00	44.12	0.00	47.95	0.00
Iso-valeric acid	t0	0.00	0.00	0.00	0.00	0.00	0.00	270.08	0.00	260.84	0.00
	tf	45.40	194.40	45.39	179.11	143.39	0.00	142.77	303.56	182.67	625.38

Initial WPC40 carbohydrate concentration was approximately 260 mg glucose L^{-1}, stabilizing at 65mg glucose L^{-1} on the fourth day. The acidogenesis rate of 1.9 d^{-1}, was close to the typical rate of 2 d^{-1} observed in similar studies(van Lier et al., 2008). COD removal and volatile solids (VS) showed similar patterns, with sCOD decreasing from 4.2 to 2.4 g L^{-1} and VS decreasing from 4.92 to 4.74 g L^{-1}. This was likely due to biomass production and organic matter oxidation. Control batches showed a decrease from 4.92 to 4.74 g L^{-1}, corroborating with COD removal results. Cheese whey alkalinity varied by 6% in all batches (1.53 to 1.45 $CaCO_3$ L^{-1}). Acidification of whey might thus have led to the production of VFAs, as seen in both control and thermal pre-treatment pH 9.0. **Table 4** shows the results of the main physicochemical analyses.

3.1.3 Inoculum thermal pre-treatment, initial pH, and non-pressurized headspace acted as selective pressure mechanisms on microbial communities during cheese whey acidogenic fermentation

In the replicate experiment performed in TU Delft, both control and inoculum thermal pre-treated microbial communities' composition and evolution were determined through 16S rRNA gene amplicon sequencing (**Figures 3** and **4**). Initial microbial communities were highly similar, with few quantitative and only minor qualitative differences being observed. They both shared 7 of their 8 main detected phyla, 10 of their 11 main detected classes, and 18 of their 19 main detected orders, as well as their 10 and 5 most important detected families and genera, respectively

As shown in **Figures 3** and **4**, the common genera included fermenters and VFAs producers (such as *Sedimentibacter* (X.-Q. Lin et al., 2019), *Longilinea*, *Leptolinea* (Dai et al., 2016), and *Christensenellaceae* R-7 group (Y. Gao et al., 2022), the lipid-accumulating and bulk and foaming *Candidatus Microthrix* (Sheik et al., 2016), microorganisms involved in sulfur and nitrogen metabolisms (*Magnetovibrio* (Bazylinski et al., 2013), *Sulfurovum* and *Sulfurimonas* (Y. Li et al., 2018), as well as the acetoclastic methanogen *Methanosaeta* (Stams et al., 2019).

Table 4 Initial and final results of the main physicochemical analyses performed in the AF experiment for 30 days. Batches consisted of control, alkaline, and thermal pre-treatments with initial pH 7.0 and 9.0 ($A_{PT}7$, $A_{PT}9$, $T_{PT}7$, and $T_{PT}9$) with pressurized (P) and non-pressurized (NP) headspaces. Analyses considered are chemical oxygen demand (COD), total organic carbon (TOC), total nitrogen (TN), total solids (TS), total volatile solids (TVS), and pH.

		Batch operational conditions									
Analyzes (mg L^{-1}) * × •	Time	Control		$A_{PT}7$		$A_{PT}9$		$T_{PT}7$		$T_{PT}9$	
		P	NP	P	NP	P	NP	P	NP	P	NP
CH4•	t0	0.00	0.00	0.00	0.00	0.00	0.00	0.00	0.00	0.00	0.00
	tf	11,086.37	5.69	0.00	0.54	52.29	0.67	0.00	0.00	0.00	0.00
COD*	t0	8,368.63	8,634.33	7,336.90	11,174.50	8,583.00	15,294.50	9,325.30	8,758.00	10,000.00	9,736.00
	tf	7,391.10	11,053.99	7,694.78	10,658.81	7,610.05	10,584.72	8,859.74	14,289.56	8,779.31	13,844.98
TOC	t0	2,005.67	1,695.33	3,280.00	1,326.00	2,890.00	1,636.00	3,467.00	2,230.00	3,691.00	2,237.00
	tf	2,284.00	1,181.00	2,229.00	1,213.00	2,385.00	1,176.00	3,133.00	1,842.00	3,266.00	1,784.00
TN	t0	333.40	617.99	309.80	69.25	306.50	100.30	468.30	219.20	463.50	216.10
	tf	279.33	174.97	268.20	157.40	403.60	136.80	544.90	317.60	484.10	284.20
C: N ratio	t0	6.02:1	2.7:1	10.59:1	19.15:1	9.43:1	16.31:1	7.40:1	10.17:1	7.96:1	10.35:1
	tf	8.18:1	6.75:1	8.31:1	7.71:1	5.91:1	8.60:1	5.75:1	5.80:1	6.75:1	6.28:1
TS	t0	0.00516	5.72	0.00478	6.69	0.00539	6.71	0.00729	7.68	0.00698	8.52
	tf	0.00323	5.50	0.00344	5.08	0.00330	4.69	0.00376	6.13	0.00401	5.64
TVS	t0	0.00453	4.98	0.00421	5.87	0.00468	5.84	0.00578	6.81	0.00600	7.40
	tf	0.00264	4.66	0.00278	4.23	0.00260	3.99	0.00311	5.10	0.00324	4.58
pH	t0	8.25	8.25	7.00	7.00	9.00	9.00	7.00	7.00	9.00	9.00
	tf	4.76	5.14	4.65	4.99	5.00	5.01	4.87	5.11	5.06	5.19

The only noticeable difference consisted of *Cyanobacteria* being detected in the inoculum thermal pre-treated population (Figure 4). Cyanobacteria are aerobic photosynthetic microorganisms (Stal & Moezelaar, 1997). However, they display mechanisms that enable them to survive in unfavorable conditions such as in hypoxic or anaerobic (Y. Li et al., 2018) environments. Although chlorophyll (Chl) deficiency can be caused by low levels of oxygen, these microorganisms can regulate Chl production by activating oxygen-independent oxidases or by inducing the transcription of genes that encodes enzymes that work in microoxic conditions (Fujita et al., 2015). In the given scenario, facultative anoxygenic photosynthesis uses sulfide as the electron donor with photosystem I-driven photo assimilation (Hamilton et al., 2018).

Control and inoculum thermal pre-treated microbial communities evolved differently along the process. The final populations presented highly similar compositions at the phylum, class, order, and family levels, sharing all or almost all the main detected taxons with only quantitative differences being perceived. Noticeable qualitative and quantitative differences were however observed at the genus level (Figures 3 and 4). Figure 5 depicts the beta diversity analysis of the samples.

In the control final microbial community, an increase was observed in fermenters, such as *Longilinea* and *Leptolinea* (Dai et al., 2016), and microorganisms involved in sulfur and nitrogen metabolisms, such as *Magnetovibrio* (Bazylinski et al., 2013), *Sulfurovum* and *Sulfurimonas* (Y. Li et al., 2018). *Arcobacter* (S. Gao et al., 2022), a sulfide oxidizer and denitrifier, also appeared and became the second genus of importance, while the two VFAs producers *Sedimentibacter* (X.-Q. Lin et al., 2019) and *Christensenelaceae* R-7 group (Y. Gao et al., 2022) strongly decreased.

In opposition, in the inoculum thermal pre-treated final microbial community, an increase was observed in VFAs and alcohols producers, such as *Clostridium* (Mockaitis et al., 2022), *Fonticella* (Joshi et al., 2021), and *Intestinimonas* (Kang et al., 2021), while fermenters such as *Longilinea* and *Leptolinea* strongly decreased. The lipid-accumulating and bulk and foaming *Candidatus Microthrix* (Sheik et al., 2016) and the *Cyanobacteria Synechocystis* (Fujita et al., 2015) increased, and *Magnetovibrio* (Bazylinski et al., 2013), *Sulfurovum* and *Sulfurimonas* (Y. Li et al., 2018), involved in sulfur and nitrogen metabolisms, slightly decreased.

Those results could explain the differences in performance observed in both processes. Methanogenesis was likely halted in the inoculum thermal pre-treated assay by the strong decrease observed in microorganisms such as *Longilinea* and *Leptolinea*, which are fermenters known to provide substrates to methanogens (Yamada et al., 2006, 2007), concomitantly with the strong increase in VFAs and alcohols producers.

The decrease, even if limited, observed in *Methanosaeta* tends to confirm that methanogens were inhibited. The presence of *Methanosaeta* could be explained by several hypotheses: (*i*) samples detected were dead biomass or spores, (*ii*) inoculum pre-treatments were sufficient to inhibit or diverge the metabolic pathway for methane formation, or (*iii*) they could have been outcompeted by acetate fermenters (Callbeck et al., 2019; Miñana-Galbis et al., 2002; Nuppunen-Puputti et al., 2018; Shi et al., 2020). Further -omics studies can clarify this finding. The presence of denitrifiers could be a response to batches' oxygen limitation since they are aerobic facultative (Skiba, 2008). They can also compete for nitrate content in cheese whey (Oliveira et al., 1995).

Initial WPC40 carbohydrate concentration was approximately 260 $mg_{glucose}$ L^{-1}, stabilizing at 65$mg_{glucose}$ L^{-1} on the fourth day. The acidogenesis rate of 1.9 d^{-1}, was close to the typical rate of 2 d^{-1} observed in similar studies(van Lier et al., 2008). COD removal and volatile solids (VS) showed similar patterns, with sCOD decreasing from 4.2 to 2.4 g L^{-1} and VS decreasing from 4.92 to 4.74 g L^{-1}. This was likely due to biomass production and organic matter oxidation. Control batches showed a decrease from 4.92 to 4.74 g L^{-1}, corroborating with COD removal results. Cheese whey alkalinity varied by 6% in all batches (1.53 to 1.45 $CaCO_3$ L^{-1}). Acidification of whey might thus have led to the production of VFAs, as seen in both control and thermal pre-treatment pH 9.0.

Table 5 VFAs spectra of replicated control and thermal pre-treatment (pH 9.0) acidogenic fermentation experiment compared to the original experiment for 10 days. Replicate results are expressed as a means average of the triplicate assays. (--) The product was not evaluated.

VFAs Production (mg COD compound L^{-1})					
		UNICAMP		TU Delft	
Products	Time	C	T	C	T
Acetic acid	t0	154.34	308.26	0.00	19.28
	tf	1,037.34	1,361.07	319.13	1,407.90
Butyric acid	t0	0.00	0.00	0.00	0.00
	tf	187.29	1121.49	5.35	106.91
Iso-butyric acid	t0	0.83	0.00	16.04	149.67
	tf	0.00	0.00	16.04	58.80
Caproic acid	t0	0.00	0.00	290.94	179.70
	tf	0.00	0.00	479.20	2,587.25
Iso-caproic acid	t0	--	--	0.00	0.00
	tf	--	--	0.00	42.79
Ethanol	t0	0.00	0.00	--	--
	tf	0.00	155.07	--	--
Formic acid	t0	0.00	0.00	4.30	4.30
	tf	0.00	0.00	0	0.00
Lactic acid	t0	0.00	1,137.59	--	--
	tf	0.00	0.00	--	--
Malic acid	t0	0.00	24.74	--	--
	tf	0.00	0.00	--	--
Propionic acid	t0	0.00	0.00	11.19	11.19
	tf	161.48	55.21	85.76	55.93
Valeric acid	t0	0.00	0.00	0.00	6.94
	tf	0.00	0.00	20.83	27.78
Iso-valeric acid	t0	0.00	0.00	0.00	20.83
	tf	46.54	235.89	20.83	83.34

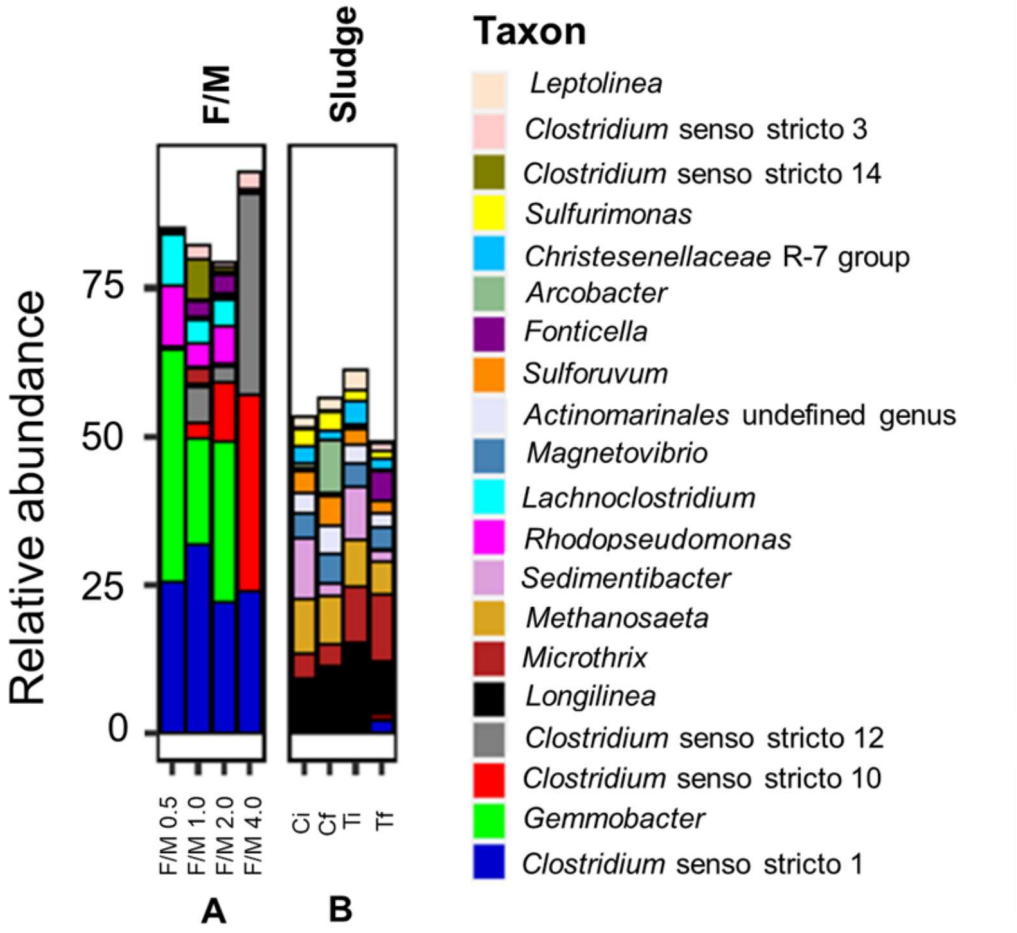


Figure 3 – Microbial communities' compositions and evolution. The 20 most abundant archaeal and bacterial genera were identified through 16S rRNA gene amplicon sequencing. A microbial population from the F/M ratios experiments (FM). B, microbial populations from the control and thermal pre-treated inoculum batches ($T_{PT}9$ NP).

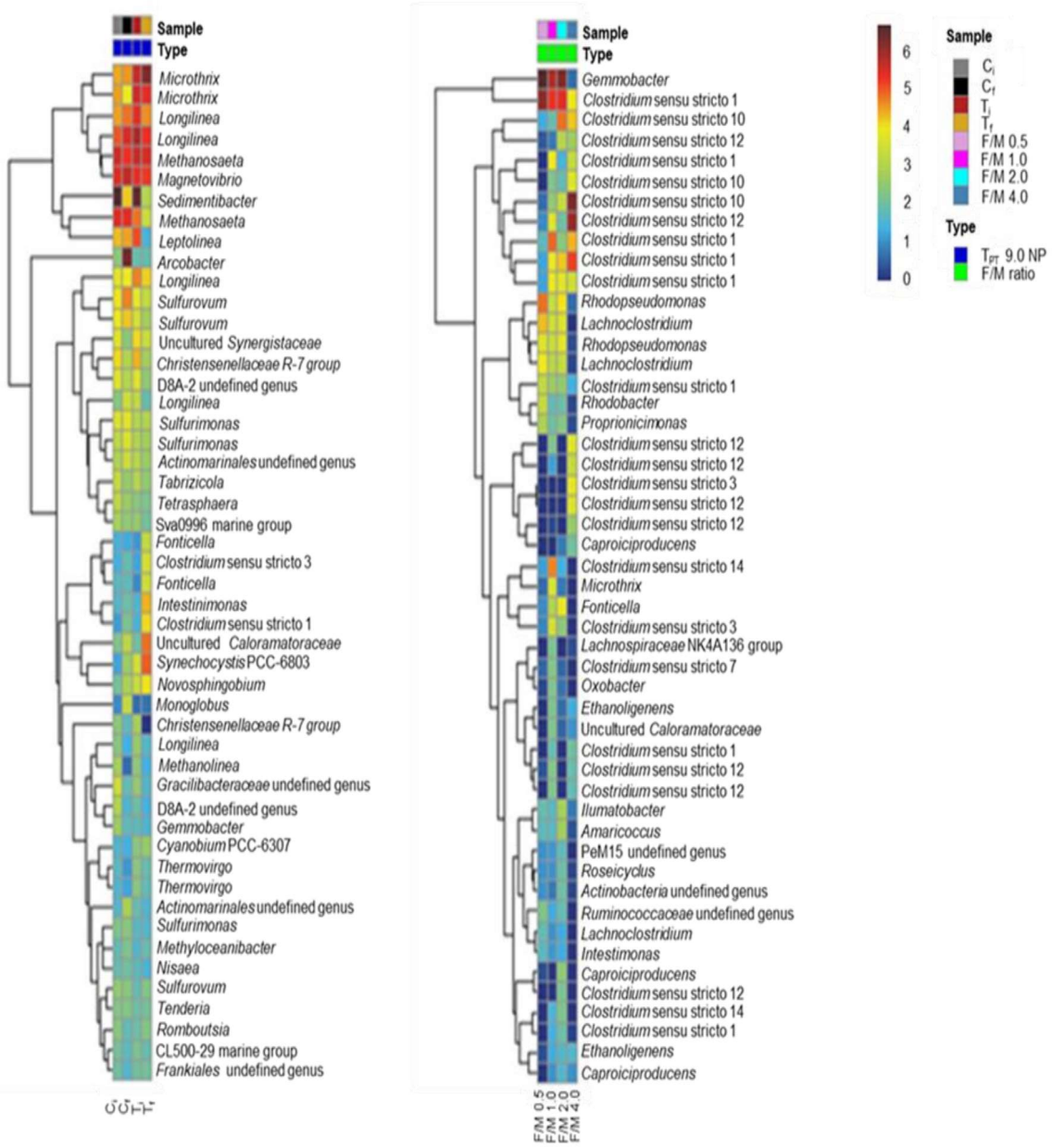


Figure 4 – ASV abundance. The 50 most abundant archaeal and bacterial ASVs detected by the AmpliconTagger pipeline. FM: F/M ratios experiments; T_{PT}NP9: thermal pre-treated inoculum batches.

3.2 Impact of F/M ratio on VFAs production during acidogenic fermentation of cheese whey

3.2.1 Lower F/M ratio is more efficient for VFAs production

Four different F/M ratios of WPC40 were evaluated in an experiment performed with a thermal pre-treated inoculum at initial pH of 9.0 and under non-pressurized conditions. Ratios were F/M 0.5, F/M 1.0, F/M 2.0, and F/M 4.0, corresponding to 0.5, 1.0, 2.0, and 4.0 g COD g VSS^{-1}, respectively.

The F/M 0.5 ratio acted as a positive control since the thermal batch in the replicate experiment presented the same F/M ratio of 0.5 g COD g VSS^{-1}. About 95% of carbohydrates were consumed by the third day, while substrate acidification started in the first couple of days F/M 0.5 (1,056 mg $COD_{compound}$ L^{-1} d^{-1}), F/M 1.0 (789 mg $COD_{compound}$ L^{-1} d^{-1}), F/M 0.2 (486 mg $COD_{compound}$ L^{-1} d^{-}1nd F/M 4.0 (390 mg $COD_{compound}$ L^{-1} d^{-1}).

As shown in **Table 6,** F/M 0.5 ratio showed the best VFA production (3,317.88 mg $COD_{compound}$ L^{-1}), whereas the F/M ratio 2.0 (345.93 mg L^{-1}) had the lowest. Non-pressurized thermal pre-treatment batch in the replicate experiment had a VFAs production of 2,568.26 mg L^{-1}. There was no production of methane in all samples which corroborates the results observed in previous experiments.

3.2.2 F/M ratios affected microbial communities' evolution

Microbial communities evolved differently during the F/M experiments. As shown in Figure 5, increasing F/M ratios significantly impacted the microbial populations' evolution, with the strongest impact observed at the highest ratio of 4.0. Under such conditions, the microbial population was ultra-dominated by a single genus, *Clostridium* (Figures 3 and 4). At lower F/M ratios, the community was mainly composed of the same four genera, which altogether represented 84.3%, 77.6%, and 74.7% of the F/M-0.5, F/M-1, and F/M-2 populations, respectively (Figure 3 and 4).

Table 6 – VFAs spectra of F/M ratios experiments. F/M 0.5, F/M 1.0, F/M 2.0, and F/M 4.0: 0.5, 1.0, 2.0, and 4.0 g COD g VSS^{-1}, respectively. F/M 0.5 acted as a positive control as it has the same 0.5 g COD g VSS^{-1} ratio as the replicated thermal pre-treatment batch in section 3.2. The experiment was performed in triplicate and lasted 10 days.

VFAs Production (mg CODcompound L^{-1})					
Products	Time	F/M 0.5	F/M 1.0	F/M 2.0	F/M 4.0
Acetic acid	t0	34.02	9.19	0.00	0.00
	tf	900.48	956.51	493.42	865.84
Butyric acid	t0	0.00	0.00	0.00	0.00
	tf	349.75	25.26	34.64	36.48
Iso-butyric acid	t0	1,707.03	78.98	60.70	25.58
	tf	43.22	38.89	19.32	12.99
Caproic acid	t0	154.28	30.42	0.00	0.00
	tf	1,823.41	1,042.24	3,620.88	194.20
Iso-caproic acid	t0	0.00	0.00	0.00	0.00
	tf	0.00	0.00	0.00	0.00
Formic acid	t0	1.85	2.21	2.89	3.33
	tf	0.00	0.00	0.30	0.00
Propionic acid	t0	5.26	0.00	0.00	0.00
	tf	66.33	34.40	7.27	23.27
Valeric acid	t0	9.79	0.00	0.00	0.00
	tf	45.21	0.00	27.19	4.90
Iso-valeric acid	t0	32.61	17.61	0.00	0.00
	tf	89.48	58.23	40.31	27.40
Total production		3,317.88	2,155.53	4,211.46	1,165.08

Those four genera were *Gemmobacter*, a poly-hydroxybutyrate-accumulating and denitrifying bacteria (S. Wang et al., 2019), *Clostridium*, a known fermenter, and VFAs producer (Mockaitis et al., 2022), *Lachnoclostridium*, a known butyrate producer (Detman et al., 2021), and *Rhodopseudomonas*, a highly metabolically versatile

bacteria capable of hydrogen production through nitrogen fixation or poly-hydroxybutyrate production (Ranaivoarisoa et al., 2019). The operational conditions applied in the F/M-0.5 experiment were thus apparently those that favor the best microbial combination to produce the highest level of VFAs. Further characterizations (i.e. metagenomics and/or metatranscriptomics analyses) have to be performed to better understand why such close microbial populations could generate different amounts of VFAs.

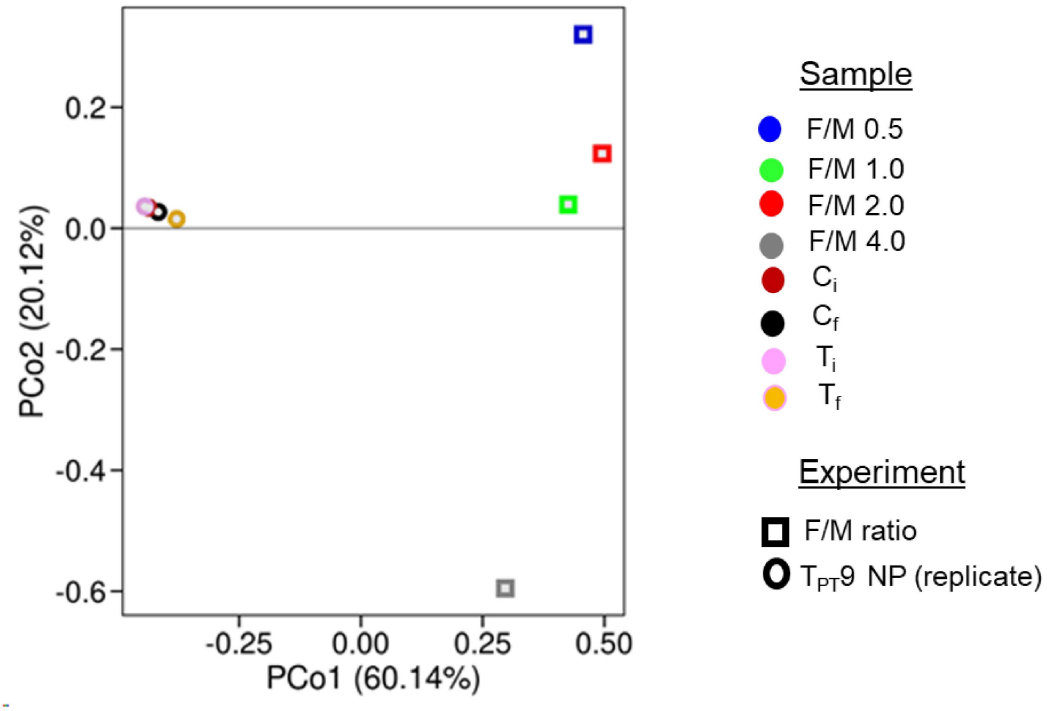


Figure 5 – Beta diversity analysis of the microbial populations. Principal Coordinates Analysis computed from Bray-Curtis dissimilarity distance matrix. FM: F/M ratios experiments; T_{PT}NP9: thermal pre-treated inoculum batches.

4 Conclusions

AF is a successful alternative for producing VFAs of economic interest out of high-strength residues such as cheese whey. Inoculum pre-treatments can play selective pressures on microbial communities, selecting microorganisms that can thrive in imposed conditions. The main conclusions from this work are the following:

1. Thermal pre-treatment of inocula was efficient to halt methanogenesis regardless of headspace pressure, pH, and F/M ratios.
2. Contrary to the literature, alkaline pre-treatment did not improve methanogenesis. However, non-pressurized headspace alkaline pre-treatment pH 9.0 did produce significant quantities of iso-butyric acid (7,677.30 mg COD_{IBA} L^{-1}) and ethanol (13,693.24 mg COD_{EtOH} L^{-1}). Further studies on the mechanisms of this pre-treatment are necessary to optimize the process.
3. *Methanosaeta* was present in the replicate of the control (pH 8.25) and thermal (pH 9.0) batches, despite the absence of methane production. Thermal pre-treatment could have either inactivated or destroyed this microorganism, which in its turn enabled the detection of *Methanosaeta* in the 16S rRNA gene amplicon sequencing analysis.
4. A low F/M ratio of 0.5 g COD g^{-1} VS selected a microbial community producing a high level of VFAs by AF.
5. The setup of parameters used as selective pressure during cheese whey AF must vary according to the desired end-product.
6. Headspace pressure directs the metabolic pathways for VFAs and alcohol production in AF. Pressurized headspace batches had a more diverse VFAs spectra, while non-pressurized batches produced higher amounts of VFAs. The exception would be iso-butyric acid and ethanol produced in non-pressurized alkaline pH 9.0 batches.
7. Another important parameter was the Initial pH of 9.0. Regardless of the headspace pressure and inoculum pre-treatment, an initial pH of 9.0 produced the greatest number of products. The drastic pH drop influences the redox

potential of the medium facilitating the uptake of compounds while setting the grounds for ecologic relationships within the microbial community.

This work aimed to verify if imposed parameters (i.e., headspace pressure, inoculum thermal and alkaline pre-treatment, and initial pH) in cheese whey AF would work as selective pressures on the inoculum microbial community. Our objectives were met when we managed to halt methanogenesis and increase acetic acid, iso-butyric acid, and ethanol. Acetate is an organic carbon source that can be used for different biological conversions (e.g., microalgal photoorganoheterotrophic processes), whereas iso-butyric and ethanol are of interest to pharmaceutical, feed, chemical, and biofuels industries.

Still, there is plenty to be understood, especially regarding the influence of these parameters on metabolic pathways and microbial interaction. The fact that thermal pre-treatment time and temperature were optimized and methanogenesis was halted, despite the presence of methanogens. Understanding the mechanism behind this can overcome competition for the substrate.

Thermal inoculum pre-treatment can be used in short fermentation processes. Nevertheless, the interaction among the factors with different substrates, inoculum, and reactor configurations must be studied to certify thermal pre-treatment efficiency. Thus, it is necessary to evaluate other configurations for process implementation and optimization.

Understanding the VFAs' production and consumption mechanisms is crucial for driving the spectrum of fermentation products to desired compounds. Future 16S rRNA metagenomics analyses will be fundamental to decreasing these knowledge gaps.

5 References

Abbasi, T., Tauseef, S. M., & Abbasi, S. A. (2012). Biogas energy. In S. A. Abbasi, Tasneem, Tauseef, S.M., Abbasi (Ed.), *Biogas Energy* (1st ed., pp. 1–169). Springer. https://doi.org/10.1007/978-1-4614-1040-9

Alibardi, L., Favaro, L., Lavagnolo, M. C., Basaglia, M., & Casella, S. (2012). Effects of heat treatment on microbial communities of granular sludge for biological hydrogen production. *Water Science and Technology*, *66*(7), 1483–1490. https://doi.org/10.2166/wst.2012.336

Angenent, L. T., Richter, H., Buckel, W., Spirito, C. M., Steinbusch, K. J., Strik, D. P. B. T. B., Grootscholten, T. I. M., Buisman, C. J. N., & Hamelers, H. V. M. (2016). Chain elongation with reactor microbiomes : open-culture biotechnology to produce biochemicals - Extensive review. *Environmental Science and Technology*, *50*(6), 2796–2810. https://doi.org/10.1021/acs.est.5b04847

APHA. (2005). *Standard Methods for the Examination of Water and Wastewater* (A. E. G. Andrew D. Eaton, Lenore S. Clesceri, M. A. H. Franson, Eugene W. Rice, Ed.; 21st ed.). American Public Health Association.

Appels, L., Lauwers, J., Degrve, J., Helsen, L., Lievens, B., Willems, K., van Impe, J., & Dewil, R. (2011). Anaerobic digestion in global bio-energy production: Potential and research challenges. *Renewable and Sustainable Energy Reviews*, *15*(9), 4295–4301. https://doi.org/10.1016/j.rser.2011.07.121

ASTM International. (2016). ASTM D8083-16 - Standard Test Method for Total Nitrogen, and Total Kjeldahl Nitrogen (TKN) by Calculation, in Water by High Temperature Catalytic Combustion and Chemiluminescence Detection. *ASTM Standard*, 1–9.

Bazylinski, D. A., Williams, T. J., Lefèvre, C. T., Trubitsyn, D., Fang, J., Beveridge, T. J., Moskowitz, B. M., Ward, B., Schübbe, S., Dubbels, B. L., & Simpson, B. (2013). *Magnetovibrio blakemorei* gen. nov., sp. nov., a magnetotactic bacterium (*Alphaproteobacteria : Rhodospirillaceae*) isolated from a salt marsh. *International Journal of Systematic and Evolutionary Microbiology*, *63*(Pt_5), 1824–1833. https://doi.org/10.1099/ijs.0.044453-0

Callbeck, C. M., Pelzer, C., Lavik, G., Ferdelman, T. G., Graf, J. S., Vekeman, B., Schunck, H., Littmann, S., Fuchs, B. M., Hach, P. F., Kalvelage, T., Schmitz, R. A., & Kuypers, M. M. M. (2019). *Arcobacter peruensis* sp. nov., a chemolithoheterotroph isolated from sulfide-and organic-rich coastal waters off Peru. *Applied and Environmental Microbiology*, *85*(24), 1–17. https://doi.org/10.1128/AEM.01344-19

Casallas-Ojeda, M. R., Marmolejo-Rebellón, L. F., & Torres-Lozada, P.

(2020). Evaluation of simultaneous incidence of head space and temperature on biochemical methane potential in food waste. *Cogent Engineering*, *7*(1), 1729514. https://doi.org/10.1080/23311916.2020.1729514

Chen, Y., Cheng, J. J., & Creamer, K. S. (2008). Inhibition of anaerobic digestion process. *Bioresource Technologyr*, *99*, 4.

Chen, Y., Jiang, S., Yuan, H., Zhou, Q., & Gu, G. (2007). Hydrolysis and acidification of waste activated sludge at different pHs. *Water Research*, *41*(3), 683–689. https://doi.org/10.1016/j.watres.2006.07.030

Corti, A., & Lombardi, L. (2007). Anaerobic co-digestion of source selected organic waste and sewage sludge. *11th International Symposium on Waste Management and Sustainable Landfilling*, 1–5.

Dai, Y., Yan, Z., Jia, L., Zhang, S., Gao, L., Wei, X., Mei, Z., & Liu, X. (2016). The composition, localization and function of low-temperature-adapted microbial communities involved in methanogenic degradations of cellulose and chitin from Qinghai-Tibetan Plateau wetland soils. *Journal of Applied Microbiology*, *121*(1), 163–176. https://doi.org/10.1111/jam.13164

Dareioti, M. A., Vavouraki, A. I., & Kornaros, M. (2014). Effect of pH on the anaerobic acidogenesis of agroindustrial wastewaters for maximization of bio-hydrogen production: A lab-scale evaluation using batch tests. *Bioresource Technology*, *162*, 218–227. https://doi.org/10.1016/j.biortech.2014.03.149

Darvekar, P., Liang, C., Karim, M. N., & Holtzapple, M. T. (2019). Effect of headspace gas composition on carboxylates production in open-culture fermentation of corn stover. *Biomass and Bioenergy*, *126*, 57–61. https://doi.org/10.1016/j.biombioe.2019.04.019

Detman, A., Laubitz, D., Chojnacka, A., Kiela, P. R., Salamon, A., Barberán, A., Chen, Y., Yang, F., Błaszczyk, M. K., & Sikora, A. (2021). Dynamics of dark fermentation microbial communities in the light of lactate and butyrate production. *Microbiome*, *9*(1), 158. https://doi.org/10.1186/s40168-021-01105-x

Deublein, D., & Steinhauser, A. (Eds.). (2011). *Biogas from renewable resources: An introduction* (2nd ed.). Wiley-VCH Verlag GmbH & Co. KGaA.

Dilallo, R., & Albertison, O. E. (1961). Volatile Acids by Direct Titration. *Journal Water Pollution Control Federation*, *33*, 356–365.

Dubois, M., Gilles, K. A., Hamilton, J. K., Rebers, P. A., & Smith, F. (1956). Colorimetric method for determination of sugars and related substances. *Analytical Chemistry*, *28*(3), 350–356.

FAO. (n.d.). *FAOSTAT - Livestock processed*. Food and Agriculture Organization of the United Nations. Retrieved June 20, 2020, from http://www.fao.org/faostat/en/?#data/QP

Fujita, Y., Tsujimoto, R., & Aoki, R. (2015). Evolutionary Aspects and Regulation of Tetrapyrrole Biosynthesis in Cyanobacteria under Aerobic and Anaerobic Environments. *Life*, *5*(2), 1172–1203. https://doi.org/10.3390/life5021172

Gao, S., Li, Z., Hou, Y., Wang, A., Liu, Q., & Huang, C. (2022). Effects of different carbon sources on the efficiency of sulfur-oxidizing denitrifying microorganisms. *Environmental Research*, *204*, 111946. https://doi.org/10.1016/j.envres.2021.111946

Gao, Y., Guo, L., Jin, C., Zhao, Y., Gao, M., She, Z., & Wang, G. (2022). Metagenomics and network analysis elucidating the coordination between fermentative bacteria and microalgae in a novel bacterial-algal coupling reactor (BACR) for mariculture wastewater treatment. *Water Research*, *215*, 118256. https://doi.org/10.1016/j.watres.2022.118256

Goud, R. K., & Mohan, S. V. (2012). Acidic and alkaline shock pretreatment to enrich acidogenic biohydrogen producing mixed culture: Long term synergetic evaluation of microbial inventory, dehydrogenase activity and bio-electro kinetics. *RSC Advances*, *2*(15), 6336–6353. https://doi.org/10.1039/c2ra20526b

Hamilton, T. L., Klatt, J. M., de Beer, D., & Macalady, J. (2018). Cyanobacterial photosynthesis under sulfidic conditions: insights from the isolate *Leptolyngbya* sp. strain hensonii. *The ISME Journal*, *12*, 568–584. https://doi.org/https://doi.org/10.1038/ismej.2017.193

Joshi, S., Robles, A., Aguiar, S., & Delgado, A. G. (2021). The occurrence and ecology of microbial chain elongation of carboxylates in soils. *The ISME Journal*, *15*(7), 1907–1918. https://doi.org/10.1038/s41396-021-00893-2

Kang, D., Saha, S., Kurade, M. B., Basak, B., Ha, G.-S., Jeon, B.-H., Lee, S. S., & Kim, J. R. (2021). Dual-stage pulse-feed operation enhanced methanation of lipidic waste during co-digestion using acclimatized consortia. *Renewable and Sustainable Energy Reviews*, *145*, 111096. https://doi.org/10.1016/j.rser.2021.111096

Kigozi, R., Muzenda, E., & Aboyade, A. O. (2014). Biogas technology: Current trends, opportunities and challenges. *6th Int'l Conf. on Green Technology, Renewable Energy & Environmental Engg. (ICGTREEE'20114)*, 311–317.

Kleerebezem, R., Joosse, B., Rozendal, R., & van Loosdrecht, M. C. M. (2015). Anaerobic digestion without biogas? *Reviews in Environmental Science and Biotechnology*, *14*(4), 787–801. https://doi.org/10.1007/s11157-015-9374-6

Li, H., Li, C., Liu, W., & Zou, S. (2012). Optimized alkaline pretreatment of sludge before anaerobic digestion. *Bioresource Technology*, *123*, 189–194. https://doi.org/10.1016/j.biortech.2012.08.017

Li, Y., Tang, K., Zhang, L., Zhao, Z., Xie, X., Chen, C.-T. A., Wang, D., Jiao, N., & Zhang, Y. (2018). Coupled Carbon, Sulfur, and Nitrogen Cycles mediated by microorganisms in the water column of a shallow-water hydrothermal ecosystem. *Frontiers in Microbiology*, *9*. https://doi.org/10.3389/fmicb.2018.02718

Lin, J.-G., Chang, C.-N., & Chang, S.-C. (1997). Enhancement of anaerobic digestion of waste activated sludge by alkaline solubilization. *Bioresource Technology*, *62*, 85–90.

Lin, X.-Q., Li, Z.-L., Liang, B., Zhai, H.-L., Cai, W.-W., Nan, J., & Wang, A.-J. (2019). Accelerated microbial reductive dechlorination of 2,4,6-trichlorophenol by weak electrical stimulation. *Water Research*, *162*, 236–245. https://doi.org/10.1016/j.watres.2019.06.068

Liu, Y., Zhang, Z., Jiang, W., & Gu, Y. (2022). Protein acetylation-mediated cross regulation of acetic acid and ethanol synthesis in the gas-fermenting *Clostridium ljungdahlii*. *Journal of Biological Chemistry*, *298*(2). https://doi.org/10.1016/j.jbc.2021.101538

López-Torres, M., & Llórens, Ma. del C. E. (2016). Effect of alkaline pretreatment on anaerobic digestion of olive mill solid waste. *Waste Management*, *58*, 160–168. https://doi.org/10.1016/j.wasman.2016.08.008

Miñana-Galbis, D., Farfán, M., Lorén, J. G., & Fusté, M. C. (2002). Biochemical identification and numerical taxonomy of *Aeromonas* spp. isolated from environmental and clinical samples in Spain. *Journal of Applied Microbiology*, *93*(3), 420–430. https://doi.org/10.1046/j.1365-2672.2002.01711.x

Mockaitis, G., Bruant, G., Foresti, E., Zaiat, M., & Guiot, S. R. (2022). Physicochemical pretreatment selects microbial communities to produce alcohols through metabolism of volatile fatty acids. *Biomass Conversion and Biorefinery*. https://doi.org/10.1007/s13399-022-02383-7

Mockaitis, G., Bruant, G., Guiot, S. R., Peixoto, G., Foresti, E., & Zaiat, M. (2020). Acidic and thermal pre-treatments for anaerobic digestion inoculum to improve hydrogen and volatile fatty acid production using xylose as the substrate. *Renewable Energy*, *145*, 1388–1398. https://doi.org/10.1016/j.renene.2019.06.134

Mockaitis, G., Ratusznei, S. M., Rodrigues, J. A. D., Zaiat, M., & Foresti, E. (2006). Anaerobic whey treatment by a stirred sequencing batch reactor (ASBR): effects of organic loading and supplemented alkalinity. *Journal of Environmental Management*, *79*(2), 198–206. https://doi.org/10.1016/j.jenvman.2005.07.001

Mulders, M., Tamis, J., Abbas, B., Sousa, J., Dijkman, H., Rozendal, R., & Kleerebezem, R. (2020). Pilot-scale polyhydroxyalkanoate production from organic waste: Process characteristics

at high pH and high ammonium concentration. *Journal of Environmental Engineering*, *146*(7), 4020049. https://doi.org/10.1061/(ASCE)EE.1943-7870.0001719

Navia, R., & Vidal, G. (2002). Alkaline pretreatment of kraft mill sludge to improve its anaerobic digestion alkaline pretreatment of kraft mill sludge to improve its anaerobic digestion. *Bull. Environ. Contam. Toxicol.*, *69*, 869–876. https://doi.org/10.1007/s00128-002-0140-4

Nuppunen-Puputti, M., Purkamo, L., Kietäväinen, R., Nyyssönen, M., Itävaara, M., Ahonen, L., Kukkonen, I., & Bomberg, M. (2018). Rare biosphere archaea assimilate acetate in Precambrian terrestrial subsurface at 2.2 km depth. *Geosciences (Switzerland)*, *8*(11), 1–20. https://doi.org/10.3390/geosciences8110418

Oliveira, C. P., Gloria, M. B. A., Barbour, J. F., & Scanlan, R. A. (1995). Nitrate, nitrite, and volatile nitrosamines in whey-containing food products. *Journal of Agricultural and Food Chemistry*, *43*(4), 967–969. https://doi.org/10.1021/jf00052a023

Ostrem, K. M., Millrath, K., & Themelis, N. J. (2004). Combining anaerobic digestion and waste-to-energy. *Proceedings of 12TH Annual North American Waste to Energy Conference,NAWTEC12*, *Nawtec 12*, 265–271. https://doi.org/10.1115/nawtec12-2231

Pang, N., Gu, X., Kirchhoff, H., Lei, H., & Roje, S. (2019). Exploiting mixotrophic for improving productivities of biomass and co-products of microalgae. *Renewable and Sustainable Energy Reviews*, *112*, 450–460. https://doi.org/10.1016/j.rser.2019.06.001

Peixoto, G., Saavedra, N. K., Varesche, M. B. A., & Zaiat, M. (2011). Hydrogen production from soft-drink wastewater in an upflow anaerobic packed-bed reactor. *International Journal of Hydrogen Energy*, *36*(15), 8953–8966. https://doi.org/10.1016/j.ijhydene.2011.05.014

Penteado, E. D., Adorno, M. A. T., & Zaiat, M. (2012, June 16). Simple and accurated method for determination of fatty acids, alcohols andcarbohydrates by HPLC with UV/DAD and RID detectors. *38th International Symposium on High Performance Liquid Phase Separation.*

Pretorius, W. A. (1987). A conceptual basis for microbial selection in biological wastewater treatment. *Water Research*, *21*(8), 891–894.

Quast, C., Pruesse, E., Yilmaz, P., Gerken, J., Schweer, T., Yarza, P., Peplies, J., & Glöckner, F. O. (2013). The SILVA ribosomal RNA gene database project: Improved data processing and web-based tools. *Nucleic Acids Research*, *41*(D1), D590–D596. https://doi.org/10.1093/nar/gks1219

Ramos-Suarez, M., Zhang, Y., & Outram, V. (2021). Current perspectives on acidogenic fermentation to produce volatile fatty acids from waste. *Reviews in Environmental Science and Bio/Technology*, *20*(2), 439–478. https://doi.org/10.1007/s11157-021-09566-0

Ranaivoarisoa, T. O., Singh, R., Rengasamy, K., Guzman, M. S., & Bose, A. (2019). Towards sustainable bioplastic production using the photoautotrophic bacterium *Rhodopseudomonas palustris* TIE-1. *Journal of Industrial Microbiology and Biotechnology*, *46*(9–10), 1401–1417. https://doi.org/10.1007/s10295-019-02165-7

Ripley, L.E., Boyle, W.C. and Converse, J. C. (1986). Improved alkalimetric monitoring for anaerobic digestion of high-strength wastes. *Journal WPCF*, *48*, 406–411.

Rognes, T., Flouri, T., Nichols, B., Quince, C., & Mahé, F. (2016). VSEARCH: A versatile open source tool for metagenomics. *PeerJ*, *2016*(10). https://doi.org/10.7717/peerj.2584

Rombouts, J. L., Mos, G., Weissbrodt, D. G., Kleerebezem, R., & van Loosdrecht, M. C. M. (2019). Diversity and metabolism of xylose and glucose fermenting microbial communities in sequencing batch or continuous culturing. *FEMS Microbiology Ecology*, *95*(2), 1–12. https://doi.org/10.1093/femsec/fiy233

Saary, P., Forslund, K., & Hildebrand, F. (2017). RTK: efficient rarefaction analysis of large datasets. *Bioinformatics*, *33*(16), 2594–2595. https://doi.org/10.1093/bioinformatics/xxxx

Saddoud, A., Hassaïri, I., & Sayadi, S. (2007). Anaerobic membrane reactor with phase separation for the treatment of cheese whey. *Bioresource Technology*, *98*(11), 2102–2108. https://doi.org/10.1016/j.biortech.2006.08.013

Sarkar, O., Butti, S. K., & Venkata Mohan, S. (2017). Acidogenesis driven by hydrogen partial pressure towards bioethanol production through fatty acids reduction. *Energy*, *118*, 425–434. https://doi.org/10.1016/j.energy.2016.12.017

Sarkar, O., Rova, U., Christakopoulos, P., & Matsakas, L. (2021). Influence of initial uncontrolled pH on acidogenic fermentation of brewery spent grains to biohydrogen and volatile fatty acids production: Optimization and scale-up. *Bioresource Technology*, *319*. https://doi.org/10.1016/j.biortech.2020.124233

Shah, F. A., Mahmood, Q., Rashid, N., Pervez, A., Raja, I. A., & Shah, M. M. (2015). Co-Digestion, pretreatment and digester design for enhanced methanogenesis. *Renewable and Sustainable Energy Reviews*, *42*, 627–642. https://doi.org/10.1016/j.rser.2014.10.053

Sheik, A. R., Muller, E. el, Audinot, J.-N., Lebrun, L. A., Grysan, P., Guignard, C., & Wilmes, P. (2016). *In situ* phenotypic heterogeneity among single cells of the filamentous bacterium *Candidatus* Microthrix parvicella. *The ISME Journal*, *10*(5), 1274–1279. https://doi.org/10.1038/ismej.2015.181

Shi, L. L., Da, Y. Y., Zheng, W. T., Chen, G. Q., & Li, Z. J. (2020). Production of polyhydroxyalkanoate from acetate by metabolically engineered *Aeromonas hydrophilia*. *Journal of Bioscience and Bioengineering*, *130*(3), 290–294. https://doi.org/10.1016/j.jbiosc.2020.05.003

Skiba, U. (2008). Denitrification. In S. E. Jorgensen & B. D. Fath (Eds.), *Encyclopedia of Ecology* (First, Vol. 1, pp. 866–871). Oxford, Elsevier.

Smithers, G. W. (2008). Whey and whey proteins-From "Gutter-to-Gold." *International Dairy Journal*, *18*(7), 695–704. https://doi.org/10.1016/j.idairyj.2008.03.008

Stal, L. J., & Moezelaar, R. (1997). Fermentation in cyanobacteria. *FEMS Microbiology Reviews*, *21*, 179–211.

Stams, A. J. M., Teusink, B., & Sousa, D. Z. (2019). Ecophysiology of Acetoclastic Methanogens. In *Biogenesis of Hydrocarbons* (pp. 1–14). Springer International Publishing. https://doi.org/10.1007/978-3-319-53114-4_21-1

Thatikayala, D., Pant, D., & Min, B. (2021). MnO_2/reduced graphene oxide nanohybrids as a cathode catalyst for the microbial reduction of CO_2 to acetate and isobutyric acid. *Sustainable Energy Technologies and Assessments*, *45*. https://doi.org/10.1016/j.seta.2021.101114

Torres, P. L. (1992). *Desempenho de um reator anaerobio de manta de lodo (uasb) de bancada no tratamento de substrato sintetico simulando esgotos sanitarios* [Doctorate]. Universidade de Sãp Paulo.

Tremblay, J. (2019). *AmpliconTagger Pipeline Databases*.

Tremblay, J. (2020). *microbiomeutils 0.9.4 : Microbiome utilities*. https://github.com/jtremblay/microbiomeutils

Tsakali, E., Petrotos, K., d'Allessandro, A., & Goulas, P. (2010). A review on whey composition and the methods used for its utilization for food and pharmaceutical products. In C. R. Centre (Ed.), *6th International Conference on Simulation and Modelling in the Food and Bio-Industry* (pp. 195–201).

USDA. (2022). *Dairy: World markets and trade*. https://apps.fas.usda.gov/psdonline/circulars/dairy.pdf

van Lier, J. B., Mahmoud, N., & Zeeman, G. (2008). Anaerobic wastewater treatment. In M. Henze, M. C. M. van Loosdrecht, G. A. Ekama, & D. Brdjanovic (Eds.), *Biological Wastewater Treatment : Principles, Modelling and Design* (1st ed., pp. 401–442). IWA Publishing. https://doi.org/10.1021/es00154a002

van Lier, J. B., Tilche, A., Ahring, B. K., Macarie, H., Moletta, R., Dohanyos, M., Pol, L. W. H., Lens, P., & Verstraete, W. (2001). New perspectives in anaerobic digestion. *Water Science and Technology*, *43*(1), 1–18.

Wang, Q., Garrity, G. M., Tiedje, J. M., & Cole, J. R. (2007). Naïve Bayesian classifier for rapid assignment of rRNA sequences into the new bacterial taxonomy. *Applied and Environmental Microbiology*, *73*(16), 5261–5267. https://doi.org/10.1128/AEM.00062-07

Wang, S., Zhao, J., Ding, X., Zhao, R., Huang, T., Lan, L., Naim Bin Nasry, A. al, & Liu, S. (2019). Effect of starvation time on NO and N_2O production during heterotrophic denitrification with nitrite and glucose shock loading. *Process Biochemistry*, *86*, 108–116. https://doi.org/10.1016/j.procbio.2019.07.023

Weissbrodt, D. G., Wells, G. F., Laureni, M., Agrawal, S., Goel, R., Russo, G., Men, Y., Johnson, D. R., Christensson, M., Lackner, S., Joss, A., Lund Nielsen, J., Bürgmann, H., Morgenroth, E., & Nielsen, L. (2020). Systems microbiology and Engineering of aerobic-anaerobic ammonium oxidation. *ChemRxiv Preprint*, 1–34. https://doi.org/10.26434/chemrxiv.12243077.v1

Wonglertarak, W., & Wichitsathian, B. (2014). Alkaline Pretreatment of Waste Activated Sludge in Anaerobic Digestion. *Journal of Clean Energy Technologies*, *January 2014*, 118–121. https://doi.org/10.7763/jocet.2014.v2.104

Yamada, T., Imachi, H., Ohashi, A., Harada, H., Hanada, S., Kamagata, Y., & Sekiguchi, Y. (2007). *Bellilinea caldifistulae* gen. nov., sp. nov. and *Longilinea arvoryzae* gen. nov., sp. nov., strictly anaerobic, filamentous bacteria of the phylum *Chloroflexi* isolated from methanogenic propionate-degrading consortia. *International Journal of Systematic and Evolutionary Microbiology*, *57*(10), 2299–2306. https://doi.org/10.1099/ijs.0.65098-0

Yamada, T., Sekiguchi, Y., Hanada, S., Imachi, H., Ohashi, A., Harada, H., & Kamagata, Y. (2006). *Anaerolinea thermolimosa* sp. nov., *Levilinea saccharolytica* gen. nov., sp. nov. and *Leptolinea tardivitalis* gen. nov., sp. nov., novel filamentous anaerobes, and description of the new classes *Anaerolineae* classis nov. and *Caldilineae* classis nov. in the bacterial phylum *Chloroflexi*. *International Journal of Systematic and Evolutionary Microbiology*, *56*(6), 1331–1340. https://doi.org/10.1099/ijs.0.64169-0

Yu, Y., Lee, C., Kim, J., & Hwang, S. (2005). Group-specific primer and probe sets to detect methanogenic communities using quantitative Real-Time Polymerase Chain Reaction. *Biotechnology and Bioengineering*, *89*(6), 670–679. https://doi.org/10.1002/bit.20347

Yuan, H., Chen, Y., Zhang, H., Jiang, S., Zhou, Q., & Gu, G. (2006). Improved bioproduction of short-chain fatty acids (SCFAs) from excess sludge under alkaline conditions. *Environmental Science and*

Technology, *40*(6), 2025–2029. https://doi.org/10.1021/es052252b

Zhang, S., Guo, H., Du, L., Liang, J., Lu, X., Li, N., & Zhang, K. (2015). Influence of NaOH and thermal pretreatment on dewatered activated sludge solubilisation and subsequent anaerobic digestion: Focused on high-solid state. *Bioresource Technology*, *185*, 171–177.

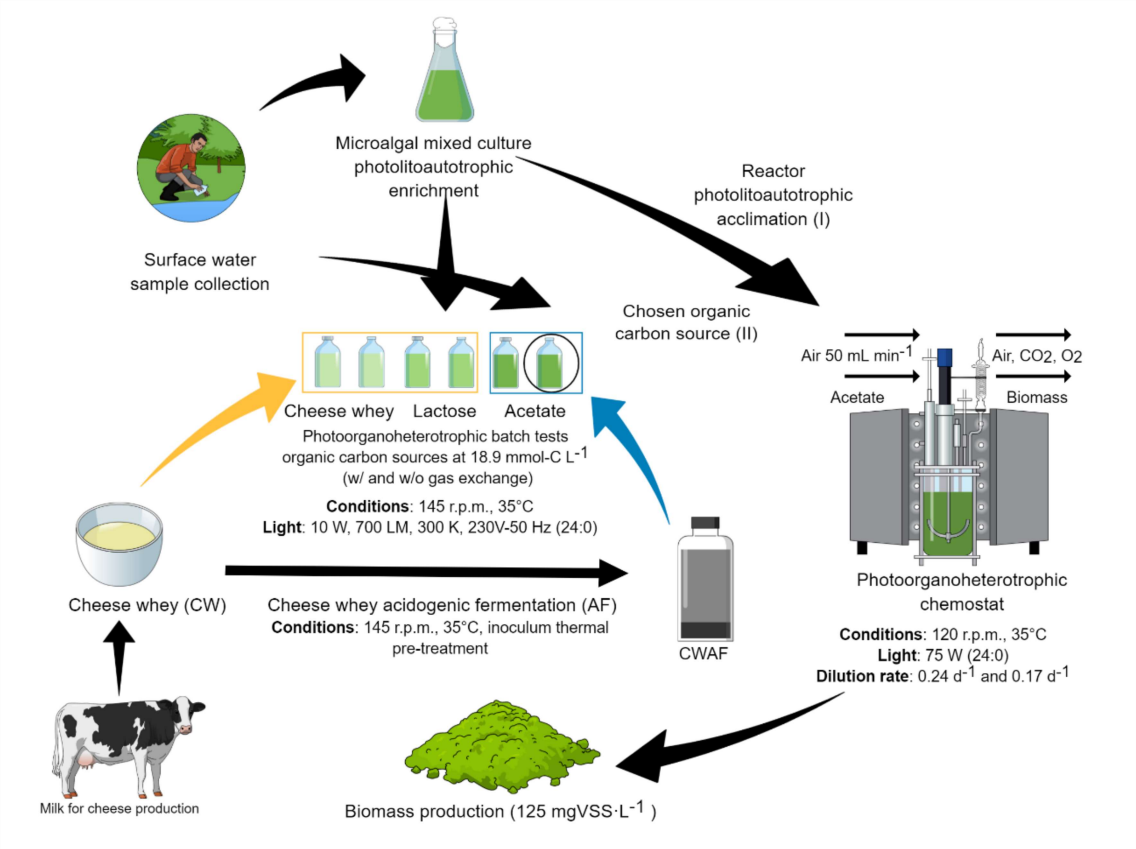
Zhang, X., Shao, Y., Tian, J., Liao, Y., Li, P., Zhang, Y., Chen, J., & Li, Z. (2019). PTrimmer: An efficient tool to trim primers of multiplex deep sequencing data. *BMC Bioinformatics*, *20*(236). https://doi.org/10.1186/s12859-019-2854-x

Zhou, M., Yan, B., Wong, J. W. C., & Zhang, Y. (2018). Enhanced volatile fatty acids production from anaerobic fermentation of food waste: A mini-review focusing on acidogenic metabolic pathways. *Bioresource Biotechnology*, *248*(Part A), 68–78. https://doi.org/https://doi.org/10.1016/j.biortech.2017.06.121

4.Beyond phycoremediation: Ecological engineering of photoorganoheterotrophic microalgal mixed cultures for cheese whey valorization

This chapter was developed in collaboration with Camille Mondini, Master student at the TU Delft in the framework of this Ph.D..Part of this work was presented to ACS Fall Meeting as: **Giulianetti de Almeida MP**°, Mondini C°, Mockaitis G, Weissbrodt DG (2020) *Ecological engineering of photoorganoheterotrophic microalgal mixed cultures to valorise cheese whey*. In: American Chemical Society (ed.) ACS Fall Meeting, San Francisco /US. (virtual). This chapter will be submitted to *ACS Sustainable Chemistry & Engineering.*

Graphical abstract



Abstract

Microalgae cultivation, and phycoremediation, can be a polishing step in wastewater treatment. Depending on the stream utilized for microalgal cultivation, biomass can be contaminated with considerable quantities of heavy metals and xenobiotics. Given the economic value of microalgae bioproducts, we suggest coupling anaerobic fermentation with microalgae mixotrophic growth. Cheese whey, a product from cheese production, has a 2022 forecast production of 160.7 million m^3 $year^{-1}$ in which about 66.5 million m^3 y^{-1} is used as animal feed, fertilizers or illegally discharged causing eutrophication. Anaerobic fermentation of cheese whey produces volatile fatty acids (VFAs) such as acetate which serves as an organic carbon source for photoorganoheterotrophic microalgal biomass growth. Our work selected three organic sources derived from cheese whey: 40% demineralized whey powder (WPC40), lactose, and acetate. In photolitoautotrophic conditions, green phototrophic growth was successful. In batch tests, acetate was the best organic carbon source among photoorganoheterotrophs with a higher yield of 1.15 mg VSS mg $Carbon^{-1}$ (C) in anaerobic conditions. Also, acetate uptake was thought to be via the glyoxylate cycle. When upscaling the experiment in a chemostat, a lower dilution rate of 0.17 d^{-1} was more suitable for green photoorganoheterotrophs selection, as they were not washed out in the process. These findings show that acetate uptake by microalgae in mixotrophic regimes must be better understood as well as reinforce the advantages of coupling microalgal biomass growth with cheese whey acidogenic fermentation, avoiding contaminations as in phycoremediation processes and fully valorizing cheese whey.

KEYWORDS: Microalgae, phycoremediation, biomass contamination, anaerobic coupled processes, cheese whey, photoorganoheterotrophy

1 Introduction

Microalgae are a common and cost-effective polishing step removing nutrients, xenobiotics, and heavy metals from wastewaters foregoing the use of sterile media (Atiku et al., 2016; Beltrán-Rocha et al., 2017; Bohutskyi et al., 2015; Chew et al., 2018; Chiu et al., 2015; de Melo et al., 2018; Fernández-Linares et al., 2017; Gonçalves, Pires, & Simões, 2017; Guldhe et al., 2017; Khan et al., 2019; Kotteswari, Murugesan, & R, 2012; Maizatul et al., 2017; Moreno García et al., 2020; Pahazri et al., 2016; Posadas et al., 2014; Renuka et al., 2015; Singh, Tiwari, & Das, 2016; Solmaz & Mustafa, 2019; Ting et al., 2017; Wang et al., 2016), thriving under stress conditions whilst maintaining their productivity (Ansari et al., 2020). Their photosynthetic activity enables them to sequestrate carbon and decreases wastewater organic and inorganic loads, resulting in biomass that can be either used as a biofertilizer or further processed into biofuels and other products. Consequently, eutrophication can be prevented (Amit & Ghosh, 2018; Bohutskyi et al., 2015; Chiu et al., 2015; Gani et al., 2015; Guldhe et al., 2017; Khan et al., 2019; Kotteswari et al., 2012; Rawat et al., 2011; Renuka et al., 2015; Singh et al., 2016) making phycoremediation a very promising technique for mitigating pollution and environmental impacts (Akthar et al., 2017; Atiku et al., 2016; Beltrán-Rocha et al., 2017; Bohutskyi et al., 2015; Chew et al., 2018; Chiu et al., 2015; de Melo et al., 2018; Fernández-Linares et al., 2017; Gonçalves et al., 2017; Guldhe et al., 2017; Kotteswari et al., 2012; Maizatul et al., 2017; Moreno García et al., 2020; Pahazri et al., 2016; Posadas et al., 2014; Renuka et al., 2015; Singh et al., 2016; Solmaz & Mustafa, 2019; Ting et al., 2017; Wang et al., 2016).

Several studies focus on the use of wastewater for microalgal biomass production (Atiku et al., 2016; Bohutskyi et al., 2015; Cheng et al., 2019; Chiu et al., 2015; Fernández-Linares et al., 2017; Hena, Fatimah, & Tabassum, 2015; Melo et al., 2018; Olguín, 2012; Pahazri et al., 2016; Posadas et al., 2014, 2016; Sahu et al., 2013). Microalgae can be cultivated on arid land (Aratboni et al., 2019; Rösch, Roßmann, & Weickert, 2018; Zeng et al., 2011), brackish or high strength waters (Aslan & Kapdan, 2006; Ho et al., 2011; Jeong, 2003; Kamyab et al., 2015; Ren et al., 2007; Wang et al., 2008; Yi, Han, & Zhuo, 2013; Zhao & Su, 2014), have high photosynthetic efficiency, sequestrate carbon dioxide (Bassi, Saxena, & Aguirre, 2014; Ho et al., 2011; Jeong, 2003; Siregar et al., 2015; Wang et al., 2008; Yi et al., 2013; Zhao & Su, 2014), have

different carbon metabolisms (Bassi et al., 2014; Chojnacka & Noworyta, 2004; Crane & Grover, 2010; Godrijan, Drapeau, & Balch, 2020; Subashchandrabose et al., 2013) and an outlet of high added value bioproducts that can be processed into (e.g., biofuels, pigments, omega-3, antioxidants, pigments, lipids, biomass, polyunsaturated fatty acids (PUFAs), polysaccharides, immune modulators, polymers) which can be used by food, aquaculture, nutraceutical, pharmaceutical, cosmetic and energetic industries (Bohutskyi et al., 2015; Chen et al., 2019; Chew et al., 2017; Chiu et al., 2015; D'Imporzano et al., 2018; Fei et al., 2015; Fernández-Linares et al., 2017; Guldhe et al., 2017; Hu et al., 2018; Moreno García et al., 2020; Odjadjare, Mutanda, & Olaniran, 2017; Posten & Schaub, 2009; Pulz & Gross, 2004; Singh et al., 2016).

Microalgae have an outlet of bioproducts of high aggregated value that depending on the substrate used during phycoremediation, there is the possibility of biomass contamination with heavy metals and xenobiotics (Markou et al., 2018). Ergo, coupled anaerobic processes for microalgal mixotrophic biomass growth avoid this contamination by feeding microalgae with only the products of the fermentation of anaerobic digestion, volatile fatty acids.

Anaerobic digestion (AD) is a sustainable option to treat and reuse organic residues, reducing their organic load and concomitantly, converting them into VFAs during fermentation. Anaerobic processes have low energy consumption and the potential to decrease greenhouse gas (GHG) emissions (Boyle, 2012). According to Atasoy et al.(2018), VFAs can serve as raw material to produce some polyhydroxyalkanoates (PHAs), biogas, electricity, and an organic carbon source for the biological removal of phosphorus and nitrogen from wastewater. Microalgae-coupled processes can use VFAs as organic carbon sources derived from anaerobic digestion processes. In our case, this organic carbon source originates from cheese whey acidogenic fermentation processes.

Cheese whey is a product from cheese processing (Archer, 1998; Tsakali et al., 2010) with high organic content (i.e., 50-102 g O_2 L^{-1} in terms of COD) (Prazeres, Carvalho, & Rivas, 2012; Tsolcha et al., 2016) making cheese whey one of the biggest agricultural pollutants (Kosseva & Webb, 2013; Prazeres et al., 2012; Stamatelatou et al., 2011; Tsolcha et al., 2016). In the year 2022, the forecast for cheese whey production among the world's biggest producers is 160.67 Mm^3 y^{-1} although only 58.6% is absorbed by industries (Tsakali et al., 2010; USDA, 2019). The remaining 66.5 Mm^3 y^{-1} of cheese whey is currently used as animal feed, fertilizers, or in some

locations (i.e., developing and developing countries and remote locations), it can be illegally discharged into water bodies (Tsakali et al., 2010).

The acidogenic fermentation of cheese whey produces mainly acetate (Hassan & Nelson, 2012). Phototrophic organisms can convert electromagnetic energy into chemical energy to maintain cellular growth (Overmann & Garcia-Pichel, 2013). Microalgae (i.e., microalgae and cyanobacteria) are phototrophic organisms capable of performing mixotrophy (Mondal et al., 2016; Salati et al., 2017).

Some microalgae can display heterotrophic and mixotrophic metabolisms (Bouarab, Dauta, & Loudiki, 2004; Hu et al., 2018; Mondal et al., 2016). The mixotrophic regime is thought to be the sum of both photolithoautotrophic and chemoorganoheterotrophic regimes (Bouarab et al., 2004). In mixotrophic microalgae mixed cultures coupled with cheese whey anaerobic digestion processes, the organic carbon source can come from the lactose, proteins, and fats present in cheese whey or, as we propose it can come as acetate, the main VFA produced in cheese whey anaerobic processes.

Another way to obtain organic carbon sources is through symbiotic relationships within ordinary heterotrophic organisms (OHO). They will degrade organic matter into carbon dioxide and in return, microalgae will produce oxygen in photosynthesis, which is essential for aerobic bacterial life (Yao et al., 2018). However, competition for substrate and predatism can be an issue in mixotrophic cultures, decreasing microalgae organic carbon uptake (Chen, Zhao, & Qi, 2015; Ramanan et al., 2016). Hence, it can influence biomass production. Mixotrophic cultures also have an economic advantage over axenic cultures as they do not require sterilization of substrate and equipment as do pure cultures to avoid contamination (Chen et al., 2015).

Our work aims to understand the ecological engineering of green photoorganoheterotrophs and their mechanisms of organic carbon uptake. We also target the best reactor regimes and parameters (i.e., dilution and hydraulic retention time) for green phototroph selection. In addition, we attempt to comprehend the symbiotic relationships between different guilds of microorganisms for upscaling the process.

2 Materials and Methods

2.1 Enrichment of mother culture

Surface water was sampled from a channel 51°59'23.3"N 4°22'53.8"E (Ruiven, 2628 CN Delft, NL). A mother microalgal culture was enriched from this sample using Allen´s Blue-Green algal medium, BG-11 (Allen, 1968; Allen & Stanier, 1968; Ripka et al., 1979), in a 1:15 ratio. Acclimation lasted 15 days. Every two weeks, the mother culture was reinoculated.

The culture was initially grown photolitoautrotophicaly in an incubator (shaker KS-15, hood TS-15, Edmund Bühler GmbH, Germany) at 145 rpm mixing and mesophilic temperature of 35°C. A led lamp (10 W, 700 LM, 300K, 230V-50 Hz, GAMMA, The Netherlands) provided continuous illumination of 80 µmol photons m^{-2} s^{-1}. Culture flasks used a sterile cotton stopper allowing gas exchange between media and atmosphere. Once culture was established, it served as an inoculum for all experiments.

2.2 Study of different phototropism regimes in batches

Table 1 describes the experimental set-up for photolitoautotrophic biomass growth with different nitrogen sources and gas exchange conditions and photoorganoheterotrophic microorganisms' selection under different carbon source sections.

2.2.1 Photolitoautotrophic growth with different nitrogen sources and gas exchange conditions

Cultivation was performed in borosilicate vials (100 mL) using a modified BG- 11 medium heated at 90°C for whole carbon source (CO_3^{2-}) dissolution. The nitrate ($NaNO_3$) content of the medium was substituted by ammonium (NH_4Cl) in equal mols (17.6 mmol N L^{-1}). Gas exchange was controlled by using open and sealed bottles which were sealed with rubber stoppers and aluminum crimp caps.

Vials were sparged with nitrogen to ensure initial anaerobic conditions. Open bottles had a sterile cotton stopper to allow gas exchange. Measurements consisted

of biomass concentration as volatile suspended solids (VSS), nutrient (N and P) consumption, pH variation, and microscope visualization. The experiment lasted for 30 days.

2.2.2 Selection of photoorganoheterotrophic microorganisms by different carbon sources

A photoorganoheterotrophic regime was applied to the mother culture using different organic carbon sources such as acetate, lactose, and 40% demineralized whey powder (WPC40). BG-11 medium was used as a substrate where each carbon source was substituted in the medium by 0.189 mM C L^{-1} and then by 100-fold higher as the original recipe. When the carbon source was substituted by WPC40, a total organic carbon (TOC) assay was performed to measure its carbon content. Cultivation was performed in 250 mL Erlenmeyer in a 1:15 ratio of inoculum and medium. Nitrate ($NaNO_3$) content in the medium was substituted by ammonium (NH_4Cl) in equal mols (17.6 mmol-N L^{-1}) as in the medium.

Sealed vials were sparged with nitrogen to ensure initial anaerobic conditions. Open bottles had a sterile cotton stopper to allow gas exchange. The experiment lasted for 10 days. An additional experiment to verify the effect of organic carbon source in biomass and pigment concentration was performed in microplates using WPC40 and acetate. Different concentrations of organic carbon (0.221, 0.947, 2.524, 6.31, 12.621 to 25.241 mM) in the forms of acetate and WPC40 replaced the carbon concentration in BG-11 medium resulting in C:N:P ratios of 1:101:1, 5:101:1, 14:101:1, 36:101:1, 72:101:1, 144:101:1. Absorbance was measured over the visible light spectrum using a microplate reader (Synergy™ HTX, BioTek, USA). The experiment lasted 10 days.

Table 1. Set up experiments for photolitoautotrophic biomass growth with different nitrogen sources and gas exchange conditions and photoorganoheterotrophic microorganisms' selection under different carbon source sections. Table 1 summarizes the experiments regarding their organic carbon and nitrogen source, aerobic or anaerobic conditions, and carbon concentration. An initial organic carbon concentration of 0.189 mM was equivalent to the inorganic carbon concentration in the BG-11 medium whereas, conditions with a concentration of 18.9 mM C L^{-1} were 100-fold BG-11 conditions. The analysis encompassed solid series, cell counting and viability, pH measurements, chlorophyll extraction, nutrient consumption, and microscopy.

Conditions	Organic carbon source	Nitrogen source	Gas exchange	Carbon concentration
A_oN	Acetate	Nitrate	Aerobic	0.189 mM
A_oA		Ammonia		
A_xA				18.9 mM
A_oA_{100}				
A_xA_{100}				
CW_oN	WPC40	Nitrate	Aerobic	0.189 mM
CW_xA_{100}		Ammonia	Anaerobic	18.9 mM
L_oA	Lactose	Ammonia	Aerobic	0.189 mM
L_xA				
L_oA_{100}				18.9 mM
L_xA_{100}				

2.2.3 Photoorganoheterotrophic growth of microalgae in a continuous-flow photobioreactor

An initial photolitoautotrophic regime on BG-11 medium was imposed on microalgae until growth stabilization in batch mode with a 0.24 $^{-1}$ dilution rate. This experiment lasted 12 days. Due to incomplete carbon dissolution, BG-11 was then heated to 90°C leading to complete carbon dissolution. Biomass growth and nutrient consumption this time was monitored for 7 days.

The reactor regime changed to photoorganoheterotrophic conditions using 18.9 mmol C L^{-1} of acetate in continuous-flow mode as established in section 2.2.2. The experiment was scaled up in a 3.5 L continuous-flow stirred-tank photobioreactor (CSTR-PBR) with a 2 L working volume. An initial photolitoautotrophic regime on BG-11 medium was imposed on microalgae until growth stabilization in batch mode. Additional nutrients were provided according to BG- 11 medium, except for the nitrogen source that was replaced by NH_4Cl in equal mols (17.6 mmol-N L^{-1}) as stated in the medium.

Both reactor regimes were continuously irradiated with a 75 W white light jacket (400- 700 nm, PhotoBioSim, Designinnova, India) at 96 µmol photons m^{-2} s^{-1} and run at a mesophilic temperature of 35°C. Photobioreactor in batch mode started with a dilution rate of 0.24 d^{-1}. Hence, the initial dilution rate of the chemostat was also 0.24 d^{-1} changing to 0.17 d^{-1} after a few days. Argon was sparged at 50 mL min^{-1}. Gas flow and off-gas CO_2 and O_2 measurements were monitored. Polyisocyanurate (PIR) boards were used to serve as an isolation hood so no external light interfered with CSTR- PBR light conditions. An anchor paddle provided CSTR_PBR mixing at 120 r.p.m. and prevented biofilm formation. Biomass growth was monitored daily until a steady state was reached with nutrient consumption afterward. **Figure 1** shows the reactor setup and the isolation hood.

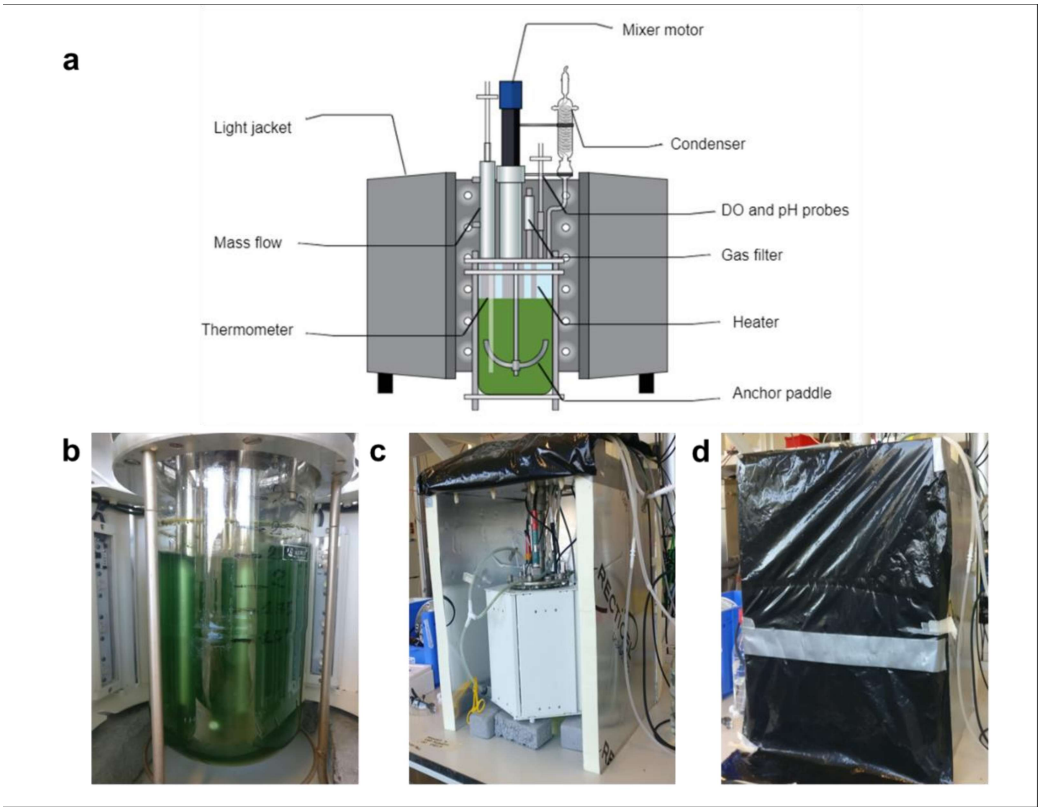


Figure 1 a. Photobioreactor set up with a light jacket surrounding it. The temperature was kept at 35°C and argon was injected in the reactor. The incoming gas was controlled by a mass flow controller, while the off-gas was cooled by a condenser and filtered with a cotton filter before it was sent to the off-gas analyzer. DO, temperature, and pH were continuously measured in all set-ups. For the chemostat regime, influent and effluent flows were regulated by pumps. Acid and base were dosed to maintain the pH at 7. **b.** Picture of the reactor the a and light jacket. **c**. Picture of the PIR-boards hood built to avoid the influences of external light and temperature. **d.** PIR-boards hood had a black plastic cover that enabled access and hinder the entry of external light.

2.3 Physical and chemical analysis

2.3.1 General analysis

The following analysis was common to most experiments, or else specified. Ammonium, nitrite, nitrate, and phosphate content were either measured by manual spectrometric method (ISO 7150-1:1984) (ISO, 1984) or by discrete analysis systems with photometric detection (ISO 15923-1:2013) (ISO, 2013).

Total organic carbon (TOC) was measured by combustion catalytic oxidation method at 720°C – standard methods 5310B (APHA, 2005) (APHA, 2005), and total nitrogen (TN) was also analyzed at 720°C by catalytic thermal decomposition

method/chemiluminescence – Standard Method 5310B(APHA, 2005). Both analyses were performed on the first and last day of the experiments.

In most experiments, dissolved oxygen (DO) and pH were measured daily by electrometry and potentiometry, respectively (APHA,2005) (APHA, 2005). Gas flow was regulated by a mass flow controller (0154 Microprocessor Flow Control & Read Out Unit, Brooks Instruments, USA). Argon was used as the off-gas carrier at 50 mL min^{-1} and CO_2 and O_2 off-gas measurements were performed by an online gas analyzer (NGA 2000, Rosemount, USA).

Solids series were analyzed according to Standard Method 2540 (APHA, 2005)(APHA, 2005). For mixed cultures observation, about 1 µL of unstained samples were fixed with alcohol 70% (v/v) to stop motility and observed by phase contrast microscopy using Axioplan 2 (Zeiss, Germany).

2.3.2 Acetate and carbohydrates consumption

VFA (acetate) and sugar (lactose, glucose, and galactose) consumption were monitored daily. A sample containing a volume of 2 mL was filtered with a 0.45 µm pore size disposable sterile polytetrafluoroethylene polymer (PTFE) syringe filter with needles for filtration. About 1 mL of sample was then detected by high-performance liquid chromatography (HPLC - Waters, USA), with a BioRad Aminex separation column (Biorad, USA HPX-87H) and a BioRad Cation-H refill cartridge guard column. Chromatographer was equipped with a 717 plus Autosampler, a 2489 UV/Vis Detector, and a 2414 Refractive Index Detector (Waters Corporation, USA). The mobile phase was a solution of 1.5 mM phosphoric acid (H_3PO_4) at 60°C and a flow rate of 0.6 mL min^{-1}. Glucose consumption was also monitored according to the phenol-sulphuric method described by Dubois (1956).

2.3.3 Cell viability and biomass analysis

Cell viability was monitored by methylene blue (MB) as proposed by Bicas et al.(2015). Two samples of 3-5 mL were taken from the culture, where one of them was heated to 90°C in a water bath for 5 minutes. After the heated sample reached room temperature, both samples were centrifuged for 3 minutes at 4000 g min^{-1}.

The supernatant was discarded and pellet resuspended into 4 mL of methylene blue (MB) solution (85 µM of MB in phosphate buffer solution 0.1 M, pH 7.4), followed vortexing and centrifugation at 4000 g min^{-1}. Supernatant was read at 664 nm and compared to the absorbance of MB solution at the same wavelength. The uptake of MB was measured with **equation 1**:

$$MB_{uptake} = 14.86 * 4 * \left(A_{664}^{solution} - A_{664}^{sample}\right) \quad \text{(Eq. 1)}$$

Cell viability was given by considering the ratio between the MB uptake of both raw and boiled samples.

Biomass concentration was determined by optical density at 750 nm (A_{750}) and the constant term of calibration (q) using a spectrophotometer (DR3900, Hach Lange, USA). A calibration curve was created for conversion of absorbance to grams of biomass per liter using **equation 2**:

$$C_{biomass}\,(g\ VSS\ L^{-1}) = m * A_{750} + q \quad \text{(Eq. 2)}$$

Other conversions such as maximum growth rates, yields, production rates, and biomass-specific rates of substrate were calculated according to the following **equations 3** to **6**, respectively:

$$\mu_{max}(d^{-1}) = \frac{\ln(C_{biomass,2}) - \ln(C_{biomass,t1})}{t_2 - t_1} \quad \text{(Eq. 3)}$$

$$Y_{VSS/C}(mgVSS\ mgC^{-1}) = \frac{C_{biomass,2} - C_{biomass,1}}{C_{Carbon,2} - C_{Carbon,1}} \quad \text{(Eq. 4)}$$

$$P_{VSS}(mgVSS\ d^{-1}) = \frac{C_{biomass}}{Q} \quad \text{(Eq.5)}$$

$$q_S(mg_{acetate}mgVSS^{-1}\ d^{-1}) = \frac{C_{acetate,2} - C_{acetate,1}}{P_{VSS}} \quad \text{(Eq. 6)}$$

2.3.4 Pigments extraction and quantification

An adaptation of Shoaf and Lium (1976) was used for pigment extraction and quantification. Samples of 2.5 mL were collected, and centrifuged at 13,300 g min^{-1} for

3 minutes. Supernatant was discarded and the pellet was resuspended in a 1:1 (v/v) solution of dimethyl sulfoxide (DMSO) and 80% acetone (80%). Eppendorffs containing samples were closed with parafilm to avoid evaporation and covered in foil paper to avoid any light interference. Samples were placed at 4°C for 24 hours. The following day, samples were centrifuged (13,300 g min^{-1}, 3 minutes) and the absorbance spectrum (350 to 750 nm, DR3900, Hach Lange, USA) was measured. A DMSO:acetone solution was used as blank. Measurements were performed in a quartz cuvette to avoid any fog common on polystyrene disposable cuvettes.

Chlorophylls a, b, and carotenoid contents were calculated according to Wellburn(Wellburn, 1994). Specific sets of equations were used to calculate contends in 80% acetone solution (**equations 7, 8**, a nd **9**) and DMSO (**equations 10, 1,1,** and **12**). After calculation, the result was given as an average of results from both solvents. According to Arnon et al.(1949) and Speziale et al.(1984), averaging results is plausible given the negligible difference between equations.

Acetone

$$C_a = 12.21 * A_{663} - 2.81 * A_{646} \quad \text{(Eq. 7)}$$

$$C_b = 20.13 * A_{646} - 5.03 * A_{663} \quad \text{(Eq. 8)}$$

$$Car = (1000 * A_{470} - 3.27 * C_a - 104 * C_b)/198 \quad \text{(Eq. 9)}$$

DMSO

$$C_a = 12.19 * A_{665} - 3.45 * A_{649} \quad \text{(Eq. 10)}$$

$$C_a = 12.19 * A_{665} - 3.45 * A_{649} \quad \text{(Eq. 11)}$$

$$Car = (1000 * A_{480} - 2.14 * C_b - 70.16 * C_b)/220 \quad \text{(Eq. 12)}$$

In addition to pigment extraction, a wavelength scan over the visible light spectrum (330 to 900 nm) was performed with a spectrophotometer (DR3900, Hach, Germany) to monitor the evolution of pigment and biomass content over the experiment.

2.4 Microbial composition gene amplicon sequencing analysis

DNA extractions for 16S and 18S rRNA were performed to identify prokaryotes and eukaryotes microorganisms in different phototrophic regimes (photolitoautotrophic, photolitoheterotrophic, and photoorganoheterotrophic) in batches and CSTR-PBR with DNeasy® UltraClean® Microbial Kit (QIAGEN, Germany).

Both DNA extractions' concentration and quality were measured by fluorescence using an Invitrogen Qubit 4.0 (Thermo Fisher Scientific, USA) and 200 µL samples of concentrated DNA (ranging from 13.9 to 95 ng μL^{-1}) were stored at - 20°C. Novogene Co., Ltd. (China) was responsible for the amplicon sequencing. At Novogene, DNA concentration and purity were evaluated on 1% agarose gels, and depending on the concentration, samples can be diluted to 1 ng μL^{-1} with mili-Q water.

Selected regions for 16S rRNA (V3-V4) and 18S rRNA (V4) were amplified by polymerase chain reaction (PCR) for library preparation. For 16S rRNA, the regions V3- V4 had the primer forward 341F (5'-CCTAYGGGRBGCASCAG-3') and reverse 806R (5'- GGACTACNNGGGTATCTAAT-3') according to Takahashi et al.(Takahashi et al., 2014). In 18S rRNA amplification, region V4 had the primer forward 528F (5'-GCGGTAATTCCAGCTCCAA-3') and reverse 706R (5'-AATCCRAGAATTTCACCTCT-3') according to Cheung et al.(Cheung et al., 2010) and Lutz et al. (Lutz et al., 2015)

Sequencing libraries were created using NEB Next Ultra ™ DNA Library Prep Kit for Illumina® (QIAGEN, Germany). Library quality was evaluated with a Qubit 2.0 Fluorometer (Thermo Scientific, USA) and Agilent Bioanalyzer 2100 system (Agilent, USA). The library was then sequenced on an Illumina platform (Illumina, USA) and 250 bp paired-end reads were generated.

PCR reactions were performed by 30µL reactions using 15µL of Phusion® High-Fidelity PCR Master Mix (New England Biolabs, USA), 0.2 µM of primers
Set, and about 10 ng of template DNA. Thermal cycling had an initial denaturation (98°C, 1 minute), followed by 30 cycles of denaturation (98℃, 10 seconds), annealing (50℃, 30 seconds), elongation (72℃, 1 minute,) and a 5 minutes step at 72℃. PCR products were quantified and qualified, then mixed in equidensity ratios. The mixed PCR products were purified with a GeneJET Gel Extraction Kit (Thermo Scientific, USA).

Data analysis constituted of identification of nucleotides (base calling), removal of chimeric sequences, and generation of operational taxonomic units (OTU) with ≥ 97% identity. OTUs were also analyzed using the SINA (v.1.2.11) aligner based on the global SILVA alignment for rRNA genes.

3 Results and Discussion

3.1 Photolithoautotrophs are set in their ways

3.1.1 Biomass growth and cell viability: thriving in BG-11

Photolithoautotrophic culture on BG-11 and gas exchange allowance displayed an increase in three units of initial pH of 7.0. Usually, carbon dioxide dissolution decreases medium pH and carbonic acid formation. Consequently, bicarbonate is formed with hydrogen ions dissolution and subsequent carbonate ion formation. However, the increase observed in pH can result from hydrogen ions absorption during microalgae photosynthesis and denitrification given the non-axenic mother culture. Increased medium turbidity and reduction in nitrogen and phosphorus levels indicated microorganisms' absorption for anabolic processes.

Biomass concentration was verified by dry weight measurement, and cell viability. Despite the pH increase, all measurements indicated biomass growth. Dry weight as volatile suspended solids (VSS) were of about 650 mg VSS L^{-1}, indicating an increase of about 13-fold the initial biomass concentration. Methylene blue (MB) cell viability measurements showed a decrease in viable cells after the tenth day reaching 17% by the end of measurements. Decrease in
absorbance is proportional to decrease in cell viability. **Figure 2** shows biomass concentration increase and cell viability.

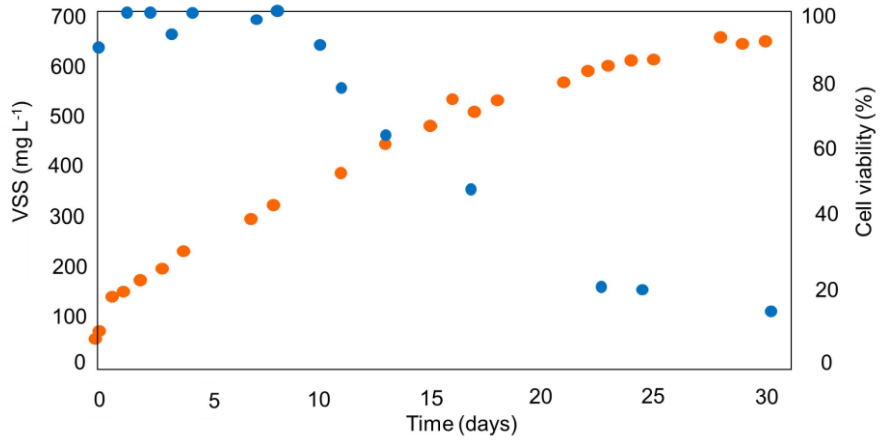


Figure 2 Photolitoautotrophic culture biomass concentration (●) and cell viability (●).

3.1.2 Pigment content increase is consistent with biomass growth

Pigments were identified in the following culture absorbance spectra peaks: 440, 630 and 680 nm which corresponded to chlorophyll *a* and *b*. Sample absorbance spectrum are shown in **figure 3**. The solvents used for pigment extraction, DMSO and acetone. The blank used was distilled water. Pigments absorbance peaks might have been slightly lowered and shifted to the left due to the difference on composition of medium and blank.

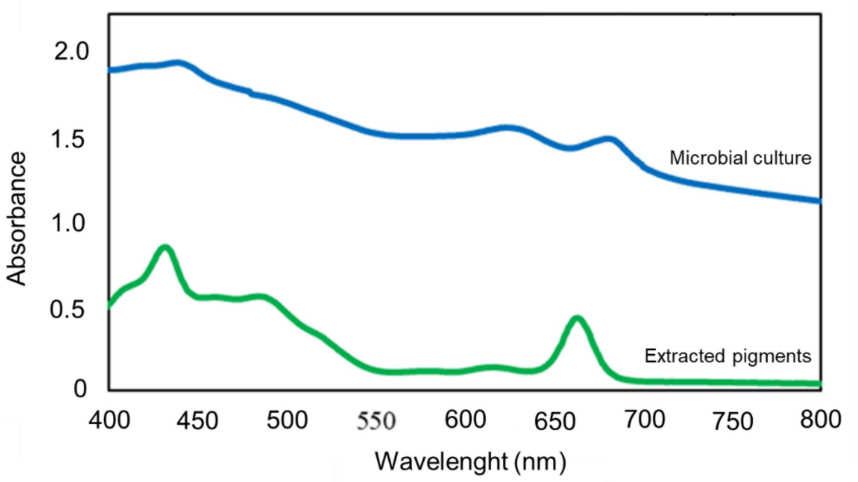


Figure 3 Absorbance spectra of the microbial culture and pigments extracted with DMSO/Acetone measured after 13th day of cultivation. The bottom curve in green regards the extracted pigments, whereas the upper curve refers to the microbial culture.

Pigments content was directly proportional to biomass concentration and increasing linearly until the last measurement after the exponential growth phase on the 16th day. Biomass specific pigment content also increased, as shown in **table 2**.

Table 2 Pigments production according to their production rate, biomass specific content and the maximum biomass specific content. *Their production rate was constant after the 5th day of measurement. ** The maximum biomass specific content refers to the end of the experiment. *Chl a* stands for chlorophyll a, *Chl b* for chlorophyll b and *Car* for carotenoids.

	Chl *a*	**Chl *b***	**Total Car**
Production rate (μg L^{-1} d^{-1})	212	143	103
Biomass specific content (μg mg VSS^{-1}) *	10.3	1.2	4.3
Max biomass specific content (μg mg VSS^{-1}) **	14.7	4.8	6.2

3.1.3 Changes in carbon and nitrogen sources are not beneficial to photoaautolitotrophic culture

Carbon and nitrogen changes in mother culture with BG-11 medium were proposed to improve cell growth and biomass concentration. Initially, incomplete medium carbonate dissolution, which was thought to hinder biomass growth, was then addressed by heating the solution of Na_2CO_3 before adding it to the medium. However, carbonate dissolution by heat caused a decrease of 48% in cell productivity and 33% in biomass concentration within the first 10 days of experiment.

In addition, a drastic increase in pH overnight from 7.0 to 10.0 indicated that most microorganisms in the photolitoautotrophic community were also intolerant to alkaline pH. The same decrease in cell productivity, biomass concentration happened when replacing the nitrogen source from nitrate ($NaNO_3$) to ammonium (NH_4Cl). However, it could be observed a decrease in pH. The aims behind these changes were to limit the action of denitrifiers and boost acidogenic fermentation, but they also led to lower biomass concentration. The proposed modifications in
BG-11 medium did not show positive changes in photolitoautotrophic cultures. **Table 3** shows the alterations in cell growth and biomass concentration consequence of changes in nitrogen and carbon sources.

Table 3 Variations in μ_{max}, biomass increase and pH evolution according different media and aerobic conditions. The number of days in which pH reached a new value are in parentheses. Initial BG-11 pH is 7.0. (Undiss) stands for undissolved and (Diss) for dissolved.

	Undiss. CO^{2-} NO_3	**Diss. CO^{2-} NO_3**	**Diss. CO^{2-} NH_3**	**Diss.CO^{2-} NH_3**
μ_{max} (d^{-1})	0.97	0.47	0.40	0.12
Final pH and period	10 (15 d)	10 (1 d)	5.2 (3 d)	7.7 (6 d)
Biomass (mg VSS L^{-1})	600	200	90	15

3.1.4 Visualization and identification of photolitoautotrophic cultures revealed microorganism's diversity

Observations in phase-contrast microscopy revealed great microorganism diversity with an abundance of green round-shaped cells of 3-4 µm diameter, mostly in aggregates. Other types of microorganisms were not as plentiful. **Figure 4** shows the composition of microorganisms in photolitoautotrophic cultures.

As for the identification of microbial populations, 16S rRNA gene amplicon sequencing confirmed microorganisms diversity as seen through phase-contrast microscopy. Cyanobacteria, mostly Cyanobium PCC-6307 sp. and Synechocystis PCC-6803 sp., corresponded to 10-20% of prokaryotic community. The phototrophic purple non-sulfur bacteria (PNSB) *Rhodobacter* sp. corresponded to 10% of initial community but they were outcompeted along the cultivation period.

All bacteria presented in initial and final cultivation were gram-negative and most of them were able to oxidize nitrate. Denitrifier bacteria are mostly facultative anaerobic chemoorganoheterotrophic microorganisms. In the BG-11 photolitoautotrophic mother culture, $NaNO_3$ was the nitrogen source. This suggests that these bacteria were able to also use the inorganic nitrogen present in the medium and the dissolved oxygen as terminal e-acceptor.

In the 18S rRNA gene amplicon sequencing, in the final sample there was a visible decrease of green microalgae genera (i.e., *Scenedesmus* sp., *Desmodesmus* sp. and

Trebouxioupheceae) found in the initial culture to an increase of unidentified Chlorophyceae. The increase of the genus Vermamoeba indicates lack of competition among microorganisms or even their predatory activities which enabled other genus of bacteria to thrive in throughout culturing. **Figure 5** shows the prokaryotic and eukaryotic diversity between initial and final samples of mother-culture.

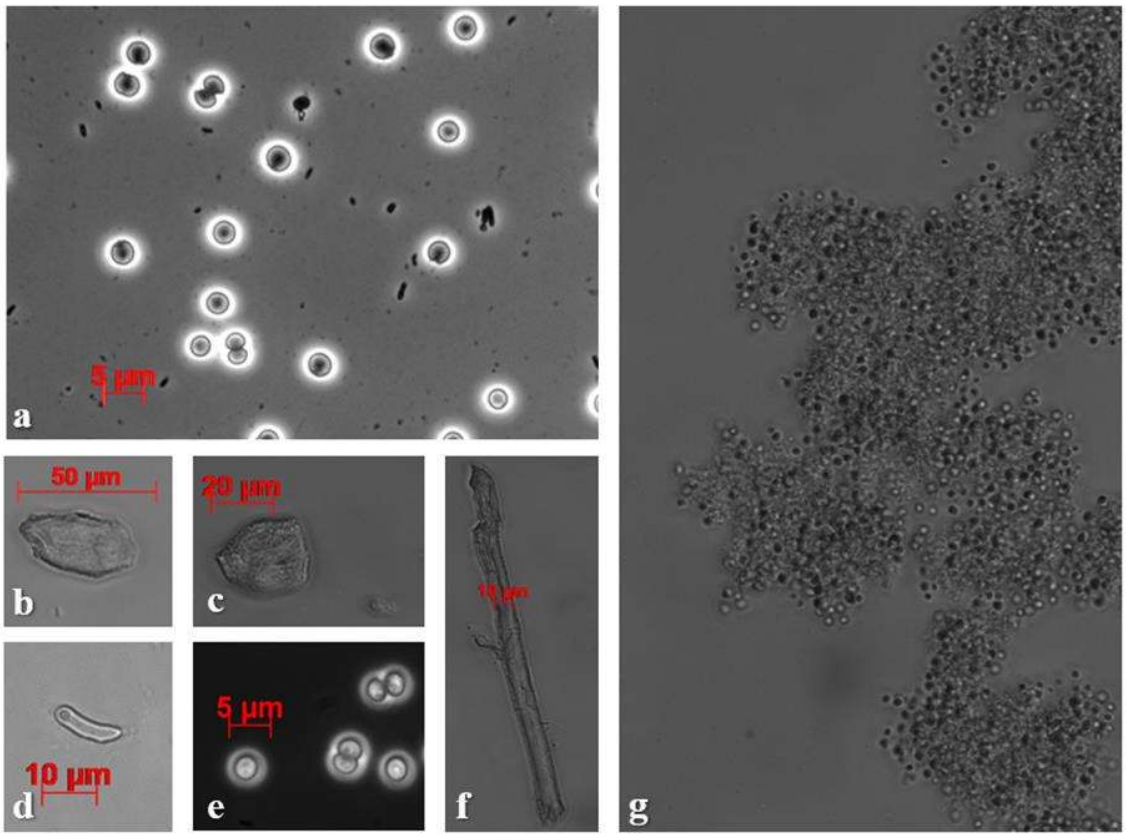


Figure 4. (***a-g***) Photolitoautotrophic culture bacterial community. Images *a*, *e* and *g* depicted the most abundant 3-4 µm diameter round-shaped cells. They tend to form aggregates as shown on image ***g***. Larger microorganisms were found on images ***b***, ***c***, ***d*** and ***f***, whereas smaller bacteria can be observed on the background of image ***a***.

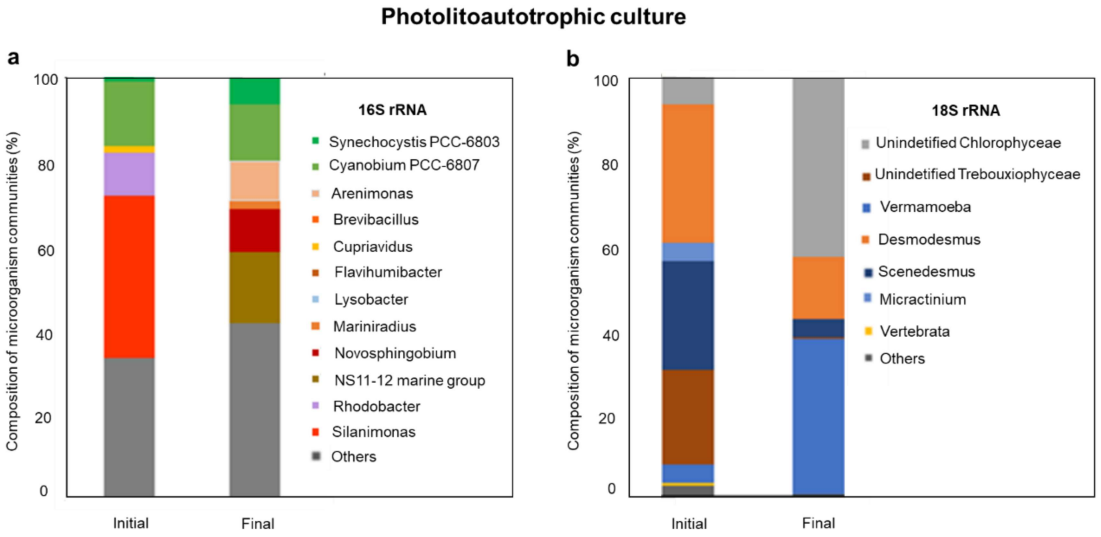


Figure 5 Composition of microbial communities. Figure **A** shows the results from 16S rRNA amplicon gene sequencing region V3-V4 and figure **B**, the results from 18S rRNA amplicon gene sequencing region V4. Only genera comprising more than 2% of the composition of communities are depicted in the graph. The remaining were classified as 'others'.

3.2 Influence of different organic carbon sources in photoorganoheterotrophic microrganisms selection

3.2.1 High concentration of organic substrates enables green phototrophs selection in mixed cultures

The medium chosen for mixed culture enrichment was BG-11 and substitution of inorganic carbon source to organic ones (e.g., WPC40, lactose and acetate) was done with 0.189 mM C L^{-1} and with 100-fold the concentration in the medium, 18.9 mM C L^{-1}. Physico-chemical, morphologic and ecologic patterns displayed by 0.189 mM C L^{-1} open bottle cultures grown on acetate and WPC40 as carbon sources, and $NaNO_3$ as nitrogen source were similar to the photolitoautotrophic culture.

In both 0.189 mM C L^{-1} close and open bottles batches, exchanging nitrogen source led to variations in cell growth patterns. Open bottles batches with acetate and lactose as organic carbon source had 0.46 d^{-1} and 0.44 d^{-1} growth rates, respectively. These rates were similar to the 0.4 d^{-1} growth rate of photolitoautotrophic conditions. A similar microorganism community pattern to photolitoautotrophic culture can be observed in **figure 6**. An additional pH decreased culture inorganic carbon uptake,

since atmospheric CO_2 absorption was limited with subsequent carbonate saturation. Consequently, it has halted biomass growth.

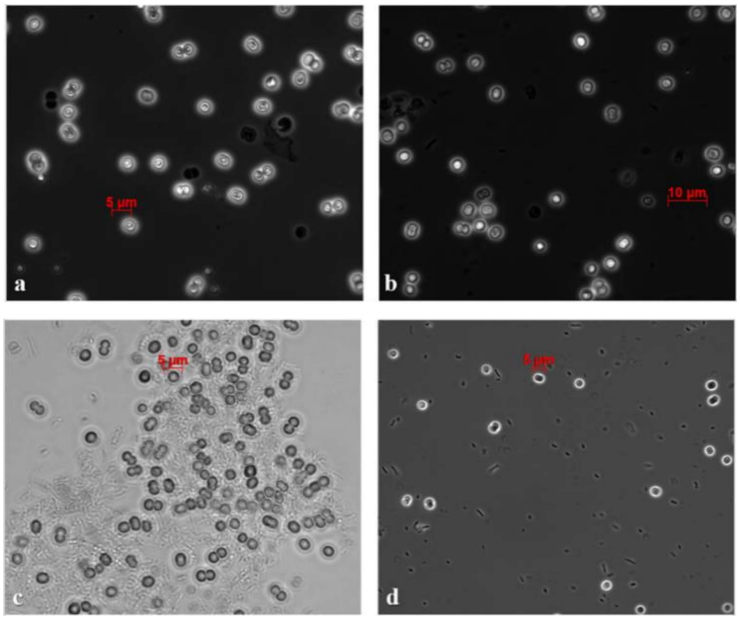


Figure 6 Microscope images from photomixotrophic cultures. Figures *a* – *d* show AxA, LoA, AxA_{100} and LxA_{100} cultures, respectively. Small phototrophic cells (3-4 µm diameter) were identified as well as smaller bacterial cells.

Anaerobic cultures, presented the highest pigment content than aerobic ones. Since the oxygen availability resulted from photosynthesis water oxidation, heterotrophic bacterial growth was disadvantageous. Hence, selection of green phototrophs was possible as some of the phototrophic microorganisms present in the photolitoautotrophic culture (e.g., *Chlorella* sp., *Micractinium* sp., *Scenedesmus* sp., *Desmodesmus* sp., *Synechocystis* sp.) display mixotrophic metabolisms. Some studies demonstrated the possibility of axenic microalgal growth in treated cheese whey (Blier, Lalibert, & de la Notie, 1995; Girard et al., 2014). However, symbiotic relationships in mixed culture are still not explored to their fullest.

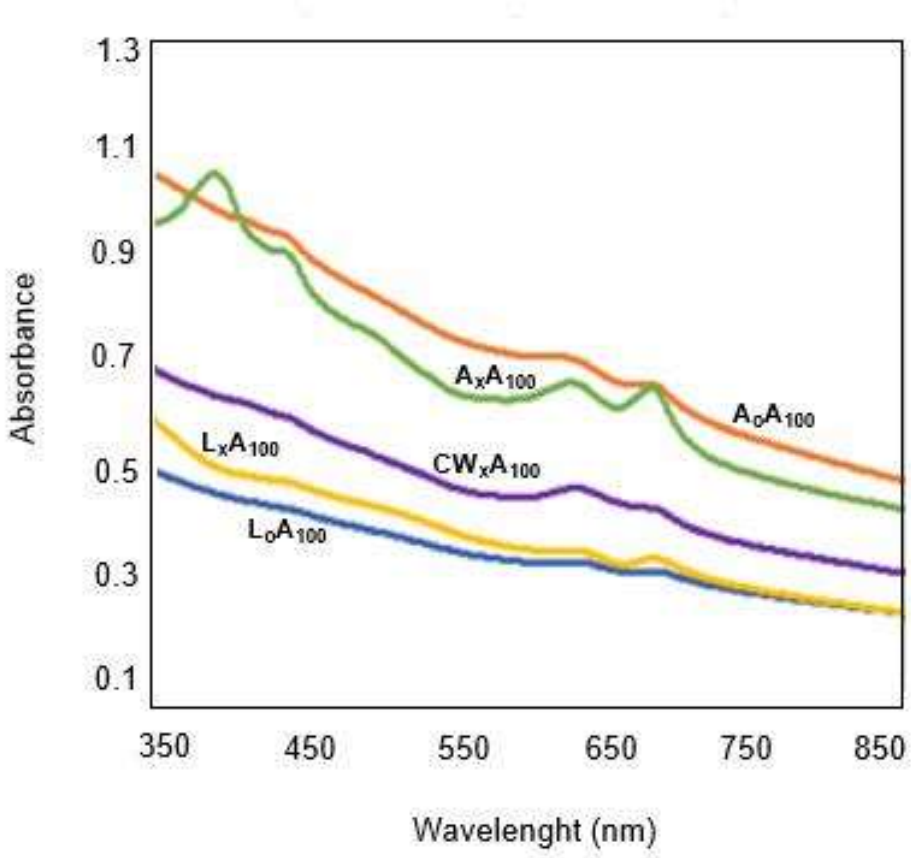


Figure 7 Absorbance spectra curves of A_oA_{100} (—), A_xA_{100} (—), L_oA_{100} (—), L_xA_{100} (—) and $CWxA_{100}$ (—) cultures. Peaks related to the presence of pigments are more visible in sealed bottles. Biomass content (A_{750}) is similar or higher in open bottles.

As seen in **figure 7**, anaerobic culture on WPC40 and ammonium (CWxA) displayed the highest μ_{max} of all substrates but did not grow as much as cultures in acetate. This can be due to the presence of ordinary heterotrophic organisms together with green phototrophs. The increase in biomass can also be justified by the additional inorganic nutrients for uptake, such as nitrogen and phosphorus that was inherent in CWxA but not in other substrates. Studies on WPC40 in open bottles did not present significant growth (data not shown). Growth rates for different carbon and nitrogen sources and gas exchange allowance are in **table 4**.

Table 4 Main characteristics of the cultures grown on ammonia and 18.9 mM-C in aerobic (o) and anaerobic (x) conditions. «+» and «-» signs indicate an increase and a decrease in pH, respectively. “Not available (n.a.)” refers to cultures in which the pigment content was not evaluated.

Experiment	L_OA_{100}	L_XA_{100}	A_OA_{100}	A_XA_{100}	CW_XA_{100}
μ_{max} (d^{-1})	0.29	0.14	0.71	0.25	0.56
Yield (mg VSS mg-C^{-1})	0.34	0.65	0.77	1.15	0.82
C_{max} (mg VSS L^{-1})	121	111	189	170	140
C consumption (%)	92	28	96	52	46
pH (final)	4.5	4.5	9.0	8.5	4.6
Chl_a (µg mg VSS^{-1})	n.a.	11.1	n.a.	20.3	8.6
Chl_b (µg mg VSS^{-1})	n.a.	9.3	n.a.	13.8	9.5
Car (µg mg VSS^{-1})	n.a.	3.3	n.a.	5.3	2.3

BG-11 medium, a standard medium for the cultivation of cyanobacteria and microalgae, is highly abundant in nitrogen. The C:N:P ratio supplied by the medium is 0.189:101:1. This is significantly imbalanced substrate considering the algal biomass theoretical composition of $C_{106}H_{263}O_{110}N_{16}P$ (Redfield, 1934). The excess of nitrogen in this medium is simply used to grow photolithoautotrophs in small batches using atmospheric CO_2 as additional carbon source.

Carbon, nitrogen, and phosphorus were not a limiting factor in both aerobic and anaerobic cultures. The same could be observed in the C:N:P experiment. However, biomass growth with a carbon concentration of 2.524 mM (C:N:P 36:101:1), showed similar absorbance peaks as the photolitoautotrophic culture. Since nitrogen and phosphorus were a fixed constant, carbon dictated both biomass and pigment concentrations. We can infer that the medium at a C:N:P ratio of 36:101:1, the carbon available was the amount required for biomass and pigment production. The same goes for higher C:N:P ratios. Perhaps, the carbon absorbed was closer to the optimal C:N:P ratio where the remaining carbon was not absorbed by green phototrophs. **Table 5** summarizes the results.

Table 5 Variation of the maximum biomass (Bms) growth (A_{750}), chlorophyll *a* content (A_{680}) and carbon content, and therefore with the C:N ratio.

C (mmol L^{-1})	C:N:P ratio	Cheese whey		Acetate	
		Bms (A_{750})	Chl (A_{680})	Bms (A_{750})	Chl (A_{680})
0.22	1:101:1	0.29	0.37	0.83	0.92
0.95	5:101:1	0.54	0.95	0.90	1.25
2.52	14:101:1	0.76	1.59	0.95	1.62
6.31	36:101:1	1.2	2.33	1.13	2.37
12.62	72:101:1	1.05	1.48	1.11	1.60
25.24	144:101:1	1.11	1.59	0.97	1.75

Overall, acetate proved to be the most suitable substrate in terms of biomass and pigment concentrations. All chosen organic substrates, WPC40, lactose and acetate, usually have acidic pH. When carbon concentration increased to 18.9 mM C L^{-1}, acetate pH increased to 9.0. Acetate cultures in aerobic conditions had a higher pH probably because of atmospheric carbon uptake that allowed a buffer system with some extra carbon availability. In that sense, biomass production could be a result from both photolitoautotrophic and photoorganoheterotrophic metabolisms. As for the acetate in anaerobic conditions, only the photoorganoheterotrophic regime was applied. Since pH was slightly lower than the one on aerobic conditions, we may say that pH was not the limiting factor. The decrease in growth rate in aerobic and anaerobic lactose-ammonium cultures (LoA_{100} and LxA_{100}) as well as $CWxA_{100}$ were directly proportional to pH decrease.

So, rather than just pH influence, the suitability of acetate over the other substrates can also be explained by (*i*) efficiency of microorganisms under anaerobic conditions. Besides not having competition with ordinary OHOs, acetate culture under anaerobic conditions microorganisms present a higher growth yield, suggesting that they are able to utilize their resources more efficiently, whereas acetate culture in aerobic conditions microorganisms have a higher growth rate at the rapidly expense of the substrate, (*ii*) the readily uptake of acetate in the glyoxylate cycle. This cycle enables growth on acetate since it bypasses the decarboxylation of the tricarboxylic acid cycle (TAC). Acetate is converted into two molecules of acetyl-CoA by acetyl-CoA synthetase.

Acetyl-CoA can be either a precursor for fatty acids biosynthesis (e.g. chain elongation) or further transformed into succinate for both anabolic and catabolic processes.

3.3 Transition of metabolic regimes and substrates in a SBR-CSTR

3.3.1 Photolitoautotrophic acclimation for selection for green phototrophs under batch mode

A stirred-tank photobioreactor was initially operated in batch mode for acclimation of photolitoautotrophic culture prior to transition of substrate and metabolic regime. During the first six days, a similar growth rate (0.99 d^{-1}) to the one with undissolved carbonate flasks was observed. When carbonate minerals were fully dissolved growth was limited, contrary to what was observed in the undissolved carbonate flasks. This can be due to complete carbon consumption in BG- 11 medium and the inability of atmospheric carbon uptake giving the anaerobic mode. The fact that the gas flow consisted of argon, limited any possibility of carbon source or inorganic nutrients entry in the system.

Nitrogen and phosphorus measurements, (>130 mg $N\text{-}NO_3^-$ L^{-1} and > 5 mg $P\text{-}PO_4^{3-}$) confirmed that the nutrients available in BG-11 were sufficient to sustain microalgae growth. Giving the initial high substrate concentration in batch regimes, microorganisms were selected according growth rate. **Figure 8** compares photolitoautotrophic biomass growth in different batch scales.

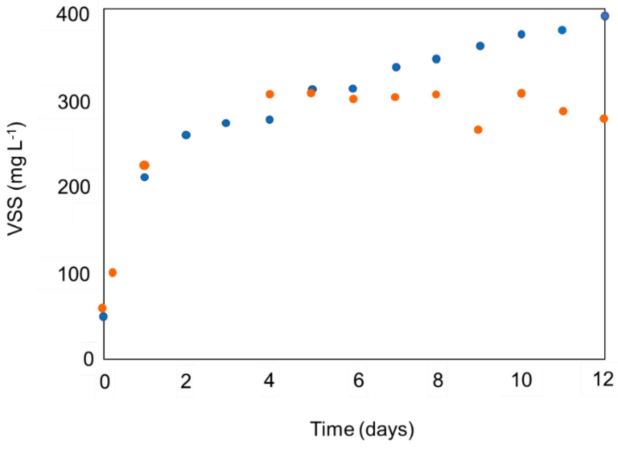


Figure 8 Biomass growth in shake-flask culture (●) and photobioreactor – batch mode (●). Growth in the photobioreactor was limited after six days due to atmospheric carbon dioxide dissolution limitation.

3.3.2 Lower dilution rate favors green phototrophs selection in a chemostat

Acetate replace BG-11 on the transition from photolitoautotrophic regime to a photoorganoheterotrophic one. An initial dilution rate of 0.24 d^{-1} displayed a biomass concentration of 41 mg VSS d^{-1}. The selection of this specific dilution rate was a result of the maximum growth rate of 0.46 d^{-1} observed in the aerobic acetate-ammonium and 0.189 mM C L^{-1}, as in BG-11. However, at this dilution rate the culture had a few phototrophic cells which can be seen in the in the absorbance spectra of the sample, especially on the wavelengths corresponding to pigments (440, 630 and 680 nm). **Figure 9** shows the morphologic characterization of microorganisms community.

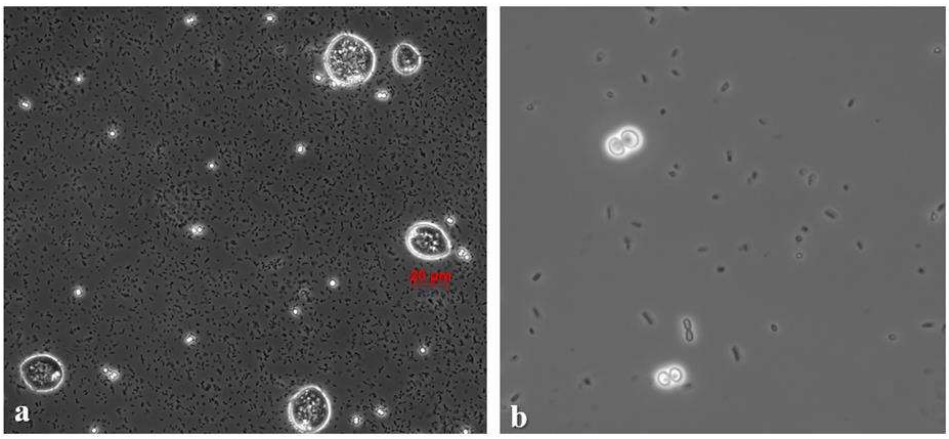


Figure 9 Microscope images of the photomixotrophic culture cultivated on acetate in the CSTR PBR. Image ***a*** was taken from the cultivation with a dilution rate of 0.25 d^{-1} and image ***b*** from the 0.17 d^{-1} dilution rate cultivation.

A different dilution rate of 0.17 d^{-1} was then selected based on the maximum growth rate of 0.25 d^{-1} observed anaerobic acetate-ammonium and 18.9 mmol C L^{-1} as the experiment in the previous section. The dilution rate alteration led to visible improvements as reactor presented a dark green content, an improved absorbance spectrum and an increase in biomass concentration from 86 to 125 mg VSS L^{-1}. Presence of ciliates and smaller bacteria was still visible in the culture although in less quantity than phototrophic cells as observed in **figure 9 *a***.

The dissolved oxygen in the culture increased from 0% to 2%. The carbon dioxide in the off-gas decreased from 0.085% to 0.058%, and the transition was oscillatory, indicating a positive symbiotic relationship with adequate retention time. A picture of the CSTR, spectra profile from batch mode and both dilution rates and biomass evolution can be seen on **figure 10**. **Table 6** depicts the CSTR growth parameters in both dilution rates.

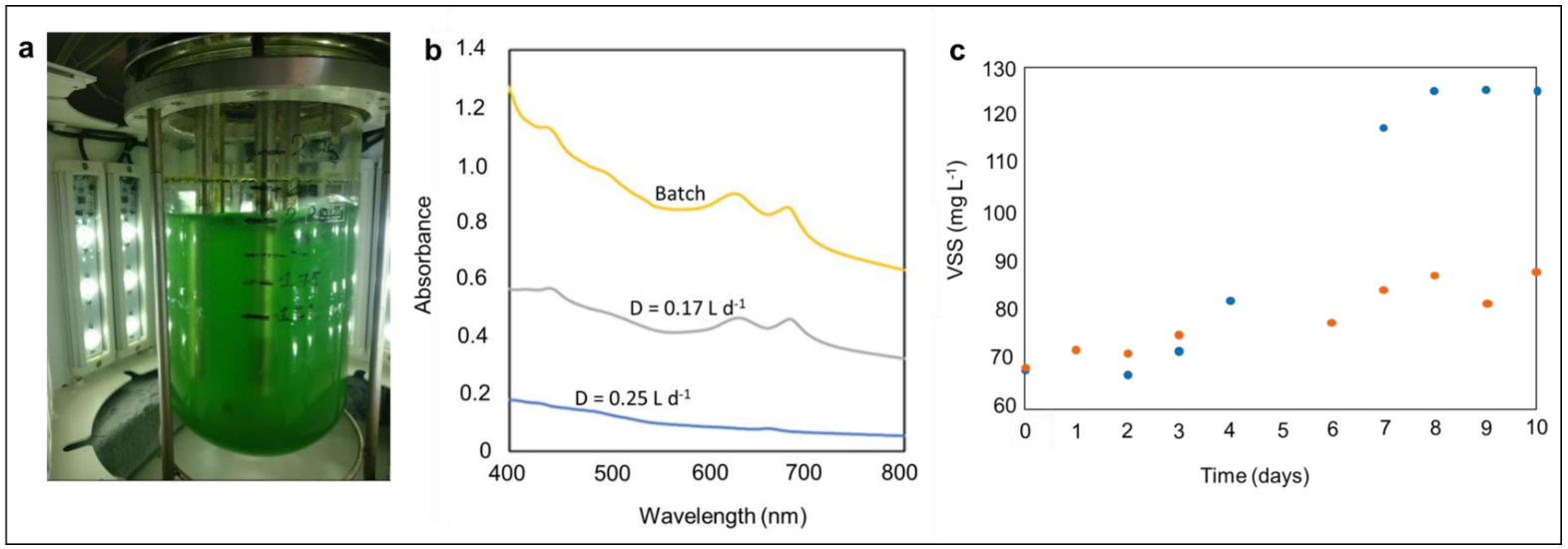


Figure 10 **a** CSTR PBR with a dilution rate of 0.17 d^{-1}, **b** Absorbance spectra of the microalgal cultivation on acetate in a CSTR with 0.17 d^{-1} and 0.25 d^{-1} dilution rates and in a batch (AxA_{b100}). Higher dilution rate caused phototrophic biomass wash out. At a lower dilution rate, absorbance peaks were identified at the same wavelengths as in the batch culture (AxA_{b100}). **c** Biomass growth at different dilution rates (0.25 d^{-1} and 0.17 d^{-1}). The 0.17 d^{-1} dilution rate allowed higher biomass growth inside the reactor. Dilution rate was the only different parameter between both experiments.

Table 6 Growth parameters of the mixed culture grown on acetate (18.9 mmol C L^{-1}), using ammonium as a N-source, in CSTR mode for two different dilution rates.

Dilution rate (d^{-1})	Yield (mg VSS mg C^{-1})	Carbon removal (%)	C_{VSS} (mg VSS L^{-1})	P_{VSS} (mg VSS d^{-1})	P_{CO2} (mL-CO_2 d^{-1})	q_s ($mg_{acetate}$ mg VSS^{-1} d^{-1})
0.24	0.45	93	86	41	62.6	1.30
0.17	0.66	95	125	45	39.6	1.38

4 Conclusions

This work aimed on the ecologic engineering of green photoorganoheterotrophic microalgal biomass growth for cheese whey full valorization. For that, we suggested the couple microalgae biomass growth process with cheese whey acidogenic fermentation processes given their potential 66.5 million m^3 y^{-1} production destined to lower aggregated-value products or depending on location, its discharge into water bodies leading to eutrophication. The following can be concluded:

1. Green phototrophs selection from channel surface water was successful and pigment content was directly proportional to biomass concentration.
2. Despite changing the nitrogen source from nitrate to ammonium, denitrifiers were able to metabolize both nitrogen sources and use the dissolved oxygen in the medium as electron acceptor.
3. In batch experiments, acetate was the most suitable organic carbon source for biomass and pigments production with a maximum growth rate of 0.25 d^{-1} and biomass concentration of 170 mg VSS d^{-1}, compared to lactose (0.29 d^{-1} and 111 mg VSS d^{-1}), and WPC40 (0.56 d^{-1} and 140 mg VSS d^{-1}). The higher growth rate presented in WPC40 can be a result of additional inorganic nutrients.
4. The uptake of acetate was is thought to take place via the glyoxylate cycle for chain elongation, given the absence of other carbon sources in the CSTR reactor.
5. Selection of green phototrophs were successful under chemostat regime with a lower dilution rate to prevent microalgae wash-out and out-competition with OHOs, displaying 125 mg L^{-1} of biomass concentration and 45 mg VSS d^{-1} of biomass production.
6. The use of argon as the off-gas carrier together with the presence of dissolved oxygen suggests a symbiotic relationship within the microbial community.

Results on the amplicon gene sequencing of batches and both chemostat dilutions are currently being assessed and will shed light on the behavior of green photoorganoheterotrophs in mixed cultures. In addition, acetate metabolism of potoorganoheterotrophs should be better understood in order to diverge their metabolism to the glyoxylate cycle and optimize the process for both upscaling and cheese whey full valorization.

5 References

Akthar, A. B. T., Yasar, A., Ali, R., & Irfan, R. (2017). Phytoremediation using aquatic macrophytes. In A. A. Ansari, S. S. R. Gill, G. Lanza, & L. Newman (Eds.), *Phytoremediation* (1st ed., pp. 1–514). Springer International Publishing. https://doi.org/10.1007/978-3-319-52381-1

Allen, M. M. (1968). Simple conditions for growth of unicellular blue-green algae on plates. *J. Phycol.*, *4*, 1–4.

Allen, M. M., & Stanier, R. Y. (1968). Growth and division of some unicellular blue-green algae. *J. Gen. Microbiol.*, *51*, 199–202.

Amit, & Ghosh, U. K. (2018). An approach for phycoremediation of different wastewaters and biodiesel production using microalgae. *Environmental Science and Pollution Research*, *25*(19), 18673–18681. https://doi.org/10.1007/s11356-018-1967-5

Ansari, A. A., Naeem, M., Gill, S. S., & AlZuaibr, F. M. (2020). Phytoremediation of contaminated waters: An eco-friendly technology based on aquatic macrophytes application. *Egyptian Journal of Aquatic Research*, *xxxx*. https://doi.org/10.1016/j.ejar.2020.03.002

APHA. (2005). *Standard Methods for the Examination of Water and Wastewater* (A. E. G. Andrew D. Eaton, Lenore S. Clesceri, M. A. H. Franson, Eugene W. Rice, Ed.; 21st ed.). American Public Health Association.

Aratboni, H. A., Rafei, N., Garcia-Granados, R., Alemzadeh, A., & Morones-Ramírez, J. R. (2019). Biomass and lipid induction strategies in microalgae for biofuel production and other applications. *Microbial Cell Factories*, *18*(178), 1–17. https://doi.org/10.1186/s12934-019-1228-4

Archer, R. H. (1998). *Whey products*. New Zealand Dairy Research Institute. https://nzic.org.nz/app/uploads/2017/10/3G.pdf

Arnon, D. I. (1949). Copper enzymes in isolated chloroplasts. Polyphenoloxidase in *Beta vulgaris*. *Plant Physiology*, *24*(1), 1–16.

Aslan, S., & Kapdan, I. K. (2006). Batch kinetics of nitrogen and phosphorus removal from synthetic wastewater by algae. *Ecological Engineering*, *18*, 64–70. https://doi.org/10.1016/j.ecoleng.2006.04.003

Atasoy, M., Owusu-Agyeman, I., Plaza, E., & Cetecioglu, Z. (2018). Bio-based volatile fatty acid production and recovery from waste streams.pdf. *Bioresource Technology*, *268*, 773–786.

Atiku, H., Mohamed, R., Al-Gheethi, A., Wurochekke, A., & Kassim, A. H. M. (2016). Harvesting of microalgae biomass from the phycoremediation process of greywater. *Environmental Science and Pollution Research*, *23*(24), 24624–24641. https://doi.org/10.1007/s11356-016-7456-9

Bassi, A., Saxena, P., & Aguirre, A. (2014). Mixotrophic algae cultivation for energy production and other

applications flat panel or plate reactor. In R. Bajpai, A. Prokop, & M. Zappi (Eds.), *Algal Biorefineries* (pp. 177–202). Springer, Dordrecht. https://doi.org/10.1007/978-94-007-7494-0

Beltrán-Rocha, J. C., Barceló-Quintal, I. D., García-Martínez, M., Osornio-Berthet, L., Saavedra-Villarreal, N., Villarreal-Chiu, J., & Javier López-Chuken, U. (2017). Polishing of municipal secondary effluent using native microalgae consortia. *Water Science and Technology*, *75*(7), 1693–1701. https://doi.org/10.2166/wst.2017.046

Bicas, J. L., Kleinegris, D. M. M., & Barbosa, M. J. (2015). Use of methylene blue uptake for assessing cell viability of colony-forming microalgae. *Algal Research*, *8*, 174–180. https://doi.org/10.1016/j.algal.2015.02.004

Blier, R., Lalibert, G., & de la Notie, J. (1995). Tertiary treatment of cheese factory anaerobic effluent with *Phormidium bohneri* and *Micractinium pusillum*. *Bioresource Technology*, *52*, 151–155.

Bohutskyi, P., Liu, K., Nasr, L. K., Byers, N., Rosenberg, J. N., Oyler, G. A., Betenbaugh, M. J., & Bouwer, E. J. (2015). Bioprospecting of microalgae for integrated biomass production and phytoremediation of unsterilized wastewater and anaerobic digestion centrate. *Appl Microbiol Biotechnol*, *99*(14), 6139–6154. https://doi.org/10.1007/s00253-015-6603-4

Bouarab, L., Dauta, A., & Loudiki, M. (2004). Heterotrophic and mixotrophic growth of *Micractinium pusillum* Fresenius in the presence of acetate and glucose : effect of light and acetate gradient concentration. *Water Research*, *38*, 2706–2712. https://doi.org/10.1016/j.watres.2004.03.021

Boyle, G. (2012). *Renewable Energy - Power for a Sustainable Future* (3rd ed.). Oxford University Press.

Chen, G., Zhao, L., & Qi, Y. (2015). Enhancing the productivity of microalgae cultivated in wastewater toward biofuel production : A critical review. *Applied Energy*, *137*, 282–291. https://doi.org/10.1016/j.apenergy.2014.10.032

Chen, J. H., Kato, Y., Matsuda, M., Chen, C. Y., Nagarajan, D., Hasunuma, T., Kondo, A., Dong, C. Di, Lee, D. J., & Chang, J. S. (2019). A novel process for the mixotrophic production of lutein with *Chlorella sorokiniana* MB-1-M12 using aquaculture wastewater. *Bioresource Technology*, *290*. https://doi.org/10.1016/j.biortech.2019.121786

Cheng, D. L., Ngo, H. H., Guo, W. S., Chang, S. W., Nguyen, D. D., & Kumar, S. M. (2019). Microalgae biomass from swine wastewater and its conversion to bioenergy. *Bioresource Technology*, *275*, 109–122. https://doi.org/10.1016/j.biortech.2018.12.019

Cheung, M. K., Au, C. H., Chu, K. H., Kwan, H. S., & Wong, C. K. (2010). Composition and genetic diversity of picoeukaryotes in subtropical coastal waters as revealed by 454 pyrosequencing. *The ISME Journal*, *4*(8), 1053–1059. https://doi.org/10.1038/ismej.2010.26

Chew, K. W., Chia, S. R., Show, P. L., Yap, Y. J., Ling, T. C., & Chang, J. S. (2018). Effects of water culture medium, cultivation systems and growth modes for microalgae cultivation: A review. *Journal of the Taiwan Institute of Chemical Engineers*, *91*, 332–344. https://doi.org/10.1016/j.jtice.2018.05.039

Chew, K. W., Yap, J. Y., Show, P. L., Suan, N. H., Juan, J. C., Ling, T. C., Lee, D. J., & Chang, J. S. (2017). Microalgae biorefinery: High value products perspectives. *Bioresource Technology*, *229*, 53–62. https://doi.org/10.1016/j.biortech.2017.01.006

Chiu, S. Y., Kao, C. Y., Chen, T. Y., Chang, Y. bin, Kuo, C. M., & Lin, C. S. (2015). Cultivation of microalgal *Chlorella* for biomass and lipid production using wastewater as nutrient resource. *Bioresource Technology*, *184*, 179–189. https://doi.org/10.1016/j.biortech.2014.11.080

Chojnacka, K., & Noworyta, A. (2004). Evaluation of *Spirulina* sp . growth in photoautotrophic , heterotrophic and mixotrophic cultures. *Enzyme and Microbial Technology*, *34*(2), 461–465. https://doi.org/10.1016/j.enzmictec.2003.12.002

Crane, K. W., & Grover, J. P. (2010). Coexistence of mixotrophs , autotrophs , and heterotrophs in planktonic microbial communities. *Journal of Theoretical Biology*, *262*(3), 517–527. https://doi.org/10.1016/j.jtbi.2009.10.027

de Melo, R. G., de Andrade, A. F., Bezerra, R. P., Correia, D. S., Souza, V. C. de, Brasileiro-Vidal, A. C., Marques, D. de A. V., & Porto, A. L. F. (2018). *Chlorella vulgaris* mixotrophic growth enhanced biomass productivity and reduced toxicity from agro-industrial by-products. *Chemosphere*, *204*, 344–350. https://doi.org/10.1016/j.chemosphere.2018.04.039

D'Imporzano, G., Veronesi, D., Salati, S., & Adani, F. (2018). Carbon and nutrient recovery in the cultivation of *Chlorella vulgaris*: A life cycle assessment approach to comparing environmental performance. *Journal of Cleaner Production*, *194*, 685–694. https://doi.org/10.1016/j.jclepro.2018.05.174

Fei, Q., Fu, R., Shang, L., Brigham, C. J., & Chang, H. N. (2015). Lipid production by microalgae *Chlorella protothecoides* with volatile fatty acids (VFAs) as carbon sources in heterotrophic cultivation and its economic assessment. *Bioprocess and Biosystems Engineering*, *38*(4), 691–700. https://doi.org/10.1007/s00449-014-1308-0

Fernández-Linares, L. C., Barajas, C. G., Páramo, E. D., & Corona, J. A. B. (2017). Assessment of *Chlorella vulgaris* and indigenous microalgae biomass with treated wastewater as growth culture medium. *Bioresource Technology*, *244*, 400–406. https://doi.org/10.1016/j.biortech.2017.07.141

Gani, P., Sunar, N. M., Matias-Peralta, H., Latiff, A. A. A., Parjo, U. K., & Razak, A. R. A. (2015). Phycoremediation of wastewaters and potential hydrocarbon from microalgae: A review. *Advances in Environmental Biology*, *9*(20), 1–8.

Girard, J. M., Roy, M. L., Hafsa, M. ben, Gagnon, J., Faucheux, N., Heitz, M., Tremblay, R., & Deschênes, J. S. (2014). Mixotrophic Cultivation of Green

Microalgae <i>Scenedesmus obliquus<i> on Cheese Whey Permeate for Biodiesel Production. *Algal Research*, *5*(1), 241–248. https://doi.org/10.1016/j.algal.2014.03.002

Godrijan, J., Drapeau, D., & Balch, W. M. (2020). Mixotrophic uptake of organic compounds by coccolithophores. *Limnology and Oceanography*, *65*, 1410–1421. https://doi.org/10.1002/lno.11396

Gonçalves, A. L., Pires, J. C. M., & Simões, M. (2017). A review on the use of microalgal consortia for wastewater treatment. *Algal Research*, *24*, 403–415. https://doi.org/10.1016/j.algal.2016.11.008

Guldhe, A., Ansari, F. A., Singh, P., & Bux, F. (2017). Heterotrophic cultivation of microalgae using aquaculture wastewater: A biorefinery concept for biomass production and nutrient remediation. *Ecological Engineering*, *99*, 47–53. https://doi.org/10.1016/j.ecoleng.2016.11.013

Hassan, A. N., & Nelson, B. K. (2012). Invited review : Anaerobic fermentation of dairy food wastewater. *Journal of Dairy Science*, *95*(11), 6188–6203. https://doi.org/10.3168/jds.2012-5732

Hena, S., Fatimah, S., & Tabassum, S. (2015). Cultivation of algae consortium in a dairy farm wastewater for biodiesel production. *Water Resources and Industry*, *10*, 1–14. https://doi.org/10.1016/j.wri.2015.02.002

Ho, S., Chen, C., Lee, D., & Chang, J. (2011). Perspectives on microalgal CO_2 -emission mitigation systems — A review. *Biotechnology Advances*, *29*(2), 189–198. https://doi.org/10.1016/j.biotechadv.2010.11.001

Hu, J., Nagarajan, D., Zhang, Q., Chang, J. S., & Lee, D. J. (2018). Heterotrophic cultivation of microalgae for pigment production: A review. *Biotechnology Advances*, *36*(1), 54–67. https://doi.org/10.1016/j.biotechadv.2017.09.009

ISO. (1984). *ISO 7150-1:1984 Water quality — Determination of ammonium — Part 1: Manual spectrometric method*. ICS : 13.060.50 Examination of Water for Chemical Substances. https://www.iso.org/standard/13742.html

ISO. (2013). *ISO 15923-1:2013 Water quality — Determination of selected parameters by discrete analysis systems — Part 1: Ammonium, nitrate, nitrite, chloride, orthophosphate, sulfate and silicate with photometric detection*. ICS : 13.060.50 Examination of Water for Chemical Substances. https://www.iso.org/standard/55559.html

Jeong, M. (2003). Carbon dioxide mitigation by microalgal photosynthesis. *Bull. Korean Chem. Soc.*, *24*(12), 1763–1766. https://doi.org/10.5012/bkcs.2003.24.12.1763

Kamyab, H., Mohd Fadhil Md, D., Keyvanfarb, A., Abd, M. Z., Majidb, Talaiekhozania, A., Shafaghat, A., Lee, C. T., Shiun, L. J., & Ismail, H. H. (2015). Efficiency of microalgae *Chlamydomonas* on the removal of POME. *Energy Procedia*, *75*, 2400–2408.

Khan, S. A., Sharma, G. K., Malla, F. A., Kumar, A., Rashmi, & Gupta, N. (2019). Microalgae based biofertilizers: A biorefinery approach to phycoremediate wastewater and harvest biodiesel and manure. *Journal of Cleaner Production*, *211*, 1412–1419. https://doi.org/10.1016/j.jclepro.2018.11.281

Kosseva, M. R., & Webb, C. (2013). *Food industry wastes assessment and recuperation of commodities* (M. R. Kosseva & C. Webb, Eds.). Academic Press. https://doi.org/10.1016/C2011-0-00035-2

Kotteswari, M., Murugesan, S., & R, R. K. (2012). Phycoremediation of Dairy Effluent by using the Microalgae Nostoc sp. *International Journal of Environmental Research and Development*, *2*(1), 35–43.

Lutz, S., Anesio, A. M., Edwards, A., & Benning, L. G. (2015). Microbial diversity on icelandic glaciers and ice caps. *Frontiers in Microbiology*, *6*(MAR), 1–17. https://doi.org/10.3389/fmicb.2015.00307

Maizatul, A. Y., Radin Mohamed, R. M. S., Al-Gheethi, A. A., & Hashim, M. K. A. (2017). An overview of the utilisation of microalgae biomass derived from nutrient recycling of wet market wastewater and slaughterhouse wastewater. *International Aquatic Research*, *9*(3), 177–193. https://doi.org/10.1007/s40071-017-0168-z

Markou, G., Wang, L., Ye, J., & Unc, A. (2018). Using agro-industrial wastes for the cultivation of microalgae and duckweeds: Contamination risks and biomass safety concerns. *Biotechnology Advances*, *36*(4), 1238–1254. https://doi.org/10.1016/j.biotechadv.2018.04.003

Melo, R. G. de, Andrade, A. F. de, Bezerra, R. P., Correia, D. S., Souza, V. C. de, Brasileiro-Vidal, A. C., Viana Marques, D. de A., & Porto, A. L. F. (2018). *Chlorella vulgaris* mixotrophic growth enhanced biomass productivity and reduced toxicity from agro-industrial by-products. *Chemosphere*, *204*, 344–350. https://doi.org/10.1016/j.chemosphere.2018.04.039

Mondal, M., Ghosh, A., Subhalaxmi, A., Tiwari, O. N., Gayen, K., Mandal, M. K., & Halder, G. N. (2016). Mixotrophic cultivation of *Chlorella* sp . BTA 9031 and *Chlamydomonas* sp . BTA 9032 isolated from coal field using various carbon sources for biodiesel production. *Energy Conversion and Management*, *124*, 297–304. https://doi.org/10.1016/j.enconman.2016.07.033

Moreno García, L., Gariépy, Y., Barnabé, S., & Raghavan, V. (2020). Biorefinery of microalgae biomass cultivated in wastewaters. In R. P. K. E. G. J. K. R. G. Baskar (Ed.), *Refining Biomass Residues for Sustainable Energy and Bioproducts - Technology, Advances, Life Cycle Assessment, and Economics* (1st ed., pp. 149–180). Elsevier Inc. https://doi.org/10.1016/b978-0-12-818996-2.00007-7

Odjadjare, E. C., Mutanda, T., & Olaniran, A. O. (2017). Potential biotechnological application of microalgae: a critical review. *Critical Reviews in Biotechnology*, *37*(1), 37–52.

https://doi.org/10.3109/07388551.2015.1108956

Olguín, E. J. (2012). Dual purpose microalgae-bacteria-based systems that treat wastewater and produce biodiesel and chemical products within a Biorefinery. In *Biotechnology Advances* (Vol. 30, Issue 5, pp. 1031–1046). https://doi.org/10.1016/j.biotechadv.2012.05.001

Overmann, J., & Garcia-Pichel, F. (2013). The phototrophic way of life. In T. F. Rosenberg E., DeLong E.F., Lory S., Stackebrandt E. (Ed.), *The Prokaryotes* (1st ed., pp. 203–246). Springer. https://doi.org/10.1007/978-3-642-30123-0

Pahazri, N. F., Mohamed, R. M. S. R., Al-Gheethi, A. A., & Kassim, A. H. M. (2016). Production and harvesting of microalgae biomass from wastewater: a critical review. *Environmental Technology Reviews*, *5*(1), 39–56. https://doi.org/10.1080/21622515.2016.1207713

Posadas, E., Bochon, S., & M. C., García-González, M. C., García-Encina, P. A., & Muñoz, R. (2014). Microalgae-based agro-industrial wastewater treatment : a preliminary screening of biodegradability. *J. Appl. Phycol.*, *26*, 2335–2345. https://doi.org/10.1007/s10811-014-0263-0

Posadas, E., Szpak, D., Lombó, F., Domínguez, A., Díaz, I., Blanco, S., García-Encina, P. A., & Muñoz, R. (2016). Feasibility study of biogas upgrading coupled with nutrient removal from anaerobic effluents using microalgae-based processes. *Journal of Applied Phycology*, *28*(4), 2147–2157. https://doi.org/10.1007/s10811-015-0758-3

Posten, C., & Schaub, G. (2009). Microalgae and terrestrial biomass as source for fuels-A process view. *Journal of Biotechnology*, *142*(1), 64–69. https://doi.org/10.1016/j.jbiotec.2009.03.015

Prazeres, A. R., Carvalho, F., & Rivas, J. (2012). Cheese whey management: A review. In *Journal of Environmental Management* (Vol. 110, pp. 48–68). https://doi.org/10.1016/j.jenvman.2012.05.018

Pulz, O., & Gross, W. (2004). Valuable products from biotechnology of microalgae. *Applied Microbiology and Biotechnology*, *65*(6), 635–648. https://doi.org/10.1007/s00253-004-1647-x

Ramanan, R., Kim, B. H., Cho, D. H., Oh, H. M., & Kim, H. S. (2016). Algae-bacteria interactions: Evolution, ecology and emerging applications. *Biotechnology Advances*, *34*(1), 14–29. https://doi.org/10.1016/j.biotechadv.2015.12.003

Rawat, I., Ranjith Kumar, R., Mutanda, T., & Bux, F. (2011). Dual role of microalgae: Phycoremediation of domestic wastewater and biomass production for sustainable biofuels production. *Applied Energy*, *88*(10), 3411–3424. https://doi.org/10.1016/j.apenergy.2010.11.025

Ren, N. Q., Chua, H., Chan, S. Y., Tsang, Y. F., Wang, Y. J., & Sin, N. (2007). Assessing optimal fermentation type for bio-hydrogen production in continuous-flow acidogenic reactors. *Bioresource Technology*, *98*(9), 1774–1780.

https://doi.org/10.1016/j.biortech.2006.07.026

Renuka, N., Sood, A., Prasanna, R., & Ahluwalia, A. S. (2015). Phycoremediation of wastewaters: a synergistic approach using microalgae for bioremediation and biomass generation. *International Journal of Environmental Science and Technology*, *12*(4), 1443–1460. https://doi.org/10.1007/s13762-014-0700-2

Ripka, R., Deruelles, J., Waterbury, J. B., Herdman, M., & Stanier, R. Y. (1979). Generic assignments , strain histories and properties of pure cultures of Cyanobacteria. *Journal of General Microbiology*, *110*(2), 1–61.

Rösch, C., Roßmann, M., & Weickert, S. (2018). Microalgae for integrated food and fuel production. *Global Change Biology - Bioenergy*, *0*, 1–9. https://doi.org/10.1111/gcbb.12579

Sahu, A. K., Siljudalen, J., Trydal, T., & Rusten, B. (2013). Utilisation of wastewater nutrients for microalgae growth for anaerobic co-digestion. *Journal of Environmental Management*, *122*, 113–120. https://doi.org/10.1016/j.jenvman.2013.02.038

Salati, S., D'Imporzano, G., Menin, B., Veronesi, D., Scaglia, B., Abbruscato, P., Mariani, P., & Adani, F. (2017). Mixotrophic cultivation of *Chlorella* for local protein production using agro-food by-products. *Bioresource Technology*, *230*, 82–89. https://doi.org/10.1016/j.biortech.2017.01.030

Shoaf, W. T., & Lium, B. W. (1976). Improved extraction of chlorophyll a and b from algae using dimethyl sulfoxide. In *Limnology and Oceanography* (Vol. 21, Issue 6, pp. 926–928). https://doi.org/10.4319/lo.1976.21.6.0926

Singh, V., Tiwari, A., & Das, M. (2016). Phyco-remediation of industrial waste-water and flue gases with algal-diesel engenderment from micro-algae: A review. *Fuel*, *173*(January), 90–97. https://doi.org/10.1016/j.fuel.2016.01.031

Siregar, K., Tambunan, A. H., Irwanto, A. K., Wirawan, S. S., & Araki, T. (2015). A comparison of life cycle assessment on oil palm (Elaeis guineensis Jacq.) and physic nut (Jatropha curcas Linn.) as feedstock for biodiesel production in Indonesia. *Energy Procedia*, *65*, 170–179. https://doi.org/10.1016/j.egypro.2015.01.054

Solmaz, A., & Mustafa, I. (2019). Polishing the secondary effluent and biomass production by microalgae submerged membrane photo bioreactor. *Sustainable Energy Technologies and Assessments*, *34*(April), 1–8. https://doi.org/10.1016/j.seta.2019.04.002

Speziale, B. J., Schreiner, S. P., Giammatteo, P. A., & Schindler, J. E. (1984). Comparison of N,N-dimethylformamide, dimethyl sulfoxide, and acetone for extraction of phytoplankton chlorophyll. *Canadian Journal of Fisheries and Aquatic Sciences*, *41*(10), 1519–1522. https://doi.org/10.1139/f84-187

Stamatelatou, K., Antonopoulou, G., Tremouli, A., & Lyberatos, G. (2011). Production of gaseous biofuels and electricity from cheese whey. *Industrial and Engineering Chemistry Research*,

50(2), 639–644. https://doi.org/10.1021/ie1002262

Subashchandrabose, S. R., Ramakrishnan, B., Megharaj, M., Venkateswarlu, K., & Naidu, R. (2013). Mixotrophic cyanobacteria and microalgae as distinctive biological agents for organic pollutant degradation. *Environment International*, *51*, 59–72. https://doi.org/10.1016/j.envint.2012.10.007

Takahashi, S., Tomita, J., Nishioka, K., Hisada, T., & Nishijima, M. (2014). Development of a prokaryotic universal primer for simultaneous analysis of Bacteria and Archaea using next-generation sequencing. *PLoS ONE*, *9*(8), 1–9. https://doi.org/10.1371/journal.pone.0105592

Ting, H., Haifeng, L., Shanshan, M., Zhang, Y., Zhidan, L., & Na, D. (2017). Progress in microalgae cultivation photobioreactors and applications in wastewater treatment: A review. *International Journal of Agricultural and Biological Engineering*, *10*(1), 1–29. https://doi.org/10.3965/j.ijabe.20171001.2705

Tsakali, E., Petrotos, K., D'Allessandro, A., & Goulas, P. (2010). A review on whey composition and the methods used for its utilization for food and pharmaceutical products. In C. R. Centre (Ed.), *6th International Conference on Simulation and Modelling in the Food and Bio-Industry* (pp. 195–201).

Tsolcha, O. N., Tekerlekopoulou, A. G., Akratos, C. S., Bellou, S., Aggelis, G., Katsiapi, M., Moustaka-Gouni, M., & Vayenas, D. v. (2016). Treatment of second cheese whey effluents using a *Choricystis*-based system with simultaneous lipid production. *Journal of Chemical Technology and Biotechnology*, *91*(8), 2349–2359. https://doi.org/10.1002/jctb.4829

USDA. (2019). *Dairy: World markets and trade*. https://www.fas.usda.gov/data/dairy-world-markets-and-trade

Wang, B., Li, Y., Wu, N., & Lan, C. Q. (2008). CO_2 bio-mitigation using microalgae. *Appl Biochem Biotechnol*, *79*, 707–718. https://doi.org/10.1007/s00253-008-1518-y

Wang, Y., Ho, S., Cheng, C., Guo, W., Nagarajan, D., Ren, N., Lee, D., & Chang, J. (2016). Perspectives on the feasibility of using microalgae for industrial wastewater treatment. *Bioresource Technology*, *222*, 485–497. https://doi.org/10.1016/j.biortech.2016.09.106

Wellburn, A. R. (1994). The spectral determination of chlorophylls a and b, as well as total carotenoids, using various solvents with spectrophotometers of different resolution. *Journal of Plant Physiology*, *144*(3), 307–313. https://doi.org/10.1016/S0176-1617(11)81192-2

Yao, S., Lyu, S., An, Y., J.Lu, Gjermansen, C., & Schramm, A. (2018). Microalgae – bacteria symbiosis in microalgal growth and biofuel production : a review. *Journal of Applied Microbiology*, *126*, 359–368. https://doi.org/10.1111/jam.14095

Yi, H., Han, Y., & Zhuo, Y. (2013). Effect of combined pretreatment of waste activated sludge for anaerobic digestion

process. *Procedia Environmental Sciences*, *18*, 716–721. https://doi.org/10.1016/j.proenv.2013.04.097

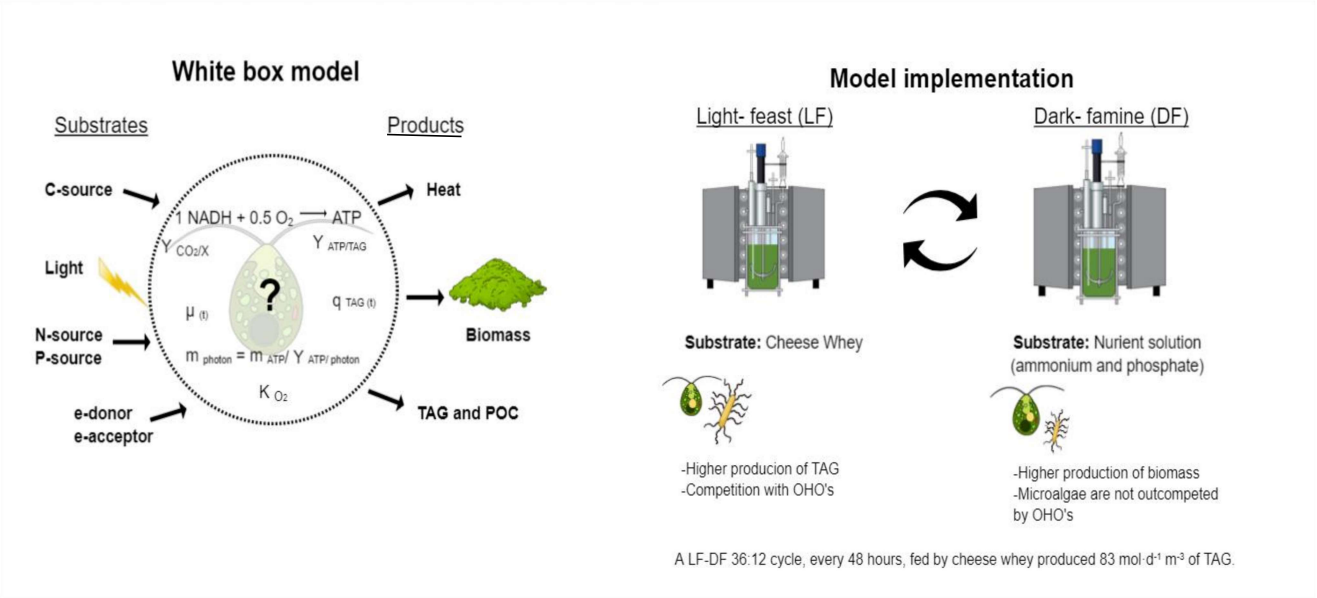
Zeng, X., Danquah, M. K., Chen, X. D., & Lu, Y. (2011). Microalgae bioengineering: From CO_2 fixation to biofuel production. *Renewable and Sustainable Energy Reviews*, *15*(6), 3252–3260. https://doi.org/10.1016/j.rser.2011.04.014

Zhao, B., & Su, Y. (2014). Process effect of microalgal-carbon dioxide fixation and biomass production : A review. *Renewable and Sustainable Energy Reviews*, *31*, 121–132. https://doi.org/10.1016/j.rser.2013.11.054

5. Green microalgae mixotrophy: A mathematical model for triacylglycerol production and cheese whey valorization

This chapter was developed in collaboration with Saman Khayat, Master student at the TU Delft in the framework of this Ph.D.. Part of this work was presented to Algal BBB 2021 conference as: Khayat S°, **Giulianetti de Almeida MP**, Mockaitis G, van Loosdrecht MCM, Ebrahimi S, Weissbrodt DG (2021) *Modelling the mixotrophy of green microalgae to produce triacylglycerol and valorize cheese whey in mixed-culture biotechnology*. In: Krause et al. (eds.) 10th International Conference on Algal Bio-mass, Biofuels and Bioproducts (Algal BBB 2021), Hawaii /US. (virtual). This chapter will be submitted to *Algal Research.*

Graphical abstract



Abstract

Our economy is currently heavily dependent on fossil fuels to meet our energy needs, but transitioning to a bioeconomy and circular economy, which relies on renewable resources like biomass, can decrease this dependence. Even though there are many computational tools available to analyze photobioprocesses, incorporating light regimes, and nutrient availability among other parameters into mathematical models remains challenging. Hence, we developed a comprehensive mathematical model to study and support the production of triacylglycerol and microalgal biomass using cheese whey, a by-product of the dairy industry, as a substrate in mixed-culture fermentation processes. Our model examined the mixotrophic metabolism of microalgae at different levels, from intracellular to extracellular constraints, such as phototrophic growth thermodynamics, triacylglycerol, poly-carbohydrate synthesis, degradation pathways, and light/dark regime shifts. By applying periodic light-feast and dark-famine cycles 36:12 every 48 hours in a continuous-flow photobioreactor fed by raw cheese whey, a high-grade enrichment of microalgae and a volumetric productivity of triacylglycerol of 83 $mol \cdot d^{-1}$ m^{-3} could be achieved. This highlights the potential for using a mixed-culture photobioreactor to valorize cheese whey and to produce microalgae-derived biofuel at lower costs. Our model can aid in experimental and process design and optimization toward commercializing large-scale production of biofuel from microalgae.

Keywords: predictive mathematical model, microalgae, mixotrophy, cheese whey, triacylglycerol, mixed-culture bioprocesses

1 Introduction

Fossil fuels still play a significant role in meeting our energy needs. However, biomass has been seen as a key factor for the successful transition to bioeconomy (BE) and circular economy (CE) by decreasing our dependency on non-renewable fuels (Antar et al., 2021; Sherwood, 2020; Solarte-Toro & Cardona Alzate, 2021). Although under the same umbrella, BE and CE have different aims.

While BE aims at the reduction of CO_2 emissions and the transition from non-renewable fuels to renewable ones (Gomez San-Juan & Bogdanski, 2021; Kircher, 2012; Solarte-Toro & Cardona Alzate, 2021), CE's main goal is to develop cascading processes that can transform by-products and materials into new added-value products by making use of renewable energy sources (Carus & Dammer, 2018; Mohan et al., 2019; Uvarova et al., 2020) and consequently, reducing the amount of waste produced during the process (Yadav et al., 2020). The cultivation of microalgae biomass in cheese whey and its derivatives can aid in the complete transition of the dairy sector into BE and CE. Throughout this work, the term microalgae stand for phototrophic microorganisms such as green microalgae and cyanobacteria.

Microalgae biomass presents various benefits as a sustainable feedstock for biofuel production. Besides displaying excellent photosynthetic efficiency and shorter biomass growth cycles (Fabris et al., 2020; Peng et al., 2018) compared to other biofuel feedstocks (e.g., rapeseed, jatropha, soybean, and palm oil) (Ahmad et al., 2011; Chowdhury & Loganathan, 2019), microalgae can be grown in arid land and brackish waters. Hence, they do not compete with land for food production (Darvehei et al., 2018). Moreover, microalgae contribute to carbon dioxide mitigation (Banu et al., 2020) by fixating it during photosynthesis while removing nutrients from wastewater (i.e., nitrogen and phosphorus) and using them in anabolic processes (Darvehei et al., 2018).

The metabolisms of microalgae are very versatile. These microorganisms can adapt themselves according to the environment and light and carbon source availability. Microalgae can be cultivated in different modes (*i*) photoautotrophic, where light acts as an energy source and inorganic carbon as a carbon source, (*ii*) heterotrophic, by using organic compounds as both carbon and energy sources, (*iii*) photoheterotrophic, where

an organic carbon source is metabolized using light as an energy source, and (*iv*) mixotrophic, a process in which microalgae can utilize both organic and inorganic carbon sources and the organic compound and light as the energy sources (Ananthi et al., 2021; Fernández et al., 2021).

In mixotrophy, the specific growth rate is computed by considering the cell growth rates that were achieved under photoautotrophic, photoheterotrophic, and chemoheterotrophic conditions (Pang et al., 2019). Low-cost organic carbon sources such as food and milk industrial wastes, wastewater, and lignocellulosic materials have been replacing expensive chemicals such as glucose and acetate (Hemalatha et al., 2019; Kiefer et al., 2021; Pawar et al., 2021).

One of the main disadvantages of mixotrophic mixed cultures is the competition between microalgae and ordinary heterotrophic organisms (OHOs) which may affect microalgae's productivity (di Caprio et al., 2022). Although microalgae axenic culture reduces the chance of contamination, it elevates the cultivation and processing costs (Talapatra et al., 2021). However, considering microbial community engineering, the implementation of selective pressure on the system (e.g., hydraulic retention time, dilution rate, nutrients availability, light cycle) can limit the competition between microalgae and OHOs (di Caprio et al., 2022; Khan, Shin, & Kim, 2018; Trebuch et al., 2020) and consequently, reduce the overall processes' operational costs.

Additionally, microalgae display high levels of neutral lipid productivity (Gumbi, Kumar, & Olaniran, 2022; Whangchai et al., 2021), and bioactive molecules (i.e., polysaccharides, proteins, carotenoids, and omega three fatty acids) that can be further processed into various products, such as food supplements, bioplastics, medicines, and cosmetics(Abu-Ghosh et al., 2021; Chénais, 2021; Mehariya et al., 2021). According to Pang et al. (2019), algal mixotrophic culture can significantly increase biomass production, while accumulating more lipids in algal cells. Additionally, anaerobic digestion of microalgae can potentially recover methane and hydrogen (Dębowski et al., 2021; Nagarajan, Lee, & Chang, 2019).

Regarding anaerobic digestion, the use of wastewater as a substrate for microalgal biomass cultivation can either increase the biomolecules' concentration or act as stressors altering microalgae's metabolic pathways depending on its composition (Moreira et al.,

2021). Hernández-García et al. (2019), reported that although biomolecules' (i.e., carbohydrates and lipids) concentration tends to increase with the use of wastewater as carbon, nitrogen, and phosphorus source, biomass productivity decreases. Additionally, the use of wastewater can improve microalgal biofuels' (i.e., biodiesel, bioethanol, biohydrogen, and biogas) cost efficiency related to cultivation, harvesting, and dewatering, making them more competitive with fossil fuels (Chen, Zhao, & Qi, 2015; Li, Li, & Ho, 2022; Moreira et al., 2021).

Cheese whey, a by-product of the dairy industry, presents a COD of 50 to 80 g O_2 L^{-1} (Carvalho, Prazeres, & Rivas, 2013; Saddoud, Hassaïri, & Sayadi, 2007) and due to its low pH level, it acidifies quickly producing VFAs such as butyrate, acetate, and propionate. In 2022, cheese whey annual production was estimated at 160.67 million m^{-3} in which. 66.5 million m^{-3} are not absorbed by the industry, being used as either animal feed or fertilizer (Tsakali et al., 2010; USDA, 2022). Depending on the location, cheese whey can be discarded into water bodies leading to eutrophication (Smithers, 2008; Tsakali et al., 2010). However, the cheese whey currently not absorbed by industry could be further valorized by serving as an organic carbon source for microalgal biomass and lipid production ensuring the complete transition of the dairy sector into the circular economy (Panghal et al., 2018).

Bioremediation of waste streams to produce lipid-enriched microalgal biomass in mixotrophic conditions has been widely acknowledged but still not economically viable. Mathematical models can be an effective tool to predict how different factors (e.g., light intensity, nutrient availability, temperature, feeding regime) affect microalgal growth, and consequently, biomass production (Solimeno et al., 2015). Modeling the kinetics of microalgae growth enables to control of the parameters that affect biomass and lipid production, thus optimizing the process (Darvehei et al., 2018; Moreno García et al., 2020).

Most models utilized to evaluate algae dynamics usually consider the (*i*) limitation of growth by a nutrient using a cell quota approach (Martínez et al., 2019), (*ii*) chlorophyll concentration as a means to anticipate light attenuation in a system (Ma et al., 2022), (*iii*) combined effects of parameters such as nutrient availability and light intensity to estimate growth rate (Perin et al., 2019), (*iv*), microalgal growth in inorganic carbon (Khoo, Lam, &

Lee, 2019; Tunay et al., 2022), (*v*) combined effect of light intensity and temperature (Khoo et al., 2019; Tunay et al., 2022), and lastly, (*vi*) a combination of different mathematical models such as Monod, Aiba, Bernard, Droop and Steele (Khoo et al., 2019; Solimeno et al., 2015; Tunay et al., 2022).

This work aimed to develop a computational model based on ASM1 (Henze et al., 2015) to predict the growth and lipid production of microalgae in different growth conditions using cheese whey and its derivatives (i.e., raw cheese whey, whey powder, and optimized version of whey) as substrate. The model accounted for the effects of light intensity and availability, as well as nutrient availability on microalgae growth. The model was tested using data from relevant literature and a microalgae cultivation experiment and was able to predict microalgae biomass growth and lipid production.

2 Materials and methods

2.1 Model assumptions

A mathematical model was developed to predict microalgal axenic and culture growth patterns, storage products, lipids, and polycarbohydrates final concentrations in batch and chemostat regimes using a photobioreactor and a continuous stirred-tank reactor (CSTR), respectively. The model also considered the following trophic regimes in mixed cultures: (*i*) photoautotrophic, (*ii*) photoheterotrophic, (*iii*) chemoautotrophic, and (*iv*) mixotrophic. The two-flow, predictive model accounted for the stoichiometry and kinetics of microalgae growth, the productivity of storage compounds, and their final concentrations, enabling the modeling to function with different carbon sources. This work used cheese whey as its carbon source. For the chemostat regime, both light-dark cycles and feast-famine regimes were applied. The nutrient feast regime was applied to the light cycle, while the famine regime occurred during the dark phase.

To build the model, we made the following assumptions:

(i) The chosen substrates for the processes consisted of raw cheese whey (RCW) and the main VFAs resulted from cheese whey acidogenic fermentation. Both

substrates were initially sparged with either common airflow or carbon dioxide-enriched airflow.

(ii) Biological and chemical processes took place in both liquid and gas phases in the photobioreactors, where chemical reactions were limited to the transfer of volatile compounds between phases.

(iii) The model processes encompassed biomass growth and decay, nutrient and substrate conversion, and production and degradation of TAG and POC.

(iv) The stoichiometry of biological conversions was based on the photosynthesis metabolic pathway considering carbon dioxide and glucose as inorganic and organic carbon sources, respectively.

(v) Given cheese whey's acidic nature, it was considered that the breakdown of lactose, cheese whey's main component, into galactose and glucose led to the full degradation of galactose into glucose in the Leloir pathway. As for the main VFAs produced in cheese whey acidogenic fermentation (i.e., acetate, butyrate, and propionate), the same degree of biodegradability as glucose was assumed once they converted into glucose via gluconeogenesis.

(vi) The regulation between POC and TAG metabolic pathways was modeled by using the principles of kinetics. Product inhibition occurred when the levels of POC or TAG were saturated and that was assumed to be the most influential factor in central carbon shifting. The maximum saturation level of the microalgae storage compound was estimated by the average of the maximum yields of different species under different cultivation modes as depicted in **table 1**.

(vii) Microalgal biomass was divided into functional biomass (X or X_f) and storage molecules (i.e., TAG and POC). It was assumed that functional biomass was mainly composed of proteins, amino acids, chlorophyll, and other pigments and had the same formula and molecular weight as the elemental composition of microbial biomass, $C_1H_{1.8}O_{0.5}N_{0.2}P_{0.03,}$ and 25.53 g $Cmol^{-1}$, respectively.

Appendix A, Table I lists the model state variables where the concentration of microbial heterotrophic biomass (X_{het}) and the concentration of microbial autotrophic (i.e., nitrifying) biomass (X_{nit}) are analogs to the activated sludge model ASM1 (Henze et al.,

2015). The remaining components are model specific. The model stated variables were divided into concentrations of soluble matter (C), particulate matter (X), and cell quota (S) within the liquid phase, as well as the mole fraction of volatile compounds (y) within the gaseous phase. Once the mass balance for these state variables was adopted, the model equations were solved using Matlab®. A sensitive analysis was then performed to determine how and to what extent the key parameter alterations affected the model performance.

2.2 Modeling microalgal mixotrophic growth

A white box metabolic network model was built assuming (*i*) the whole microalgal metabolism as a set of chemical reactions, (*ii*) that the entire metabolism was broken down into sub-metabolisms according to their main function (e.g. functional biomass synthesis, Calvin cycle, and phosphorylation), (*iii*) that these sub-metabolisms were connected by stoichiometry coefficients within the whole metabolism (i.e., yields) which were calculated using compounds balance, (*iv*) that rate equations were formulated using kinetics parameters and calculated yields, and (*v*) that rate equations were implemented according to the principals of mass balance in both batch and chemostat reactors.

2.2.1 Stoichiometry of microalgae metabolisms

According to our proposed model, the stoichiometry of microalgae growth metabolism was investigated in light-feast and dark-famine conditions. During photoautotrophy, microalgae require light and an inorganic carbon source to grow, whereas in photoheterotrophic mode the presence of light and an organic carbon source for assimilation is preferred. In chemoheterotrophy, the organic carbon source is metabolized without a light supply. The stoichiometry of the mixotrophic regime was assumed to be the sum of all three metabolisms.

2.2.2 Light-feast regime

2.2.2.1 Photoautotrophic regime

Photoautotrophic metabolism involves six metabolic reactions consisting of (*a-i*) non-cyclic photophosphorylation resulting in ATP and NADPH derived from photons

energy, (*a-ii*) cyclic photophosphorylation, presenting higher ATP yield than the previous reaction, (*a-iii*, *a-iv,* and *a-v*) encompassing the synthesis of functional biomass, TAG and POC from an inorganic carbon source (i.e., CO_2), respectively and the (*a-vi*) formation of glycerol. The equations for photoautotrophic metabolism equations are depicted in **Appendix B, Table II**.

To achieve photoautotrophy stoichiometric yields NADH, NADPH, and ATP were considered conserved moieties. Hence, to these moieties, all reactions were coupled resulting in three main energetically balanced reactions encompassing growth (*a-i, a-ii, a-iii,* and *a-vi*), TAG (*a-i, a-ii, a-iv,* and *a-vi*) and POC (*a-i, a-ii,* and *a-v*) production. Cyclic photophosphorylation (*a-ii*) was considered catabolism during maintenance since the energy provided for maintenance was more efficient than in non-cyclic photophosphorylation (*a-i*). **Table 2** presents the photoautotrophic stoichiometric yields considering both the non-cyclic and cyclic oxidative phosphorylation efficiency (δ and Δ, respectively).

2.2.2.2 Photoheterotrophic regime

The photoheterotrophic regime is also composed of six metabolic reactions in which was assumed that photophosphorylation is cyclic with a higher yield of ATP as NADPH would be supplied by an organic carbon source (i.e., glucose) via the pentose phosphate pathway. The reactions are (*b-i*) cyclic phosphorylation, with the oxidation of an organic carbon source, (*b-ii*) the pentose phosphate pathway, (*b-iii* to *b-v*) with the synthesis of biomass, TAG, and POC, respectively, ending with glycerol formation (*b-vi*). **Appendix B, Table III**. as in the photoautotrophic regime NADH, NADPH, and ATP were also considered conserved moieties. Therefore, the metabolism consisted of overall growth (*b-i* to *b-iii*), TAG (*b-i, b-ii,* and *b-iv*) and POC synthesis (*b-i* and *b-v*) and catabolism for maintenance represented by reaction *b-ii*. **Table 3** depicts the stoichiometric yields of the phototrophic regime.

Table 1 Overview of maximum biomass, POC, and TAG productivity on different microalgae species. In the table: photoheterotrophy (PhT), chemoheterotrophy (Cht), photoautotrophy (PaT), glucose (Glc,), and acetate (AcO^-).

Species	Trophic regime	Carbon source	Max. specific growth rate (day^{-1})	Max. biomass productivity (g VSS $L\ day^{-1}$)	Max. lipid productivity (g l_{lipid} $L\ day^{-1}$)	Max. POC productivity (g $_{POC}$ $L\ day^{-1}$)	Max. TAG yield (g $_{lipid}$ g VSS^{-1})	Max. POC yield (g $_{POC}$ g VSS^{-1})	References
C. vulgaris	ChT	Glc		0.151	0.035		0.23		Liang et al., 2009
		Glc	0.70	0.033		0.072		2.18	Choix et al., 2012
		Glc	0.42	0.031					Perez-Garcia et al., 2011
		AcO^-		0.087	0.027		0.31		Liang et al., 2009
		AcO^-	0.73	0.057		0.052		0.91	Choix et al, 2012
		AcO^-	0.49	0.047					Perez-Garcia et al., 2011
	PaT)	CO_2		0.010	0.004				Liang et al., 2009
		CO_2		1.440		0.63		0.43	Ho et al., 2013
		CO_2		0.037		0.021		0.57	Illman et al., 2000
C. sorokiniana	ChT	Glc	0.67	0.033		0.066		2.00	Choix et al., 2012
		AcO^-	0.72	0.037		0.055		1.49	Choix et al., 2012
	PaT	CO_2		0.230	0.045		0.20		Rodolfi et al., 2009
C. protothecoides	ChT	Whey		1.300	0.550		0.42		Espinosa-Gonzalez et al., 2014
		Whey		2.450	0.791		0.32		Espinosa-Gonzalez et al., 2014
		Glc		2.560	1.160		0.45		Liang et al., 2009
		Glc		0.660	0.310		0.47		Lu et al., 2010
		Glc		3.200	1.560		0.49		Xiong et al., 2010
	PhT	Glc		6.400	2.900		0.45		Xiong et al., 2010
		Glc		23.900	11.800		0.49		Xiong et al., 2010
S. obliquus	ChT	Whey	0.70	0.207	0.028		0.14		Girard et al., 2014
		Glc		0.230	0.045		0.20		Liang et al., 2009
	PaT	CO_2	0.27	0.061	0.037		0.61		Girard et al., 2014
		CO_2		0.380		0.112		0.29	Ho et al., 2013
Microalgae consortium	ChT	Organic					0.33	1.65	Estimated (average of above data)
	PaT	CO_2					0.41	0.43	
	PhT	Organic					0.47		

Table 2 Photoautotrophic stoichiometric yields are expressed as a function of the non-cyclic and cyclic oxidative phosphorylation efficiency (δ and Δ, respectively).

	Growth	Catabolism for maintenance	Production of TAG	Production of POC
CO_2	$Y_{\frac{CO_2}{X}} = -6.823$		$Y_{\frac{CO_2}{TAG}} = -3.760$	$Y_{\frac{CO_2}{POC}} = -1$
O_2	$Y_{\frac{O_2}{X}} = \frac{2.931 - 1.961\,\delta + 7.843\,\Delta}{\Delta}$	$Y_{\frac{O_2}{photon}} = 0.125$	$Y_{\frac{O_2}{TAG}} = \frac{3.055 - 1.16\,\delta + 4.64\,\Delta}{\Delta}$	$Y_{\frac{O_2}{POC}} = \frac{0.459 - 0.25\,\delta + \Delta}{\Delta}$
Glycerol	$Y_{\frac{Gly}{X}} = 1.941$		$Y_{\frac{Gly}{TAG}} = 0.92$	
Photon	$Y_{\frac{photon}{X}} = -\frac{23.449 + 15.686\,(\Delta - \delta)}{\Delta}$		$Y_{\frac{photon}{TAG}} = -\frac{12.22 + 9.28\,(\Delta - \delta)}{\Delta}$	$Y_{\frac{photon}{POC}} = -\frac{3.167 + 2\,(\Delta - \delta)}{\Delta}$
NH_4^+	$Y_{\frac{NH_4^+}{X}} = -0.2$			
PO_4^{3-}	$Y_{\frac{PO_4^{3-}}{X}} = -0.03$			
ATP		$Y_{\frac{ATP}{photon}} = -\Delta$		

Table 3 Photoheterotrophic regime stoichiometry yields considering cyclic oxidative photophosphorylation (Δ) as the efficiency function.

	Growth	Catabolism for maintenance	Production of TAG	Production of POC
$C_6H_{12}O_6$	$Y_{\frac{Glc}{X}} = -\frac{0.404\,\Delta + 0.473}{\Delta}$	$Y_{\frac{Glc}{photon}} = 0.25$	$Y_{\frac{Glc}{TAG}} = -\frac{0.775\,\Delta + 0.253}{\Delta}$	$Y_{\frac{Glc}{POC}} = -\frac{0.167\,\Delta + 0.083}{\Delta}$
CO_2	$Y_{\frac{CO_2}{X}} = \frac{0.248\,\Delta + 2.836}{\Delta}$	$Y_{\frac{CO_2}{photon}} = -1.5$	$Y_{\frac{CO_2}{TAG}} = \frac{0.885\,\Delta + 1.516}{\Delta}$	$Y_{\frac{CO_2}{POC}} = \frac{0.499}{\Delta}$
Glycerol	$Y_{\frac{Gly}{X}} = +0.392$		$Y_{\frac{Gly}{TAG}} = +0.922$	
Photon	$Y_{\frac{photon}{X}} = -\frac{1.891}{\Delta}$		$Y_{\frac{photon}{TAG}} = -\frac{1.011}{\Delta}$	$Y_{\frac{photon}{POC}} = -\frac{0.333}{\Delta}$
NH_4^+	$Y_{\frac{NH_4^+}{X}} = -0.2$			
PO_4^{3-}	$Y_{\frac{PO_4^{3-}}{X}} = -0.03$			
ATP		$Y_{\frac{ATP}{photon}} = -\Delta$		

2.2.2.3 Chemoheterotrophic regime

Chemoheterotrophic metabolism is composed of eight reactions beginning with glycolysis and Krebs Cycle (*c-i*) generating ATP and co-factors NADH and $FADH_2$ from oxidation of an organic carbon source; (*c-ii*) the pentose phosphate pathway which is the only reaction providing $FADH_2$; the synthesis of functional biomass, TAG and POC (*c-iii* to *c-v*, respectively); oxidative phosphorylation with the production of ATP by donating electrons to oxygen which acts as an electron receptor (*c-vii*) and lastly, glycerol formation (*c-viii*). **Table IV** (see **Appendix B**) shows the reactions describing chemoheterotrophic metabolism and **Table 4**, the stoichiometric yields under chemoheterotrophic metabolism. To calculate the maximum yields during the chemotrophic regime, $FADH_2$ was also treated as a conserved moiety. Additionally, all reactions (*c-i* to *c-viii*) were assumed to be coupled. Hence, reactions were balanced within the whole metabolism consisting of overall growth (c-i to c-iii, c-vi, and c-vii), TAG (*c-ii*, *civ*, *c-vi,* and *cv- iii*), and POC (*c-i*, *c-v* to *c-vii*) production, and catabolism for maintenance (*c-vi* and *c-vii*).

Table 4 Chemoheterotrophic regime stoichiometric yields.

	Growth	Catabolism for maintenance	Production of TAG	Production of POC
$C_6H_{12}O_6$	$Y_{\frac{Glc}{X}} = -0.280$	$Y_{\frac{Glc}{Glc}} = 1$	$Y_{\frac{Glc}{TAG}} = -0.522$	$Y_{\frac{Glc}{POC}} = -0.189$
CO_2	$Y_{\frac{CO_2}{X}} = 0.680$	$Y_{\frac{CO_2}{Glc}} = -6$	$Y_{\frac{CO_2}{TAG}} = 0.885$	$Y_{\frac{CO_2}{POC}} = 0.132$
O_2	$Y_{\frac{O_2}{X}} = -0.629$	$Y_{\frac{O_2}{Glc}} = +6$	$Y_{\frac{O_2}{TAG}} = -0.252$	$Y_{\frac{O_2}{POC}} = -0.130$
Glycerol			$Y_{\frac{Gly}{TAG}} = 0.417$	
NH_4^+	$Y_{\frac{NH_4^+}{X}} = -0.2$			
PO_4^{3-}	$Y_{\frac{PO_4^{3-}}{X}} = -0.03$			
ATP		$Y_{\frac{ATP}{Glc}} = -15.334$		

2.2.3 Dark-famine regime

The dark-famine phase is devoid of both light and carbon sources leading to microalgal chemoheterotrophic metabolism where the necessary energy for maintenance and further growth is supplied by the degradation of their storage of carbon-based molecules (i.e., TAG and starch) into acetyl Co-A (AcCoA). This intermediate molecule is a precursor in both anabolic and catabolic reactions. Therefore, the dark-famine metabolism comprises seven reactions: degradation of TAG to AcCoA via beta-oxidation (*d-i*), POC degradation to AcCoA via glycolysis (*d-ii*), the pentose phosphate pathway (*d-iii*), Krebs Cycle from AcCoA (*div*), oxidative phosphorylation of NADH and $FADH_2$ (*d-v* and *d-vi*, respectively), and synthesis of functional biomass after the degradation of an organic carbon source (e.g., glucose and acetate) to AcCoA (*d-vii*). **Table V** (see **Appendix C**) summarizes the dark-famine metabolic reactions considering the synthesis of functional biomass on a carbon-mole base and excluding the following compounds from the balance: ADP, Pi, H_2O, CoA-SH, and H^+.

All reactions were coupled to achieve an energetically independent overall growth reaction, reducing the degree of freedom. Additionally, AcCoA was also considered a conserved moiety together with ATP and reduced co-factors NADH, $FADH_2$, and NADPH. As a result, no net accumulation of AcCoA is expected in overall growth.

Thus, anabolic and catabolic pathways will depend on the storage molecule utilized by green phototrophs. When TAG acts as a sole carbon and energy source, the overall growth comprised all reactions but *d-ii*, whereas catabolism for maintenance comprised reactions *d-i* and *div* to *d-vi*.

However, when POC is the carbon and energy source, the overall growth comprised all reactions but *d-i*, and catabolism for maintenance comprised reactions *d-ii* and *d-iv* to *d-vi*. **Table 5** summarizes the maximum yields during dark-famine anabolism and catabolism reactions considering the storage precursor used.

2.2.4 Kinetics of microalgal growth

To precisely estimate microalgal growth, co-limitation between cell building blocks and light intensity as well as their interactions were assumed to control microalgal growth. We have developed a joint kinetics model accounting for threshold and multiplicative models which are two distinctive models based on the co-limitation concept (Lee, Jalalizadeh, & Zhang, 2015).

In this model, the co-limitation of nutrients (i.e., N and P) required for biomass synthesis and the light and carbon dioxide availability for photoautotrophic photosynthesis were separately described by the threshold model whilst their interaction was described by the multiplicative model, as shown on **equation 1**.

$$\mu = \mu^{max} \times min\big(g(F_1), g(F_2), \dots g(F_n)\big) \times min\big(h(F_1), h(F_2), \dots h(F_n)\big) \qquad \text{(Eq. 1)}$$

where, g (F_n) stands for a function of a limiting factor required for energy generation as well as biomass synthesis, and h (F_n) stands for a function of a nutrient factor. Depending on the type of cultivation mode, the enrolling functions may vary. Microalgae kinetics was studied in both light-feast and dark-famine regimes.

Table 5 Stoichiometric yields under the dark-famine regime, derived from the metabolic reactions and balances for the conserved moieties.

	TAG utilization as a carbon and energy source		**POC utilization as a carbon and energy source**	
	Growth on TAG	**Catabolism on TAG**	**Growth on POC**	**Catabolism on POC**
CO_2	$Y_{\frac{CO_2}{X}} = 1.286$	$Y_{\frac{CO_2}{TAG}} = -1$	$Y_{\frac{CO_2}{X}} = 1.873$	$Y_{\frac{CO_2}{POC}} = -1$
O_2	$Y_{\frac{O_2}{X}} = -2.200$	$Y_{\frac{O_2}{TAG}} = 1.421$	$Y_{\frac{O_2}{X}} = -1.824$	$Y_{\frac{O_2}{POC}} = 1$
TAG	$Y_{\frac{TAG}{X}} = -2.286$			
POC			$Y_{\frac{POC}{X}} = -2.875$	
NH_4^+	$Y_{\frac{NH_4^+}{X}} = -0.2$		$Y_{\frac{NH_4^+}{X}} = -0.2$	
PO_4^{3-}	$Y_{\frac{PO_4^{3-}}{X}} = -0.03$		$Y_{\frac{PO_4^{3-}}{X}} = -0.03$	
ATP	$Y_{\frac{ATP}{TAG}} = -1.955$			$Y_{\frac{ATP}{POC}} = -1.555$

2.2.4.1 Kinetics of light-feast regime

During the light-feast regime, microalgae growth depends on nutrient availability (i.e., N and P), carbon, and light. The substrate uptake rate (q_S), biomass specific growth rate (μ), and poly-carbohydrate production rate (q_{PO}), functioned as independently-derived rates, since each was modeled considering the maximum rate and with limitations or/and inhibitions saturation terms according to **equation 1**.

Conversely, the TAG production rate was based on overflow metabolism, making it dependent on independently-derived rates. Hence, the influent's nutrient availability exerts on independently-derived rates is straightforward. Regardless of the cultivation mode, the biomass-specific growth rate was regulated by intracellular nutrient concentration availability which was entailed by the concept of cell quota (*S*) in the term $min\ (1 - S_N^{min}/S_N, 1 - S_P^{min}/S_P\ )$.

Consumption of any of the limiting nutrients (i.e., N or P) below the cell quota (S^{min}), changes the specific growth rate to zero. Consequently, the surplus fixed carbon is channelled to the production of starch (POC) as its primary storage compound, which is modeled by the term $min\ \left(S_N^{min}/S_N, S_P^{min}/S_P\right)$ in POC production rate. When both N and P are abundant, the real cell quota is above its minimum value, so POC production is impeded due to carbon being diverted to cell growth.

As opposed to nutrients limitation, the effect that light and carbon source exercise on independently-derived rates is subject to microalgae cultivation mode. Depending on the growth mode, both POC production rate and biomass specific growth rate may be limited by organic or inorganic carbon and light availability, or both. Regarding carbon source uptake, the impact of carbon availability is modeled by the Monod saturation term as in $C_{CO2}/(C_{CO2} + K_{CO2})$ or $C_{GLC}/(C_{GLC} + K_{GLC})$. However, the impact of light is more complicated. In order to achieve the optimum growth rate, microalgae need specific light intensity referred hereafter as, saturated light level. When light intensity is below the saturation level, the growth will be limited by light. This limitation could be occasioned by either insufficient light incidence or adsorption due to culture turbidity, also known as cell attenuation.

According to Molina Grima et al. (1994), the term $I_{avg}^{n}/(I_{avg}^{n} + I_{K}^{n})$ estimates light limitation influence associated with cell attenuation. The average light intensity (I_{avg}) was then determined by the light path (*R*), culture density (*X*), light adsorption factor (α), and incident light intensity (I_{in}), which represents the average of microalgae cells light absorption in the medium as shown in **equation 2**.

$$I_{avg} = \frac{I_{in} \cdot \left(1 - e^{(-\alpha \cdot X \cdot R)}\right)}{\alpha \cdot X \cdot R} \qquad \text{(Eq.2)}$$

In this case, the culture density (X) is presumably equal to the total biomass concentration, including functional biomass and storage molecules ($X_f + C_{TAG} + C_{POC}$). However, when light intensity is beyond the saturation level, microalgal growth is photoinhibited. The term $I_{avg}/(I_{avg} + (I_{avg}^{2})/K_I)$ represents the photoinhibition effect by incorporating an inhibition term in the denominator.

Likewise, inhibition by storage product considered that POC production rate could be inhibited by a higher POC content, which is represented by the term $1 - (f_{POC}/f_{POC}^{max})$^$w$, where f_{POC} and f_{POC}^{max} stand for real and maximum POC microalgae cell content, respectively. The relative rate of POC formation to algal biomass production ($\tilde{Y}_{\frac{POC}{X}}$) was assumed to be equal to the value of f_{POC}^{max}.

Maintenance, another independently-derived rate, was equal to the constant of biomass specific ATP consumption rate *(m_{ATP})*. Due to maintenance, the substrate consumption rate (i.e., photon or glucose consumption rates) could be then calculated with the ATP stoichiometric yield on the substrate (i.e., photon or glucose), as shown in **equation 3**.

$$m_S = \frac{m_{ATP}}{Y_{\frac{ATP}{S}}} \qquad \text{(Eq. 3)}$$

The remainder rates such as TAG production rate, carbon dioxide evolution or uptake rate, oxygen evolution or uptake rate, and glucose uptake rate were derived from known independently-derived rates with the stoichiometric yields, according to the Herbert-Pirt model.

TAG production rate followed the overflow metabolism, as the total substrate uptake would be allocated for growth, maintenance, and POC and TAG production. Thus,

unconsumed substrate was allocated to TAG production as a secondary storage compound. Similarly to POC production rate, TAG production rate is inhibited by the term $1 - (f_{TAG}/f_{TAG}^{max})\hat{}u$, in case the real TAG content (f_{TAG}) reaches its maximum amount ($f_{TAG,\ max}$), which was assumed to be equal to the relative rate of TAG formation to algal biomass production ($\widetilde{Y}_{\frac{TAG}{X}}$). **Equation 4** demonstrates a general form of TAG production rate.

$$q_{TAG\,(t)} = Y_{\frac{TAG}{S}}.\left(q_{S\,(t)} - Y_{\frac{S}{X}}.\mu_{(t)} - m_S - Y_{\frac{S}{POC}}.q_{POC\,(t)}\right).\left(1 - \left(\frac{f_{TAG\,(t)}}{f_{TAG,\ max}}\right)^{u}\right) \qquad \text{(Eq. 4)}$$

The nutrient uptake rate also followed the Herbert-Pirt model given the extracellular nutrient concentration ($C_{NH_4^+}$ or $C_{PO_4^{3-}}$) limitation, characterized by negative feedback. The latter displayed a linear dependency on the nutrient cell quota depicted in **equations 5** and **6**, respectively. Both the nutrient uptake rate and the intracellular nutrient concentration decreased linearly, reaching their maximum when S = S^{min} and zero when S = S^{max}. The saturation parameter (S^m was also accounted for the maximum nutrient quota that could be stored in algal cells.

$$q_{N\,(t)} = Y_{\frac{NH_4^+}{X}}.\ \mu^{max}.\left(\frac{C_{NH_4^+}}{C_{NH_4^+} + K_{NH4}}\right).\left(\frac{S_N^{max} - S_N}{S_N^{max} - S_N^{min}}\right) \qquad \text{(Eq.5)}$$

$$q_{P\,(t)} = Y_{\frac{PO_4^{3-}}{X}}.\ \mu^{max}.\left(\frac{C_{PO_4^{3-}}}{C_{PO_4^{3-}} + K_{PO4}}\right).\left(\frac{S_P^{max} - S_P}{S_P^{max} - S_P^{min}}\right) \qquad \text{(Eq. 6)}$$

We have assumed that the maximum specific growth rate of microalgae biomass during mixotrophy was equal to the sum of all individual trophic modes' maximum specific growth rates, as shown in **equation 7**. The same approach was applied to TAG and POC production rates (**equations 8 and 9**). **Table 6** displays the model kinetics under the light-feast phase for different trophic modes.

$$\mu_{(t)}^{MIX} = \mu_{(t)}^{PLA} + \mu_{(t)}^{COH} + \mu_{(t)}^{POH} \qquad \text{(Eq. 7)}$$

$$q_{POC\,(t)}^{MIX} = q_{POC\,(t)}^{PLA} + q_{TAG\,(t)}^{COH} + q_{TAG\,(t)}^{POH} \qquad \text{(Eq. 8)}$$

$$q_{TAG\,(t)}^{MIX} = q_{TAG\,(t)}^{PLA} + q_{POC\,(t)}^{COH} + q_{POC\,(t)}^{POH} \qquad \text{(Eq. 9)}$$

Table 6 Model kinetics under light-feast phase for photoautotrophy, chemoheterotrophy, and photoheterotrophy.

Rate equations of photoautotrophy	
Photon uptake	$q^{PLA}_{photon\,(t)} = q^{PLA}_{photon,\ max}.min\left[\left(\frac{I^n_{avg}}{I^n_{avg}+\ I^n_K}\right),\left(\frac{I_{avg}}{I_{avg}+\frac{I^2_{avg}}{K_I}}\right),\left(\frac{C_{CO_2}}{C_{CO_2}+\ K_{CO2}}\right)\right]$
Growth	$\mu^{PLA}_{(t)} = \mu^{PLA}_{max}.min\left[\left(\frac{I^n_{avg}}{I^n_{avg}+\ I^n_K}\right),\left(\frac{I_{avg}}{I_{avg}+\frac{I^2_{avg}}{K_I}}\right),\left(\frac{C_{CO_2}}{C_{CO_2}+\ K_{CO2}}\right)\right].min\ (1-\frac{S^{min}_N}{S_N}, 1-\frac{S^{min}_P}{S_P})$
Maintenance	$m^{PLA}_{photon} = \frac{m_{ATP}}{Y_{\frac{ATP}{photon}}}$
POC production	$q^{PLA}_{POC\,(t)} = q^{PLA}_{POC,\ max}.\left[\left(\frac{I^n_{avg}}{I^n_{avg}+\ I^n_K}\right),\left(\frac{I_{avg}}{I_{avg}+\frac{I^2_{avg}}{K_I}}\right),\left(\frac{C_{CO_2}}{C_{CO_2}+\ K_{CO2}}\right)\right].min\left(\frac{S^{min}_N}{S_N},\frac{S^{min}_P}{S_P}\right).\left(1-\left(\frac{f_{POC\,(t)}}{f^{max}_{POC}}\right)^w\right)$
TAG production	$q^{PLA}_{TAG\,(t)} = \left(q^{PLA}_{photon\,(t)} - Y_{\frac{photon}{X}}.\mu^{PLA}_{(t)} - m^{PLA}_{photon} - Y_{\frac{photon}{POC}}.q^{PLA}_{POC\,(t)}\right).\frac{1}{Y_{\frac{photon}{TAG}}}\left(1-\left(\frac{f_{TAG\,(t)}}{f^{PLA}_{TAG,\ max}}\right)^u\right)$
CO_2 evolution	$q^{PLA}_{CO_2\,(t)} = Y_{\frac{CO_2}{X}}.\mu^{PLA}_{(t)} + Y_{\frac{CO_2}{TAG}}.q^{PLA}_{TAG\,(t)} + Y_{\frac{CO_2}{POC}}.q^{PLA}_{POC\,(t)}$
O_2 uptake	$q^{PLA}_{O_2\,(t)} = Y_{\frac{O_2}{X}}.\mu^{PLA}_{(t)} + Y_{\frac{O_2}{TAG}}.q^{PLA}_{TAG\,(t)} + Y_{\frac{O_2}{POC}}.q^{PLA}_{POC\,(t)} + Y_{\frac{O_2}{photon}}.m^{PLA}_{photon\,(t)}$
Nitrogen uptake	$q_{N\,(t)} = q^{max}_N.\left(\frac{C_{NH^+_4}}{C_{NH^+_4}+K_{NH4}}\right).\left(\frac{S^{max}_N - S_N}{S^{max}_N - S^{min}_N}\right)$
Phosphorus uptake	$q_{P\,(t)} = q^{max}_P.\left(\frac{C_{PO^{3-}_4}}{C_{PO^{3-}_4}+K_{PO4}}\right).\left(\frac{S^{max}_P - S_P}{S^{max}_P - S^{min}_P}\right)$
	$q^{max}_P = Y_{\frac{PO^{3-}_4}{X}}.\ \mu^{max}$

Table 6 (Continued)

Rate equations of chemoheterotrophy	
Glucose uptake	$q^{COH}_{Glc\,(t)} = q^{COH}_{Glc,\ max}.min\left[\left(\frac{C_{Glc}}{C_{Glc}+\ K_{Glc}}\right),\left(\frac{C_{O_2}}{C_{O2}+\ K_{O2}}\right)\right]$
Growth	$\mu^{COH}_{(t)} = \mu^{COH}_{max}.min\left[\left(\frac{C_{Glc}}{C_{Glc}+\ K_{Glc}}\right),\left(\frac{C_{O_2}}{C_{O_2}+\ K_{O2}}\right)\right].min\left(1-\frac{S_N^{min}}{S_N},1-\frac{S_P^{min}}{S_P}\right)$
Maintenance	$m^{COH}_{Glc\,(t)} = \frac{m_{ATP\,(t)}}{Y_{\frac{ATP}{Glc}}}$
POC production	$q^{COH}_{POC\,(t)} = q^{COH}_{POC,\ max}.min\left[\left(\frac{C_{Glc}}{C_{Glc}+\ K_{Glc}}\right),\left(\frac{C_{O_2}}{C_{O_2}+\ K_{O2}}\right)\right].min\left(\frac{S_N^{min}}{S_N},\frac{S_P^{min}}{S_P}\right).\left(1-\left(\frac{f_{POC\,(t)}}{f^{max}_{POC}}\right)^{w}\right)$
TAG production	$q^{COH}_{TAG\,(t)} = \left(q^{COH}_{Glc\,(t)} - Y_{\frac{Glc}{X}}.\mu^{COH}_{(t)} - m^{COH}_{Glc\,(t)} - Y_{\frac{Glc}{POC}}.q^{COH}_{POC\,(t)}\right).\frac{1}{Y_{\frac{Glc}{TAG}}}.\left(1-\left(\frac{f_{TAG\,(t)}}{f^{COH}_{TAG,\ max}}\right)^{u}\right)$
CO_2 evolution	$q^{COH}_{CO_2\,(t)} = Y_{\frac{CO_2}{X}}.\mu^{COH}_{(t)} + Y_{\frac{CO_2}{TAG}}.q^{COH}_{TAG\,(t)} + Y_{\frac{CO_2}{POC}}.q^{COH}_{POC\,(t)} + Y_{\frac{CO_2}{Glc}}.m^{COH}_{Glc\,(t)}$
O_2 uptake	$q^{COH}_{O_2\,(t)} = Y_{\frac{O_2}{X}}.\mu^{COH}_{(t)} + Y_{\frac{O_2}{TAG}}.q^{COH}_{TAG\,(t)} + Y_{\frac{O_2}{POC}}.q^{COH}_{POC\,(t)} + Y_{\frac{O_2}{Glc}}.m^{COH}_{Glc\,(t)}$
Nitrogen uptake	$q_{N\,(t)} = q_N^{max}.\left(\frac{C_{NH_4^+}}{C_{NH_4^+}+K_{NH4}}\right).\left(\frac{S_N^{max}-S_N}{S_N^{max}-S_N^{min}}\right)$ $q_N^{max} = Y_{\frac{NH_4^+}{X}}.\ \mu^{max}$
Phosphorus uptake	$q_{P\,(t)} = q_P^{max}.\left(\frac{C_{PO_4^{3-}}}{C_{PO_4^{3-}}+K_{PO4}}\right).\left(\frac{S_P^{max}-S_P}{S_P^{max}-S_P^{min}}\right)$ $q_P^{max} = Y_{\frac{PO_4^{3-}}{X}}.\ \mu^{max}$

Table 6 (Continued)

Rate equations of photoheterotrophy	
Photon uptake	$q^{POH}_{photon\,(t)} = q^{POH}_{photon,\ max}.min\left[\left(\frac{I^n_{avg}}{I^n_{avg}+\ I^n_K}\right),\left(\frac{I_{avg}}{I_{avg}+\frac{I^2_{avg}}{K_I}}\right),\left(\frac{C_{Glc}}{C_{Glc}+\ K_{Glc}}\right)\right]$
Growth	$\mu^{POH}_{(t)} = \mu^{POH}_{max}.min\left[\left(\frac{I^n_{avg}}{I^n_{avg}+\ I^n_K}\right),\left(\frac{I_{avg}}{I_{avg}+\frac{I^2_{avg}}{K_I}}\right),\left(\frac{C_{Glc}}{C_{Glc}+\ K_{Glc}}\right)\right].min\ (1-\frac{S^{min}_N}{S_N}, 1-\frac{S^{min}_P}{S_P})$
Maintenance	$m^{POH}_{photon\,(t)} = \frac{m_{ATP\,(t)}}{Y_{\frac{ATP}{photon}}}$
POC production	$q^{POH}_{POC\,(t)} = q^{POH}_{POC,\ max}.\left[\left(\frac{I^n_{avg}}{I^n_{avg}+\ I^n_K}\right),\left(\frac{I_{avg}}{I_{avg}+\frac{I^2_{avg}}{K_I}}\right),\left(\frac{C_{Glc}}{C_{Glc}+\ K_{Glc}}\right)\right].min\left(\frac{S^{min}_N}{S_N},\frac{S^{min}_P}{S_P}\right).\left(1-\left(\frac{f_{POC\,(t)}}{f^{POH}_{POC,\ max}}\right)^w\right)$
TAG production	$q^{POH}_{TAG\,(t)} = \left(q^{POH}_{photon\,(t)} - Y_{\frac{photon}{X}}.\mu^{POH}_{(t)} - m^{POH}_{photon\,(t)} - Y_{\frac{photon}{POC}}.q^{POH}_{POC\,(t)}\right).\frac{1}{Y_{\frac{photon}{TAG}}}\ .\left(1-\left(\frac{f_{TAG\,(t)}}{f^{POH}_{TAG,\ max}}\right)^u\right)$
CO_2 evolution	$q^{POH}_{CO_2\,(t)} = Y_{\frac{CO_2}{X}}.\mu_{(t)} + Y_{\frac{CO_2}{TAG}}.q_{TAG\,(t)} + Y_{\frac{CO_2}{POC}}.q_{POC\,(t)}$
O_2 uptake	$q^{POH}_{O_2\,(t)} = Y_{\frac{O_2}{X}}.\mu_{(t)} + Y_{\frac{O_2}{TAG}}.q_{TAG\,(t)} + Y_{\frac{O_2}{POC}}.q_{POC\,(t)} + Y_{\frac{O_2}{photon}}.m_{photon\,(t)}$
Glucose uptake	$q^{POH}_{Glc\,(t)} = Y_{\frac{Glc}{X}}.\mu_{(t)} + Y_{\frac{Glc}{TAG}}.q_{TAG\,(t)} + Y_{\frac{Glc}{POC}}.q_{POC\,(t)} + Y_{\frac{Glc}{photon}}.m_{photon\,(t)}$
Nitrogen uptake	$q_{N\,(t)} = q^{max}_N.\left(\frac{C_{NH^+_4}}{C_{NH^+_4}+K_{NH4}}\right).\left(\frac{S^{max}_N - S_N}{S^{max}_N - S^{min}_N}\right)$ $q^{max}_N = Y_{\frac{NH^+_4}{X}}.\ \mu^{max}$
Phosphorus uptake	$q_{P\,(t)} = q^{max}_P.\left(\frac{C_{PO^{3-}_4}}{C_{PO^{3-}_4}+K_{PO4}}\right).\left(\frac{S^{max}_P - S_P}{S^{max}_P - S^{min}_P}\right)$ $q^{max}_P = Y_{\frac{PO^{3-}_4}{X}}.\ \mu^{max}$

2.2.4.2 Kinetics of dark-famine regime

During the dark-famine regime, microalgae growth depends on nutrient availability for cell reproduction. Storage compounds (i.e., POC and TAG) are then used as organic carbon sources enabling microalgal growth. We assumed that POC and TAG were concomitantly used with different degradation rates. Thus, each storage molecule was defined with two biomass-specific growth rates where their sum gave the practical value for biomass-specific growth rate under the dark-famine regime.

Microalgae usually prefer starch as the organic carbon source for cell growth. Therefore, the model assumed a higher biomass maximum specific growth rate for POC than TAG ($\mu_{max}^{Dark,\ POC} > \mu_{max}^{Dark,\ TAG}$). Considering the Herbert-Pirt model, known stoichiometry yields were adopted for POC and TAG degradation, CO_2 evolution, and O_2 uptake rates. Nutrient uptake rates adopted the approach applied within the light-feast regime. **Table 7** shows the equations for the model kinetics under the dark-famine regime.

Table 7 Model kinetics under dark-famine regime

Growth	$\mu_{TAG\ (t)}^{Dark} = \mu_{max}^{Dark,\ TAG}.\left(\frac{C_{TAG}}{C_{TAG}+K_{TAG}}\right).min\ (1-\frac{S_N^{min}}{S_N}, 1-\frac{S_P^{min}}{S_P})$
	$\mu_{POC\ (t)}^{Dark} = \mu_{max}^{Dark,\ POC}.\left(\frac{C_{POC}}{C_{POC}+K_{POC}}\right).min\ (1-\frac{S_N^{min}}{S_N}, 1-\frac{S_P^{min}}{S_P})$
	$\mu_{(t)}^{Dark} = \mu_{TAG\ (t)}^{Dark} + \mu_{POC\ (t)}^{Dark}$
Maintenance	$m_{POC\ (t)}^{Dark} = \frac{m_{ATP\ (t)}}{Y_{\frac{ATP}{POC}}}$
	$m_{TAG\ (t)}^{Dark} = \frac{m_{ATP\ (t)}}{Y_{\frac{ATP}{TAG}}}$
POC degradation	$q_{POC\ (t)}^{Dark} = Y_{\frac{POC}{X}}.\mu_{(t)}^{Dark,\ POC} + m_{POC\ (t)}^{Dark}$
TAG degradation	$q_{TAG\ (t)}^{Dark} = Y_{\frac{TAG}{X}}.\mu_{(t)}^{Dark,\ TAG} + m_{TAG\ (t)}^{Dark}$
TAG degradation	$q_{TAG\ (t)}^{Dark} = Y_{\frac{TAG}{X}}.\mu_{(t)}^{Dark,\ TAG} + m_{TAG\ (t)}^{Dark}$
CO_2 evolution	$q_{CO_2\ (t)}^{Dark} = Y_{\frac{CO_2}{X}}.\mu_{(t)}^{Dark,\ POC} + m_{POC\ (t)}^{Dark}.Y_{\frac{CO_2}{POC}} + Y_{\frac{CO_2}{X}}.\mu_{(t)}^{Dark,\ TAG} + m_{TAG\ (t)}^{Dark}.Y_{\frac{CO_2}{TAG}}$
O_2 uptake	$q_{O_2\ (t)}^{Dark} = Y_{\frac{O_2}{X}}.\mu_{(t)}^{Dark,\ POC} + m_{POC\ (t)}^{Dark}.Y_{\frac{O_2}{POC}} + Y_{\frac{O_2}{X}}.\mu_{(t)}^{Dark,\ TAG} + m_{TAG\ (t)}^{Dark}.Y_{\frac{O_2}{TAG}}$
Nitrogen uptake	$q_{N\ (t)}^{Dark} = q_N^{Dark,\ max}.\left(\frac{C_{NH_4^+}}{C_{NH_4^+}+K_{NH4}}\right).\left(\frac{S_N^{max}-S_N}{S_N^{max}-S_N^{min}}\right)$
	$q_N^{max} = Y_{\frac{NH_4^+}{X}}.\mu_{max}^{Dark,\ TAG} + Y_{\frac{NH_4^+}{X}}.\mu_{max}^{Dark,\ POC}$
Phosphorus uptake	$q_{P\ (t)}^{Dark} = q_P^{Dark,\ max}.\left(\frac{C_{PO_4^{3-}}}{C_{PO_4^{3-}}+K_{PO4}}\right).\left(\frac{S_P^{max}-S_P}{S_P^{max}-S_P^{min}}\right)$
	$q_P^{max} = Y_{\frac{PO_4^{3-}}{X}}.\mu_{max}^{Dark,\ TAG} + Y_{\frac{PO_4^{3-}}{X}}.\mu_{max}^{Dark,\ POC}$

2.3 Microbial chemotrophic growth

Hitherto, our mathematical model covered the stoichiometry and kinetics of microalgal axenic cultures. However, in mixed cultures, the model must cover not only microalgal behavior but also their symbiotic relationships with other microorganisms. So, the ASM1(Henze et al., 2015) was incorporated covering chemoautotrophic and heterotrophic microbial growth (i.e., nitrifying bacteria). We assumed that denitrifiers grew under aerobic and anoxic conditions, whereas fermenters grew in anaerobic ones. To simplify the model, heterotrophic denitrifications and chemoautotrophic nitrification were modeled as a one-step process, where NO_3^- would be converted to N_2 and NH_4^+ would be directly converted to NO_3^-, respectively. **Figure 1** depicts the relationships among these microorganisms in a mixed culture.

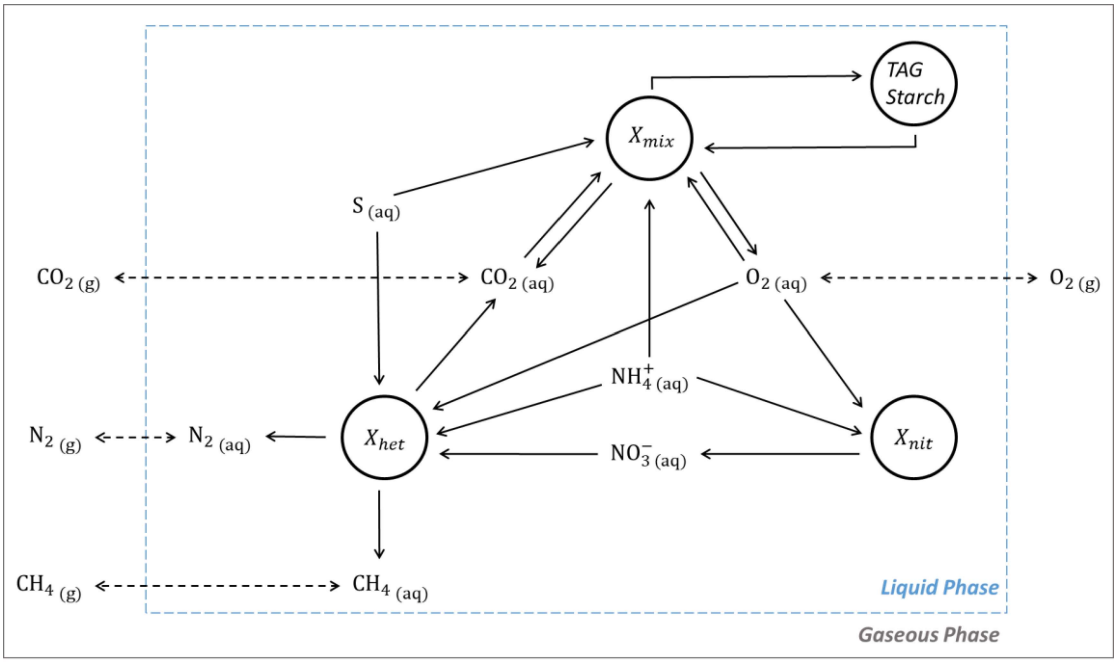


Figure 1 Microorganisms symbiotic relationships (i.e., conversion process and interactions) in mixed cultures considering gas exchange between liquid and gaseous phases, where (X_{mix}) stands for mixotrophic microalgae biomass and (X_{het}) and (X_{nit}) for heterotrophic and nitrifiers microbial biomass, respectively. Unbroken lines ( ) cover biological encompass conversion processes and dashed lines (---) the transfer processes between phases.

In terms of the symbiotic relationship, the stoichiometry and kinetics of microbial growth assumed that microalgae would produce intracellular storage compounds but no extracellular polymeric material. Besides that, heterotrophic and autotrophic bacteria would not have microalgal biodegradable biomass to serve as a carbon source in their metabolism, thus growing either using the COD present in the feedstock or the products of catabolic conversions (e.g., O_2 and CO_2) during commensalism or mutualism (see **Figure 1**).

The ASM1 underwent some alterations to express the kinetics of bacterial growth. Thus, the adjustment considered the fact that in mixed cultures, both microalgal and bacterial growth rates were modeled according to the joint model expression depicted in **equation 1** instead of the threshold model. Therefore, all impacts of inconsistent assumptions were removed. **Table 8** summarizes the the maximum yields predicted by microbial growth stoichiometry and **Table 9** the kinetic of heterotrophic and autotrophic bacteria rate equations.

2.4 Culture medium and feedstock properties

Under a light-feast regime, 40% demineralized whey concentrate (WPC40) and the VFAs produced during the acidogenic fermentation of cheese whey were considered suitable feedstocks to model microalgae biomass growth, kinetics, and TAG and POC production. For WPC40, it was considered that 1 g L^{-1} of WPC corresponds to 1 g O_2 L^{-1} in COD terms.

According to Saddoud (2007), cheese whey has an organic load of 50 to 80 g O_2 L^{-1}, in terms of COD. Yadav (2014), stated that cheese whey had a COD of about 68 g O_2 L^{-1}, in terms of COD. Assuming that all CW COD was soluble, a dissolution of 65.7g of WPC was considered after applying the principle of linear proportionality. **Table 10** shows the characteristics of the CW solution adopted for our model.

Table 8 Stoichiometric yields for microbial growth expressed as the function of the yield of heterotrophs (Y_H) on glucose and the yield of nitrifiers (Y_N) on nitrate.

	Aerobic heterotrophs	**Anoxic heterotrophs**	**Anaerobic heterotrophs**	**Nitrifiers**
$C_6H_{12}O_6$	$Y_{\frac{GLC}{X_{het}}} = \frac{1}{Y_H}$	$Y_{\frac{GLC}{X_{het}}} = \frac{1}{Y_H}$	$Y_{\frac{GLC}{X_{het}}} = \frac{1}{Y_H}$	
CO_2	$Y_{\frac{CO_2}{X_{het}}} = \frac{1}{0.16\ Y_H} - 0.99$	$Y_{\frac{CO_2}{X_{het}}} = -\frac{1}{0.16\ Y_H} - 0.99$	$Y_{\frac{CO_2}{X_{het}}} = -\frac{1}{0.33\ Y_H} - 0.45$	$Y_{\frac{CO_2}{X_{nit}}} = -1$
O_2	$Y_{\frac{O_2}{X_{het}}} = \frac{1}{0.16\ Y_H} + 1.08$			$Y_{\frac{O_2}{X_{nit}}} = -\frac{1}{0.5\ Y_N} + 1.08$
NO_3^-		$Y_{\frac{NO_3^-}{X_{het}}} = \frac{1}{0.21\ Y_H} + 0.86$		$Y_{\frac{NO_3^-}{X_{nit}}} = \frac{1}{Y_N}$
N_2		$Y_{\frac{N_2}{X_{het}}} = -\frac{1}{0.42\ Y_H} - 0.43$		
CH_4			$Y_{\frac{CH_4}{X_{het}}} = -\frac{1}{0.33\ Y_H} - 0.54$	
NH_4^+	$Y_{\frac{NH4^+}{X_{het}}} = -0.2$	$Y_{\frac{NH4^+}{X_{het}}} = -0.2$	$Y_{\frac{NH4^+}{X_{het}}} = -0.2$	$Y_{\frac{NH4^+}{X_{nit}}} = -\frac{1}{Y_N} - 0.2$
PO_4^{3-}	$Y_{\frac{PO_4^{3-}}{X_{het}}} = -0.03$	$Y_{\frac{PO_4^{3-}}{X_{het}}} = -0.03$	$Y_{\frac{PO_4^{3-}}{X_{het}}} = -0.03$	$Y_{\frac{PO_4^{3-}}{X_{nit}}} = -0.03$

Table 9 The kinetics of heterotrophic and autotrophic bacteria rate equations.

Nitrifiers	
Growth	$\mu_{(t)}^{Nit} = \mu_{max}^{Nit}.min\left(\frac{C_{CO_2}}{C_{CO_2} + K_{CO2}^{Nit}}, \frac{C_{O_2}}{C_{O_2} + K_{O2}^{Nit}}\right).min\left(\frac{S_{Nmin}^{Nit}}{S_N^{Nit}}, \frac{S_{Pmin}^{Nit}}{S_P^{Nit}}\right)$
O_2 uptake	$q_{O_2}^{Nit} = Y_{\frac{O_2}{X_{nit}}}.\mu_{(t)}^{Nit}$
CO_2 uptake	$q_{CO_2}^{Nit} = Y_{\frac{CO_2}{X_{nit}}}.\mu_{(t)}^{Nit}$
Nitrate evolution	$q_{NO_3}^{Nit} = Y_{\frac{NO_3^-}{X_{nit}}}.\mu_{(t)}^{Nit}$
Nitrogen (ammonia) uptake	$q_{NH_4}^{Nit} = Y_{\frac{NH_4^+}{X_{nit}}}.\mu_{(t)}^{Nit}.\left(\frac{C_{NH_4^+}}{C_{NH_4^+} + K_{NH4}^{Nit}}\right).\left(\frac{S_{Nmax}^{Nit} - S_N^{Nit}}{S_{Nmax}^{Nit} - S_{Nmin}^{Nit}}\right)$
Heterotrophs	
Phosphate uptake	$q_{PO_4}^{Nit} = Y_{\frac{PO_4^{3-}}{X_{nit}}}.\mu_{(t)}^{Nit}.\left(\frac{C_{PO_4^{3-}}}{C_{PO_4^{3-}} + K_{PO4}^{Nit}}\right).\left(\frac{S_{Pmax}^{Nit} - S_P^{Nit}}{S_{Pmax}^{Nit} - S_{Pmin}^{Nit}}\right)$
Growth	
Aerobic	$\mu_{(t)}^{Het,\ Aerobic} = \mu_{max}^{Het,\ Aerobic}.min\left(\frac{C_S}{C_S + K_S^{Het}}, \frac{C_{O_2}}{C_{O_2} + K_{O2}^{Het}}\right).min\left(\frac{S_{Nmin}^{Het}}{S_N^{Het}}, \frac{S_{Pmin}^{Het}}{S_P^{Het}}\right)$
Anoxic	$\mu_{(t)}^{Het,\ Anoxic} = \mu_{max}^{Het,\ Anoxic}.min\left(\frac{C_S}{C_S + K_S^{Het}}, \frac{C_{NO_3^-}}{C_{NO_3^-} + K_{NO3}^{Het}}, \frac{K_{O2}^{Het}}{C_{O_2} + K_{O2}^{Het}}\right).min\left(\frac{S_{Nmin}^{Het}}{S_N^{Het}}, \frac{S_{Pmin}^{Het}}{S_P^{Het}}\right)$
Anaerobic	$\mu_{(t)}^{Het,\ Anaerobic} = \mu_{max}^{Het,\ Anaerobic}.min\left(\frac{C_S}{C_S + K_S^{Het}}, \frac{K_{NO_3^-}^{Het}}{C_{NO_3^-} + K_{NO3}^{Het}}, \frac{K_{O_2}^{Het}}{C_{O_2} + K_{O2}^{Het}}\right).min\left(\frac{S_{Nmin}^{Het}}{S_N^{Het}}, \frac{S_{Pmin}^{Het}}{S_P^{Het}}\right)$
Overall	$\mu_{(t)}^{Het} = \mu_{(t)}^{Het,\ Aerobic} + \mu_{(t)}^{Het,\ Anoxic} + \mu_{(t)}^{Het,\ Anaerobic}$

Table 9 (Continued)

Heterotrophs	
O_2 uptake	$q_{O_2}^{Het} = Y_{\frac{O_2}{X_{het}}}^{Aerobic} . \mu_{(t)}^{Het,\ Aerobic}$
CO_2 evolution	$q_{CO_2}^{Het} = Y_{\frac{CO_2}{X_{het}}}^{Aerobic} . \mu_{(t)}^{Het,\ Aerobic} + Y_{\frac{CO_2}{X_{het}}}^{Anoxic} . \mu_{(t)}^{Het,\ Anoxic} + Y_{\frac{CO_2}{X_{het}}}^{Anaerobic} . \mu_{(t)}^{Het,\ Anaerobic}$
Nitrate uptake	$q_{NO_3}^{Het} = Y_{\frac{NO_3^-}{X_{het}}}^{Anoxic} . \mu_{(t)}^{Het,\ Anoxic}$
N_2 evolution	$q_{N_2}^{Het} = Y_{\frac{N_2}{X_{het}}}^{Anoxic} . \mu_{(t)}^{Het,\ Anoxic}$
Glucose uptake	$q_{GLC}^{Het} = Y_{\frac{GLC}{X_{het}}}^{Aerobic} . \mu_{(t)}^{Het,\ Aerobic} + Y_{\frac{GLC}{X_{het}}}^{Anoxic} . \mu_{(t)}^{Het,\ Anoxic} + Y_{\frac{GLC}{X_{het}}}^{Anaerobic} . \mu_{(t)}^{Het,\ Anaerobic}$
CH_4 evolution	$q_{CH_4}^{Het} = Y_{\frac{CH_4}{X_{het}}}^{Anaerobic} . \mu_{(t)}^{Het,\ Anaerobic}$
Nitrogen (ammonia) uptake	$q_{NH_4}^{Nit} = Y_{\frac{NH_4^+}{X_{het}}} . \mu_{(t)}^{Het} . \left(\frac{C_{NH_4^+}}{C_{NH_4^+} + K_{NH4}^{Het}}\right) . \left(\frac{S_{Nmax}^{Het} - S_N^{Het}}{S_{Nmax}^{Het} - S_{Nmin}^{Het}}\right)$
Phosphate uptake	$q_{PO_4}^{Nit} = Y_{\frac{PO_4^{3-}}{X_{het}}} . \mu_{(t)}^{Het} . \left(\frac{C_{PO_4^{3-}}}{C_{PO_4^{3-}} + K_{PO4}^{Het}}\right) . \left(\frac{S_{Pmax}^{Het} - S_P^{Het}}{S_{Pmax}^{Het} - S_{Pmin}^{Het}}\right)$

Table 10 Preliminary characteristics of the cheese whey solution implemented in the mathematical model. (TS) total solids, (VS) volatile solids, (TSS) total suspended solids, (COD_S) soluble COD, (TOC) total organic carbon, (TN) total nitrogen

TS (gL^{-1})	VS (gL^{-1})	TSS (gL^{-1})	$_SCOD$ ($g_{COD}L^{-1}$)	Sugar (gL^{-1})	TOC (g_CL^{-1})	TN (g_NL^{-1})	$N-NH_4^+$ (mg_NL^{-1})	$P-PO_4^{3-}$ (mg_PL^{-1})
64.71	60.94	1.15	68.0	52.56	24.64	410	18.23	361.51

Table 10 provided the values of chosen parameters of cheese whey to be implemented in the model. However, these values needed to be altered to be implemented in the model and consequently, modeling would run without additional issues regarding units.

These alterations comprised the conversion of sCOD values to their glucose-equivalent ones. Additionally, we assumed that total nitrogen (TN) was only comprised of (NH_4^+). Hence, the practical concentration values of RCW were calculated and shown in **Table 11**. The same premise was applied to PCW assuming the values of **Chapter 3**. Phosphorus concentration was assumed to be the same as RCW.

Regarding the MCW an ideal C: N ratio was hypothesized for optimal TAG production. Since the main characteristics of MCW were unknown, they were obtained by solving the model equations considering the effect of the C: N ratio on TAG production efficiency. The main difference between all three substrates was the C: N and the C:P ratios which directly affect microalgae metabolism. A synthetic carbon-free and nutrient-rich substrate (NS) was designed to be implemented during dark-famine regime with $C_{NH_4^+}^{In} = 50\ \mathrm{mol\ m^{-3}}$, and $C_{PO_4^{3-}}^{In} = 20\ \mathrm{mol\ m^{-3}}$, which can be seen on **Table 11**.

Table 11 Practical characteristics of culture medium/feedstock, Cheese whey (RCW), Products of CW (PCW), Modified CW (MCW), and Nutrient Stream (NS), to be implemented in the model

	C_S^{In} (mol COD m^{-3})	C_{GLC}^{In} (mol GLC m^{-3})	$C_{NH_4^+}^{In}$ (mol NH_4^+ m^{-3})	$C_{PO_4^{3-}}^{In}$ (mol PO_4^{3-} m^{-3})
RCW	2,053.3	342.2	29.3	11.7
PCW	1,430.6	238.4	42.5	11.7
MCW	$C_{S,\ MCW}^{In}$	$C_{GLC,\ MCW}^{In}$	$C_{NH_4^+,\ MCW}^{In}$	$C_{PO_4^{3-},\ MCW}^{In}$
NS	0	0	50	20

The gas influent was composed of common airflow (A_F) and a carbon dioxide-enriched airflow (CEA_F) of 40,000 ppm, thus enhancing microalgal photoautotrophic growth. **Table 12** shows the mole fraction of both gas-influent streams.

Table 12 Practical characteristics of gaseous flow, CO_2 enriched airflow (CEA_F), and Air flow (A_F), to be implemented in the model.

	$y_{CO_2}^{In}$ (mol_{CO2} mol_{Air}^{-1})	$y_{O_2}^{In}$ (mol_{O2} mol_{Air}^{-1})	$y_{N_2}^{In}$ (mol_{N2} mol_{Air}^{-1})	$y_{CH_4}^{In}$ (mol_{N2} mol_{Air}^{-1})
CEA_F	0.04	0.202	0.758	0
A_F	0.0004	0.210	0.780	0

2.5 Reactor configuration and set of ODEs

Concerning the modeling of microalgae biomass growth, the use of a photobioreactor with specific operation configurations was assumed, even though other types of bioreactor configurations could also be adapted to the model.

A photobioreactor (PBR) able to operate under batch and chemostat regimes and, with a working volume of 20 L given the vessel radius (R_r) of 0.147 m, a height (H_h) of 0.294 m and a diameter over height (β) of 1.0 m was chosen for the model implementation. Other assumptions included the airflow sparge in the reactor for CO_2, N_2, and O_2 supply, which would then transform into air bubbles
contributing to a more efficient contact between gas and liquid phases. Both influent and effluent liquid flows were considered for the chemostat regime and a butterfly paddle would provide the continuous agitation.

Regarding the illumination patterns, the light would be provided by a light jacket encircling the PBR and emitting radiation in the range of visible wavelengths. The light-feast and dark-famine phases occurred on the premise that the CSTR-PBR would operate constantly under a chemostat regime. The switch between light-feast and dark-famine phases would happen once the light jacket would be turned on and off, respectively. Additionally, the influent substrate would change from a carbon-rich feedstock (i.e., CW, PCW, and MCW) for the light-feast phase and a carbon-free substrate (i.e., NS) during the dark-famine phase. **Figure 2** shows two different light cycles that were implemented for each

carbon-rich and carbon-free substrate or additional comparison. Those were alternated light-feast and dark-famine 24:24 h and 36:12h cycles.

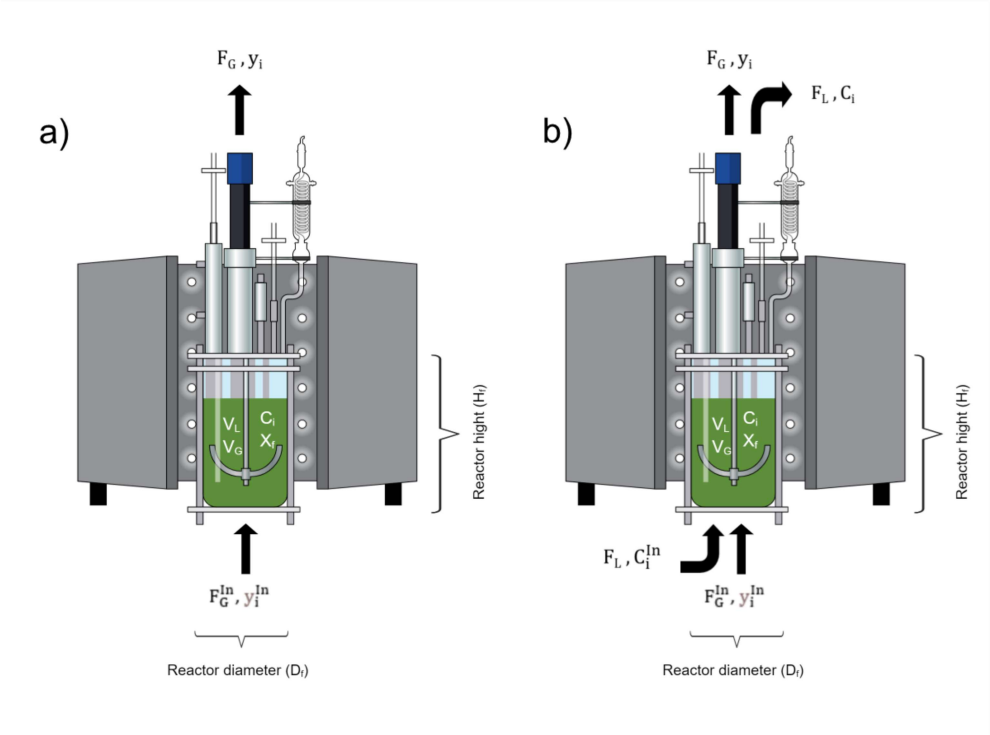


Fig 2 a) Batch photobioreactor regime assumed for microalgal axenic culture growth where the reactor is filled with culture medium with an initial concentration of compounds (C_i). The reactor would operate until the consumption of all essential compounds. b) CSTR photobioreactor conditions assumed for both axenic and mixed culture under the chemostat regime. The reactor would be continuously fed by an influent feedstock (F_L) until reaching a steady state.

The value of state variables over time was determined based on the principle of mass conservation, where the difference between the overall mass entering the system and the one which is already present there would be equal to the accumulation of mass within the system.

However, accumulation can also derive from mass consumption or generation. Thus, it is important to account not only for the rearrangement of mass in the system but its change to form other compounds rather than just the input and output of mass in the system.

A set of ordinary differential equations (ODEs) for the mass balances of state variables under batch and chemostat regimes were adopted based on **equation 10**.

Accumulation = Input – Output + Generation - Consumption (Eq. 10)

The only state variables of interest in batch culture were the ones within the liquid phase, whereas, in a batch regime photobioreactor without the input and output of liquids, the expression of mass balance was simplified to mass generation and consumption giving the biological conversions and transfer to and from the gaseous phase. Subsequently, the material balance for non-volatile variables (TAG, POC, Glc, X) in the liquid phase was derived as

$$\frac{\mathrm{dC_i}}{\mathrm{dt}} = \mathrm{q_i}.\mathrm{X_{mix}} \quad \text{(Eq. 11)}$$

where $\mathrm{q_i}$ is the conversion rate of component *i*, calculated in the kinetics **section 2.2.4.**

For gaseous compounds such as O_2, CO_2, N_2, and CH_4, the gas-liquid transfer rate considered the volumetric transfer coefficient and was obtained by the difference between the maximum soluble concentration and saturated concentration ($\mathrm{C_i^{sat}}$) of the gas compound, as well as the actual gas concentration in the liquid phase.

$$\frac{dC_i}{dt} = q_i.X_{mix} + kLa.(C_i^{sat} - C_i) \quad \text{(Eq.12)}$$

where $\mathrm{C_i^{sat}}$ depended on the compound partial pressure *i* during the gas phase via Henry's coefficient ($\mathrm{H_i}$) as depicted in **equation 13**.

$$C_i^{sat} = y_i \times H_i \times P_{tot} \quad \text{(Eq.13)}$$

The material balance for nutrients cell quota (S_N and S_P) also followed the same approach depicted in **equation 13.** The intracellular nutrient content within microalgal cells, defined as the nutrient cell quota multiplied by the functional biomass concentration, was dependent on microalgae nutrient uptake shown in **equation 14.**

$$\frac{d(S_i.X_{mix})}{dt} = -q_i.X_{mix} \quad \text{(Eq. 14)}$$

Expanding $(S_i.X_{mix})$ gave the nutrient cell quota of the functional biomass as **equation 15.**

$$\frac{dS_i}{dt} = -\frac{q_i.X_{mix} + S_i.\frac{dX_{mix}}{dt}}{X_{mix}} \quad \text{(Eq.15)}$$

Substituting $\frac{\mathrm{dX_{mix}}}{\mathrm{dt}}$ with its equality based on **equation 11**, the simplified expression of cell quota balance was derived as **equation 16.**

$$\frac{dS_i}{dt} = -q_i - S_i.(\mu^{PLA} + \mu^{COH} + \mu^{POH}) \quad \text{(Eq. 16)}$$

A summary of the state variables' mass balances in a batch photobioreactor under the light-feast phase is provided in **Table 13.**

Table 13 Ordinary differential equations (ODEs) for microalgal pure culture in a batch photobioreactor under light-feast phase

$\frac{dC_{CO_2}}{dt} = q_{CO_2}.X_{mix} + kLa.(C_{CO_2}^{sat} - C_{CO_2})$
$\frac{dC_{O_2}}{dt} = q_{O_2}.X_{mix} + kLa.(C_{O_2}^{sat} - C_{O_2})$
$\frac{dC_{GLC}}{dt} = q_{GLC}.X_{mix}$
$\frac{dC_{NH_4^+}}{dt} = q_N.X_{mix}$
$\frac{dS_N}{dt} = -q_N - S_N.(\mu^{PLA} + \mu^{COH} + \mu^{POH})$
$\frac{dC_{PO_4^{3-}}}{dt} = q_P.X_{mix}$
$\frac{dS_P}{dt} = -q_P - S_P.(\mu^{PLA} + \mu^{COH} + \mu^{POH})$
$\frac{dC_{TAG}}{dt} = (q_{TAG}^{PLA} + q_{TAG}^{COH} + q_{TAG}^{POH}).X_{mix}$
$\frac{dC_{POC}}{dt} = (q_{POC}^{PLA} + q_{POC}^{COH} + q_{POC}^{POH}).X_{mix}$
$\frac{dX_{mix}}{dt} = (\mu^{PLA} + \mu^{COH} + \mu^{POH}).X_{mix} - K_d.X_{mix}$

The equations in **Table 12** were expanded accounting for the continuous inflow and outflow of liquid to and from the system, thus applying the chemostat regime. **Equations 17, 18,** and **19** demonstrate the material balance in a chemostat photobioreactor regime for the concentration of non-volatile components, concentration of volatile components, and cell quota, respectively.

$$\frac{dC_i}{dt} = \frac{F_L}{V_L}.(C_i^{In} - C_i) + q_i.X_{mix} \quad \text{(Eq.17)}$$

$$\frac{dC_i}{dt} = \frac{F_L}{V_L}.(C_i^{In} - C_i) + q_i.X_{mix} + kLa.(C_i^{sat} - C_i) \quad \text{(Eq.18)}$$

$$\frac{dS_i}{dt} = \frac{F_L}{V_L}.\left(\frac{X_{mix}^{In}.S_i}{X_{mix}} - S_i\right) - q_i - S_i.(\mu^{PLA} + \mu^{COH} + \mu^{POH}) \quad \text{(Eq.19)}$$

where F_{LR} stands for the inlet and outlet volumetric liquid flow rate, and V_L for the liquid phase volume.

The chemostat regime model was then improved once accounting for both the state variables in the liquid phase and the mole fraction of gaseous compounds in the gaseous phase. The material balances for the gas phase can also be derived for a gaseous component *i* as shown in **equation 20**.

$$\frac{dy_i}{dt} = \frac{F_G^{In}}{V_G}.(y_i^{In} - y_i) + \frac{V_L.R_c.T}{V_G.P_{tot}}.kLa.\left(y_i.\sum_{j=all\ gases}(C_j^{sat} - C_j) - (C_i^{sat} - C_i)\right)$$

(Eq.20)

where F_G^{In} stands for the volumetric inlet gas flow rate, V_G for the gas phase volume, R_c for the ideal gas constant, and T for temperature. **Table 14** summarizes the material balances for the state variables in a CSTR photobioreactor under light-feast and dark-famine regimes.

The same principles used to perform the mass balance of microalgae axenic culture were applied to the non-axenic culture with few adjustments. The term corresponding to the consumption and generation of components resulted from biological conversions was expanded considering different microbial activities such as (*i*) nitrifiers influencing the concentration of dissolved CO_2 by consuming it for biomass production which is represented by $q_{CO2}^{Nit}.X_{nit}$ and, (*ii*) CO_2 generation by heterotrophic bacteria through the oxidation of organics which is represented by $q_{CO2}^{Het}.X_{het}$. Additionally, the number of state variables included in the model increased so microbial activities (e.g., nitrate concentration, $CH_{4\ (g)}$ mole fraction, heterotrophs nitrogen cell quota) were considered. **Table 15** depicts the material balances for all state variables in a CSTR photobioreactor for microalgae mixed culture under light-feast and dark-famine regimes.

Table 14 ODEs for microalgal axenic culture in a CSTR photobioreactor under both light-feast and dark-famines regimes.

Light-feast	Dark-famine
$\frac{dC_{CO_2}}{dt} = \frac{F_L}{V_L}.\left(C_{CO_2}^{In} - C_{CO_2}\right) + q_{CO_2}.X_f + kLa.\left(C_{CO_2}^{sat} - C_{CO_2}\right)$	$\frac{dC_{CO_2}}{dt} = \frac{F_L}{V_L}.\left(C_{CO_2}^{In} - C_{CO_2}\right) + q_{CO_2}^{Dark}.X_f + kLa.\left(C_{CO_2}^{sat} - C_{CO_2}\right)$
$\frac{dC_{O_2}}{dt} = \frac{F_L}{V_L}.\left(C_{O_2}^{In} - C_{O_2}\right) + q_{O_2}.X_f + kLa.\left(C_{O_2}^{sat} - C_{O_2}\right)$	$\frac{dC_{O_2}}{dt} = \frac{F_L}{V_L}.\left(C_{O_2}^{In} - C_{O_2}\right) + q_{O_2}^{Dark}.X_f + kLa.\left(C_{O_2}^{sat} - C_{O_2}\right)$
$\frac{dC_{GLC}}{dt} = \frac{F_L}{V_L}.\left(C_{GLC}^{In} - C_{GLC}\right) + q_{GLC}.X_f$	$\frac{dC_{GLC}}{dt} = \frac{F_L}{V_L}.\left(C_{GLC}^{In} - C_{GLC}\right) + q_{GLC}^{Dark}.X_f$
$\frac{dC_{NH_4^+}}{dt} = \frac{F_L}{V_L}.\left(C_{NH_4^+}^{In} - C_{NH_4^+}\right) + q_N.X_f$	$\frac{dC_{NH_4^+}}{dt} = \frac{F_L}{V_L}.\left(C_{NH_4^+}^{In} - C_{NH_4^+}\right) + q_N^{Dark}.X_f$
$\frac{dS_N}{dt} = \frac{F_L}{V_L}.\left(\frac{X_f^{In}.S_N}{X_f} - S_N\right) - q_N - S_N.\left(\mu^{PLA} + \mu^{COH} + \mu^{POH}\right)$	$\frac{dS_N}{dt} = \frac{F_L}{V_L}.\left(\frac{X_f^{In}.S_N}{X_f} - S_N\right) - q_N^{Dark} - S_N.\mu^{Dark}$
$\frac{dC_{PO_4^{3-}}}{dt} = \frac{F_L}{V_L}.\left(C_{PO_4^{3-}}^{In} - C_{PO_4^{3-}}\right) + q_P.X_f$	$\frac{dC_{PO_4^{3-}}}{dt} = \frac{F_L}{V_L}.\left(C_{PO_4^{3-}}^{In} - C_{PO_4^{3-}}\right) + q_P^{Dark}.X_f$
$\frac{dS_P}{dt} = \frac{F_L}{V_L}.\left(\frac{X_f^{In}.S_P}{X_f} - S_P\right) - q_P - S_P.\left(\mu^{PLA} + \mu^{COH} + \mu^{POH}\right)$	$\frac{dS_P}{dt} = \frac{F_L}{V_L}.\left(\frac{X_f^{In}.S_P}{X_f} - S_P\right) - q_P^{Dark} - S_P.\mu^{Dark}$
$\frac{dC_{TAG}}{dt} = \frac{F_L}{V_L}.\left(C_{TAG}^{In} - C_{TAG}\right) + \left(q_{TAG}^{PLA} + q_{TAG}^{COH} + q_{TAG}^{POH}\right).X_f$	$\frac{dC_{TAG}}{dt} = \frac{F_L}{V_L}.\left(C_{TAG}^{In} - C_{TAG}\right) + q_{TAG}^{Dark}.X_f$
$\frac{dC_{POC}}{dt} = \frac{F_L}{V_L}.\left(C_{POC}^{In} - C_{POC}\right) + \left(q_{POC}^{PLA} + q_{POC}^{COH} + q_{POC}^{POH}\right).X_f$	$\frac{dC_{POC}}{dt} = \frac{F_L}{V_L}.\left(C_{POC}^{In} - C_{POC}\right) + q_{POC}^{Dark}.X_f$
$\frac{dX_f}{dt} = \frac{F_L}{V_L}.\left(X_f^{In} - X_f\right) + \left(\mu^{PLA} + \mu^{COH} + \mu^{POH}\right).X_f - K_d.X_f$	$\frac{dX_f}{dt} = \frac{F_L}{V_L}.\left(X_f^{In} - X_f\right) + \mu^{Dark}.X_f - K_d.X_f$

Table 13 (Continued)

General
$\frac{dy_{CO_2}}{dt} = \frac{F_G^{In}}{V_G}.\left(y_{CO_2}^{In} - y_{CO_2}\right) + \frac{V_L.R_c.T}{V_G.P_{tot}}.kLa.\left(y_{CO_2}.\sum_{j=all\ gases}\left(C_j^{sat} - C_j\right) - \left(C_{CO_2}^{sat} - C_{CO_2}\right)\right)$
$\frac{dy_{O_2}}{dt} = \frac{F_G^{In}}{V_G}.\left(y_{O_2}^{In} - y_{O_2}\right) + \frac{V_L.R_c.T}{V_G.P_{tot}}.kLa.\left(y_{O_2}.\sum_{j=all\ gases}\left(C_j^{sat} - C_j\right) - \left(C_{O_2}^{sat} - C_{O_2}\right)\right)$

Table 15 Ordinary differential equations (ODEs) for microalgal mixed culture in a CSTR photobioreactor under light-feast and dark-famine regimes.

Light-feast
$\frac{dC_{CO_2}}{dt} = \frac{F_L}{V_L}.\left(C_{CO_2}^{In} - C_{CO_2}\right) + q_{CO_2}.X_{mix} + q_{CO_2}^{Nit}.X_{nit} + q_{CO_2}^{Het}.X_{het} + kLa.\left(C_{CO_2}^{sat} - C_{CO_2}\right)$
$\frac{dC_{O2}}{dt} = \frac{F_L}{V_L}.\left(C_{O_2}^{In} - C_{O_2}\right) + q_{O_2}.X_f + q_{O2}^{Nit}.X_{nit} + q_{O_2}^{Het}.X_{het} + kLa.\left(C_{O_2}^{sat} - C_{O_2}\right)$
$\frac{dC_{GLC}}{dt} = \frac{F_L}{V_L}.\left(C_{GLC}^{In} - C_{GLC}\right) + q_{GLC}.X_{mix} + q_{GLC}^{Het}.X_{het}$
$\frac{dC_{NH_4^+}}{dt} = \frac{F_L}{V_L}.\left(C_{NH_4^+}^{In} - C_{NH_4^+}\right) + q_N.X_{mix} + q_{NH_4}^{Nit}.X_{nit} + q_{NH_4}^{Het}.X_{het}$
$\frac{dS_N}{dt} = \frac{F_L}{V_L}.\left(\frac{X_{mix}^{In}.S_N}{X_{mix}} - S_N\right) - q_N - S_N.\left(\mu^{PLA} + \mu^{COH} + \mu^{POH}\right)$
$\frac{dC_{PO_4^{3-}}}{dt} = \frac{F_L}{V_L}.\left(C_{PO_4^{3-}}^{In} - C_{PO_4^{3-}}\right) + q_P.X_{mix} + q_{PO_4}^{Nit}.X_{nit} + q_{PO_4}^{Het}.X_{het}$
$\frac{dS_P}{dt} = \frac{F_L}{V_L}.\left(\frac{X_{mix}^{In}.S_P}{X_{mix}} - S_P\right) - q_P - S_P.\left(\mu^{PLA} + \mu^{COH} + \mu^{POH}\right)$
$\frac{dC_{TAG}}{dt} = \frac{F_L}{V_L}.\left(C_{TAG}^{In} - C_{TAG}\right) + \left(q_{TAG}^{PLA} + q_{TAG}^{COH} + q_{TAG}^{POH}\right).X_{mix}$
$\frac{dC_{POC}}{dt} = \frac{F_L}{V_L}.\left(C_{POC}^{In} - C_{POC}\right) + \left(q_{POC}^{PLA} + q_{POC}^{COH} + q_{POC}^{POH}\right).X_{mix}$
$\frac{dX_{mix}}{dt} = \frac{F_L}{V_L}.\left(X_{mix}^{In} - X_{mix}\right) + \left(\mu^{PLA} + \mu^{COH} + \mu^{POH}\right).X_{mix} - K_d.X_{mix}$

Table 15 (Continued)

Dark-famine
$\frac{dC_{CO_2}}{dt} = \frac{F_L}{V_L}.\left(C_{CO_2}^{In} - C_{CO_2}\right) + q_{CO_2}^{Dark}.X_{mix} + q_{CO_2}^{Nit}.X_{nit} + q_{CO_2}^{Het}.X_{het} + kLa.\left(C_{CO_2}^{sat} - C_{CO_2}\right)$
$\frac{dC_{O_2}}{dt} = \frac{F_L}{V_L}.\left(C_{O_2}^{In} - C_{O_2}\right) + q_{O_2}^{Dark}.X_f + q_{O_2}^{Nit}.X_{nit} + q_{O_2}^{Het}.X_{het} + kLa.\left(C_{O_2}^{sat} - C_{O_2}\right)$
$\frac{dC_{GLC}}{dt} = \frac{F_L}{V_L}.\left(C_{GLC}^{In} - C_{GLC}\right) + q_{GLC}^{Dark}.X_{mix} + q_{GLC}^{Het}.X_{het}$
$\frac{dC_{NH_4^+}}{dt} = \frac{F_L}{V_L}.\left(C_{NH_4^+}^{In} - C_{NH_4^+}\right) + q_N^{Dark}.X_{mix} + q_{NH_4}^{Nit}.X_{nit} + q_{NH_4}^{Het}.X_{het}$
$\frac{dS_N}{dt} = \frac{F_L}{V_L}.\left(\frac{X_{mix}^{In}.S_N}{X_{mix}} - S_N\right) - q_N^{Dark} - S_N.\mu^{Dark}$
$\frac{dC_{PO_4^{3-}}}{dt} = \frac{F_L}{V_L}.\left(C_{PO_4^{3-}}^{In} - C_{PO_4^{3-}}\right) + q_P^{Dark}.X_{mix} + q_{PO_4}^{Nit}.X_{nit} + q_{PO_4}^{Het}.X_{het}$
$\frac{dS_P}{dt} = \frac{F_L}{V_L}.\left(\frac{X_{mix}^{In}.S_P}{X_{mix}} - S_P\right) - q_P^{Dark} - S_P.\mu^{Dark}$
$\frac{dC_{TAG}}{dt} = \frac{F_L}{V_L}.\left(C_{TAG}^{In} - C_{TAG}\right) + q_{TAG}^{Dark}.X_{mix}$
$\frac{dC_{POC}}{dt} = \frac{F_L}{V_L}.\left(C_{POC}^{In} - C_{POC}\right) + q_{POC}^{Dark}.X_{mix}$
$\frac{dX_{mix}}{dt} = \frac{F_L}{V_L}.\left(X_{mix}^{In} - X_{mix}\right) + \mu^{Dark}.X_{mix} - K_d.X_{mix}$
General
$\frac{dC_{N_2}}{dt} = \frac{F_L}{V_L}.\left(C_{N_2}^{In} - C_{N_2}\right) + q_{N2}^{Het}.X_{het} + kLa.\left(C_{N_2}^{sat} - C_{N_2}\right)$
$\frac{dC_{CH_4}}{dt} = \frac{F_L}{V_L}.\left(C_{CH_4}^{In} - C_{CH_4}\right) + q_{N2}^{Het}.X_{het} + kLa.\left(C_{CH_4}^{sat} - C_{CH_4}\right)$
$\frac{dC_{NO_3^-}}{dt} = \frac{F_L}{V_L}.\left(C_{NO_3^-}^{In} - C_{NO_3^-}\right) + q_{NO_3}^{Nit}.X_{nit} + q_{NO_3}^{Het}.X_{het}$
$\frac{dX_{het}}{dt} = \frac{F_L}{V_L}.\left(X_{het}^{In} - X_{het}\right) + \left(\mu^{Het,\ aerobic} + \mu^{Het,\ anoxic} + \mu^{Het,\ anaerobic}\right).X_{het} - K_d^{Het}.X_{het}$
$\frac{dX_{het}}{dt} = \frac{F_L}{V_L}.\left(X_{het}^{In} - X_{het}\right) + \left(\mu^{Het,\ aerobic} + \mu^{Het,\ anoxic} + \mu^{Het,\ anaerobic}\right).X_{het} - K_d^{Het}.X_{het}$
$\frac{dX_{nit}}{dt} = \frac{F_L}{V_L}.\left(X_{nit}^{In} - X_{nit}\right) + \mu^{Nit}.X_{nit} - K_d^{Nit}.X_{nit}$
$\frac{dS_N^{Het}}{dt} = \frac{F_L}{V_L}.\left(\frac{X_{het}^{In}.S_N^{Het}}{X_{het}} - S_N^{Het}\right) - q_{NH_4}^{Het} - S_N^{Het}.\left(\mu^{Het,\ aerobic} + \mu^{Het,\ anoxic} + \mu^{Het,\ anaerobic}\right)$
$\frac{dS_P^{Het}}{dt} = \frac{F_L}{V_L}.\left(\frac{X_{het}^{In}.S_P^{Het}}{X_{het}} - S_P^{Het}\right) - q_{PO_4}^{Het} - S_P^{Het}.\left(\mu^{Het,\ aerobic} + \mu^{Het,\ anoxic} + \mu^{Het,\ anaerobic}\right)$
$\frac{dS_N^{Nit}}{dt} = \frac{F_L}{V_L}.\left(\frac{X_{nit}^{In}.S_N^{Nit}}{X_{nit}} - S_N^{Nit}\right) - q_{NH_4}^{Nit} - S_N^{Nit}.\mu^{Nit}$
$\frac{dS_P^{Nit}}{dt} = \frac{F_L}{V_L}.\left(\frac{X_{nit}^{In}.S_P^{Nit}}{X_{nit}} - S_P^{Nit}\right) - q_{PO_4}^{Nit} - S_P^{Nit}.\mu^{Nit}$

Table 15 (Continued)

General
$\frac{dy_{CO_2}}{dt} = \frac{F_G^{In}}{V_G}.\left(y_{CO_2}^{In} - y_{CO_2}\right) + \frac{V_L.R_c.T}{V_G.P_{tot}}.kLa.\left(y_{CO_2}.\sum_{j=all\ gases}\left(C_j^{sat} - C_j\right) - \left(C_{CO_2}^{sat} - C_{CO_2}\right)\right)$
$\frac{dy_{O_2}}{dt} = \frac{F_G^{In}}{V_G}.\left(y_{O_2}^{In} - y_{O_2}\right) + \frac{V_L.R_c.T}{V_G.P_{tot}}.kLa.\left(y_{O_2}.\sum_{j=all\ gases}\left(C_j^{sat} - C_j\right) - \left(C_{O_2}^{sat} - C_{O_2}\right)\right)$
$\frac{dy_{N_2}}{dt} = \frac{F_G^{In}}{V_G}.\left(y_{N_2}^{In} - y_{N_2}\right) + \frac{V_L.R_c.T}{V_G.P_{tot}}.kLa.\left(y_{N_2}.\sum_{j=all\ gases}\left(C_j^{sat} - C_j\right) - \left(C_{N2}^{sat} - C_{N2}\right)\right)$
$\frac{dy_{CH_4}}{dt} = \frac{F_G^{In}}{V_G}.\left(y_{CH_4}^{In} - y_{CH_4}\right) + \frac{V_L.R_c.T}{V_G.P_{tot}}.kLa.\left(y_{CH_4}.\sum_{j=all\ gases}\left(C_j^{sat} - C_j\right) - \left(C_{CH_4}^{sat} - C_{CH_4}\right)\right)$

The differential equations used for mass balance under a chemostat regime were simplified assuming the reactor steady-state where the accumulation term is zero. This enabled the final value for the constant for state variables to be calculated. **Table 16** shows all model parameters (i.e., stoichiometry, kinetics, transfer, and operational parameters).

Table 16 Overview of all model parameters (a) Assumed the same as for TAG; (b) Assumed the same as for microalgae

Model parameter	Symbol	Value	Unit	Reference
Stoichiometry parameters				
Relative rate of triacylglycerol formation to photoautotrophic algal biomass production	$\tilde{Y}^{PLA}_{\frac{TAG}{X}}$	0.66	$\frac{\text{cmol TAG}}{\text{cmol } X_f}$	Table 1
Relative rate of poly-carbohydrate formation to photoautotrophic algal biomass production	$\tilde{Y}^{PLA}_{\frac{POC}{X}}$	0.41	$\frac{\text{cmol POC}}{\text{cmol } X_f}$	Table 1
Relative rate of triacylglycerol formation to chemoheterotrophic algal biomass production	$\tilde{Y}^{COH}_{\frac{TAG}{X}}$	0.53	$\frac{\text{cmol TAG}}{\text{cmol } X_f}$	Table 1
Relative rate of poly-carbohydrate formation to chemoheterotrophic algal biomass production	$\tilde{Y}^{COH}_{\frac{POC}{X}}$	1.56	$\frac{\text{cmol TAG}}{\text{cmol } X_f}$	Table 1
Relative rate of triacylglycerol formation to photoheterotrophic algal biomass production	$\tilde{Y}^{POH}_{\frac{TAG}{X}}$	0.76	$\frac{\text{cmol (TAG)}}{\text{cmol } (X_f)}$	Table 1
Relative rate of poly-carbohydrate formation to photoheterotrophic algal biomass production	$\tilde{Y}^{POH}_{\frac{POC}{X}}$	0.76	$\frac{\text{cmol TAG}}{\text{cmol } X_f}$	Assumed[(a)]
Minimum nitrogen cell quota	S_{Nmin}	0.076	$\frac{\text{mol N}}{\text{cmol } X_f}$	Adesanya et al., 2014
Minimum phosphorus cell quota	S_{Pmin}	0.0051	$\frac{\text{mol P}}{\text{cmol } X_f}$	Adesanya et al., 2014
Maximum nitrogen cell quota	S_{Nmax}	0.225	$\frac{\text{mol N}}{\text{cmol } X_f}$	Adesanya et al., 2014

Table 16 (Continued) (a) Assumed the same as for TAG; (b) Assumed the same as for microalgae

Model parameter	Symbol	Value	Unit	Reference
Stoichiometry parameters				
Maximum phosphorus cell quota	S_{Pmax}	0.015	$\frac{\text{mol P}}{\text{cmol X}_f}$	Adesanya et al., 2014
Efficiency of none-cyclic photophosphorylation	δ	1	$\frac{\text{mol ATP}}{\text{mol photon}}$	Arnon, 1984
Efficiency of cyclic photophosphorylation	Δ	2	$\frac{\text{mol ATP}}{\text{mol photon}}$	Arnon, 1984
ATP requirement for transport of storage molecules	k	1.0	$\frac{\text{mol ATP}}{\text{cmol POC (TAG)}}$	Assumed
Yield of heterotrophic bacteria on glucose	Y_H	-3.6	$\frac{\text{mol X}_{het}}{\text{mol GLC}}$	Henze et al., 2015
Yield of nitrifying bacteria on nitrate	Y_N	0.1	$\frac{\text{mol X}_{nit}}{\text{mol NO}_3^-}$	Henze et al., 2015
Minimum nitrogen cell quota for nitrifiers	S_{Nmin}^{Nit}	0.076	$\frac{\text{mol N}}{\text{cmol X}_{nit}}$	Assumed[(b)]
Minimum phosphorus cell quota nitrifiers	S_{Pmin}^{Nit}	0.0051	$\frac{\text{mol P}}{\text{cmol X}_{nit}}$	Assumed[(b)]
Maximum nitrogen cell quota nitrifiers	S_{Nmax}^{Nit}	0.225	$\frac{\text{mol N}}{\text{cmol X}_{nit}}$	Assumed[(b)]

Table 16 (Continued) (a) Assumed the same as for TAG; (b) Assumed the same as for microalgae

Model parameter	Symbol	Value	Unit	Reference
Stoichiometry parameters				
Maximum phosphorus cell quota nitrifiers	S_{Pmax}^{Nit}	0.015	$\frac{\text{mol P}}{\text{cmol X}_{nit}}$	Assumed[(b)]
Minimum nitrogen cell quota for heterotrophs	S_{Nmin}^{Het}	0.076	$\frac{\text{mol N}}{\text{cmol X}_{het}}$	Assumed[(b)]
Minimum phosphorus cell quota for heterotrophs	S_{Pmin}^{Het}	0.0051	$\frac{\text{mol P}}{\text{cmol X}_{het}}$	Assumed[(b)]
Maximum nitrogen cell quota for heterotrophs	S_{Nmax}^{Het}	0.225	$\frac{\text{mol N}}{\text{cmol X}_{het}}$	Assumed[(b)]
Maximum phosphorus cell quota for heterotrophs	S_{Pmax}^{Het}	0.015	$\frac{\text{mol P}}{\text{cmol X}_{het}}$	Assumed[(b)]
Kinetics parameters				
Maximum specific photoautotrophic growth rate of microalgae	μ_{max}^{PLA}	2.5	day^{-1}	Assumed
Maximum specific chemoheterotrophic growth rate of microalgae	μ_{max}^{COH}	1.5	day^{-1}	Assumed
Maximum specific photoheterotrophic growth rate of microalgae	μ_{max}^{POH}	2.5	day^{-1}	Mondini, 2019
Maximum specific growth rate of microalgae on TAG during darkness	$\mu_{max}^{Dark,\ TAG}$	0.1	day^{-1}	Assumed

Table 16 (Continued) (a) Assumed the same as for TAG; (b) Assumed the same as for microalgae

Model parameter	Symbol	Value	Unit	Reference
Kinetics parameters				
Maximum specific growth rate of microalgae on POC during darkness	$\mu_{max}^{Dark,\ POC}$	2.0	day^{-1}	Assumed
Photoautotrophic decay rate of microalgae	K_d^{PLA}	0.15	day^{-1}	Assumed
Chemoheterotrophic decay rate of microalgae	K_d^{COH}	0.08	day^{-1}	Assumed
Photoheterotrophic decay rate of microalgae	K_d^{POH}	0.15	day^{-1}	Assumed
Decay rate of microalgae during darkness	K_d^{Dark}	0.1	day^{-1}	Assumed
Maximum photoautotrophic biomass specific photon uptake rate	$q_{photon,\ max}^{PLA}$	*-10*	day^{-1}	Assumed
Maximum photoheterotrophic biomass specific photon uptake rate	$q_{photon,\ max}^{POH}$	*-2*	day^{-1}	Assumed
Maximum chemoheterotrophic biomass specific glucose uptake rate	$q_{GLC,\ max}^{COH}$	*-0.1*	day^{-1}	Assumed
Maximum photoautotrophic biomass specific poly-carbohydrate production rate	$q_{POC,\ max}^{PLA}$	*10*	day^{-1}	Assumed
Maximum photoheterotrophic biomass specific poly-carbohydrate production rate	$q_{POC,\ max}^{POH}$	*10*	day^{-1}	Assumed
Maximum chemoheterotrophic biomass specific poly-carbohydrate production rate	$q_{POC,\ max}^{COH}$	*10*	day^{-1}	Assumed

Table 16 (Continued) (a) Assumed the same as for TAG; (b) Assumed the same as for microalgae

Model parameter	Symbol	Value	Unit	Reference
Kinetics parameters				
Biomass specific ATP requirement for maintenance	m_{ATP}	0.1	day^{-1}	Assumed
O_2 half-saturation coefficient	K_{O2}	0.3	$\frac{mol\ O_2}{m^3}$	Wolf et al., 2007
CO_2 half-saturation coefficient	K_{CO2}	0.1	$\frac{mol\ CO_2}{m^3}$	Goldman, 1999
Glucose half-saturation coefficient	K_{GLC}	1	$\frac{mol\ GLC}{m^3}$	Assumed
Poly-carbohydrate half-saturation coefficient	K_{POC}	1	$\frac{mol\ POC}{m^3}$	Assumed
Triacylglycerol half-saturation coefficient	K_{TAG}	1	$\frac{mol\ TAG}{m^3}$	Assumed
Ammonia half-saturation coefficient	K_{NH4}	0.004	$\frac{mol\ NH_4^+}{m^3}$	Adesanya et al., 2014
Phosphate half-saturation coefficient	K_{PO4}	0.004	$\frac{mol\ PO_4^{3-}}{m^3}$	Adesanya et al., 2014
Photo-inhibition constant	K_I	1000	$\left(\frac{\mu E}{m^2.s}\right)^2$	Assumed
Microalgal affinity for light	I_K	160	$\frac{\mu E}{m^2.s}$	Henze et al., 2015
Exponent constant	n	1.49	Dimensionless	Concas et al., 2013

Table 16 (Continued) (a) Assumed the same as for TAG; (b) Assumed the same as for microalgae

Model parameter	Symbol	Value	Unit	Reference
Kinetics parameters				
Poly-carbohydrate inhibition power constant	w	0.5	Dimensionless	Assumed
Triacylglycerol inhibition power constant	u	1	Dimensionless	Assumed
Cell adsorption factor	α	2.57	$\frac{m^2}{cmol\ X}$	Concas et al., 2013
Maximum specific growth rate of nitrifying bacteria	μ_{max}^{N}	1	day^{-1}	Concas et al., 2013
Maximum specific growth rate of ordinary heterotrophic bacteria (i.e., aerobic growth)	μ_{max}^{H}	5.5	day^{-1}	Henze et al., 2015
Maximum specific growth rate of denitrifying heterotrophic bacteria (i.e., anoxic growth)	μ_{max}^{DN}	1.6	day^{-1}	Henze et al., 2015
Maximum specific growth rate of fermentative heterotrophic bacteria (i.e., anaerobic growth)	μ_{max}^{M}	0.8	day^{-1}	Henze et al., 2015
Decay rate constant for nitrifying bacteria	K_d^{Nit}	0.15	day^{-1}	Henze et al., 2015
Decay rate constant for heterotrophic bacteria	K_d^{Het}	0.4	day^{-1}	Henze et al., 2015
O_2 half-saturation coefficient nitrifying bacteria	K_{O2}^{Nit}	0.0156	$\frac{mol\ O_2}{m^3}$	Henze et al., 2015

Table 16 (Continued) (a) Assumed the same as for TAG; (b) Assumed the same as for microalgae

Model parameter	Symbol	Value	Unit	Reference
Kinetics parameters				
O_2 half-saturation coefficient heterotrophic bacteria	K_{O2}^{Het}	0.3	$\frac{mol\ O_2}{m^3}$	Assumed[(a)]
CO_2 half-saturation coefficient nitrifying bacteria	K_{CO2}^{Nit}	0.1	$\frac{mol\ CO_2}{m^3}$	Henze et al., 2015
Glucose half saturation coefficient heterotrophic bacteria	K_{GLC}^{Het}	1	$\frac{mol\ GLC}{m^3}$	Assumed[(b)]
Nitrate half-saturation coefficient heterotrophic bacteria	K_{NO3}^{Het}	0.036	$\frac{mol\ NO_3^-}{m^3}$	Henze et al., 2015
Ammonia half-saturation coefficient nitrifying bacteria	K_{NH4}^{Nit}	0.004	$\frac{mol\ NH_4^+}{m^3}$	Assumed[(b)]
Phosphate half-saturation coefficient nitrifying bacteria	K_{PO4}^{Nit}	0.004	$\frac{mol\ PO_4^{3-}}{m^3}$	Assumed[(b)]
Ammonia half-saturation coefficient heterotrophic bacteria	K_{NH4}^{Het}	0.004	$\frac{mol\ NH_4^+}{m^3}$	Assumed[(b)]
Phosphate half-saturation coefficient heterotrophic bacteria	K_{PO4}^{Het}	0.004	$\frac{mol\ PO_4^{3-}}{m^3}$	Assumed[(b)]

Table 16 (Continued) (a) Assumed the same as for TAG; (b) Assumed the same as for microalgae

Model parameter	Symbol	Value	Unit	Reference
Transfer parameters				
Volumetric air transfer coefficient	kLa	1000	day^{-1}	Assumed
Henry's coefficient for O_2	H_{O_2}	1.3	$\frac{mol\ Air}{m^3.atm}$	Loomis, 1928
Henry's coefficient for CO_2	H_{CO_2}	34	$\frac{mol\ Air}{m^3.atm}$	Morgan & Maass, 1931
Henry's coefficient for N_2	H_{N_2}	0.61	$\frac{mol\ Air}{m^3.atm}$	Kavanaugh & Trussell, 1980
Henry's coefficient for CH_4	H_{CH_4}	1.3	$\frac{mol\ Air}{m^3.atm}$	Kavanaugh & Trussell, 1980
Operational parameters				
Laboratory-scale reactor volume	V_r^{Lab}	0.02	m^3	
Reactor diameter over height ratio	β	1	Dimensionless	
Inlet/Outlet liquid flow rate	F_L	variable	$m^3.day^{-1}$	
Volumetric inlet gas flow rate	F_G^{In}	10	$m^3.day^{-1}$	
Ideal gas constant	R_c	8.314	$J.mol^{-1}.K^{-1}$	
Temperature	T	300	$Kelvin$	Assumed
Dilution rate	D	F_L/V_R^{Lab}	day^{-1}	
Incident light intensity	I_{in}	variable	$\frac{\mu E}{m^2.s}$	
Total pressure	P_{tot}	101.325	Kpa	Assumed

3 Result and Discussion

This model was built to predict microalgae growth behavior patterns under different trophic modes in batch and chemostat regimes. The transition of the batch regime to chemostat was studied in microalgae axenic cultures during mixotrophy, where the impacts of light intensity, dilution, rate, and feedstock used were investigated.

Regarding mixed cultures, both microalgal and bacterial growth was modeled in a CSTR, with posterior simulations of periodic cycles of light-feast and dark famine to overcome one of the main bottlenecks in microalgae cultivation, which is culture contamination.

3.1. Microalgae axenic culture under the batch regime

Microalgae cellular growth, represented by functional biomass production, as well as storage compound production display the same patterns regardless of the trophic regime employed for microalgal cultivation where cellular growth is preferred over storage compound production.

Hence, in a nutrient-rich environment microalgae will spend their energy on biomass production and when storage compounds are considered, the production of POC is also preferred over TAG. The main reason for the increase in POC concentration rather than TAG is the fact that POC is prioritized as an energy reserve for microalgal usage. However, once the concentration of POC reaches the saturation level, TAG production occurs more rapidly.

The patterns for microalgal growth under different trophic regimes in a batch reactor are depicted in **Figure 3** and **appendix C** is shown the influence of different patterns (i.e., nutrient concentrations and dissolved gas) in microalgal growth.

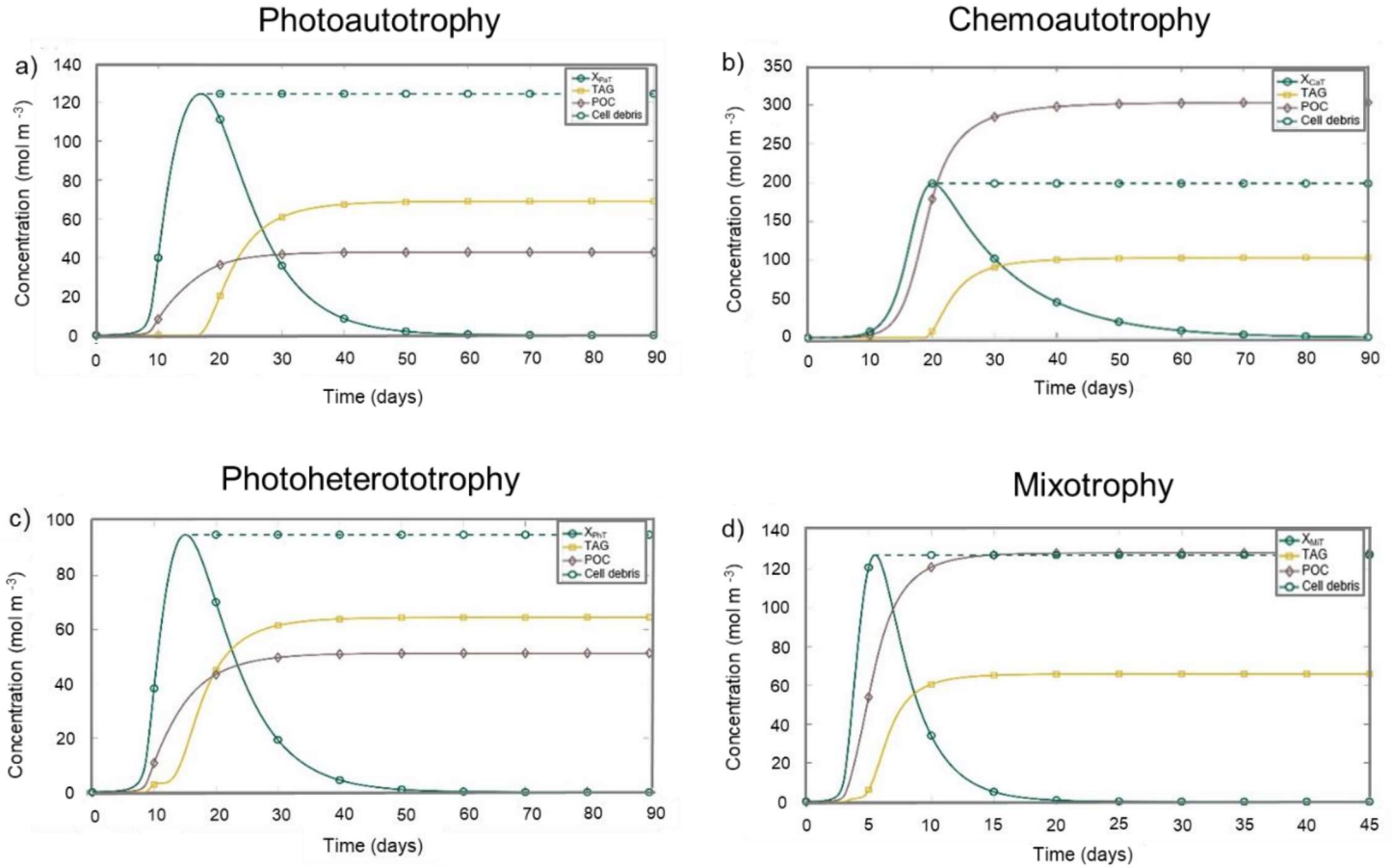


Figure 3 Microalgae growth pattern given in biomass concentration over time, under different trophic regimes in a batch reactor: a) photoautotrophy, b) chemoautotrophy, c) photoheterotrophy and d) mixotrophy; where (⊖) stands for functional biomass; (⊟) for TAG and (◈) for POC.

As seen in **Figure 3**, the growth patterns and the production of storage compounds in microalgae pure culture were modeled in a batch reactor, using CW as substrate. In **appendix D**, the complete microalgal growth patterns under different trophic regimes are displayed considering different parameters such as nutrients dissolved CO_2 and O_2 levels and organic carbon source Hence, when cultivation reaches a certain point (t_{end}), the concentration of active functional biomass dropped, reaching zero. This decrease represented the rate of microalgal decay considered in the growth equation.

Consequently, all biological conversions ceased remaining only the total biomass containing cell debris as well as the final concentration of the storage compounds produced during the process. The concentration of total biomass continued constant after reaching t_{end} since there was no other change applied to the system. However, the final values of biomass, POC, and TAG concentrations varied among the different trophic modes regardless of the growth patterns and similarities presented in the different trophic regimes.

Although photoautotrophic and photoheterotrophic growth patterns display similar profiles, there are relevant differences. The maximum biomass concentration reached its peak on the nineteenth day with 125.0 mol m^{-3}, whereas in the photoheterotrophic regime, biomass concentration reached 95.0 mol m^{-3} around the fifteenth day. This could be because in photoheterophy biomass growth depended on both light and organic carbon sources. POC and TAG productions in both photoautotrophic and photoheterotrophic regimes reached their maximum around the thirtieth and fortieth day, respectively. During photoheterotrophy, it was inferred that 30.6 % (mol mol^{-1}) of the total biomass consisted of TAG.

The chemoheterotrophy regime presented the highest concentration of biomass compared to all trophic modes with 198.9 mol m^{-3} as well as POC and TAG concentrations with 103.3 and 303.1 mol m^{-3}, respectively. In contrast, compared to all trophic regimes depicted in **figure 3** chemotrophic regime took the longest time to complete the entire process with a t_{end} of 80 days.

For each trophic regime, the best growth conditions were implemented. During the first five days of the mixotrophic regime, the functional biomass was more rapidly produced than the storage compounds, given the high concentration of nutrients which

resulted in high levels of nutrient cell quota. Once the nutrients are consumed, the value of the nutrient cell quota was below the minimum required for growth. Hence, TAG accumulation was favored until it reached its maximum value on the twelfth day. Concomitantly, the rates of functional biomass and POC production decreased.

Compared to all trophic regimes, mixotrophy presented the shortest cycle of 20 days. Both photoautotrophic and photoheterotrophic regimes displayed a cycle of 50 days and the chemoheterotrophic regime which presented a 70 days cycle. Assuming that mixotrophy is the sum of the maximum specific growth rates of all trophic regimes aforementioned, it is reasonable to state that the mixotrophic regime is unsurpassed. Despite presenting a lower final concentration for TAG and functional biomass production compared to the chemoheterotrophic regime, the overall TAG and biomass production was higher given its short t_{end}, which is depicted in **Table 17**.

The results presented in this section corresponded to the specific conditions imposed on each trophic regime, where CW was the common substrate and light intensity of 500 $W.m^{-2}$ (= 2300 $\mu E\ m^{-2}\ s^{-1}$). Thus, any changes regarding the variables used for this specific modeling would result in different outputs accordingly.

Since the most efficient cultivation mode discussed is mixotrophy, the focus of this work hereinafter will be on this trophic regime.

3.2 Modeling light intensity, dilution rate, and type of substrate for cultivation of microalgae axenic culture under mixotrophy in a chemostat regime

Since mixotrophy was the most efficient trophic regime for axenic microalgal growth in batches due to its shortest cycle (i.e., t_{end}), there was the need to investigate the best light intensity, dilution rate, and substrate to optimize the growth pattern and TAG and POC production of axenic microalgae under mixotrophy and in a CSTR.

Table 17 Main results obtained from the modeling of microalgae axenic culture under the batch regime, where t_{end} stands for the ending time of each cycle, X_f for functional, biomass concentration, C_{TAG} for TAG concentration, C_{POC} for POC concentration, TAG_C for TAG content and P_{TAG} for TAG productivity. The trophic regimes are defined by photoautotrophy (PaT), chemoheterotrophy (ChT), photohetertropy (PhT), and mixotrophy (MiT).

Growth mode	t_{end} (day)	X_f (mol X_f m^{-3})	C_{TAG} (mol TAG m^{-3})	C_{POC} (mol TAG m^{-3})	TAG_C (% mol TAG mol X^{-1})	P_{TAG} (mol TAG m^{-3} d^{-1})
PaT	58	124.4	69.0	42.8	29.2	1.2
ChT	80	198.9	103.3	303.1	17.1	1.3
PhT	55	95.0	64.5	51.2	30.6	1.2
MiT	20	127.2	65.8	128.2	20.4	3.3

3.2.1 Studying the impact of light for optimizing incident light intensity value

Light intensity and photoperiod cycles exert great influence on microalgae growth patterns and the steady-state concentration of its biomass. Different light intensity requirements can be implemented depending on the concentration of biomass produced and culture composition. The same applies to photoperiods of light and dark when cultivating microalgae. **Figure 4** shows the influence of different light intensities on the growth pattern and POC and TAG production during microalgae cultivation in a chemostat under a mixotrophic regime.

As seen in **Figure 4a**, when light intensity is lower than 100 W m^{-2} (i.e., 460 µmol m^{-2} s^{-1}), the functional biomass concentration was also low at approximately 40 mol m^{-3}. According to the model, light limitation did not influence the lag phase much. On the other hand, the log phase displayed a lower functional biomass concentration at approximately 40 mol m^{-3} and a POC concentration of 15 mol m^{-3}. The light intensity chosen for modeling was unable to present any production of TAG.

The increase of light intensity 100-fold as shown in **Figure 4d** also failed to promote cell growth and storage compounds production. After reaching the light saturation limit, microalgae did not manage to use the excess light intensity available. The culture reached the exponential phase after the thirtieth day for biomass and POC production. As in **Figure 4a**, there was no TAG production under a light intensity of 10,000 W m^{-2}.

Additionally, both biomass and POC concentration was negligible compared to the other light intensities modeled being lower than 3 W m^{-2}, thus, confirming photoinhibition.

Figures 4b and **4c** depicted the growth patterns and concentration of storage compounds of mixotrophic microalgae under light intensities of 800 W m^{-2} and 4,000 W m^{-2} (i.e., 3,680 and 18,400 µmol m^{-2} s^{-1}). Despite presenting similar profiles, at a light intensity of 4,000 W m^{-2}, both biomass and storage compounds presented higher concentrations than at 800 W m^{-2}.

The concentration of TAG almost doubled from 38.5 to 64.4 mol m^{-3} and POC concentration showed an increase of 33%, whereas biomass increased by 25%. However, as light intensity increased, a delay of 15 days to reach the steady state was observed. Consequently, we can infer that before reaching photoinhibition, the increase in product concentrations was directly proportional to the time needed for the culture to reach the steady state.

The relationship between the light limitation and photoinhibition was then examined to establish the optimal light intensity for biomass and storage compounds production. Hence, the derivatives of the photoinhibition and light limitation terms related to the average light intensity were derived and evaluated.

As a result, the derivative function of the light limitation term was always positive (**equation 21**) thus, the light limitation term was assumed to be on the interval of (0, + ∞). This meant that as the average light intensity increased, the output of the light limitation term also increased, minimizing its limitation on growth.

$$f_{\mathrm{Limit}} = \frac{I_{avg}^{n}}{I_{avg}^{n} + I_{K}^{n}} \rightarrow f'_{\mathrm{Limit}} = \frac{n.I_{avg}^{n-1}.(2\,I_{avg}^{n} + I_{K}^{n})}{(I_{avg}^{n} + I_{K}^{n})^{2}} > 0 \qquad \text{(Eq. 21)}$$

Conversely, the derivative function of the photoinhibition term was always negative (**equation 22**), so the photoinhibition function was strictly descending. That is to say that, the limitation on growth was conditioned to the increase of the average light intensity.

Subsequently, the output of the photoinhibition function decreased, which enhanced growth limitation.

$$f_{\text{Inhibit}} = \frac{I_{avg}}{I_{avg}+\frac{I_{avg}^2}{K_I}} \rightarrow f'_{\text{Inhibit}} = \frac{-\frac{I_{avg}^2}{K_I}}{\left(I_{avg}+\frac{I_{avg}^2}{K_I}\right)^2} < 0 \qquad \text{(Eq. 22)}$$

Given the fact that both light limitation and photoinhibition terms influence microalgae growth and have opposite effects, the ideal average light intensity would be a value in which both limitation and photoinhibition terms would display the same results. So, the optimum average light intensity was calculated by equating both terms 334 μmol m^2 s^{-1} which resulted in n, I_K, and K_I. These values were the same ones provided in **Table 16.**

$$f_{\text{limit}} = f_{\text{inhibit}} \rightarrow I_{avg}^{optimum} = 334\ \frac{\mu mol}{m^2\ s} \qquad \text{(Eq. 23)}$$

Therefore, the optimal light intensity as a function of cell density was derived by calculating the optimized value for the average light intensity, cell adsorption factor, and light path (i.e., reactor radius). Hence, the optimal light intensity was not a constant value, changing according to the culture cell density.

$$I_{in\ (X)}^{optimum} = \frac{126.18\ X}{1-\exp\left(-0.38\ X\right)} \qquad \text{(Eq. 24)}$$

A flexible source of illumination with adjustable light intensity (e.g., a light jacket) could solve the issues of light limitation and photoinhibition which were related to the final biomass productivity and growth exponential phase delay, respectively.

Thus, when biomass concentration is low, in the early stage of a process, the light intensity could be adjusted to a value that would neither prevent light limitation nor impose photoinhibition. As cell culture density increased, the light intensity would be proportionally adjusted providing enough light to prevent light limitation.

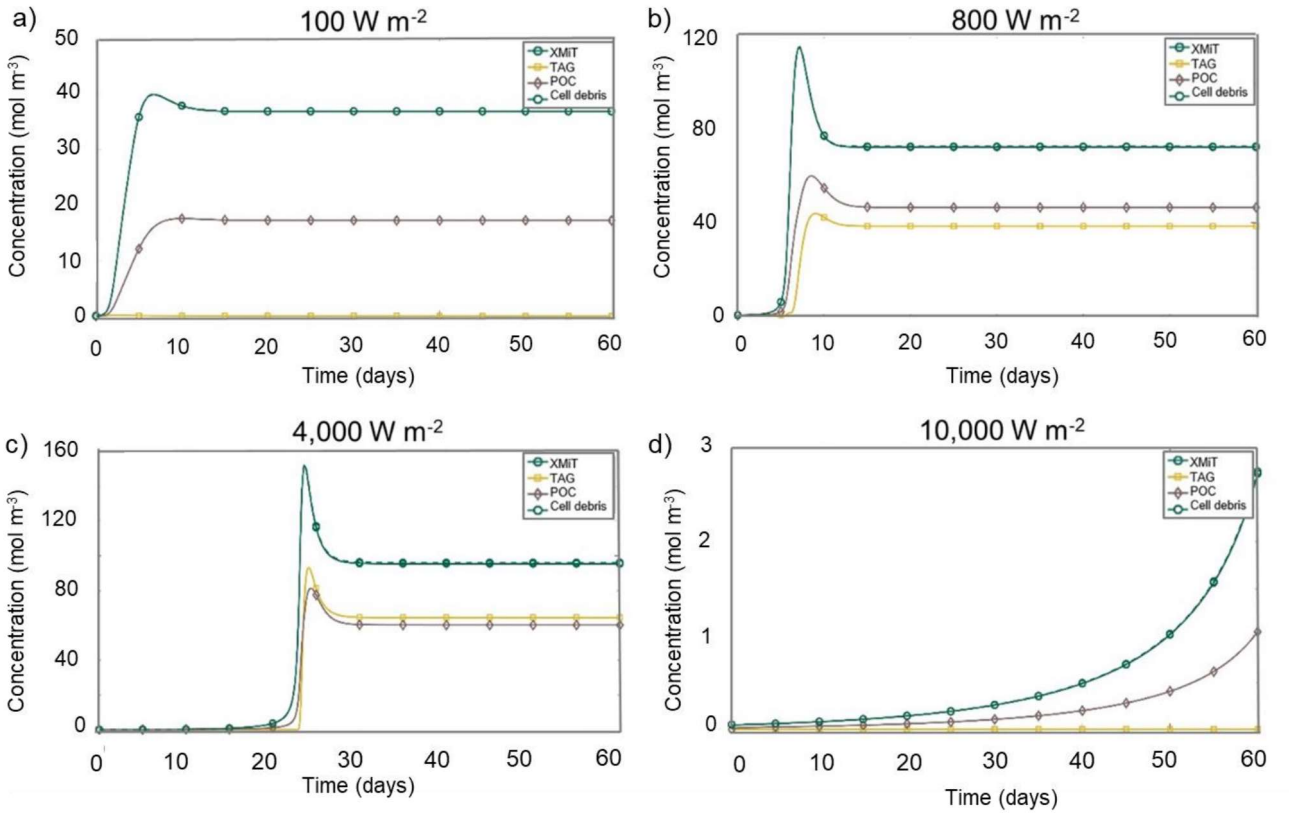


Figure 4 Influence of different light intensities on microalgae mixotrophic growth patterns and POC and TAG production under the chemostat regime, indicated as biomass. Light intensities were implemented as follows: a) L_{in} of 100 W m^{-2}; b) L_{in} of 800 W m^{-2}; c) L_{in} of 4,000 W m^{-2} , and d) L_{in} of 10,000 W m^{-2}. The dilution rate of 0.25 day^{-1} and the substrate as CW was equal for all modeled conditions. The symbol (⊸) represents functional biomass; (⊸) TAG and (⊸) POC.

3.2.2 Studying the impact of dilution rate for optimizing dilution rate value

As the dilution rate increased up to 0.45 day^{-1}, the steady-state concentration of functional biomass (F_B) also increased, whereas the steady-state concentration of TAG (C_{TAG}) linearly decreased. Hence, it could be assumed that the volumetric load of the influent (i.e., values of dilution rate) resulted in lower C_{TAG} and higher F_B, which meant a lower TAG content within the total biomass. Higher dilution rates led to microalgal cells wash-out from the media, as shown in **Figure 5**.

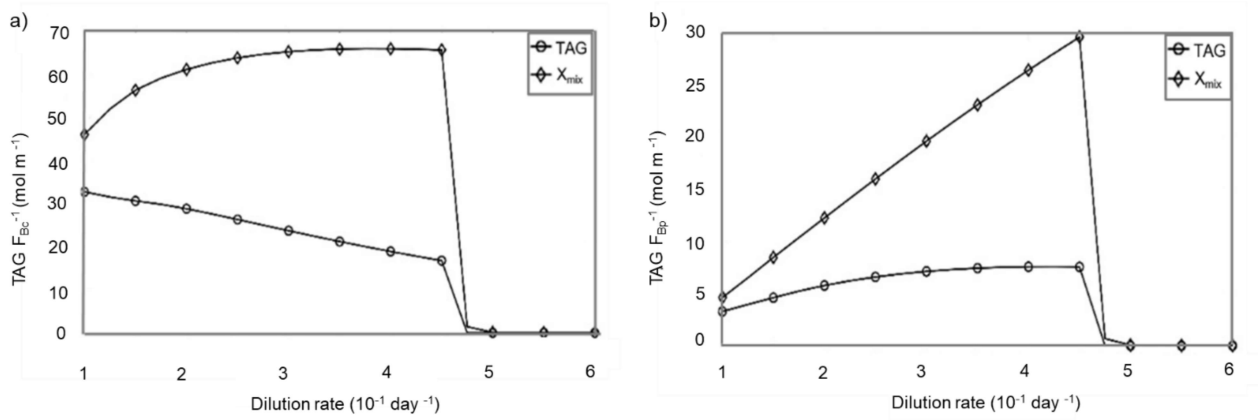


Figure 5 Influence of dilution rate on a) TAG over functional biomass content (F_{Bc}) and b) TAG over functional biomass productivity (F_{Bp}) considering a light intensity of 500 W m^{-2}, and CW as feedstock: a) TAG F_{Bc}^{-1} over dilution rate and b) Microalgae TAG F_{Bp}^{-1} over dilution rate. (◆) functional biomass; (●) TAG.

The productivity of a component depends on the dilution rate. Thus, when the dilution rate was increased to 0.45 day^{-1}, TAG productivity slightly increased while the concentration of TAG decreased. However, dilution rates above 0.45 day^{-1} halted any TAG productivity. According to **figure 5b**, the optimal dilution rate for microalgal mixotrophic growth under the chemostat regime was 0.45 day^{-1} when both TAG and functional biomass productivity reached their peak (i.e., 7.5 and 30 $mol.m^{-3}.day^{-1}$, respectively).

3.2.3 Results for microalgae axenic culture under the chemostat regime

Once the optimal dilution rate and light intensity were known, the normal and optimal environmental conditions could be modeled. Therefore, the impacts on biomass concentration and productivity of each condition in a CSTR could be compared. **Figure 6** shows the growth patterns of axenic microalgae cultures under mixotrophy and the production of storage compounds in each condition under the chemostat regime. A complete version of these diagrams together with additional results for another state variables such as the concentration of nutrients and dissolved gases are provided in **appendix E** (**figure E i** to **E iv**)

As seen in **Figure 6**, light intensity influenced both the growth patterns and the constant biomass concentration once the steady state was reached. The level of functional biomass was low (i.e., < 40 mol m^{-3}) under a low light intensity of 100 W m^{-2} (= 460 µE.m^{-2} s^{-1}). In this scenario, TAG was not produced (**Figure 6a**) given the light limitation. Microalgal growth was impaired under the high light intensity of 10,000 W m^{-2} (46,000 µE.m^{-2} s^{-1}) which was attributed to the photoinhibition effect (**Figure 6d**).

Figures 6b and **6c** show that the steady state was delayed by 15 days once the light intensity was increased from 800 to 4,000 W m^{-2} (i.e., 3,680 to 18,400 µE.m^{-2}.s^{-1}). However, the concentration of TAG in the steady state increased from 38.5 to 64.4 mol m^{-3}. Hence, it can be inferred that the light intensity is directly proportional to the concentration of functional biomass and storage compounds in a steady state. **Figure 6c** shows a higher concentration of TAG over POC during a steady state at a light intensity of 4,000 W m^{-2}.

The increase in biomass level resulted from microalgae overcoming photoinhibition as high-light intensity availability was increased. To determine the optimal light intensity, it is important to analyze the relationship between photoinhibition and light limitation was analyzed by deriving the photoinhibition and light limitation terms. The light limitation term's derivative function is positive (**equation 21**) assuming the interval of (0, + ∞). This enabled its adjustment based on the average light intensity. As the average light intensity increased, so did the output of the light limitation term, thus decreasing microorganisms'

growth limitation. The opposite is observed with the derivative function of the photoinhibition term (**equation 22**).

The optimum average light intensity, where limitation and photoinhibition terms have equal production, was calculated by equating both terms. It equals 334 μE m^{-2} s^{-1} for n, I_K, and K_I (**equation 23**), which are the same as their values provided in **table 16**. As a function of cell density, the optimum light intensity (**equation 24**) was derived by calculating the cell adsorption factor, the optimized value for average light intensity, and the light path (i.e., reactor radius).

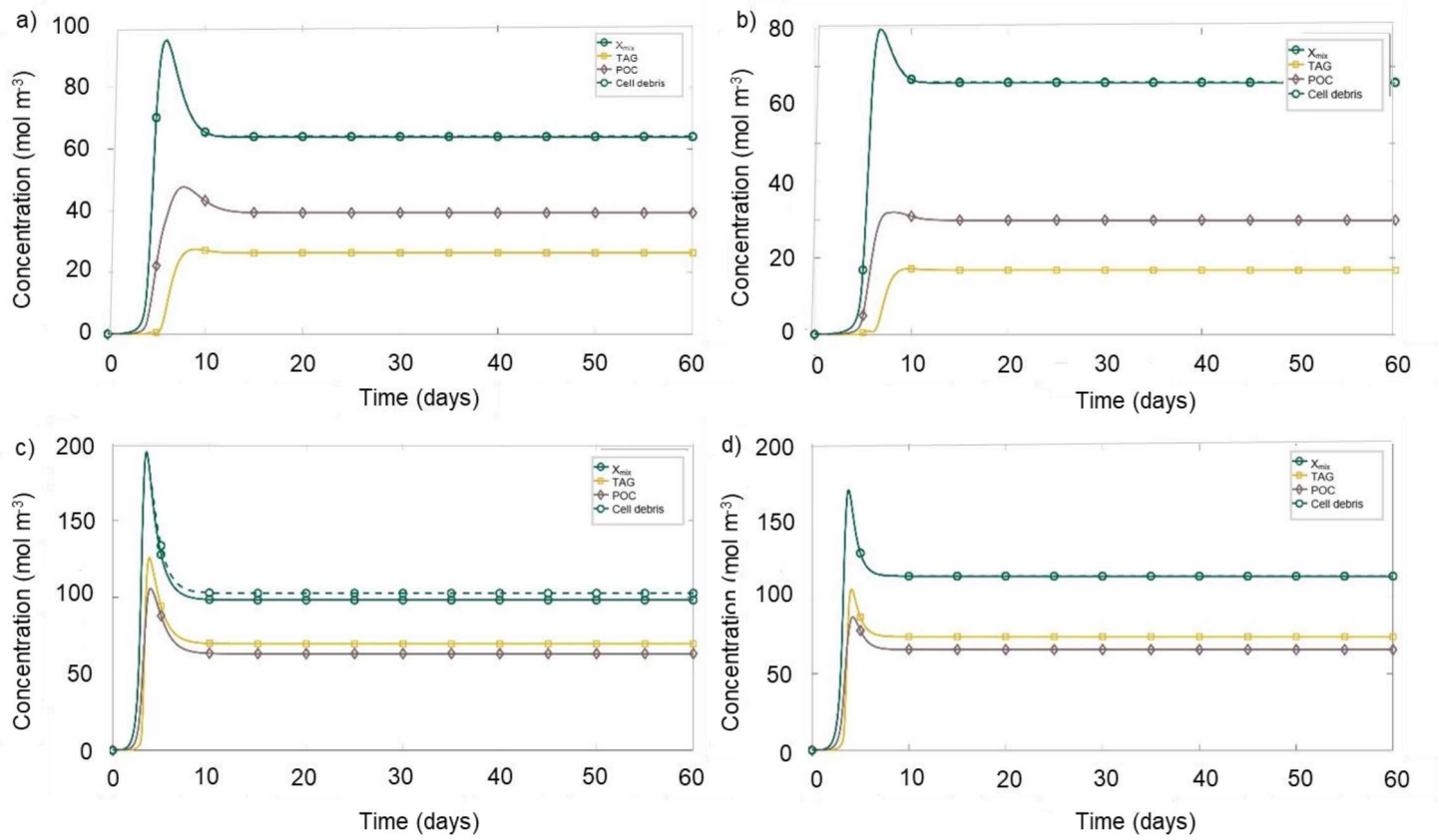


Figure 6 Microalgae mixotrophic growth pattern under different light intensity during chemostat regime where a): I_{in}= 100 W m^{-2}, b): I_{in}= 800 W m^{-2}, c): I_{in}= 4,000 W m^{-2}, and d): I_{in}= 10,000 W m^{-2}. The dilution rate was kept at 0.25 day^{-1} and CW was used as feedstock. (-○-) stands for functional biomass; (-□-) for TAG; and (-◇-) for POC.

The use of a flexible source of illumination can help solve the problems of light limitation and photoinhibition during the final stages of biomass production. It can also prevent light from being restricted during the growth phase.

3.2.4 Studying the impact of dilution rate for optimizing dilution rate value

The concentration and productivity of functional biomass and TAG during steady-state in a CSTR are shown in **Figure 7** using different values of dilution rate (0.1 – 0.6 day $^{-1}$). In **Figure 7a**. it can be observed that as the dilution rate increased to 0.45 day^{-1}, so did the biomass concentration at steady-state. Meanwhile, TAG concentration decreased linearly. Although higher dilution rates result in lower TAG content within the total biomass, microalgal cells are washed out from the media with dilution rates above 0.45 day^{-1}.

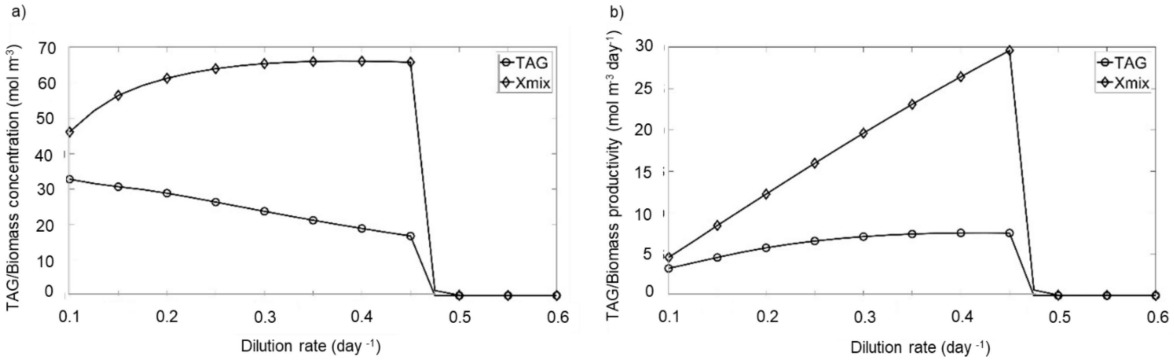


Figure 7 a) Influence of dilution rate (day^{-1}) on TAG over functional biomass content (mol m^{-3}), and b) influence of dilution rate (day^{-1}) on TAG over functional biomass productivity (mol m^{-3} day^{-1}). Light intensity was kept at 500 W m^{-2}, and RCW was used as substrate. (◆) stands for functional biomass and (●) for TAG.

The productivity of a component depends on the dilution rate. So, increasing the dilution rate from 0.45 to 0.50 day^{-1} had a positive effect on TAG productivity, despite the decreasing trend in TAG concentration observed in **Figure 7b**. The optimal microalgal mixotrophic growth under a chemostat regime could be observed at a dilution rate of

0.45 day^{-1}, for which TAG and functional biomass productivity reached 7.5 and 30 mol m^{-3} day^{-1}, respectively.

3.2.5 Results for microalgae axenic culture under the chemostat regime

The effects of different environmental conditions (i.e., light intensity and dilution rate) on the production and concentration of axenic microalgae biomass CSTR revealed that a light intensity of 500 W m^{-2} and a dilution rate of 0.45 day^{-1} improved the efficiency of the chemostat regime, as seen in **Figure 8.** The impact of other state variables, such as dissolved gases and nutrient availability on microalgal growth is displayed in **appendix E.**

Figures 8a and **8b**, show that when the dilution rate increases, the carbon allocated to the synthesis of storage molecule shifts to the synthesis of functional biomass which could be inferred by the decrease in TAG and POC concentrations, and an increase in biomass concentration. **Table 18** also corroborates these findings.

When the light intensity is the only variable adjusted (**Figures 8a** and **8c**) the concentration of storage molecules increased within the total biomass. TAG concentration increased by 164% after adjusting the light intensity. Consequently, its productivity was also higher, regardless of the adjustment in dilution rate.

The adjustment of both dilution rate (D= 0.45 day^{-1}) and light intensity ($I_{in}= I_{in\,(X)}^{optimum}$ W m^{-2}) to optimal conditions (**Figure 8d**) increased TAG productivity from 6.59 to 33.37 mol m^{-3} day^{-1}, an improvement of almost 400% to initial conditions (**Figure 8a**).

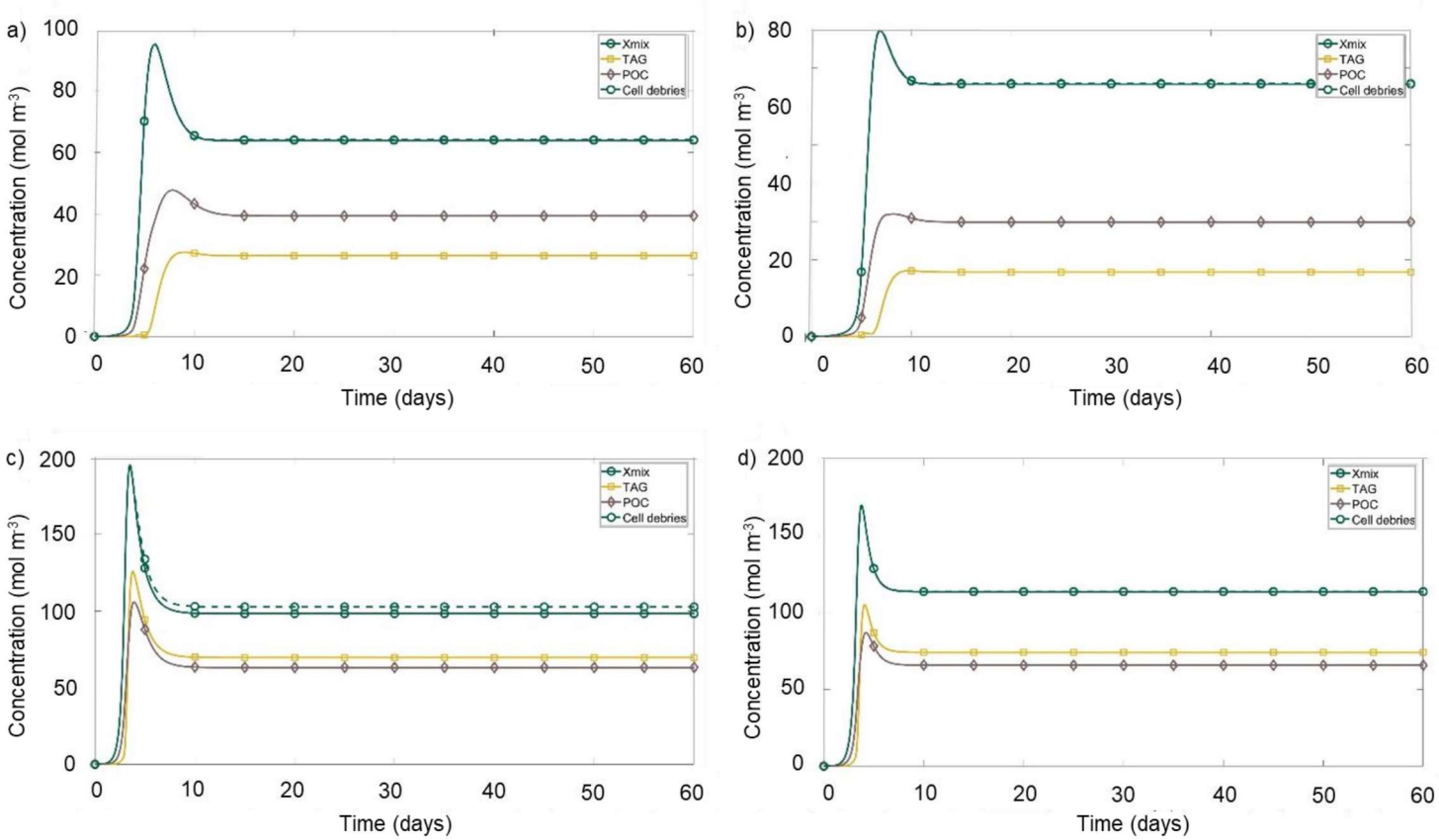


Figure 8 Microalgae mixotrophic growth pattern under chemostat regime and using RCW as substrate considering light intensities and dilution rates: a) I_{in}= 500 W m^{-2} and D = 0.25 day^{-1}, b) I_{in}= 500 W m^{-2} and D = 0.45 day^{-1}, c) I_{in}= $I_{in\,(X)}^{optimum}$ W m^{-2} and D = 0.25 day^{-1}, and d) I_{in}= $I_{in\,(X)}^{optimum}$ W m^{-2} and D = 0.45 day^{-1}. (—●—) functional biomass; (—■—) TAG; (—◆—) POC.

Table 18 TAG content/productivity value under different environmental conditions

	Normal condition I_{in}= 500 W/m^2 D = 0.25 day^{-1}	Only D is tuned I_{in}= 500 W/m^2 D = 0.45 day^{-1}	Only I_{in} is tuned $I_{in}= I_{in\,(X)}^{optimum}$ D = 0.25 day^{-1}	Both D and I_{in} are tuned (optimal condition) $I_{in}= I_{in\,(X)}^{optimum}$ and D = 0.25 day^{-1}
TAG content $(\%\frac{\text{molTAG}}{\text{mol X}})$	20.3	14.9	30.1	29.2
TAG productivity $(\frac{\text{mol TAG}}{\text{m}^3\text{.day}})$	6.59	7.57	17.39	33.37

3.2.6 Studying the impact of feedstock

The previous sections contemplated the effects of dilution rate and light intensity under a CSTR regime using RCW as a substrate. In this section, we discuss the results found for two other substrates: PCW and MCW. These substrates differ in the C: N ratios, which consequently affects TAG's content and productivity, as seen in **Figure 9.**

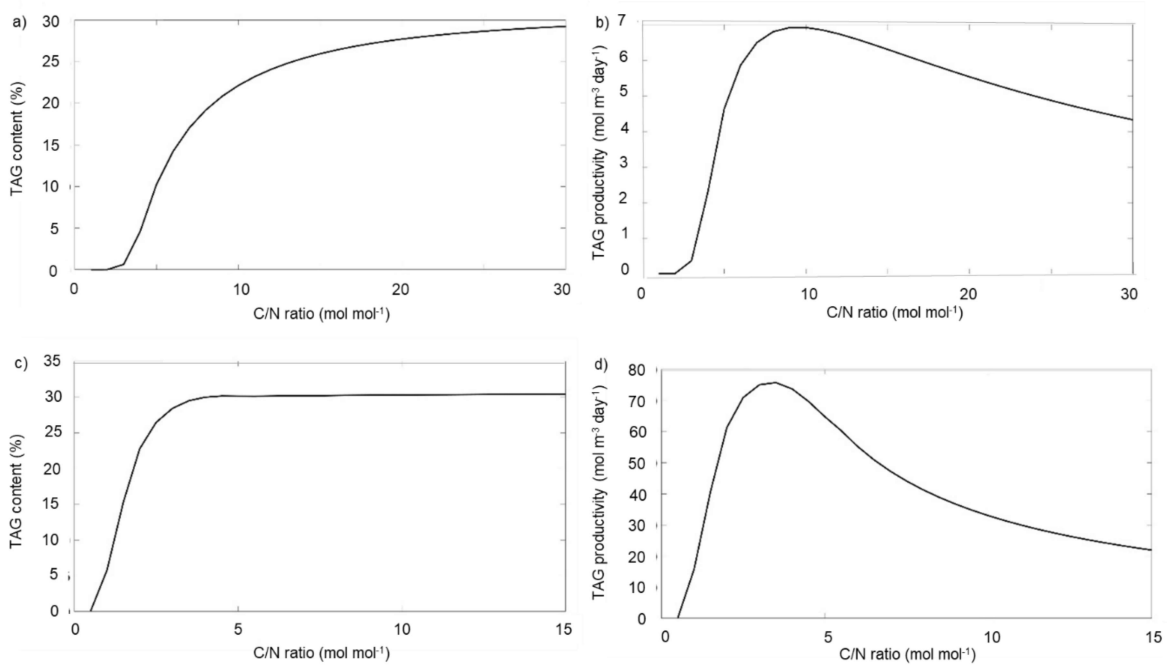


Figure 9 Influence of C: N ratio on TAG content and productivity during microalgae mixotrophic growth under chemostat regime and different light intensity and dilution rates: a) TAG content in total biomass (%) over the C: N ratio on normal culture conditions (I_{in}= 500 W m^{-2} and D = 0.25 day^{-1}); b) TAG productivity (mol m^{-3} day^{-1}) over the C N ratio on normal culture conditions; c) TAG content in total biomass (%) over C: N ratio under optimum culture conditions (I_{in}= $I_{in\,(X)}^{optimum}$ W m^{-2} and D = 0.45 day^{-1}), and d) TAG productivity (mol m^{-3} day^{-1}) over C: N ratio on optimum culture condition.

According to **Figures 9a** and **9c**, the influence of the C: N ratio on TAG content could be described as an increase to a turning point followed by a conversion to an asymptotic

line representing the maximum possible TAG content, which was about 30% of the total biomass. This trend could be observed regardless of the presence of other variables such as dilution rate and light intensity. Therefore, TAG content could be assumed to range around this value. Low C: N ratios displayed a negligible TAG content due to carbon being allocated for biomass synthesis, whereas a high C: N ratio led to TAG content reaching its most saturated level.

It is important to note that biomass with high TAG content does not mean high TAG productivity, as the latter is defined by the TAG content within total biomass times the total biomass productivity. High C: N ratios have limited nitrogen availability of nitrogen for microalgal growth. Thus, TAG productivity remained very low (**Figures 9b** and **9d**). Conversely, an optimum C: N ratio for maximum TAG productivity must present moderate values. According to **Figures 9b** and **9d**, under normal conditions (I_{in}= 500 W m^{-2} and D = 0.25 day^{-1}), the optimal C:N ratio was 10.0, which is close to RCW C: N ratio of 11.7, while under optimum conditions (I_{in}= $I_{in\,(X)}^{optimum}$W m^{-2} and D = 0.45 day^{-1}), it was 4.0, being closer to PCW C:N ratio of 5.6.

Since the optimal C: N ratio can vary with the changes in the system's conditions, there cannot be a unique MCW. Notwithstanding, a C: N ratio of 4.0 can be considered for describing the substrate's characteristics assuming optimal environmental conditions. **Table 19** presents MCW characteristics.

Table 19 Characteristics of MCW

	$C_S^{In}\ \left(\frac{mol\ COD}{m^3}\right)$	$C_{GLC}^{In}\ \left(\frac{mol\ GLC}{m^3}\right)$	$C_{NH_4^+}^{In}\ \left(\frac{mol\ NH_4^+}{m^3}\right)$	$C_{PO_4^{3-}}^{In}\ \left(\frac{mol\ PO_4^{3-}}{m^3}\right)$
Modified Cheese Whey (MCW)	1741.9	290.3	72.6	72.6

Table 20 summarizes the concentration of biomass, POC, TAG, TAG content, and productivity for RCW, PCW, and MCW used as substrates on normal and optimum conditions. TAG productivity was assumed to be its maximum value of 73.68 mol m^{-3} day^{-1}) under the optimum environmental conditions (I_{in}= $I_{in\,(X)}^{optimum}$W m^{-2} and D = 0.45 day^{-1}) and substrate (MCW).

3.3 Microalgal-microbial non-axenic culture under chemostat regime

The growth pattern of a non-axenic culture in a chemostat regime consisted of substrate (i.e., C, N, P) competition between microalgae and ordinary heterotrophic microorganisms (OHO). **Figure 10** illustrates the growth pattern of non-axenic cultures grown in PCW-fed in the CSTR regime under regular and optimized conditions.

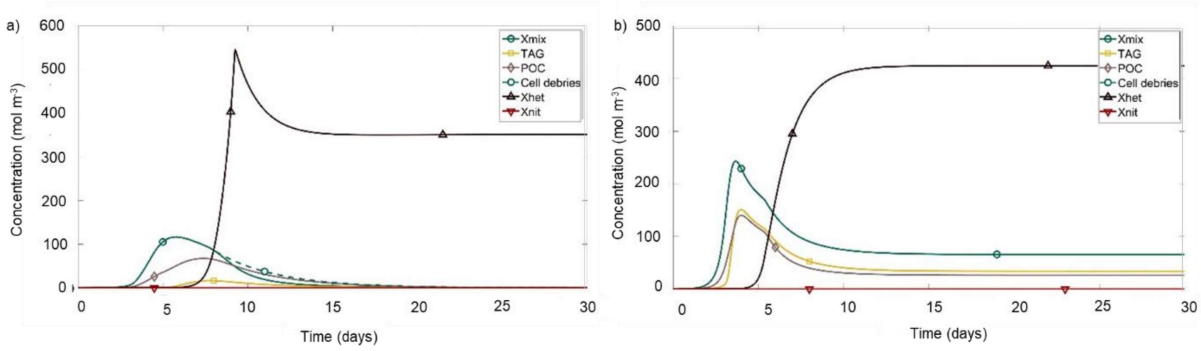


Figure 10 Microalgal growth pattern in non-axenic culture under chemostat regime using PCW as substrate. Left a): during regular light intensity and dilution rate (I_{in}= 500 Wm^{-2} and D = 0.25 day^{-1}). Right b): during optimum light intensity and dilution rate (I_{in}= $I_{in\,(X)}^{optimum}$ W/m^2 and D = 0.45 day^{-1}). (⊖) functional biomass; (▭) TAG; (◈) POC; (▲) heterotrophs; (▼) nitrifiers (See **appendix F** for supplementary diagrams).

Table 20 Microalgae axenic culture patterns in a chemostat regime and different substrates

Feedstock	TAG concentration C_{TAG} $(\frac{mol\ TAG}{m^3})$	POC concentration C_{POC} $(\frac{mol\ POC}{m^3})$	Biomass concentration X_f $(\frac{mol\ X_f}{m^3})$	TAG content $(\%\frac{mol\ TAG}{mol\ X})$	TAG productivity P_{TAG} $(\frac{mol\ TAG}{m^3.day})$
Normal condition: $D = 0.25\frac{1}{day}, I_{in} = 500\frac{w}{m^2}$					
RCW	26.36	39.32	63.96	20.3%	6.59
PCW	22.57	56.63	82.90	13.9%	5.64
MCW	9.49	63.41	127.14	4.7%	2.37
Optimum condition: $D = 0.45\frac{1}{day}, I_{in} = I_{in\ (X)}^{optimum}$					
RCW	74.15	65.82	113.70	29.2%	33.37
PCW	107.95	102.61	165.34	28.7%	48.58
MCW	163.74	118.46	263.89	30.0%	73.68

As seen in **figure 10a** OHOs completely outcompeted microalgae, which were washed out during steady-state in regular light intensity and dilution rate conditions (I_{in}= 500 W m^{-2} and D = 0.25 day^{-1}) with a biomass concentration of 350 $mol.m^{-3}$. Given the increase in dissolved carbon dioxide concentration and the observed decrease in dissolved oxygen concentration during the exponential growth of microbial biomass (see **appendix F**), it could be inferred that these microorganisms were mostly (facultative) aerobic. The absence of dinitrogen gas and methane gas, products of anoxic and anaerobic heterotrophic metabolisms, respectively, corroborates with the postulation. Microalgae sustained growth with optimized conditions (I_{in}= $I_{in\,(X)}^{optimum}$ W m^{-2} and D = 0.45 day^{-1}) as seen in **Figure 10** regardless the predominance of OHOs. Thus, different parameters were adjusted to improve microalgal biomass concentration. Considering the predominance of aerobic heterotrophic microorganisms, the depletion of oxygen supply in the airflow could favor microalgae growth over OHOs. The absence of oxygen not only hampers aerobic heterotrophic growth but also microalgae chemoheterotrophic growth. However, microalgal growth was possible due to photoautotrophic and photoheterotrophic processes. **Figure 11** shows the non-axenic culture growth patterns in the function of oxygen availability under optimal conditions in a CSTR using PCW as substrate.

A symbiotic relationship between microalgae and bacteria can be inferred since microbial and microalgal biomass concentrations did not present drastic changes during steady-state and oxygen depletion (**Figure 11**). Heterotrophic microorganisms utilized the oxygen produced by microalgae during photosynthesis. Consequently, we tested the influence of different substrates (i.e., RCW and MCW) in microalgal growth patterns using the same optimal conditions in a CSTR regime (**Figure 12**).

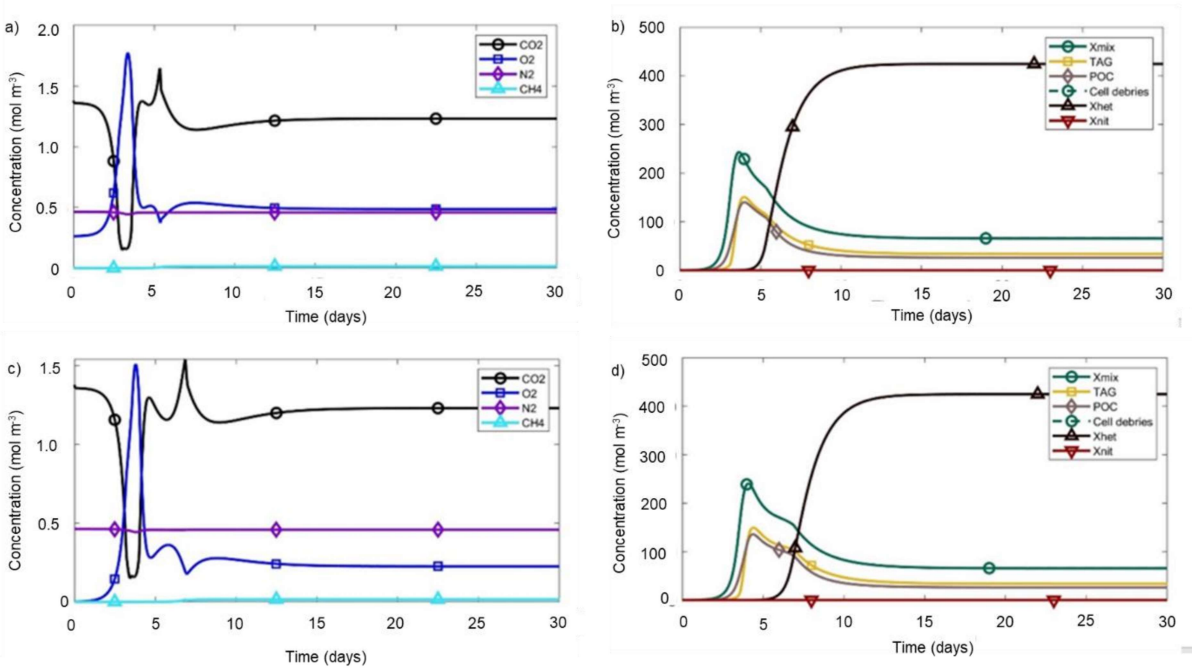


Figure 11 Growth pattern of non-axenic culture growth pattern during optimum conditions (I_{in}= $I_{in\,(X)}^{optimum}$ W m^{-2} and D = 0.45 day^{-1}) under chemostat regime using PCW as substrate. In **Figures 11a** and **11b**, the O_2 mole fraction of the influent was set at 0.202 whereas, in **Figures 11c** and **11d**, the influent's O_2 mole fraction was zero (oxygen depletion). Figures a and c display the concentration of the following dissolved gases in the liquid phase: (⊖) CO_2; (⊟) O_2; (◈) N_2; and (△) CH_4. Figures **11b** and **11d** present the concentrations of the following components and microorganisms in microbial and microalgal biomass: (⊖) functional biomass; (⊟) TAG; (◈) POC; (▲) heterotrophs; (▽) nitrifiers (see **appendix F**).

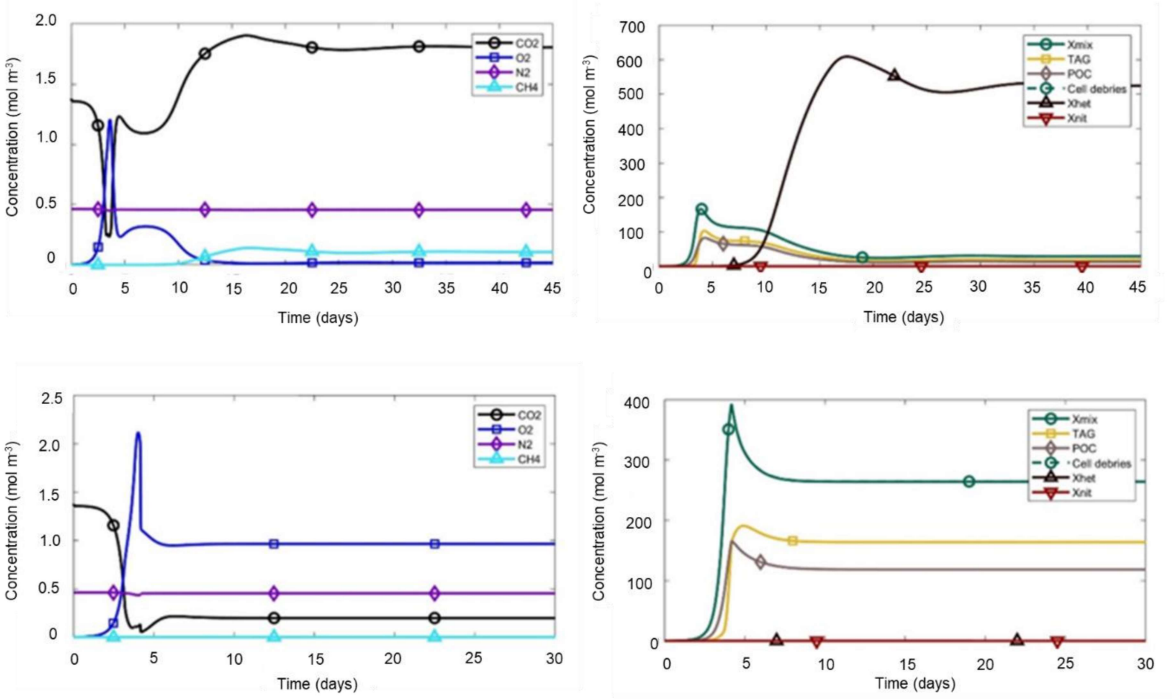


Figure 12 Microalgae non-axenic culture growth pattern, indicated as biomass concentration profile over time, under optimal conditions (I_{in}= $I_{in\,(X)}^{optimum}$ W m^{-2} and D = 0.45 day^{-1}), O_2 depletion and in a chemostat regime. and mole. **Figures 12a** and **12b** used RCW as substrate while figures c and d utilized MCW. Figures a and c display the concentration of the following dissolved gases in the liquid phase: (⊖) CO_2; (▭) O_2; (◈) N_2; and (△) CH_4. **Figures 12b** and **12d** present the concentrations of the following components and microorganisms in microbial and microalgal biomass: (⊖) functional biomass; (▭) TAG; (◈) POC; (▲) heterotrophs; (▼) nitrifiers (see **appendix F** for supplementary diagrams).

As shown in **Figure 12a**, the use of RCW as a substrate did not prevent the growth of microbial organisms. However, it can be assumed that microorganisms were predominantly anaerobic (facultative) by observing both the production and accumulation of methane. The switch in the metabolism is due to a higher C: N ratio of RCW compared to PCW combined with the absence of oxygen in the medium.

However, the use of MCW as a substrate favored microalgal growth over OHOs (**Figure 12b**). Considering that MCW had an ideal C: N ratio hypothesized for optimal TAG production, the application of a periodic switch between light-feast and dark-famine

regimes allowed the use of the available substrates for microalgal biomass growth (i.e., RCW and PCW).

3.4 Microalgae axenic culture under cyclic chemostat regime

The application of periodic cycles of light-famine and dark-famine to the system required assuming that only light cycle and feed were controlling factors in it. Unlike the switch between dark and light conditions, the control between feast and famine regimes had to be calibrated in a way that organic carbon concentration (i.e., glucose) reached zero before and during the famine phase. The concentration of organic carbon would then increase with the reintroduction of cheese whey. Therefore, the dilution rate was adjusted during the dark-famine cycle while it remained at 0.45 day^{-1} during the light-feast cycle.

As depicted in **Figure 13**, a longer period of light-feast (i.e., 36 hours) with a shorter dark-famine period (i.e., 12 hours) led to higher yields of TAG. The increased production and lower consumption of TAG during extended light-feast and reduced dark-famine cycles were expected. In the early stages of the light-feast cycle, microalgae tend to produce functional biomass and POC over TAG. During the dark-famine phase, the availability of POC reduces the microalgal consumption of TAG for anabolic processes.

In both scenarios, LF-DF (24:24) and LF-DF (36:12), biomass concentration exhibited the same pattern, increasing in LF and decreasing in DF. However, dark-famine periods are indispensable in guaranteeing that OHOs are washed out. The decrease of both TAG and POC during DF was attributed to component degradation and effluent washout. In its turn, the observed decrease in functional biomass resulted from effluent washout even though TAG and POC production prevents its depletion.

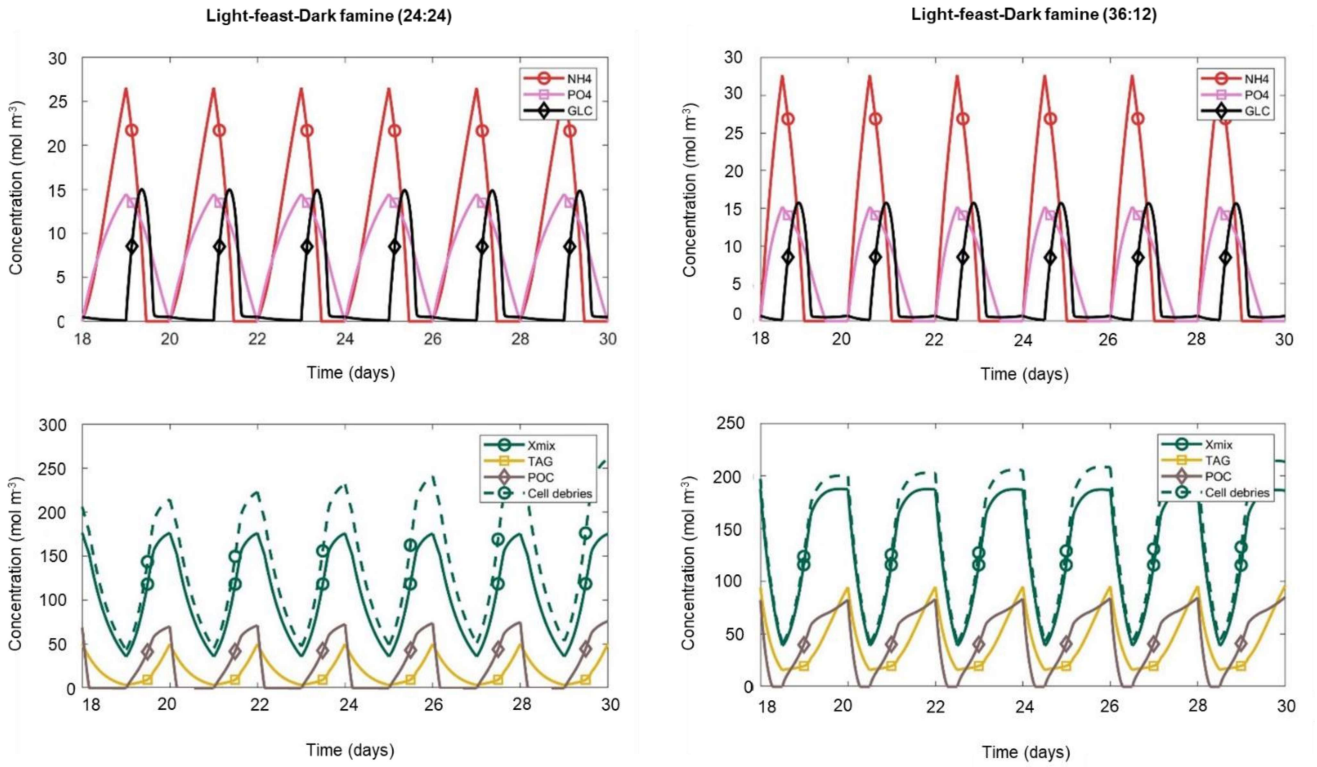


Figure 13 Microalgae mixotrophic growth under CSTR regime and PCW as substrate. Regular light-feast/dark-famine cycles and optimum dilution rate were implemented (I_{in}= $I_{in\,(X)}^{optimum}$ W m^{-2} and D = 0.45 day^{-1}, and D^{dark}= 4 day^{-1}). The experiment lasted 12 days. Left: LF-DF (24:24): 24 hours light-feast and 24 hours dark-famine. Right: LF-DF (36:12): 36 hours light-famine and 12 hours dark-famine. Top: concentration of nutrients (N and P) as well as biodegradable sCOD in form of glucose versus time; (-◆-) glucose; (-○-) ammonium (NH_4^+); (-□-) phosphate (PO_4^{3-}). Bottom: biomass concentration versus time; (-○-) functional biomass; (-□-) TAG; (-◇-) POC. (See **appendix G** for supplementary diagrams).

3.5. Microalgal-microbial non-axenic culture under cyclic chemostat regime

Non-axenic microalgal biomass growth was modeled under a CSTR regime with an LF-DF (36:12) cycle and using PCW (**Figure 14**) and RCW (**Figure 15**) as substrates.

As seen in **Figures 14** and **15**, the implementation of light-feast and dark-famine cycles contributed to the dominance of microalgal biomass in the photobioreactor once the system reached semi-steady-state conditions. **Table 21** illustrates the results for non-axenic culture under a cyclic chemostat regime The heterotrophic biomass (i.e., OHOs) were outcompeted being washed out from the system. Axenic microalgal culture produced a significant amount of TAG (see **Table 21**).

The scenario in which RCW was utilized as a substrate had TAG productivity estimated at 83.1 mol m^{-3}·day^{-1}. This production equals 1.3 kg m^{-3}.day^{-1}, making scaling up viable. Considering the production of a 10 m^3 photobioreactor in ideal scenario conditions, daily production of 13 kg of TAG could be expected. It is valid to note that results for larger photobioreactors will vary accordingly.

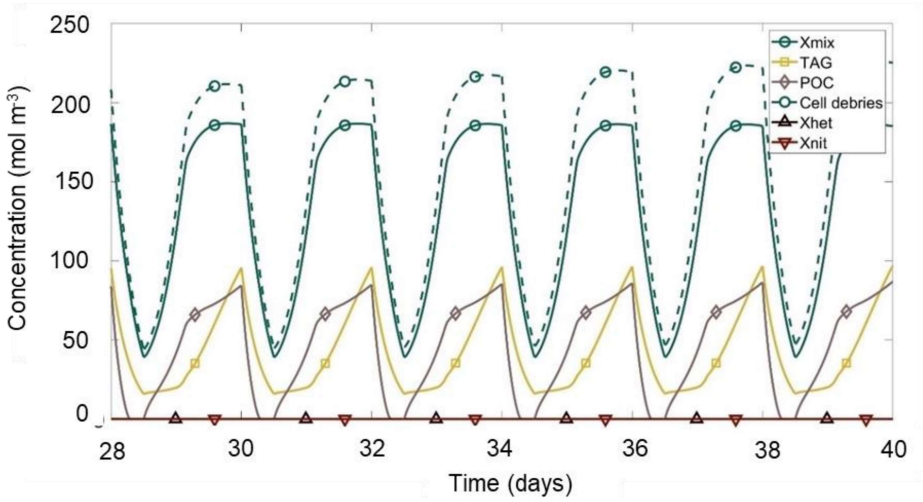


Figure 14 Non-axenic microalgae growth pattern under CSTR regime, fed with PCW, and a LF-DF (36:12) cycle. Dilution rate varied according the phase (I_{in}= $I_{in\,(X)}^{optimum}$ W m^{-2} and D^{Light} = 0.45 day^{-1}, and D^{dark}= 3 day^{-1}). The experiment lasted 12 days. (⊖) functional biomass; (⊟) TAG; (◈) POC; (▲) heterotrophs; (▼) nitrifiers; (See **appendix H** for supplementary diagrams).

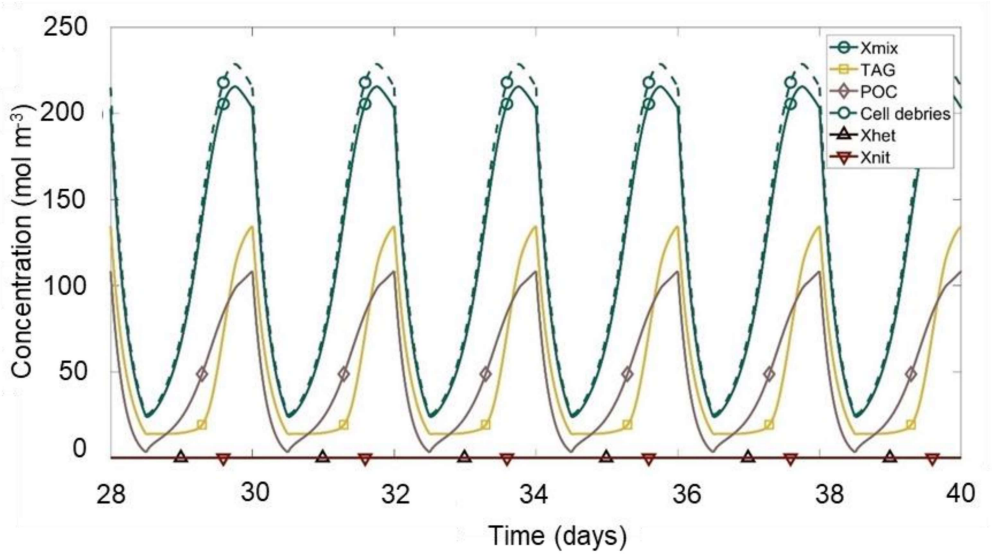


Figure 15 Non-axenic microalgae growth pattern under CSTR regime, fed with RCW, and a LF-DF (36:12) cycle. Dilution rate varied according the phase (I_{in}= $I_{in\,(X)}^{optimum}$ W m^{-2} and D^{Light} = 0.45 day^{-1}, and D^{dark}= 3 day^{-1}). Experiment lasted 12 days. (⊖) functional biomass; (⊟) TAG; (◈) POC; (▲) heterotrophs; (▼) nitrifiers; (See **appendix H** for supplementary diagrams).

Table 21 Observable results for non-axenic culture under cyclic chemostat regime for RCW and PCW. (Cfb) stands for functional biomass average concentration, (C_{TAG}) TAG average concentration, (TAGc) TAG average content, (Pfb) Functional biomass average productivity, (P_{TAG}) TAG average productivity

	Cfb $\overline{C_{X_f}}\left(\frac{\text{mol } X_f}{m^3}\right)$	C_{TAG} $\overline{C_{TAG}}\left(\frac{\text{mol TAG}}{m^3}\right)$	TAGc $\left(\%\frac{\text{mol TAG}}{\text{mol X}}\right)$	Pfb $\overline{P_{X_f}}\left(\frac{\text{mol } X_f}{m^3.day}\right)$	P_{TAG} $\overline{P_{TAG}}\left(\frac{\text{mol TAG}}{m^3.day}\right)$	Heterotrophic bacteria
RCW	132.4	64.8	25.7	447.9	83.1	Washed out
PCW	129.0	43.0	19.8	325.2	48.0	Washed out

4 Conclusion

The goal of this study was to develop a predictive model for the growth of microalgal biomass using a combination of computational analysis and theoretical knowledge of the metabolic conversions, stoichiometry, and kinetics of microalgal growth. This model can be used to study the various processes that affect the development of microalgal biomass and neutral lipids accumulation such as light cycle and intensity, dilution rate, and nutrient availability. It can also aid in the design and optimization of photobioreactors processes for the scaled-up production of microalgal-based biofuels. The model considered the *(i)* differences and similarities of microalgae trophic modes under batch and chemostat regimes; *(ii)* implementation of non-axenic microalgae cultures over axenic ones, representing real-life systems; and *(iii)* influence of light-feast and dark-famine cycles on TAG production. The model simulation enabled us to draw 5 main conclusions:

1. Microalgae mixotrophic growth displayed higher biomass production as they can metabolize both organic and inorganic carbon sources for their anabolic processes. Consequently, mixotrophic microalgae presented higher TAG production compared to other trophic modes, resulting in a more sustainable valorization of cheese whey.

2. For a more efficient TAG productivity in chemostat regimes, a higher dilution rate (D= 0.45 day^{-1}) and adjusted light intensity (I_{in}= $I_{in\,(X)}^{optimum}$ W m^{-2}) are required.

3. A longer light-feast cycle together with a shorter dark-famine cycle (36:12) led to higher TAG production compared to light-feast and dark-famine cycles of equal duration (24:24).

4. Considering the optimization of parameters such as light intensity (I_{in}= $I_{in\,(X)}^{optimum}$ W m^{-2}), light cycle (LF-DF 36:12) and dilution rate (D= 0.45 day^{-1}), both cheese whey and the VFAs resulted from cheese whey acidogenic fermentation are good substrates for microalgae biomass and TAG production.

5. The optimized model parameters (i.e., light intensity (I_{in}= $I_{in\,(X)}^{optimum}$ W m^{-2}), light cycle (LF-DF 36:12) and dilution rate (D= 0.45 day^{-1}) successfully halted the competition between OHOs and microalgae during mixotrophic growth in non-axenic cultures.

The mathematical model demonstrates the feasibility of growing microalgae biomass mixotrophically for TAG production using cheese whey as a substrate. Notwithstanding,

the model must be further calibrated and validated to improve its accuracy. Factors such as acid-base reactions, reactor designs, and the interactions between microorganisms in non-axenic microalgae cultures can also be accounted for to refine the results and identify the best levels of biomass and TAG productivity. The findings of this paper should be viewed as a theoretical exploration that may be adjusted to fit a specific experimental design.

5 Matlab codes

The Matlab codes developed for this mathematical model can be found at github.com at https://github.com/samankhayat/M.Sc.-Thesis.

6 References

Abu-Ghosh, S., Dubinsky, Z., Verdelho, V., & Iluz, D. (2021). Unconventional high-value products from microalgae: A review. *Bioresource Technology*, *329*, 124895. https://doi.org/10.1016/j.biortech.2021.124895

Adesanya, V. O., Davey, M. P., Scott, S. A., & Smith, A. G. (2014). Kinetic modelling of growth and storage molecule production in microalgae under mixotrophic and autotrophic conditions. *Bioresource Technology*, *157*, 293–304. https://doi.org/10.1016/j.biortech.2014.01.032

Ahmad, A. L., Yasin, N. H. M., Derek, C. J. C., & Lim, J. K. (2011). Microalgae as a sustainable energy source for biodiesel production: A review. *Renewable and Sustainable Energy Reviews*, *15*(1), 584–593. https://doi.org/10.1016/j.rser.2010.09.018

Ananthi, V., Raja, R., Carvalho, I. S., Brindhadevi, K., Pugazhendhi, A., & Arun, A. (2021). A realistic scenario on microalgae based biodiesel production: Third generation biofuel. *Fuel*, *284*, 118965. https://doi.org/10.1016/j.fuel.2020.118965

Antar, M., Lyu, D., Nazari, M., Shah, A., Zhou, X., & Smith, D. L. (2021). Biomass for a sustainable bioeconomy: An overview of world biomass production and utilization. *Renewable and Sustainable Energy Reviews*, *139*, 110691. https://doi.org/10.1016/j.rser.2020.110691

Arnon, D. I. (1984). The discovery of photosynthetic phosphorylation. *Trends in Biochemical Sciences*, *9*(6), 258–262. https://doi.org/10.1016/0968-0004(84)90159-2

Banu, J. R., Preethi, S. K., Gunasekaran, M., & Gopalakrishnan, K. (2020). Microalgae based biorefinery promoting circular bioeconomy-techno economic and life-cycle analysis. *Bioresource Technology*, *302*, 122822. https://doi.org/10.1016/j.biortech.2020.122822

Carus, M., & Dammer, L. (2018). The Circular Bioeconomy—Concepts, opportunities, and limitations. *Industrial Biotechnology*, *14*(2), 83–91. https://doi.org/10.1089/ind.2018.29121.mca

Carvalho, F., Prazeres, A. R., & Rivas, J. (2013). Cheese whey wastewater: Characterization and treatment. In *Science of the Total Environment* (Vols. 445–446, pp. 385–396). https://doi.org/10.1016/j.scitotenv.2012.12.038

Chen, G., Zhao, L., & Qi, Y. (2015). Enhancing the productivity of microalgae cultivated in wastewater toward biofuel production: A critical review. *Applied Energy*, *137*, 282–291. https://doi.org/10.1016/j.apenergy.2014.10.032

Chénais, B. (2021). Algae and microalgae and their bioactive molecules for human health. *Molecules*, *26*(4), 1185. https://doi.org/10.3390/molecules26041185

Choix, F. J., de-Bashan, L. E., & Bashan, Y. (2012). Enhanced accumulation of starch and total carbohydrates in alginate-immobilized *Chlorella* spp. induced by *Azospirillum brasilense*: II. Heterotrophic conditions. *Enzyme and Microbial Technology*, *51*(5), 300–309. https://doi.org/10.1016/j.enzmictec.2012.07.012

Chowdhury, H., & Loganathan, B. (2019). Third-generation biofuels from microalgae: A review. *Current Opinion in Green and Sustainable Chemistry*, *20*, 39–44. https://doi.org/10.1016/j.cogsc.2019.09.003

Concas, A., Pisu, M., & Cao, G. (2013). Mathematical modelling of *Chlorella vulgaris* growth in semi-batch photobioreactors fed with pure CO2. *Chemical Engineering Transactions*, *13*, 1021–1026.

Darvehei, P., Bahri, P. A., & Moheimani, N. R. (2018). Model development for the growth of microalgae: A review. In *Renewable and Sustainable Energy Reviews* (Vol. 97, pp. 233–258). Elsevier Ltd. https://doi.org/10.1016/j.rser.2018.08.027

Dębowski, M., Dudek, M., Zieliński, M., Nowicka, A., & Kazimierowicz, J. (2021). Microalgal hydrogen production in relation to other biomass-based technologies—A review. *Energies*, *14*(19), 6025. https://doi.org/10.3390/en14196025

di Caprio, F., Proietti Tocca, G., Stoller, M., Pagnanelli, F., & Altimari, P. (2022). Control of bacterial contamination in microalgae cultures integrated with wastewater treatment by applying feast and famine conditions. *Journal of Environmental Chemical Engineering*, *10*(5), 108262. https://doi.org/10.1016/j.jece.2022.108262

Espinosa-Gonzalez, I., Parashar, A., & Bressler, D. C. (2014). Heterotrophic growth and lipid accumulation of *Chlorella protothecoides* in whey permeate, a dairy by-product stream, for biofuel production. *Bioresource Technology*, *155*, 170–176. https://doi.org/10.1016/j.biortech.2013.12.028

Fabris, M., Abbriano, R. M., Pernice, M., Sutherland, D. L., Commault, A. S., Hall, C. C., Labeeuw, L., McCauley, J. I., Kuzhiuparambil, U., Ray, P., Kahlke, T., & Ralph, P. J. (2020). Emerging technologies in algal biotechnology: Toward the establishment of a sustainable, algae-based bioeconomy. *Frontiers in Plant Science*, *11*(279). https://doi.org/10.3389/fpls.2020.00279

Fernández, F. G. A., Reis, A., Wijffels, R. H., Barbosa, M., Verdelho, V., & Llamas, B. (2021). The role of microalgae in the bioeconomy. *New Biotechnology*, *61*, 99–107. https://doi.org/10.1016/j.nbt.2020

Girard, J. M., Roy, M. L., Hafsa, M. ben, Gagnon, J., Faucheux, N., Heitz, M.,

Tremblay, R., & Deschênes, J. S. (2014). Mixotrophic Cultivation of Green Microalgae <i>Scenedesmus obliquus<i> on Cheese Whey Permeate for Biodiesel Production. *Algal Research*, *5*(1), 241–248. https://doi.org/10.1016/j.algal.2014.03.002

Goldman, J. C. (1999). Inorganic carbon availability and the growth of large marine diatoms. *Marine Ecology Progress Serie*, *180*, 81–91.

Gomez San-Juan, M., & Bogdanski, A. (2021). *How to mainstream sustainability and circularity into the bioeconomy? A compendium of bioeconomy good practices and polices.* FAO. https://doi.org/10.4060/cb5798en

Gumbi, S. T., Kumar, A., & Olaniran, A. O. (2022). Lipid productivity and biosynthesis gene response of indigenous microalgae *Chlorella* sp. T4 strain for biodiesel production under different nitrogen and phosphorus load. *BioEnergy Research*, *15*(4), 2090–2101. https://doi.org/10.1007/s12155-022-10419-z

Hemalatha, M., Sravan, J. S., Min, B., & Venkata Mohan, S. (2019). Microalgae-biorefinery with cascading resource recovery design associated to dairy wastewater treatment. *Bioresource Technology*, *284*, 424–429. https://doi.org/10.1016/J.BIORTECH.2019.03.106

Henze, M., Gujer, W., Mino, T., & van Loosedrecht, M. (2015). Activated Sludge Models ASM1, ASM2, ASM2d and ASM3. *Water Intelligence Online*, *5*(0), 9781780402369–9781780402369. https://doi.org/10.2166/9781780402369

Hernández-García, A., Velásquez-Orta, S. B., Novelo, E., Yáñez-Noguez, I., Monje-Ramírez, I., & Orta Ledesma, M. T. (2019). Wastewater-leachate treatment by microalgae: Biomass, carbohydrate and lipid production. *Ecotoxicology and Environmental Safety*, *174*, 435–444. https://doi.org/10.1016/j.ecoenv.2019.02.052

Ho, S.-H., Huang, S.-W., Chen, C.-Y., Hasunuma, T., Kondo, A., & Chang, J.-S. (2013). Characterization and optimization of carbohydrate production from an indigenous microalga *Chlorella vulgaris* FSP-E. *Bioresource Technology*, *135*, 157–165. https://doi.org/10.1016/j.biortech.2012.10.100

Illman, A. M., Scragg, A. H., & Shales, S. W. (2000). Increase in *Chlorella* strains calorific values when grown in low nitrogen medium. *Enzyme and Microbial Technology*, *27*(8), 631–635. https://doi.org/10.1016/S0141-0229(00)00266-0

Kavanaugh, M. C., & Trussell, R. R. (1980). Design of aeration towers to strip volatile contaminants from drinking water. *Journal - American Water Works Association*, *72*(12), 684–692. https://doi.org/10.1002/j.1551-8833.1980.tb04613.x

Khan, M. I., Shin, J. H., & Kim, J. D. (2018). The promising future of microalgae: current status, challenges, and optimization of a sustainable and renewable industry for biofuels, feed, and

other products. *Microbial Cell Factories*, *17*(36), 36. https://doi.org/10.1186/s12934-018-0879-x

Khoo, C. G., Lam, M. K., & Lee, K. T. (2019). Microscale and macroscale modeling of microalgae cultivation in photobioreactor: A review and perspective. In *Advances in Feedstock Conversion Technologies for Alternative Fuels and Bioproducts* (pp. 1–19). Elsevier. https://doi.org/10.1016/B978-0-12-817937-6.00001-1

Kiefer, D., Merkel, M., Lilge, L., Henkel, M., & Hausmann, R. (2021). From Acetate to Bio-Based Products: Underexploited Potential for Industrial Biotechnology. *Trends in Biotechnology*, *39*(4), 397–411. https://doi.org/10.1016/j.tibtech.2020.09.004

Kircher, M. (2012). The transition to a bio-economy: emerging from the oil age. *Biofuels, Bioproducts and Biorefining*, *6*(4), 369–375. https://doi.org/10.1002/bbb.1352

Lee, E., Jalalizadeh, M., & Zhang, Q. (2015). Growth kinetic models for microalgae cultivation: A review. *Algal Research*, *12*, 497–512. https://doi.org/10.1016/j.algal.2015.10.004

Li, S., Li, X., & Ho, S.-H. (2022). Microalgae as a solution of third world energy crisis for biofuels production from wastewater toward carbon neutrality: An updated review. *Chemosphere*, *291*, 132863. https://doi.org/10.1016/j.chemosphere.2021.132863

Liang, Y., Sarkany, N., & Cui, Y. (2009). Biomass and lipid productivities of *Chlorella vulgaris* under autotrophic, heterotrophic and mixotrophic growth conditions. *Biotechnology Letters*, *31*(7), 1043–1049. https://doi.org/10.1007/s10529-009-9975-7

Loomis, A. G. (1928). Solubilities of gases in water. In E. W. Washburn, C. J. West, N. E. Dorsey, F. R. Bichowsky, & A. Klemenc (Eds.), *International Critical Tables of Numerical Data, Physics, Chemistry and Technology: Vol. III* (pp. 255–261). McGraw-Hill, Inc.

Lu, Y., Zhai, Y., Liu, M., & Wu, Q. (2010). Biodiesel production from algal oil using cassava (*Manihot esculenta* Crantz) as feedstock. *Journal of Applied Phycology*, *22*(5), 573–578. https://doi.org/10.1007/s10811-009-9496-8

Ma, S., Zeng, W., Huang, Y., Zhu, Xianqing, Xia, A., Zhu, Xun, & Liao, Q. (2022). Revealing the synergistic effects of cells, pigments, and light spectra on light transfer during microalgae growth: A comprehensive light attenuation model. *Bioresource Technology*, *348*, 126777. https://doi.org/10.1016/j.biortech.2022.126777

Martínez, C., Mairet, F., Plaza, L., Sciandra, A., & Bernard, O. (2019). Quantifying the potential of microalgae to remove nutrients from wastewater. *IFAC-PapersOnLine*, *52*(26), 287–292. https://doi.org/10.1016/j.ifacol.2019.12.272

Mehariya, S., Goswami, R. K., Karthikeysan, O. P., & Verma, P. (2021).

Microalgae for high-value products: A way towards green nutraceutical and pharmaceutical compounds. *Chemosphere*, *280*, 130553. https://doi.org/10.1016/j.chemosphere.2021.130553

Mohan, S. V., Chiranjeevi, P., Chandrasekhar, K., Babu, P. S., & Sarkar, O. (2019). Acidogenic biohydrogen production from wastewater. In A. Pandey, S. V. Mohan, J.-S. Chang, P. C. Hallenbeck, & C. Larroche (Eds.), *Biohydrogen* (2nd ed., pp. 279–320). Elsevier B.V. https://doi.org/10.1016/B978-0-444-64203-5.00011-3

Molina Grima, E., García Camacho, F., Sánchez Pérez, J. A., Fernandéz Sevilla, J. M., Acién Fernandéz, F. G., & Contreras Gómez, A. (1994). A mathematical model of microalgal growth in light-limited chemostat culture. *J. Chem. Tech. Biotechnol.*, *61*, 167–173.

Mondini, C. (2019). *Ecological engineering of acidogenic and photoorganoheterotrophic microbial metabolisms to valorise cheese whey* [Master dissertation]. TU Delft.

Moreira, J. B., Santos, T. D., Duarte, J. H., Bezerra, P. Q. M., de Morais, M. G., & Costa, J. A. V. (2021). Role of microalgae in circular bioeconomy: from waste treatment to biofuel production. *Clean Technologies and Environmental Policy*. https://doi.org/10.1007/s10098-021-02149-1

Moreno García, L., Gariépy, Y., Barnabé, S., & Raghavan, V. (2020). Biorefinery of microalgae biomass cultivated in wastewaters. In R. P. K. E. G. J. K. R. G. Baskar (Ed.), *Refining Biomass Residues for Sustainable Energy and Bioproducts - Technology, Advances, Life Cycle Assessment, and Economics* (1st ed., pp. 149–180). Elsevier Inc. https://doi.org/10.1016/b978-0-12-818996-2.00007-7

Morgan, O. M., & Maass, O. (1931). An inverstigation of the equilibria existing in gas-water systems forming electrolytes. *Canadian Journal of Research*, *5*(2), 162–199. https://doi.org/10.1139/cjr31-062

Nagarajan, D., Lee, D.-J., & Chang, J.-S. (2019). Integration of anaerobic digestion and microalgal cultivation for digestate bioremediation and biogas upgrading. *Bioresource Technology*, *290*, 121804. https://doi.org/10.1016/j.biortech.2019.121804

Pang, N., Gu, X., Kirchhoff, H., Lei, H., & Roje, S. (2019). Exploiting mixotrophic for improving productivities of biomass and co-products of microalgae. *Renewable and Sustainable Energy Reviews*, *112*, 450–460. https://doi.org/10.1016/j.rser.2019.05.223

Panghal, A., Patidar, R., Jaglan, S., Chhikara, N., Khatkar, S. K., Gat, Y., & Sindhu, N. (2018). Whey valorization: current options and future scenario – a critical review. *Nutrition & Food Science*, *48*(3), 520–535. https://doi.org/10.1108/NFS-01-2018-0017

Pawar, P. R., Rao, P., Prakash, G., & Lali, A. M. (2021). Organic waste streams as feedstock for the production of high volume-low value products.

Environmental Science and Pollution Research, *28*(10), 11904–11914. https://doi.org/10.1007/s11356-020-07985-0

Peng, K., Li, J., Jiao, K., Zeng, X., Lin, L., Pan, S., & Danquah, M. K. (2018). The bioeconomy of microalgal biofuels. In E. , Jacob-Lopes, L. , Queiroz Zepka, & M. Queiroz (Eds.), *Energy from microalgae. Green energy and technology.* (1st ed., pp. 157–169). Springer, Cham. https://doi.org/10.1007/978-3-319-69093-3_7

Perez-Garcia, O., Escalante, F. M. E., De-Bashan, L. E., & Bashan, Y. (2011). Heterotrophic cultures of microalgae: Metabolism and potential products. *Water Research*, *45*(1), 11–36. https://doi.org/10.1016/j.watres.2010.08.037

Perin, G., Bellan, A., Bernardi, A., Bezzo, F., & Morosinotto, T. (2019). The potential of quantitative models to improve microalgae photosynthetic efficiency. *Physiologia Plantarum*, *166*(1), 380–391. https://doi.org/10.1111/ppl.12915

Rodolfi, L., Chini Zittelli, G., Bassi, N., Padovani, G., Biondi, N., Bonini, G., & Tredici, M. R. (2009). Microalgae for oil: Strain selection, induction of lipid synthesis and outdoor mass cultivation in a low-cost photobioreactor. *Biotechnology and Bioengineering*, *102*(1), 100–112. https://doi.org/10.1002/bit.22033

Saddoud, A., Hassaïri, I., & Sayadi, S. (2007). Anaerobic membrane reactor with phase separation for the treatment of cheese whey. *Bioresource Technology*, *98*(11), 2102–2108. https://doi.org/10.1016/j.biortech.2006.08.013

Sherwood, J. (2020). The significance of biomass in a circular economy. *Bioresource Technology*, *300*, 122755. https://doi.org/10.1016/J.BIORTECH.2020.122755

Solarte-Toro, J. C., & Cardona Alzate, C. A. (2021). Biorefineries as the base for accomplishing the sustainable development goals (SDGs) and the transition to bioeconomy: Technical aspects, challenges and perspectives. *Bioresource Technology*, *340*, 125626. https://doi.org/10.1016/j.biortech.2021.125626

Solimeno, A., Samsó, R., Uggetti, E., Sialve, B., Steyer, J. P., Gabarró, A., & García, J. (2015). New mechanistic model to simulate microalgae growth. In *Algal Research* (Vol. 12, pp. 35–224 . Elsevier. https://doi.org/10.1016/j.algal.2015.09.008

Talapatra, N., Gautam, R., Mittal, V., & Ghosh, U. K. (2021). A comparative study of the growth of microalgae-bacteria symbiotic consortium with the axenic culture of microalgae in dairy wastewater through extraction and quantification of chlorophyll. *Materials Today: Proceedings*. https://doi.org/10.1016/j.matpr.2021.06.227

Trebuch, L. M., Oyserman, B. O., Janssen, M., Wijffels, R. H., Vet, L. E. M., & Fernandes, T. V. (2020). Impact of hydraulic retention time on community assembly and function of photogranules

for wastewater treatment. *Water Research*, *173*, 115506. https://doi.org/10.1016/j.watres.2020.115506

Tsakali, E., Petrotos, K., D'Allessandro, A., & Goulas, P. (2010). A review on whey composition and the methods used for its utilization for food and pharmaceutical products. In C. R. Centre (Ed.), *6th International Conference on Simulation and Modelling in the Food and Bio-Industry* (pp. 195–201).

Tunay, D., Yildirim, O., Ozkaya, B., & Demir, A. (2022). Determination of photoautotrophic growth and inhibition kinetics by the Monod and the Aiba models and bioenergetics of local microalgae strain. *Chemosphere*, *292*, 133330. https://doi.org/10.1016/j.chemosphere.2021.133330

USDA. (2022). *Dairy: World markets and trade*. https://apps.fas.usda.gov/psdonline/circulars/dairy.pdf

Uvarova, I., Atstaja, D., Grinbergs, U., Petersons, J., Gegere-Zetterstroma, A., & Kraze, S. (2020). Transition to the circular economy and new circular business models – an in-depth study of the whey recycling. *IOP Conference Series: Earth and Environmental Science*, *578*(1), 012019. https://doi.org/10.1088/1755-1315/578/1/012019

Whangchai, K., Mathimani, T., Sekar, M., Shanmugam, S., Brindhadevi, K., van Hung, T., Chinnathambi, A., Alharbi, S. A., & Pugazhendhi, A. (2021). Synergistic supplementation of organic carbon substrates for upgrading neutral lipids and fatty acids contents in microalga. *Journal of Environmental Chemical Engineering*, *9*(4), 105482. https://doi.org/10.1016/j.jece.2021.105482

Wolf, G., Picioreanu, C., & van Loosdrecht, M. C. M. (2007). Kinetic modeling of phototrophic biofilms: The PHOBIA model. *Biotechnology and Bioengineering*, *97*(5), 1064–1079. https://doi.org/10.1002/bit.21306

Xiong, W., Liu, L., Wu, C., Yang, C., & Wu, Q. (2010). 13C-tracer and gas Chromatography-mass spectrometry analyses reveal metabolic flux distribution in the oleaginous microalga *Chlorella protothecoides*. *Plant Physiology*, *154*(2), 1001–1011. https://doi.org/10.1104/pp.110.158956

Yadav, B., Chavan, S., Atmakuri, A., Tyagi, R. D., & Drogui, P. (2020). A review on recovery of proteins from industrial wastewaters with special emphasis on PHA production process: Sustainable circular bioeconomy process development. *Bioresource Technology*, *317*, 124006. https://doi.org/10.1016/j.biortech.2020.124006

Yadav, J. S. S., Bezawada, J., Elharche, S., Yan, S., Tyagi, R. D., & Surampalli, R. Y. (2014). Simultaneous single-cell protein production and COD removal with characterization of residual protein and intermediate metabolites during whey fermentation by K. marxianus. *Bioprocess and Biosystems Engineering*, *37*(6), 1017–1029. https://doi.org/10.1007/s00449-013-1072-6

Appendices

Appendix A – State variables of the mathematical model

Table I. State variables of the model with their respective units.

State variable	Unit	Definition
C_{CO_2}	mol CO_2 m^{-3}	Concentration of dissolved carbon dioxide gas
C_{O_2}	mol CO_2 m^{-3}	Concentration of dissolved oxygen gas
C_{N_2}	mol O_2 m^{-3}	Concentration of dissolved nitrogen gas
C_{CH_4}	mol CH_4 m^{-3}	Concentration of dissolved methane gas
C_S	mol COD m^{-3}	Concentration of readily biodegradable organic compound
C_{GLC}	mol Glc m^{-3}	Concentration of readily biodegradable glucose
$C_{NH_4^+}$	mol m^{-3}	Concentration of ammonium
$C_{NO_3^-}$	mol m^{-3}	Concentration of nitrate
$C_{PO_4^{3-}}$	mol m^{-3}	Concentration of phosphate
C_{TAG}	cmol TAG m^{-3}	Concentration of internally stored triacylglycerol
C_{POC}	cmol POC m^{-3}	Concentration of internally stored poly-carbohydrate (starch)
X_{mix}	cmol X m^{-3}	Concentration of microalgal mixotrophic biomass
X_{het}	cmol X m^{-3}	Concentration of microbial heterotrophic biomass
X_{nit}	Cmol X m^{-3}	Concentration of microbial autotrophic (nitrifying) biomass
S_N	mol N cmol X^{-1}	Nitrogen quota for microalgal biomass
S_P	mol P cmol X^{-1}	Phosphorus quota for microalgal biomass
S_N^{het}	mol N cmol X^{-1}	Nitrogen quota for microbial heterotrophic biomass
S_P^{het}	mol P cmol X^{-1}	Phosphorus for microbial heterotrophic biomass
S_N^{nit}	mol N cmol X^{-1}	Nitrogen quota for microbial nitrifying biomass
S_P^{nit}	mol P cmol X^{-1}	Phosphorus for microbial nitrifying biomass
y_{CO_2}	mol CO_2 mol Air $^{-1}$	Molar fraction of carbon dioxide gas
y_{O_2}	mol O_2 mol Air $^{-1}$	Molar fraction of oxygen gas
y_{N_2}	mol N_2 mol Air $^{-1}$	Molar fraction of nitrogen gas
y_{CH_4}	mol CH_4 mol Air^{-1}	Molar fraction of methane gas

Appendix B – Stoichiometry of microalgae metabolisms

2 Light-feast regime

2.1 Photoautotrophic mode

Photoautotrophic metabolism considered the following metabolic reactions: (*a-i*) non-cyclic photophosphorylation resulting in ATP and NADPH derived from photons energy, (*a-ii*) cyclic photophosphorylation, presenting higher ATP yield than the previous reaction, (*a-iii*, *a-iv*, and *a-v*) encompassing the synthesis of functional biomass, TAG and POC from an inorganic carbon source (i.e., CO_2) and the (*a-vi*) formation of glycerol.

In order to achieve photoautotrophy stoichiometric yields NADH, NADPH, and ATP were considered conserved moieties with neither net consumption nor generation. All reactions were coupled and energetically balanced encompassing growth (a-i, a-ii, a-iii and a-vi), TAG (a-I, a-ii, a-iv, and a-vi), and POC (a-i, a-ii, and a-v) production. Cyclic photophosphorylation (a-ii) was considered catabolism during maintenance since it the energy provided for maintenance was more efficient than in non-cyclic photophosphorylation (a-i). **Appendix 2 Table II** displays the equations and stoichiometry yields during photoautotrophy.

Table II. Summary of photoautotrophic metabolic reactions. The syntheses of functional biomass, TAG, and POC were based on carbon-mole and compounds such as ADP, Pi, H_2O, CoA-SH, and H^+ were not considered in the balance.

a-i. Photophosphorylation	$\text{photon} \rightarrow 1\ \text{NADPH} + 0.5\ \text{O}_2 + \delta\ \text{ATP}$
a-ii. Photophosphorylation (Cyclic)	$\text{photon} \rightarrow 0.125\ \text{O}_2 + 0.25\ \text{H}_2 + \Delta\ \text{ATP}$
a-iii. Synthesis of functional biomass	$1\ \text{CO}_2 + 4.04\ \text{NADPH} + 0.2\ \text{NH}_4^+ + 0.03\ \text{po}_4^{3-} + 5.980\ \text{ATP} \rightarrow 1\ \text{X}_\text{f} + 1.941\ \text{NADH}$
a-iv. Synthesis of TAG	$1\ \text{CO}_2 + 3.76\ \text{NADPH} + 3.94\ \text{ATP} \rightarrow 1\ \text{TAG} + 0.92\ \text{NADH}$
a-vi. Synthesis of POC	$1\ \text{CO}_2 + 2\ \text{NADPH} + 3.167\ \text{ATP} \rightarrow 1\ \text{POC}$
a-vi. Formation of glycerol	$3\ \text{CO}_2 + 6\ \text{NADPH} + 1\ \text{NADH} + 9\ \text{ATP} \rightarrow 1\ \text{C}_3\text{H}_8\text{O}_3$

2.2 Photoheterotrophic mode

The photoheterotrophic metabolism encompasses six metabolic reactions with a critical assumption: it has been assumed that the photophosphorylation is cyclic, producing higher yield of ATP as NADPH could be supplied from an organic carbon source (i.e., glucose) through the pentose phosphate pathway. Accordingly, the reactions are *(*b-i*)* cyclic photophosphorylation, in which the organic carbon source donates electrons and become oxidized; *(*b-ii*)* pentose phosphate pathway; *(b-iii)*, *(b-iv)*, and *(b-v)* synthesis of functional biomass, TAG, and POC from organic carbon source (i.e., glucose), respectively; and *(b-vi)* formation of glycerol.

Table III. Reactions considered in the metabolic network model under *photoheterotrophy*

b-i. Photophosphorylation (cyclic)	$0.25\ \mathrm{Glc} + \mathrm{photon} \rightarrow 1.5\ \mathrm{CO_2} + 3\ \mathrm{H_2} + \Delta\ \mathrm{ATP}$
b-ii Pentose Phosphate pathway	$1\ \mathrm{Glc} + 1\ \mathrm{ATP} \rightarrow 6\ \mathrm{CO_2} + 12\ \mathrm{NADPH}$
b-iii Synthesis of functional biomass	$0.175\ \mathrm{Glc} + 0.392\ \mathrm{NADPH} + 0.2\ \mathrm{NH_4^+} + 0.03\ \mathrm{po_4^{3-}} + 1.466\ \mathrm{ATP} \rightarrow 1\ \mathrm{X_f} + 0.392\ \mathrm{NADH} + 0.05\ \mathrm{CO_2}$
b-iv Synthesis of TAG	$0.245\ \mathrm{Glc} + 0.823\ \mathrm{NADPH} + 0.02\ \mathrm{ATP} \rightarrow 1\ \mathrm{TAG} + 0.922\ \mathrm{NADH} + 0.471\ \mathrm{CO_2}$
b-v Synthesis of POC	$0.167\ \mathrm{Glc} + 0.333\ \mathrm{ATP} \rightarrow 1\ \mathrm{POC}$
b-vi Formation of glycerol	$0.5\ \mathrm{Glc} + 1\ \mathrm{NADH} + 1\ \mathrm{ATP} \rightarrow 1\ \mathrm{C_3H_8O_3}$

2.3 Chemoheterotrophic regime

The chemoheterotrophic metabolism involves eight metabolic reactions: (c-i) glycolysis and Krebs cycle, which provide ATP and cofactors NADH and $FADH_2$ through oxidizing organic carbon source (i.e., glucose); (c-ii) pentose phosphate pathway, which is the only supplier of NADPH; (c-iii), (c-iv), and (c-v) synthesis of functional biomass, TAG, and POC from organic carbon source (i.e., glucose), respectively; (c-vi) and (c-vii) oxidative phosphorylation that produced further ATP via donating electrons to the oxygen as the electron acceptor; and (c-viii) formation of glycerol. **Table IV** provides a summary of chemoheterotrophic metabolic reactions with the same alterations as the previous section.

Table IV Reactions considered in the metabolic network model under *chemoheterotrophy*

c-i Glycolysis and Krebs cycle	$1\ \mathrm{Glc} \rightarrow 6\ \mathrm{CO_2} + 10\ \mathrm{NADH} + 2\ \mathrm{FADH_2} + 4\ \mathrm{ATP}$
c-ii Pentose Phosphate pathway	$1\ \mathrm{Glc} + 1\ \mathrm{ATP} \rightarrow 6\ \mathrm{CO_2} + 12\ \mathrm{NADPH}$
c-iii Synthesis of functional biomass	$0.175\ \mathrm{Glc} + 0.392\ \mathrm{NADPH} + 0.2\ \mathrm{NH_4^+} + 0.03\ \mathrm{PO_4^{3-}} + 1.466\ \mathrm{ATP} \rightarrow 1\ \mathrm{X_f} + 0.392\ \mathrm{NADH} + 0.05\ \mathrm{CO_2}$
c-iv Synthesis of TAG	$0.245\ \mathrm{Glc} + 0.823\ \mathrm{NADPH} + 0.02\ \mathrm{ATP} \rightarrow 1\ \mathrm{TAG} + 0.922\ \mathrm{NADH} + 0.471\ \mathrm{CO_2}$
c-v Synthesis of POC	$0.167\ \mathrm{Glc} + 0.333\ \mathrm{ATP} \rightarrow 1\ \mathrm{POC}$
c-vi Oxidative phosphorylation, NADH	$1\ \mathrm{NADH} + 0.5\ \mathrm{O_2} \rightarrow 1\ \mathrm{ATP}$
c-vii Oxidative phosphorylation, $FADH_2$	$1\ \mathrm{FADH_2} + 0.5\ \mathrm{O_2} \rightarrow 0.667\ \mathrm{ATP}$
c-viii Formation of glycerol	$0.5\ \mathrm{Glc} + 1\ \mathrm{NADH} + 1\ \mathrm{ATP} \rightarrow 1\ \mathrm{C_3H_8O_3}$

3. Dark-famine phase

The dark-famine phase occurs in the absence of light and carbon sources. Therefore, microalgae degrade their internal organic carbon-based molecules (i.e., starch and TAG) into acetyl-CoA to obtain the energy they need for catabolic processes. Other more readily biodegradable organic carbon sources, such as glucose and acetate can also be metabolized during this phase. Our study considered the formation of acetyl-CoA from the degradation of TAG or starch. Hence, the dark-famine phase consists of (*d-i*) the degradation of TAG into acetyl-CoA via the beta-oxidation pathway, (*d-ii*) the degradation of POC into acetyl-CoA via glycolysis, (*d-iii*) the pentose- phosphate pathway, (*d-iv*) the Krebs cycle, (*d-v* and *d-vi*) the oxidative phosphorylation of NADH and $FADH_2$, respectively, and (*d-vii*) synthesis of functional biomass having acetyl-CoA as carbon source. Table V summarizes the dark-famine metabolic reactions with the same alteration as the previous sections.

Table V Reactions considered in the metabolic network model under dark-famine phase, where k is the ATP requirement for transfer of storage molecules.

d-i Degradation of TAG	$1\ \mathrm{TAG} + (0.078 + \mathrm{k})\ \mathrm{ATP} \rightarrow 0.490\ \mathrm{Ac-CoA} + 0.02\ \mathrm{CO_2} + 0.471\ \mathrm{NADH} + 0.412\ \mathrm{FADH_2}$
d-ii Degradation of POC	$1\ \mathrm{POC} + (\mathrm{k} - 0.33)\ \mathrm{ATP} \rightarrow 0.333\ \mathrm{Ac-CoA} + 0.333\ \mathrm{CO_2} + 0.667\ \mathrm{NADH}$
d-iii Pentose phosphate pathway	$1\ \mathrm{Ac-CoA} + 1\ \mathrm{ATP} \rightarrow 2\ \mathrm{CO_2} + 3\ \mathrm{NADPH} + 0.5\ \mathrm{NADH} + 0.5\ \mathrm{FADH_2}$
d-iv Krebs cycle	$1\ \mathrm{Ac-CoA} \rightarrow 2\ \mathrm{CO_2} + 3\ \mathrm{NADH} + 1\ \mathrm{FADH_2} + 1\ \mathrm{ATP}$
d-v Oxidative phosphor. NADH	$1\ \mathrm{NADH} + 0.5\ \mathrm{O_2} \rightarrow 1\ \mathrm{ATP}$
d-vi Oxidative phosphor. $FADH_2$	$1\ \mathrm{FADH_2} + 0.5\ \mathrm{O_2} \rightarrow 0.667\ \mathrm{ATP}$
d-vii Synthesis of functional biomass	$0.608\ \mathrm{Ac-CoA} + 0.392\ \mathrm{NADPH} + 0.2\ \mathrm{NH_4^+} + 0.03\ \mathrm{PO_4^{3-}} + 1.724\ \mathrm{ATP} \rightarrow 1\ \mathrm{X_f} + 0.725\ \mathrm{NADH} + 0.216\ \mathrm{CO_2}$

Appendix C – Different trophic modes diagrams under the batch regime (complete version)

Figures I, **II**, **III**, and **IV** provide the complete version of the diagrams of **figure 3.**

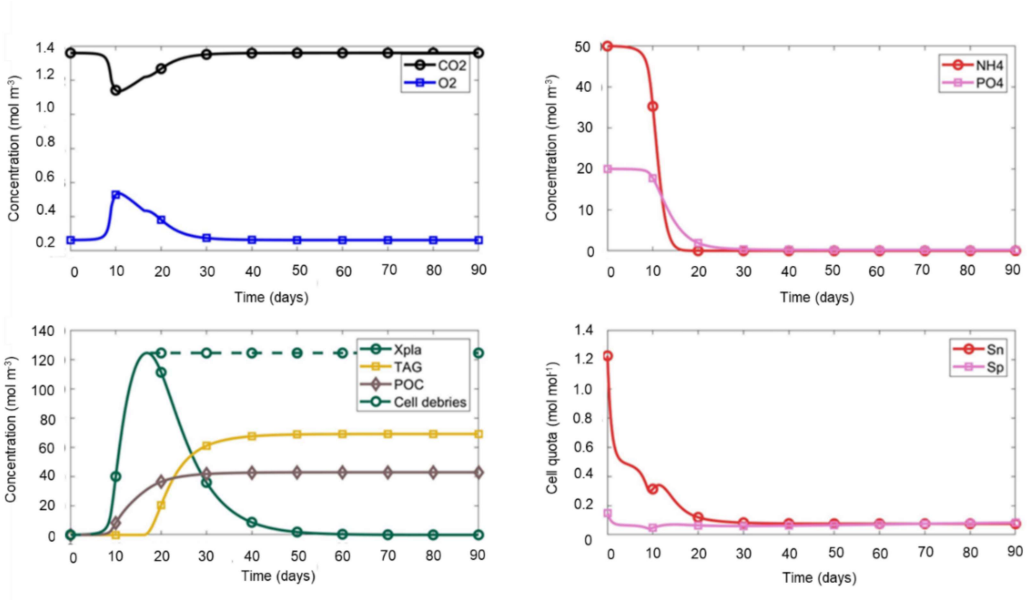


Figure I. Microalgae photoautotrophic growth and other state variables patterns under a batch regime where (●) stands for dissolved CO_2, (■) dissolved O_2, (●) ammonium (NH_4^+), (■) phosphate (PO_4^{3-}) (upper right), (●) functional biomass; (■) TAG; (◆) POC, (●) nitrogen cell quota, and (■) phosphorus cell quota (bottom-right).

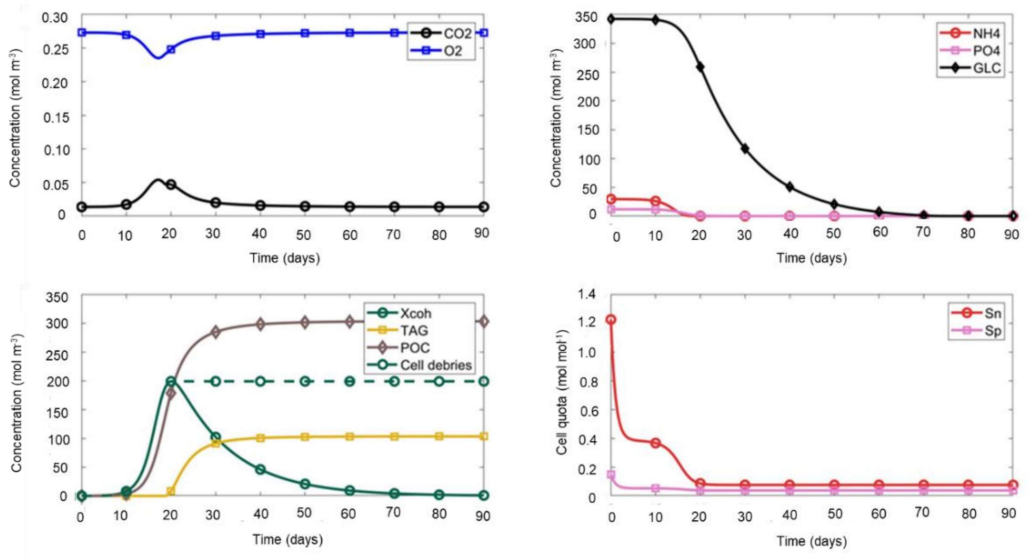


Figure II. Microalgae chemoheterotrophic growth and other state variables patterns under a batch regime where (●) stands for dissolved CO_2, (■) dissolved O_2, (◆) glucose; (●) ammonium (NH_4^+), (■) phosphate (PO_4^{3-}) (upper right), (●) functional biomass, (■) TAG, (◆) POC, (●) nitrogen cell quota, and (■) phosphorus cell quota (bottom-right).

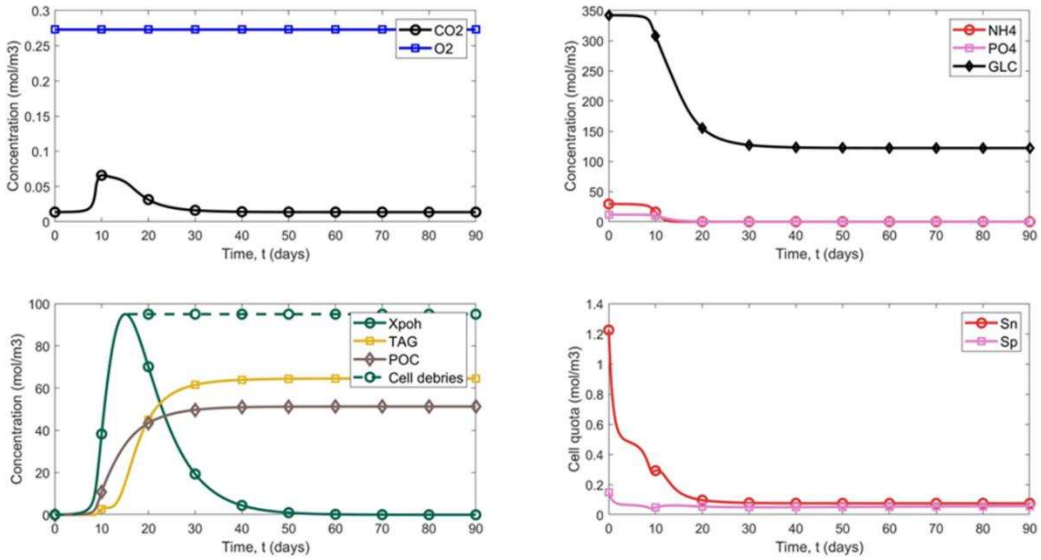


Figure III Microalgae photoheterotrophic growth and other state variables changing patterns under a batch regime where (⊖) sands for dissolved CO_2, (▬) dissolved O_2. Top-Right: conce , (◆) glucose; (⊖) ammonium (NH_4^+), (▬) phosphate (PO_4^{3-}) (upper right), (⊖) functional biomass, (▬) TAG, (◆) POC, (⊖) nitrogen cell quota, and (▬) phosphorus cell quota (bottom-right).

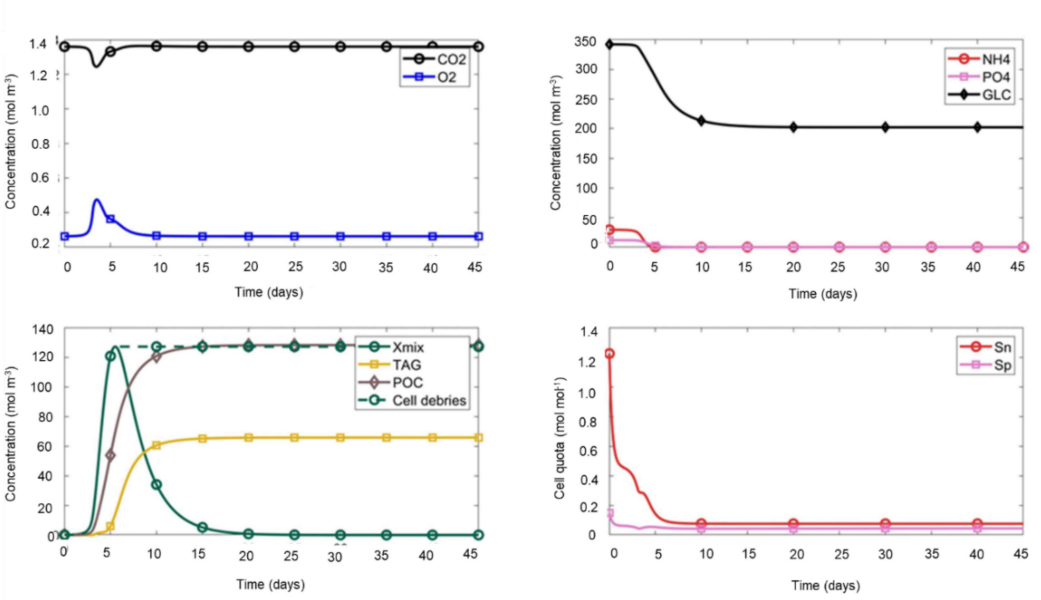


Figure IV Microalgae mixotrophic growth and other state variables changing patterns under a batch regime where (⊖) sands for dissolved CO_2, (▬) dissolved O_2. Top-Right: conce , (◆) glucose; (⊖) ammonium (NH_4^+), (▬) phosphate (PO_4^{3-}) (upper right), (⊖) functional biomass, (▬) TAG, (◆) POC, (⊖) nitrogen cell quota, and (▬) phosphorus cell quota (bottom-right).

Appendix D – Diagrams for mixotrophic microalgae under chemostat regime (complete version)

Figures V, **VI**, **VII**, and **VIII** provide the complete version of the diagrams of **figure 6.**

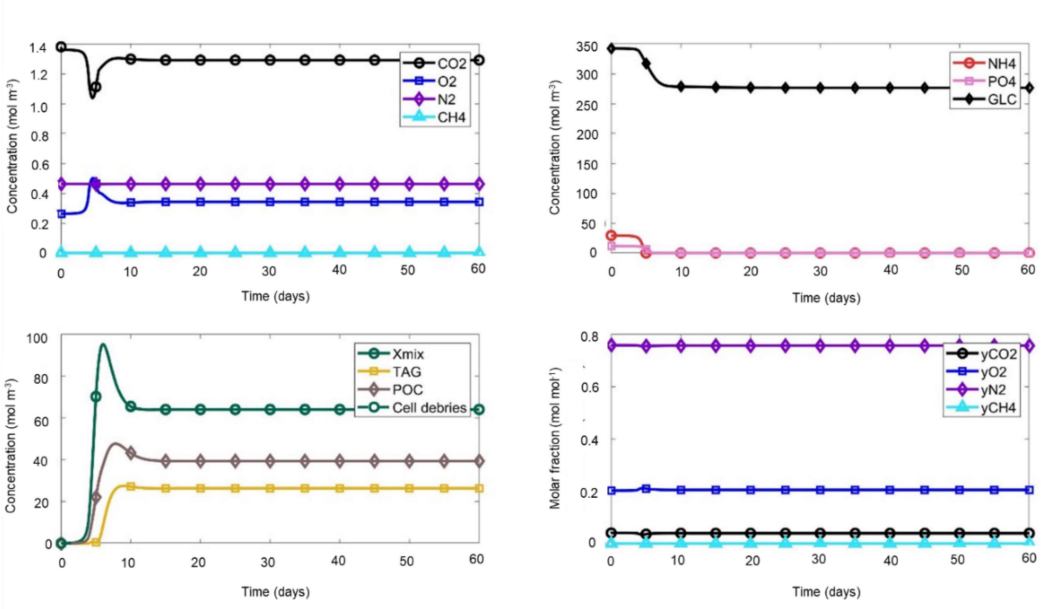


Figure V Microalgae mixotrophic growth and other state variables patterns under chemostat regime for I_{in}= 500 W m^{-2} and D = 0.25 day^{-1}, where (⊖) stands for dissolved CO_2, (⊟) dissolved O_2, (◈) dissolved N_2, (△) dissolved CH_4 (upper-left), (◆) glucose, (⊖) ammonium (NH_4^+), (⊟) phosphate (PO_4^{3-}), (⊖) functional biomass, (⊟) TAG, (◈) POC, (⊖) CO2, (⊟) O_2, (◈) N_2, (△) CH_4 (bottom-right).

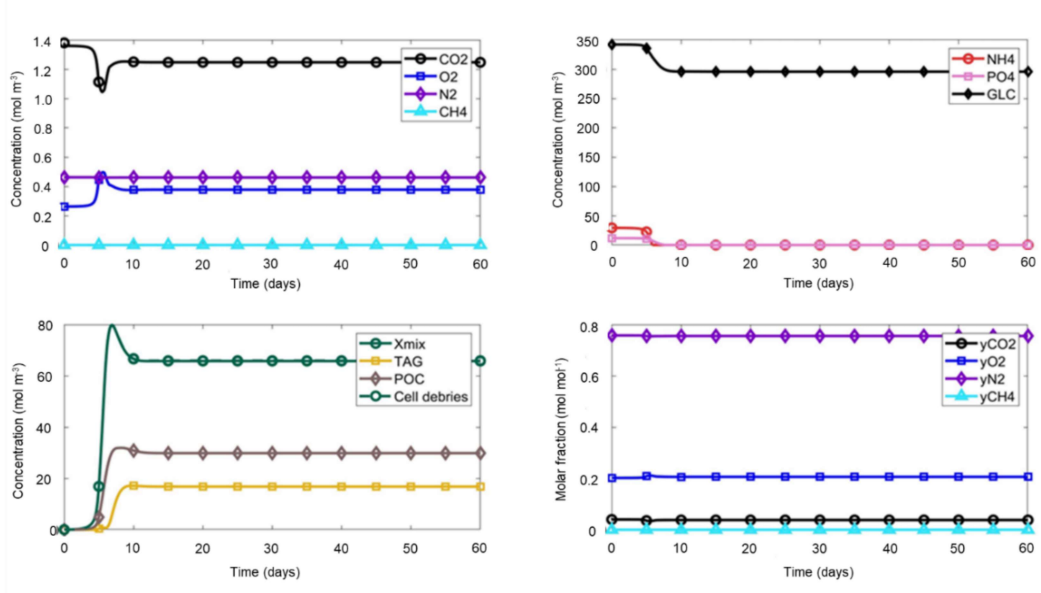


Figure VI. Microalgae mixotrophic growth and other state variables patterns under chemostat regime for I_{in}= 500 W m^{-2} and D = 0.45 day^{-1}, where (⊖) stands for dissolved CO_2, (⊟) dissolved O_2, (◈) dissolved N_2, (△) dissolved CH_4 (upper-left), (◆) glucose, (⊖) ammonium (NH_4^+), (⊟) phosphate (PO_4^{3-}), (⊖) functional biomass, (⊟) TAG, (◈) POC, (⊖) CO2, (⊟) O_2, (◈) N_2, (△) CH_4 (bottom-right).

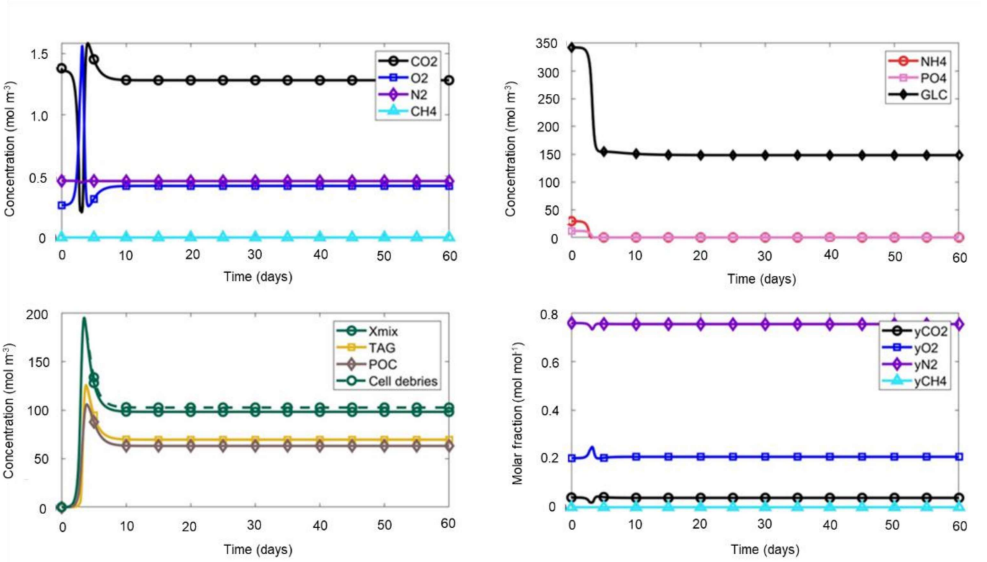


Figure VII Microalgae mixotrophic growth and other state variables patterns under chemostat regime for I_{in}= $I_{in\,(X)}^{optimum}$ W m^{-2} and D = 0.25 day^{-1}, where (⊖) stands for dissolved CO_2, (⊟) dissolved O_2, (◈) dissolved N_2, (△) dissolved CH_4 (upper-left), (◆) glucose, (⊖) ammonium (NH_4^+), (⊟) phosphate (PO_4^{3-}), (⊖) functional biomass, (⊟) TAG, (◈) POC, (⊖) CO2, (⊟) O_2, (◈) N_2, (△) CH_4 (bottom-right).

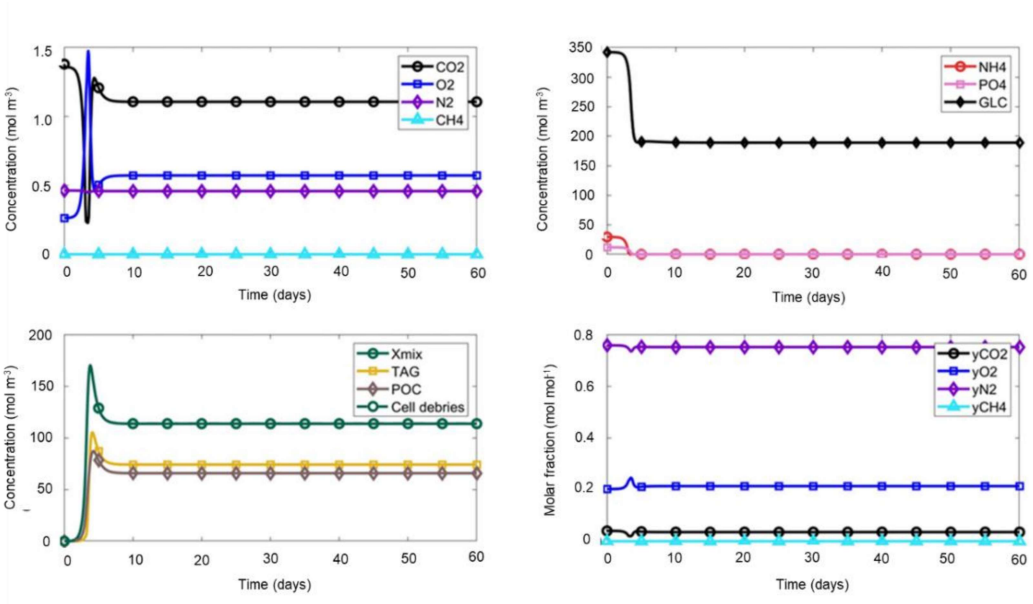


Figure VIII Microalgae mixotrophic growth and other state variables patterns under chemostat regime for I_{in}= $I_{in\,(X)}^{optimum}$ W m^{-2} and D = 0.45 day^{-1}, where (⊖) stands for dissolved CO_2, (⊟) dissolved O_2, (◈) dissolved N_2, (△) dissolved CH_4 (upper-left), (◆) glucose, (⊖) ammonium (NH_4^+), (⊟) phosphate (PO_4^{3-}), (⊖) functional biomass, (⊟) TAG, (◈) POC, (⊖) CO2, (⊟) O_2, (◈) N_2, (△) CH_4 (bottom-right).

Appendix E – Diagrams for non-axenic culture under chemostat regime (complete version)

Figures IX and **X** provide the diagrams referring to **figure 10. Figure XI** shows the diagrams related to **figure 11**, while **figures XII** and **XIII** to **figure 12.**

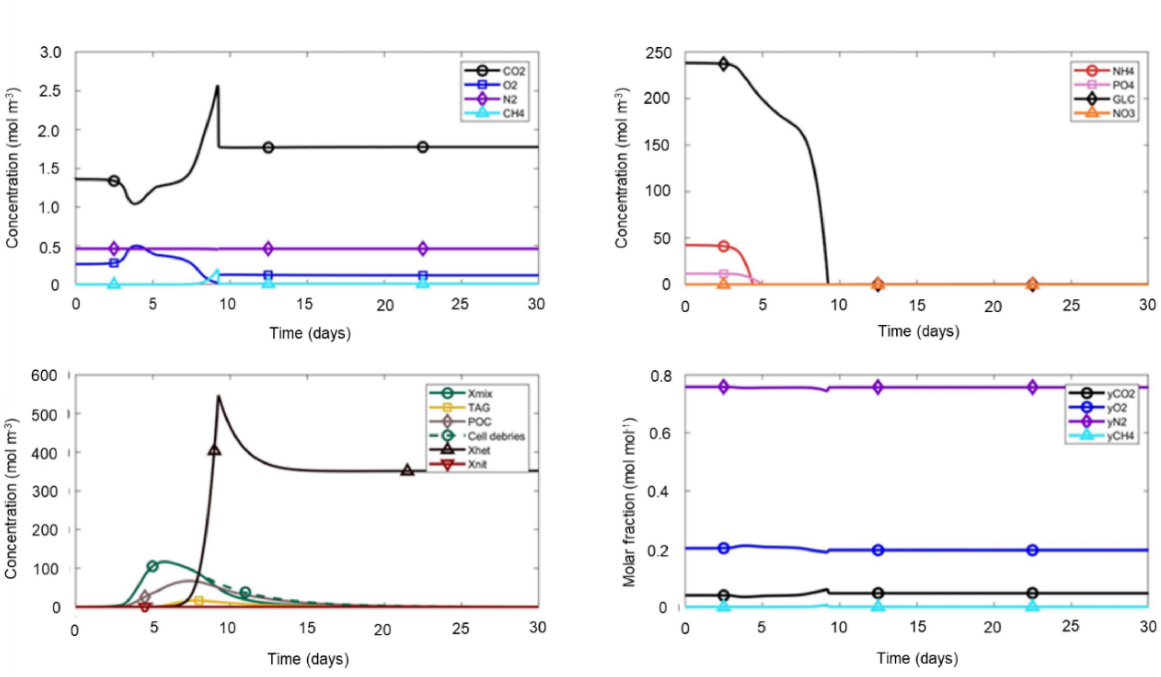


Figure IX Non-axenic culture growth and other state variables patterns, under chemostat regime using PCW as substrate, normal incident light intensity, and dilution rate of I_{in} = 500 W m^{-2} and D = 0.25 day^{-1}, respectively where (⊖) sands for dissolved CO_2, (⊟) dissolved O_2, (◈) dissolved N_2, (△) dissolved CH_4 (upper-left), (◆) glucose, (⊖) ammonium (NH_4^+), (⊟) phosphate (PO_4^{3-}), (△) Nitrate (NO_3^-), (⊖) functional biomass, (⊟) TAG, (◈) POC, (▲) heterotrophs, (▼) nitrifiers, and in the bottom-right the mole fraction of airflow components like (⊖) CO2, (⊟) O_2, (◈) N_2, and (△) CH_4.

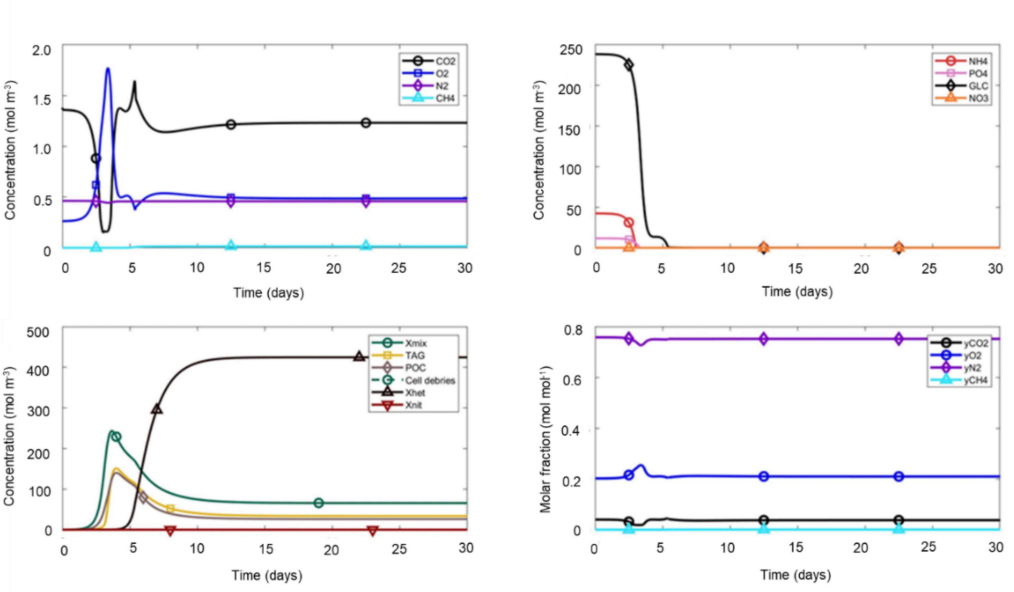


Figure X Non-axenic culture growth and other state variables patterns, under chemostat regime using PCW as substrate, optimal incident light intensity, and dilution rate of I_{in}= $I_{in\,(X)}^{optimum}$ W m^{-2} and D = 0.45 day^{-1}, respectively, where (⊖) sands for dissolved CO_2, (⊟) dissolved O_2, (◈) dissolved N_2, (△) dissolved CH_4 (upper-left), (◆) glucose, (⊖) ammonium (NH_4^+), (⊟) phosphate (PO_4^{3-}), (△) Nitrate (NO_3^-), (⊖) functional biomass, (⊟) TAG, (◈) POC, (▲) heterotrophs, (▼) nitrifiers, and in the bottom-right the mole fraction of airflow components like (⊖) CO2, (⊟) O_2, (◈) N_2, and (△) CH_4.

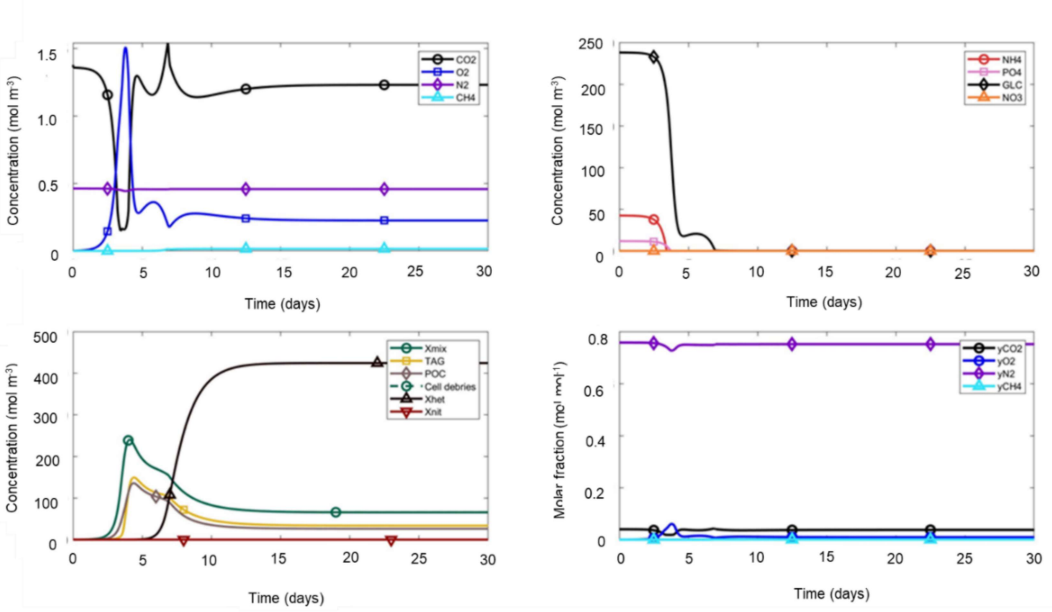


Figure XI Non-axenic culture growth and other state variables patterns, under chemostat regime using PCW as substrate, optimal incident light intensity, and dilution rate of I_{in}= $I_{in\,(X)}^{optimum}$ W m^{-2} and D = 0.45 day^{-1}, respectively, and a and O_2 mole fraction of zero, where (⊖) sands for dissolved CO_2, (⊟) dissolved O_2, (◈) dissolved N_2, (△) dissolved CH_4 (upper-left), (◆) glucose, (⊖) ammonium (NH_4^+), (⊟) phosphate (PO_4^{3-}), (△) Nitrate (NO_3^-), (⊖) functional biomass, (⊟) TAG, (◈) POC, (▲) heterotrophs, (▼) nitrifiers, and in the bottom-right the mole fraction of airflow components like (⊖) CO2, (⊟) O_2, (◈) N_2, and (△) CH_4.

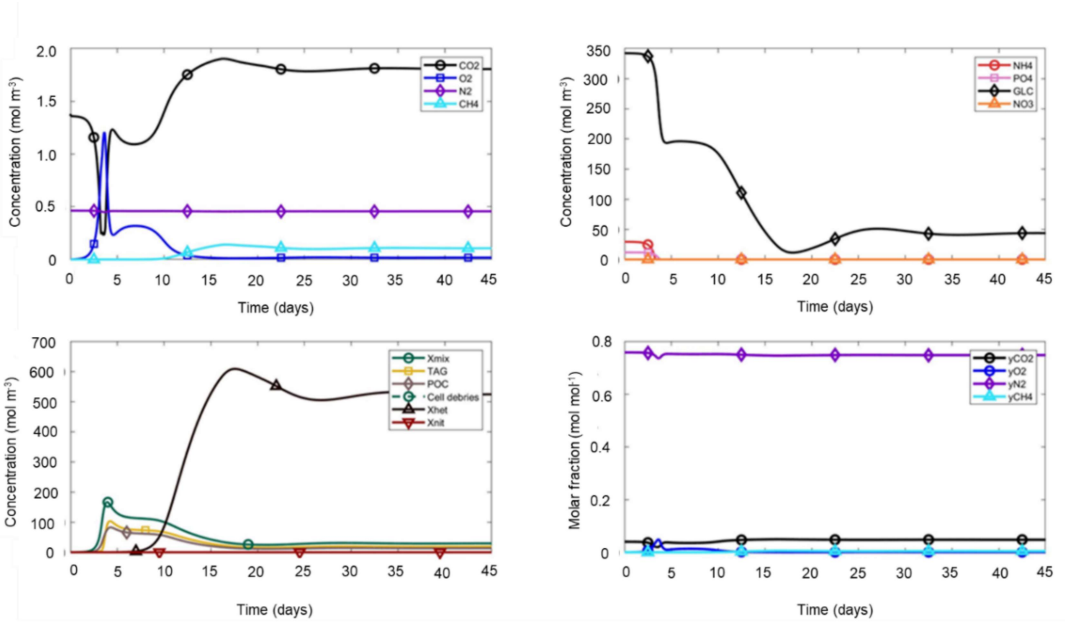


Figure XII. Non-axenic culture growth and other state variables patterns under chemostat regime using RCW as substrate, optimal incident light intensity, and dilution rate of I_{in}= $I_{in\,(X)}^{optimum}$ W m^{-2} and D = 0.45 day^{-1}, respectively, and a and O_2 mole fraction of zero, where (⊖) sands for dissolved CO_2, (⊟) dissolved O_2, (◈) dissolved N_2, (△) dissolved CH_4 (upper-left), (✦) glucose, (⊖) ammonium (NH_4^+), (⊟) phosphate (PO_4^{3-}), (△) Nitrate (NO_3^-), (⊖) functional biomass, (⊟) TAG, (◈) POC, (▲) heterotrophs, (▼) nitrifiers, and in the bottom-right the mole fraction of airflow components like (⊖) CO2, (⊟) O_2, (◈) N_2, and (△) CH_4

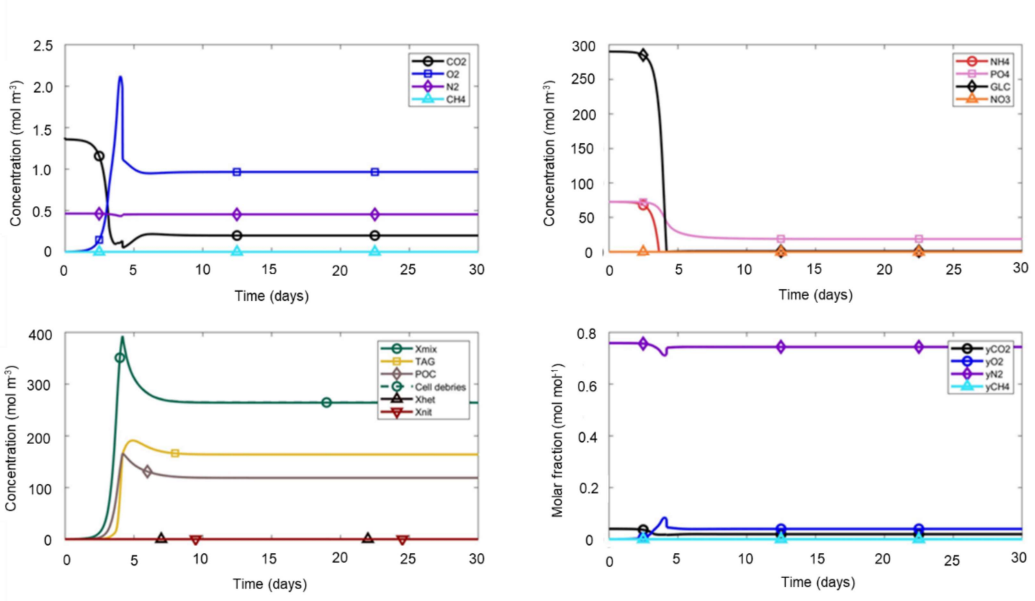


Figure XIII Non-axenic culture growth and other state variables patterns under chemostat regime using MCW as substrate, optimal incident light intensity, and dilution rate of I_{in}= $I_{in\,(X)}^{optimum}$ W m^{-2} and D = 0.45 day^{-1}, respectively, and a and O_2 mole fraction of zero, where (⊖) sands for dissolved CO_2, (⊟) dissolved O_2, (◈) dissolved N_2, (△) dissolved CH_4 (upper-left), (✦) glucose, (⊖) ammonium (NH_4^+), (⊟) phosphate (PO_4^{3-}), (△) Nitrate (NO_3^-), (⊖) functional biomass, (⊟) TAG, (◈) POC, (▲) heterotrophs, (▼) nitrifiers, and in the bottom-right the mole fraction of airflow components like (⊖) CO2, (⊟) O_2, (◈) N_2, and (△) CH_4.

Appendix F – Diagrams for mixotrophic microalgae under light-feast and dark-famine cycles (complete version)

Figures XIV and XV show the complete version of the diagrams in figure 12.

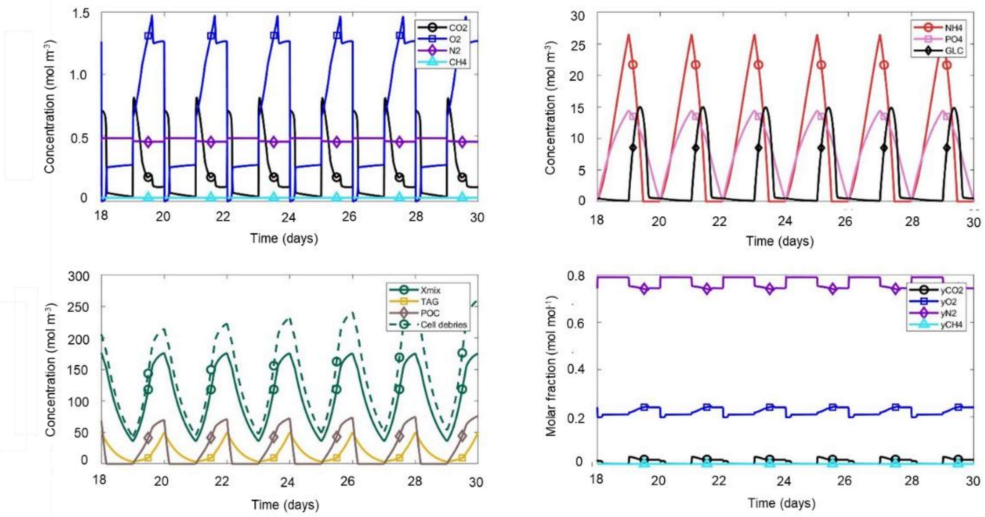


Figure XIV Microalgae mixotrophic growth in a CSTR under 24 hours light-feast and 24 hours dark-famine cycles using PCW as substrate, optimum culture condition (I_{in}= $I_{in\,(X)}^{optimum}$ W m^{-2} and D = 0.45 day^{-1}) over 12 days , where. (⊖) sands for dissolved CO_2, (▭) dissolved O_2, (◈) dissolved N_2, (△) dissolved CH_4 (upper-left), (◆) glucose, (⊖) ammonium (NH_4^+), (▭) phosphate (PO_4^{3-}), (△) Nitrate (NO_3^-), (⊖) functional biomass, (▭) TAG, (◈) POC, (▲) heterotrophs, (▼) nitrifiers, and in the bottom-right the mole fraction of airflow components like (⊖) CO2, (▭) O_2, (◈) N_2, and (△) CH_4.

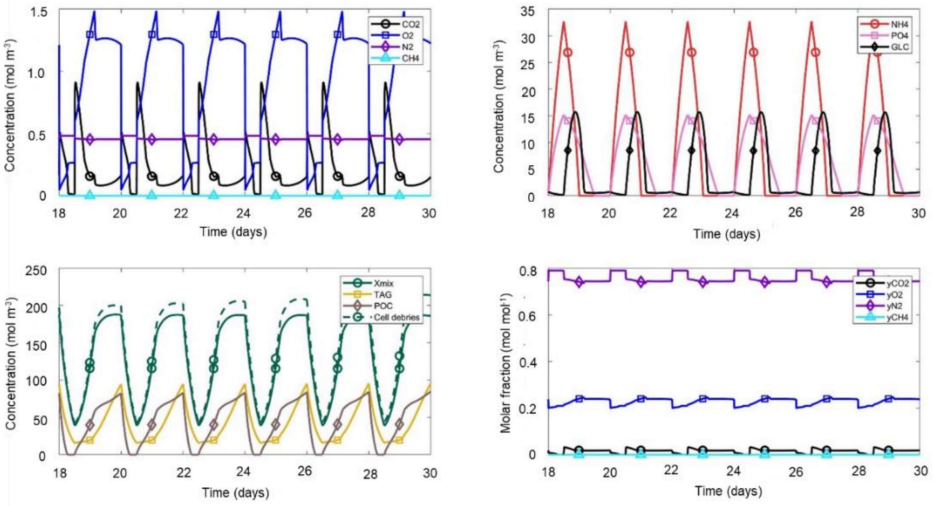


Figure XV Microalgae mixotrophic growth in a CSTR under 36 hours light-feast and 12 hours dark-famine cycles using PCW as substrate, optimum culture condition (I_{in}= $I_{in\,(X)}^{optimum}$ W m^{-2} and D = 0.45 day^{-1}) over 12 days, where. (⊖) sands for dissolved CO_2, (▭) dissolved O_2, (◈) dissolved N_2, (△) dissolved CH_4 (upper-left), (◆) glucose, (⊖) ammonium (NH_4^+), (▭) phosphate (PO_4^{3-}), (△) Nitrate (NO_3^-), (⊖) functional biomass, (▭) TAG, (◈) POC, (▲) heterotrophs, (▼) nitrifiers, and in the bottom-right the mole fraction of airflow components like (⊖) CO2, (▭) O_2, (◈) N_2, and (△) CH_4.

Appendix G – Diagrams for non-axenic culture under light-feast and dark-famine cycles

Figures XVI and **XVII** provide the complete version of **figures 14** and **15**, respectively.

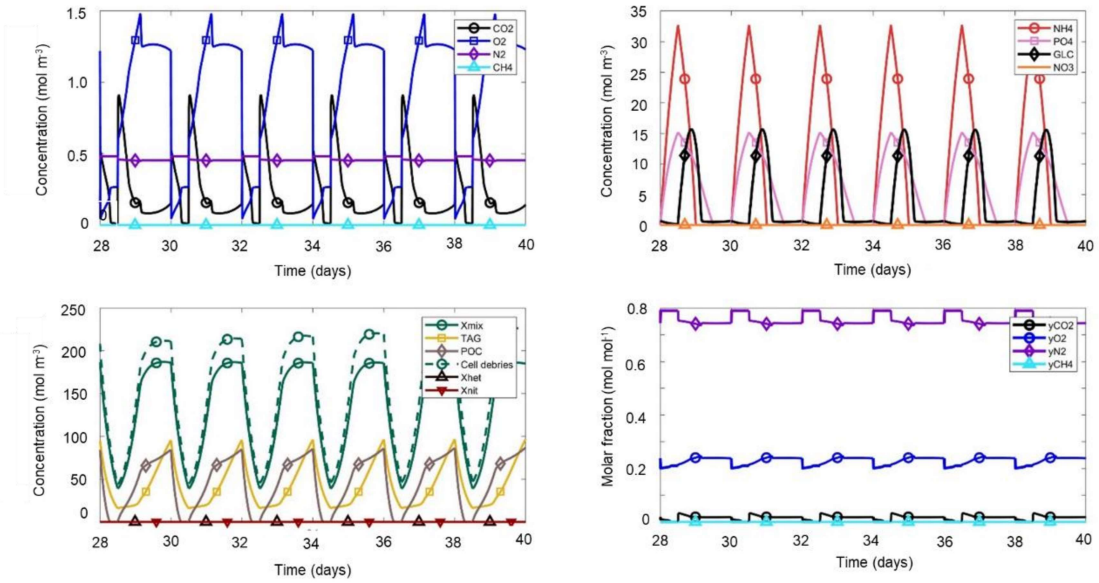


Figure XVI Non-axenic microalgae culture growth in a CSTR under 36 hours light-feast and 12 hours dark-famine cycles using PCW as substrate, optimum culture condition (I_{in}= $I_{in\,(X)}^{optimum}$ W m^{-2} and D^{light}= 0.45 day^{-1}, and D^{dark} = 3 day $^{-1}$) over 12 days, where. (⊖) sands for dissolved CO_2, (⊟) dissolved O_2, (◈) dissolved N_2, (△) dissolved CH_4 (upper-left), (◆) glucose, (⊖) ammonium (NH_4^+), (⊟) phosphate (PO_4^{3-}), (△) Nitrate (NO_3^-), (⊖) functional biomass, (⊟) TAG, (◈) POC, (▲) heterotrophs, (▼) nitrifiers, and in the bottom-right the mole fraction of airflow components like (⊖) CO2, (⊟) O_2, (◈) N_2, and (△) CH_4.

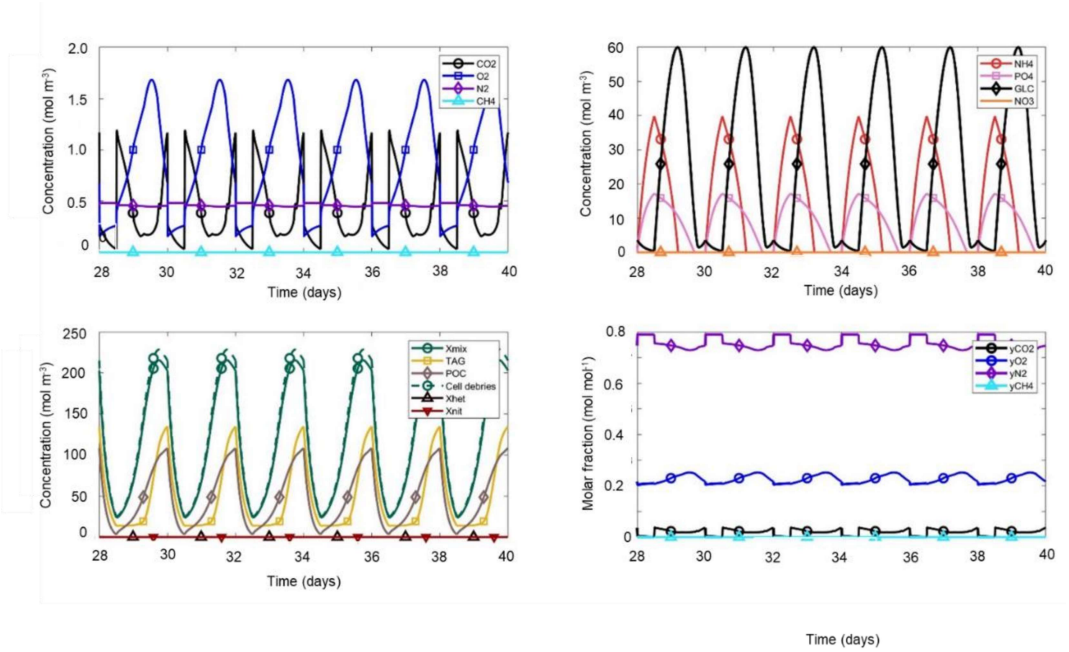


Figure XVII Non-axenic microalgae culture growth in a CSTR under 36 hours light-feast and 12 hours dark-famine cycles using RCW as substrate, optimum culture condition (I_{in}= $I_{in\,(X)}^{optimum}$ W m^{-2} and D^{light}= 0.45 day^{-1}, and D^{dark} = 3 day^{-1}) over 12 days, where. (—●—) sands for dissolved CO_2, (—■—) dissolved O_2, (—◆—) dissolved N_2, (—▲—) dissolved CH_4 (upper-left), (—◆—) glucose, (—●—) ammonium (NH_4^+), (—■—) phosphate (PO_4^{3-}), (—▲—) Nitrate (NO_3^-), (—●—) functional biomass, (—■—) TAG, (—◆—) POC, (—▲—) heterotrophs, (—▼—) nitrifiers, and in the bottom-right the mole fraction of airflow components like (—●—) CO2, (—■—) O_2, (—◆—) N_2, and (—▲—) CH_4.

Appendix H – TAG average productivity under the semi-steady-state condition

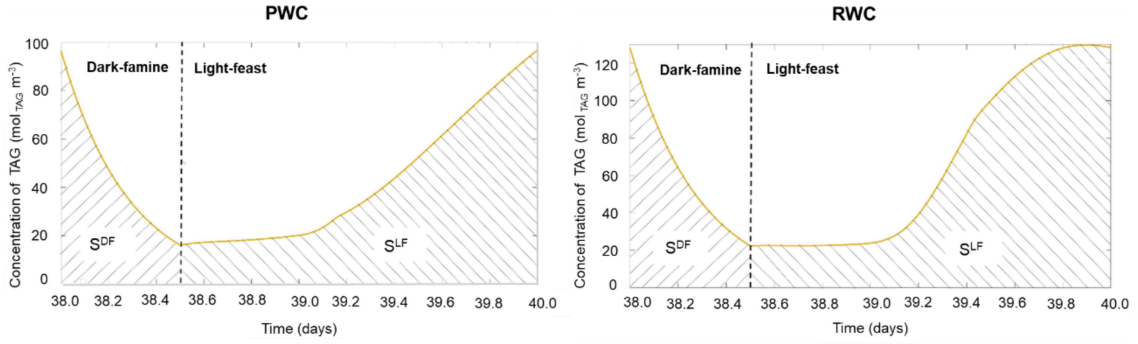


Figure XVIII TAG concentration profile over one cycle period (2 days) for Non-axenic culture grown under CSTR regime, a 36 hours light-feast and 12 hours dark-famine cycles, and optimum culture condition (I_{in}= $I_{in\,(X)}^{optimum}$ W/m^2 and D^{light} = 0.45 day^{-1}, and D^{dark}= 3 day^{-1}and 4 day^{-1} for PCW and RCW, respectively) over a period of 2 days. The area below the curve estimates the average TAG concentration and productivity in a fluctuating system.

The equation I calculates TAG productivity under the chemostat regime.

$$P_{TAG\,(t)} = \frac{C_{TAG\,(t)}^{LF} \times F_L^{LF} + C_{TAG\,(t)}^{DF} \times F_L^{DF}}{V_R} \left[\frac{mol}{m^3.day}\right] \quad \text{(Eq. I)}$$

where LF and DF stands for light-feast and dark-famine phases, respectively. The average TAG productivity was then calculated by integrating the TAG productivity over time as **equation II**.

$$\overline{P_{TAG}} = \frac{\int P_{TAG\,(t)}.dt}{\int dt} = \frac{\int\left(\frac{C_{TAG\,(t)}^{LF} \times F_L^{LF} + C_{TAG\,(t)}^{DF} \times F_L^{DF}}{V_R}\right).dt}{\int dt}$$

$$\overline{P_{TAG}} = \frac{\int C_{TAG\,(t)}^{LF}.F_L^{LF}.dt + \int C_{TAG\,(t)}^{DF}.F_L^{DF}.dt}{V_R.\int dt} = \frac{F_L^{LF} \times \int C_{TAG\,(t)}^{LF}.dt + F_L^{DF} \times \int C_{TAG\,(t)}^{DF}.dt}{V_R.\int dt}$$

$$\overline{P_{TAG}} = \frac{D^{LF} \times S^{LF} + D^{DF} \times S^{DF}}{\Delta t} \quad \text{(Eq. II)}$$

where S is the area below the curve and D is dilution rate. The average TAG productivity for both RCW and PCW-fed systems was calculated using **equation II**.

$$\overline{P_{TAG}^{RCW}} = \frac{0.45 \times 99.2 + 4.0 \times 30.4}{2} = 83.1 \left[\frac{mol}{m^3.day}\right]$$

$$\overline{P_{TAG}^{PCW}} = \frac{0.45 \times 63.5 + 3.0 \times 22.5}{2} = 48.0 \left[\frac{mol}{m^3.day}\right]$$

6. Discussion

1 Discussion

Understanding the symbiotic relationships between microalgae and bacteria is important not only to prevent eutrophication processes but to valorize agro-industrial wastes that are not entirely absorbed by industry, such as cheese whey residuals. The dairy by-products can be efficiently valorized by coupling acidogenic fermentation to solubilize the organic materials and produce fermentation products like volatile fatty acids (VFAs) and photoorganoheterotrophy (or photomixotrophy) to concentrate the organics and the nitrogen and phosphorus nutrients by producing microalgae biomass. This can contribute to transitioning the dairy sector into the circular economy while safeguarding the environment by preventing the direct release of dairy residuals into surface water.

This discussion chapter delves into the main findings obtained from the research **chapters 2** to **5** of the thesis. The chapters investigated the: (*i*) valorization potential of cheese whey, the issues hindering it, and different scenarios for this valorization; (*ii*) acidogenic fermentation of cheese whey for the production of fermentation products of added value (i.e., VFAs and ethanol); (*iii*) use of cheese whey organic substrates and derivatives (e.g., lactose, acetate) as carbon sources and electron donors for microalgae biomass growth in batch and continuous mixed cultures; and (*iv*) a mathematical model to enhance the selection of microalgal biomass and production of triacylglycerides (TAGs) in mixed cultures using cheese whey by-products and derivatives as substrates.

1.1 One size does not fit all: The implementation of a cheese whey biorefinery according to a location's specific needs and updated information on whey production …

Cheese whey residuals, about 66.5 M m^{-3} $year^{-1}$, pose an environmental threat when not properly managed and directly discharged into the aquatic ecosystem. Technologies for treatment and resource recovery are available to treat and repurpose cheese whey into additional added-value by-products (Tsakali et al., 2010; USDA, 2022). Hence, **chapter 2** assessed the full valorization potential of cheese whey. Success cases have been demonstrated internationally for repurposing 94.15 M m^{-3} $year^{-1}$ of cheese whey into whey powder concentrate (WPC), isolate (WPI) and

hydrolysate (WPH), galactooligosaccharides (GOS), caseins and caseinates, probiotics, and prebiotics, of pharmaceutical, nutraceutical, food, and animal feed industries interests (Božanić et al., 2014; Dinika & Utama, 2019; Gillies, 1974; Ibrahim, 2018; Ko & Kwak, 2009; Lappa et al., 2019; Onwulata & Huth, 2008; Tsakali et al., 2010; USDA, 2022; Zheng et al., 2019). Information sharing and access are very important to transfer technologies to regions around the globe where the dairy industry is active.

From an industrial ecology perspective, it is currently difficult to accurately estimate the real dimension of cheese whey impacts and the current extent of reuse pathways. Data need to be updated and made accessible on the production and composition of cheese whey residuals around the world. Externalities need to get internalized (Eidelwein et al., 2018). Better insights should be gained from dairy practice at regional levels on: (*i*) how many dairy farms and cooperatives are active, (*ii*) what are their total production of cheese whey, and (*iii*) how they handle the cheese whey residuals. Despite the availability of technologies for cheese whey treatment and recovery, national and regional actions should be developed to better manage cheese whey and dairy residuals.

The geographic location of producers, desuetude laws, limited access to information, and lack of or limited R&D for processing the cheese whey currently not absorbed by the industry are hindrances to cheese whey management that must be addressed (Kemp-Benedict, 2015; Lammifyad, 2020). The study highlighted the need for the implementation of tools such as stakeholder analysis and decision analysis (Brugha & Varvasovszky, 2000; Kiker et al., 2005). The stakeholder analysis will identify the different parties that must be involved in the decision-making process (Brugha & Varvasovszky, 2000) while decision analysis tools account for factors (e.g., economic, environmental, and socio-political) that will select the relevant criteria to address these issues and promote the valorization of cheese whey (Kiker et al., 2005) such as improving technology availability, developing more effective legislation, and forging partnerships between producers, industries, and governments.

Technologically, the envisioned scenario for the management and valorization of cheese whey surpluses involves anaerobic digestion or acidogenic fermentation (*i.e.*, digestion without biogas production) coupled with the photoorganoheterotrophic production of a microalgae biomass rich in organics and nutrients. By implementing a

closed-loop system, the organic matter and nutrients in whey can be repurposed by producing either biogas (as a source of biofuel, electricity, or heat) or VFAs that can be used as bulk chemicals, as templates for chain elongation into hexanoate or octanoate biofuels, or as a substrate for the mixotrophic production of microalgae biomass. These different valorization pathways are attractive for the industry and the circular economy (González-Fernández et al., 2016; Kleerebezem et al., 2015; Lagoa-Costa et al., 2020; Pais-Chanfrau et al., 2020).

Besides the organic fraction, phosphorus and nitrogen can be recovered from the digestate to produce a fertilizer (Lee et al., 2014). Mixotrophic microalgae are further an attractive alternative since able to concentrate simultaneously C, P, and N by assimilation, resulting in biomass rich in lipids and nutrients that can act both as biofuels and fertilizers, respectively.

The biorefinery concept developed in this thesis can help address the environmental issues linked to cheese whey management while presenting an attractive alternative for resource biorecovery. Valorization scenarios should be made adaptable to the needs and resources available in a specific location.

1.2 Selective pressure steers acidogenic fermentation to direct the product spectrum

Chapter 3 demonstrated the feasibility of acidogenic fermentation for recovering VFAs and alcohol from high-strength organic waste streams like cheese whey (i.e., 50 to 80 g O2 L-1, in terms of chemical oxygen demand (COD)) (Saddoud et al., 2007). The study identified that the abiotic factors such as inoculum pre-treatment (thermal or alkaline), headspace pressure, initial pH, and food-to-microorganism (F/M) ratio acted as selective pressures influencing the adaptation and metabolism of fermentative microorganisms within the microbial community. Generating a selective environment is the key to directed outputs in microbial community engineering (Kleerebezem & van Loosdrecht, 2007). The role of factors that can be used as selective pressures must be adapted according to the desired process outputs. Here, the goal was to select a fermentative microbial community that was capable to produce high levels of VFAs from cheese whey in batches.

The implementation of **thermal inoculum pre-treatment** was validated as a method to efficiently halt methanogenesis in the short term in batch reactors (Mockaitis

et al., 2020). Inoculum thermal pre-treatment efficiently halted methanogenesis, regardless of the presence of the other selective pressure parameters in the system, making it a useful tool for cheese whey acidogenic fermentation. Unlike other works in the literature (López-Torres & Llórens, 2016), inoculum alkaline pre-treatment did not favor methanogenesis given the different variables used.

In both the control and thermally treated batches, 16S rRNA gene amplicon sequencing identified the presence of DNA residues of **acetoclastic methanogen *Methanosaeta*** in the microbial community despite the absence of methane production. It is presumed that thermal pre-treatment temporarily inactivated these microorganisms and did not suppress them *per se*. Further research is needed to investigate the long-term effect of a thermal pre-treatment on the out-selection of methanogens, or whether additional measures are needed to effectively suppress them. This can for instance involve the application of a relatively short hydraulic retention time (HRT) of 5.5 (Hernández-Mendoza & Buitrón, 2014)to 12 hours (Yun & Cho, 2017).

The **headspace pressure** impacted the metabolic pathways of alcohol and VFA productions in acidogenic fermentation. Compared to pressurized batches, the non-pressurized headspace batches (*i.e.*, by emptying the bottle's headspace) presented a higher production of VFAs. More specifically, non-pressurized batches operated at an initial alkaline pH of 9.0 batches resulted in the production of acetate (1.4 g COD_{AcOH} L^{-1}), iso-butyric acid (7.7 g COD_{IBA} L^{-1}), and ethanol (13.7 g COD_{EtOH} L^{-1}) from 4 g COD L^{-1} of cheese whey used as substrate.

A high yield in VFA production from cheese whey (3,317.88 mg $COD_{compound}$ L^{-1}) was achieved using a **lower F/M ratio** of 0.5 g COD g^{-1} VS compared to 2,155.53 mg $COD_{compound}$ L^{-1} in an F/M ratio of 1.0 g COD g^{-1} VS and 1,165.08 mg $COD_{compound}$ L^{-1} in 4. Interestingly, an F/M ratio of 2.0 g COD g^{-1} VS produced 4,211.46 mg $COD_{compound}$ L^{-1} consisting mainly of caproic (i.e., 3,620.88 mg COD_{CA} L^{-1}) and acetic acid (i.e., 493.42 mg COD_{AcOH} L^{-1}).

The **initial pH of the medium** significantly impacted the number of products present in the fermentation spectrum. Regardless of the headspace pressure and inoculum pre-treatment, a high initial pH of 9.0 increased the VFA and alcohol production rates with 21,360.54 mg$COD_{compound}$ L^{-1} (i.e., 7,677.30 mg COD_{IBA} L^{-1} and 13,683.24 mg COD_{EtOH} L^{-1}). The redox potential was influenced by the uncontrolled

pH, enabling the uptake of compounds while providing the basis for the ecologic relationships within the microbial ecosystem.

Selective pressure mechanisms such as inoculum pre-treatment, headspace pressure, initial pH, and F/M ratio are therefore effective tools to tailor batch processes for the AF of cheese whey. Inhibiting methanogenesis could improve the production of VFAs and alcohols of industrial interest.

1.3 Acetate is a viable organic carbon source and electron donor for microalgal biomass production by mixotrophy non-axenic mixed cultures

VFAs like acetate produced by AF can further be utilized as organic carbon sources and electron donors for different biological processes such as photoorganoheterotrophic microalgal biomass growth while acetate, iso-butyric, and ethanol are commonly used in the feed, pharmaceutical, chemical, and biofuel industries. **Chapter 4** aimed at understanding the ecological engineering of green photoorganoheterotrophic or photomixotrophic mixed cultures to valorize either directly cheese whey (lactose) or the VFAs produced by AF of cheese whey.

While photolithoautotrophs produce their biomass by fixing CO_2 (*i.e.*, fully oxidized carbon, γ_{CO2} = 0 mol e^- C-mol^{-1}), photoorganotrophs and photomixotrophs have a unique capability to start their biosynthesis from organic compounds with a degree of reduction ($\gamma_{acetate}$ = 4 mol e^- C-mol^{-1}) close to biomass ($\gamma_{acetate}$ = 4.2 mol e^- C-mol^{-1}), using light to energize the electrons present in the substrate. While photoorganoheterotrophs, like green and purple non-sulfur bacteria (Alloul et al., 2020; Cerruti et al., 2020; Mas, 1995), are anoxygenic primarily using the organic substrate as e-donor and C-source, photomixotrophs can be oxygenic microorganisms (like cyanobacteria or eukaryotic microalgae) that primarily fix CO_2 for photosynthesis but can also use an organic compound for maximizing their growth.

This study identified the best reactor regimes and conditions for the uptake of organic substrates (raw cheese whey, lactose, acetate) and the selection of green anoxygenic photoorganoheterotrophs or oxygenic photomixotrophs. An additional goal was to understand the competitive and symbiotic relationship between phototrophs and chemotrophs in the mixed culture and in future works, their impact on process efficiency.

A microalgal mixed culture (i.e., cyanobacteria and eukaryotic microalgae) able to capture organics was successfully selected and grown out of an inoculum collected from a surface water channel. An enrichment was first produced by photolithoautotrophic cultivation supplying bicarbonate in the medium. The biomass concentration and pigment contents were directly proportional in the microalgae mixed culture. Although the nitrogen source was changed from nitrate to ammonium, denitrifiers were able to metabolize the available nitrogen source, suggesting that the dissolved oxygen within the medium acted as an electron acceptor.

As one of the main products of cheese whey fermentation, acetate was a favorable organic carbon source and electron donor for the photoorganoheterotrophic growth of the microalgae biomass. Compared to other organic carbon sources derived from cheese whey such as raw demineralized cheese whey (WPC40) and lactose, acetate was the best organic source leading to a maximum growth rate of 0.25 d^{-1} and microalgae biomass productivity of 170 mg VSS d^{-1}. The values presented by both WPC40 and lactose could be due to the presence of inorganic matter.

A green phototrophic mixed culture was further successfully selected in a chemostat fed with acetate, leading to a biomass concentration of 125 mg L^{-1} and biomass production of 45 mg VSS d^{-1} at a steady state. A relatively low dilution rate of 0.17 d^{-1} helped to retain microalgae in the system and prevent their out-competition by ordinary heterotrophic organisms (OHOs).

In this chemostat flushed with argon gas to prevent the introduction of exogenous oxygen, aerobic chemoorganoheterotrophs could develop on acetate by using the oxygen produced by the microalgae. Thus, a certain fraction of the organic substrate gets dissimilated by the OHOs, potentially affecting the yield of phototrophic biomass production. Future research could examine the pros and cons of selecting anoxygenic photoorganoheterotrophs *vs.* oxygenic photomixotrophs for carbon and nutrient capture efficiency. Beyond the interesting symbiotic relationship between microalgae and OHOs, being able to out-select OHOs is an important target for process efficiency.

Regarding the microalgal population, 16S rRNA gene amplicon sequencing confirmed that 10-20% of prokaryotic population was composed of Cyanobium PCC-6307 sp. and Synechocystis PCC-6803 sp.. In the 18S rRNA gene amplicon sequencing, eukaryotic microalgae (i.e., Scenedesmus sp., Desmodesmus sp., and

Trebouxioupheceae) found in the initial culture decreased while unidentified Chlorophyceae in the final culture increased.

1.4 A microalgal mixed culture rich in triacylglycerides can be successfully produced by mixotrophy using cheese whey and VFAs

The competition between mixotrophic microalgae and OHOs was finally examined by developing a predictive mathematical model. This model accounted for not only microalgal selection but also for their propensity to accumulate lipids like triacylglycerides (TAGs).

The model combined theoretical knowledge of microalgae growth and incorporated factors such as light cycle and intensity, nutrient availability, and dilution rate in continuous cultures. The model considered different trophic modes photoautotrophic, photoheterotrophic, chemoautotrophic, and mixotrophic, in axenic and non-axenic cultures, as well as in different reactor configurations such as in batch and continuous stirred-tank reactors (CSTR). The influence of light/dark combined to feast/famine regimes (*i.e.*, light-feast and dark-famine cycles) was also investigated on microbial selection and TAG production.

Shorter growth cycles, longer light-feast and shorter dark-famine cycles (36:12 h), higher dilution rate, and optimized light intensity were parameters that hampered competition between OHOs and microalgae in non-axenic cultures during mixotrophy. Microalgal growth by mixotrophy led to higher production of biomass of 127.2 mol X_f m^{-3} and TAG content of 65.8 mol TAG m^{-3} in the shortest cycle (20 days) compared to other trophic modes (i.e., photoautotrophy 124.4 mol X_f m^{-3} in 58 days and 69.0 mol TAG m^{-3}, chemoautotrophy 198.9 mol X_f m^{-3} and 103.3 mol TAG m^{-3} in 80 days, and photoheterotrophy 95.0 mol X_f m^{-3} and 64.5 mol TAG m^{-3} in 55 days), given that both organic and inorganic carbon sources are metabolized during mixotrophy. According to the model, TAG productivity is improved in chemostat with a higher dilution rate (D= 0.45 day^{-1}) compared to 0.25 day^{-1} and adjusted light intensity (I_{in}= $I_{in\,(X)}^{optimum}$ W m^{-2}) compared to I_{in}= 500 Wm^{-2}. The light is not at a constant value but it varies according to the culture's cell density. Moreover, longer light-feast and shorter dark-famine cycles (36:12 h) were able to increase the production of TAG (VALUE!) compared to light-feast 24:24 h cycles (VALUE!).

According to the model, both cheese whey (i.e., 132.4 mol X_f m^{-3} and 64.8 mol TAG m^{-3}) and the VFAs resulting from cheese whey acidogenic fermentation (i.e., 129.0 mol X_f m^{-3} and 43.0 mol TAG m^{-3}) are suitable substrates for microalgae biomass, and TAG production considering the aforementioned parameters.

1.5 Take home message

In coupled acidogenic fermentation and photoorganoheterotrophic processes, a series of ecological relationships occur within the microbial community. Oftentimes, microorganisms compete for substrates and their adaptability to imposed selective pressures (e.g., temperature, pH, pressure, light, physical and chemical pre-treatments, hydraulic retention time, and dilution rate) will dictate the metabolic route and consequently, their thriving.

However, microorganisms such as bacteria and microalgae (i.e., cyanobacteria and green microalgae) can also coexist in symbiotic relationships. The metabolites produced by bacteria in dark fermentation can serve as an organic carbon source for mixotrophic microalgae. Therefore, the acidogenic fermentation process can be tailored for specific product recovery.

The work demonstrated the role of different selective pressures directing the fermentation process towards the production of VFAs and microalgal biomass, as well as the inhibition of methanogenesis. The biorecovery of volatile fatty acids and alcohol of industrial interest from cheese whey can further valorize the surplus which is currently not absorbed by the industry or is used as fertilizer and animal feed, thus contributing to the full transition of the dairy industry to a circular economy.

7. Conclusion and Outlook

1 Conclusion

The main goal of the thesis was to understand the symbiotic relationships between microalgae and bacteria during coupled acidogenic fermentation and photoorganoheterotrophic processes for cheese whey valorization. In nature, these processes are part of eutrophication, posing dire consequences for the environment. This work provides the following take-home messages:

1. **As high as 66.5 million m^3 y^{-1} of residual cheese whey** need to be treated and can be upgraded in a closed-loop biorefinery value chain, although technologies are available for valorizing cheese whey and its derivatives in food, medical, and nutrition industries. Such a biorefinery concept can contribute to reduce environmental impacts linked to the management of cheese whey residuals. It simultaneously presents an attractive economic alternative for resource biorecovery, reinjecting carbon and nutrient feedstocks in the circular economy.
2. **Acidogenic fermentation** is central to solubilize cheese whey and other residual substrates of the food industry. Fermentation products like volatile fatty acids can then be efficiently captured together with residual nitrogen and phosphorus nutrients by producing nutrient-rich microalgal biomass. Selecting photoorganoheterotrophic microorganisms in mixed culture is an advantage for maximizing the yield of carbon and nutrient capture. These organisms can efficiently assimilate organic compounds (with a degree of reduction close to biomass) by energizing electrons with light and minimizing carbon dissipation.
3. **Selective pressures** such as inoculum pre-treatment, headspace gas pressure, initial pH, and food-to-microorganism (F/M) ratio are effective tools to tailor the product spectrum by acidogenic fermentation. These factors influence the metabolic adaptability of microorganisms in a selective environment and direct their fermentation pathways.
4. **Inhibiting methanogenesis** is an important endpoint in the mixed-culture fermentation process to prevent the dissipation of organics such as methane. In batch reactor regimes, thermal pre-treatment of the inoculum could improve the production of VFAs and alcohol of industrial interests. In a continuous-flow

reactor, combining it with the management of the sludge retention time will be necessary to prevent the growth of slow-growing methanogens.

5. **Green photomixotrophs** (i.e., Cyanobium PCC-6307 sp. and Synechocystis PCC-6803 sp., *Scenedesmus* sp.*, Desmodesmus* sp.*,* Trebouxioupheceae, and some unidentified Chlorophyceae) were successfully selected on a synthetic organic feed mimicking a pre-fermented feedstock rich in volatile fatty acids (using acetate as model compound) in a chemostat operated at a low dilution rate (0.17 d^{-1}) avoiding their wash-out or being outcompeted by ordinary chemoorganoheterotrophic organisms. Nitrification of the ammonium nitrogen source into nitrite and nitrate was detected to some extent in the mixed culture, suggesting that dissolved oxygen was present in the system. Given that argon gas was sparged to prevent the inlet of exogenous O_2 in the photobioreactor, it demonstrated that oxygenic photomixotrophic microorganisms (with capabilities to capture both CO_2 and organics, instead of solely anoxygenic photoorganoheterotrophic ones) were selected in the mixed culture. The oxygen produced by them fed a symbiotic relationship between microalgae and aerobic microorganisms in the closed system.
6. **Acetate** was the best organic carbon source for enabling selection and growth of the microalgal biomass. Pre-fermenting the carbohydrates (lactose) present in cheese whey by acidogenic fermentation in volatile fatty acids like acetate is a key step for preventing the competition between photomixotrophs and fermentative organisms which can hardly break down acetate further.Acetate uptake by microalgae likely occured via the glyoxylate cycle bypassing the decarboxylation of the tricarboxylic acid (TCA) cycle.
7. A **mathematical model** was successfully developed to address the selection of mixotrophic microalgae and their competition with chemoorganoheterotrophic microorganisms in mixed-culture photobioreactors whether lactose or acetate is primarily supplied in the system. The model outputs showed that photomixotrophy is the preferred trophic regime for enabling a substantial production of microalgal biomass and intracellular content of triacylglyceride (TAG) lipids useful for the biofuel and food industries. In chemostat regimes, a higher dilution rate, optimal light intensity, and feast-famine regimes (with longer light-feast and shorter dark-

famine cycles) enhanced the production of TAG while hindering competition by chemoorganoheterotrophs in non-axenic mixed cultures.

This research emphasized the roles of microbial community ecology, fermentation, and phototrophic processes for the development of ecological engineering principles for the full valorization of cheese whey in mixed-culture environmental biotechnologies. The scientific outputs of this work will contribute to a smoother transition of the dairy sector into the circular economy. Still, a next set of scientific studies are needed to complement and enrich this present work.

2 Outlook

The findings obtained in the Ph.D. thesis open interesting investigation lines for future research, that can be categorized along the following topics for the processing and valorization of cheese whey residuals:

1. **Life cycle analysis and techno-economic assessments of the value chain:** Perform LCA studies (cradle-to-grave) on various cheese whey biorefinery scenarios, and Techno-economic assessments (TEA) to evaluate the feasibility and scalability of coupled processes (i.e., acidogenic fermentation and microalgae photoorganoheterotrophic processes) for cheese whey valorization.
2. **Stakeholder analysis and policy development:** Conduct case studies to identify the stakeholders and analysis techniques and develop an Action Plan in a particular cheese whey biorefinery scenario. Studies to revise obsolete legislation that hinders the proper management of water resources and the full valorization of agroindustrial waste (i.e., cheese whey) should also be performed.
3. **Product-selective mixed-culture fermentation:** Performing experiments aiming at the optimization of selective pressure variables such as inoculum pre-treatment, pH, temperature, and headspace pressure to maximize the yield of specific products (i.e., VFAs, hydrogen, alcohols, methane). Up-scaling cheese whey acidogenic fermentation process using different reactors configurations.

4. **Microbial community engineering of photomixotrophic processes:** Up-scaling non-axenic microalgal biomass production during mixotrophic processes. Studying the microbial ecology in microalgae mixed cultures during mixotrophy. Conducting the study of microalgae acetate metabolism during mixotrophic regimes. Validating and refining the mathematical model presented in this thesis for optimal TAG production.

8. References

References

Abo, B. O., Odey, E. A., Bakayoko, M., & Kalakodio, L. (2019). Microalgae to biofuels production: A review on cultivation, application and renewable energy. *Reviews on Environmental Health*, *34*(1), 91–99. https://doi.org/10.1515/reveh-2018-0052

Alloul, A., Cerruti, M., Adamczyk, D., Weissbrodt, D. G., & Vlaeminck, S. E. (2020). Control tools to selectively produce purple bacteria for microbial protein in raceway reactors. *BioRxiv*, 2020.01.20.912980. https://doi.org/10.1101/2020.01.20.912980

Božanić, R., Barukčić, I., Kl, J., & Tratnik, L. (2014). Possibilities of whey utilisation. *Austin J Nutri Food Sci*, *2*(7), 1036–1042.

Brugha, R., & Varvasovszky, Z. (2000). Stakeholder analysis: a review. *Health Policy and Planning*, *15*(3), 239–246.

Caporgno, M. P., & Mathys, A. (2018). Trends in microalgae incorporation into innovative food products with potential health benefits. *Frontiers in Nutrition*, *5*(58), 58. https://doi.org/10.3389/fnut.2018.00058

Cerruti, M., Stevens, B., Ebrahimi, S., Alloul, A., Vlaeminck, S. E., & Weissbrodt, D. G. (2020). Enrichment and aggregation of purple non-sulfur bacteria in a mixed-culture sequencing-batch photobioreactor for biological nutrient removal from wastewater. *Frontiers in Bioengineering and Biotechnology*, *8*, 557234. https://doi.org/10.3389/fbioe.2020.557234

Chen, Y., Jiang, S., Yuan, H., Zhou, Q., & Gu, G. (2007). Hydrolysis and acidification of waste activated sludge at different pHs. *Water Research*, *41*(3), 683–689. https://doi.org/10.1016/j.watres.2006.07.030

Christensen, A. D., Kádár, Z., Oleskowicz-Popiel, P., & Thomsen, M. H. (2011). Production of bioethanol from organic whey using *Kluyveromyces marxianus*. *Journal of Industrial Microbiology and Biotechnology*, *38*(2), 283–289. https://doi.org/10.1007/s10295-010-0771-0

Crane, K. W., & Grover, J. P. (2010). Coexistence of mixotrophs , autotrophs , and heterotrophs in planktonic microbial communities. *Journal of Theoretical Biology*, *262*(3), 517–527. https://doi.org/10.1016/j.jtbi.2009.10.027

Davila-vazquez, G., León-Rodríguez, A. de, Alatriste-Mondragón, F., & Razo-Flores, E. (2011). The buffer composition impacts the hydrogen production and the microbial community composition in non-axenic cultures. *Biomass and Bioenergy*, *35*, 3174–2181. https://doi.org/10.1016/j.biombioe.2011.04.046

Dinika, I., & Utama, G. L. (2019). Cheese whey as potential resource for antimicrobial edible film and active packaging production. *Foods and Raw Materials*, *7*(2), 229–239.

Eidelwein, F., Collatto, D. C., Rodrigues, L. H., Lacerda, D. P., & Piran, F. S. (2018). Internalization of environmental externalities: Development of a method for elaborating the statement of economic and environmental results. *Journal of Cleaner Production*, *170*, 1316–1327. https://doi.org/10.1016/j.jclepro.2017.09.208

Gameiro, T., Novais, R. M., Correia, C. L., Carvalheiras, J., Seabra, M. P., Labrincha, J. A., Duarte, A. C., & Capela, I. (2020). Red mud-based inorganic polymer spheres : Innovative and environmentally friendly anaerobic digestion enhancers. *Bioresource Technology*, *316*. https://doi.org/10.1016/j.biortech.2020.123904

Gillies, M. T. (1974). *Whey processing and utilization : economic and technical aspects*. Noyes Data Corp.

González Siso, M. I. (1996). The biotechnological utilization of cheese whey: A review. In *Bioresource Technology* (Vol. 57, Issue 1, pp. 1–11). Elsevier Science Ltd. https://doi.org/10.1016/0960-8524(96)00036-3

González-Fernández, C., Mahdy, A., Ballesteros, I., & Ballesteros, M. (2016). Impact of Temperature and Photoperiod on Anaerobic Biodegradability of Microalgae Grown in Urban Wastewater. *International Biodeterioration and Biodegradation*, *106*, 16–23. https://doi.org/10.1016/j.ibiod.2015.09.016

Gonzalez-Fernandez, C., Sialve, B., & Molinuevo-Salces, B. (2015). Anaerobic digestion of microalgal biomass: Challenges, opportunities and research needs. *Bioresource Technology*, *198*, 896–906. https://doi.org/10.1016/j.biortech.2015.09.095

Hernández-Mendoza, C. E., & Buitrón, G. (2014). Suppression of methanogenic activity in anaerobic granular biomass for hydrogen production. *Journal of Chemical Technology and Biotechnology*, *89*(1), 143–149. https://doi.org/10.1002/jctb.4143

Ibrahim, O. (2018). A new low calorie tagatose sweetner D-Tagatose from lactose in cheese whey as a nutraceutical value-added product. *Journal of Food Health & Technology Innovations*, *1*(1), 11–28.

Kemp-Benedict, E. (2015). *3 key steps to a more sustainable economy*. World Economic Forum - Future of Economic Progress Sustainable Development. https://www.weforum.org/agenda/2015/09/3-key-steps-to-a-more-sustainable-economy/

Kiker, G. A., Bridges, T. S., Varghese, A., Seager, P. T. P., & Linkov, I. (2005). Application of multicriteria decision analysis in environmental decision making. In *Integrated environmental assessment and management* (Vol. 1, Issue 2, pp. 95–108). https://doi.org/10.1897/IEAM_2004a-015.1

Kim, B., Ramanan, R., Cho, D., Oh, H., & Kim, H. (2014). Role of Rhizobium , a plant growth promoting bacterium , in enhancing algal biomass through mutualistic interaction. *Biomass and Bioenergy*, *69*, 95–105. https://doi.org/10.1016/j.biombioe.2014.07.015

Kleerebezem, R., Joosse, B., Rozendal, R., & Van Loosdrecht, M. C. M. (2015). Anaerobic digestion without

biogas? *Reviews in Environmental Science and Biotechnology*, *14*(4), 787–801. https://doi.org/10.1007/s11157-015-9374-6

Kleerebezem, R., & van Loosdrecht, M. C. (2007). Mixed culture biotechnology for bioenergy production. In *Current Opinion in Biotechnology* (Vol. 18, Issue 3, pp. 207–212). https://doi.org/10.1016/j.copbio.2007.05.001

Ko, S., & Kwak, H.-S. (2009). Bioactive components in whey products. In Y. W. Park (Ed.), *Bioactive Components in Milk and Dairy Products* (pp. 263–285). Wiley-Blackwell.

Kucera, D., Pernicová, I., Kovalcik, A., Koller, M., Mullerova, L., Sedlacek, P., Mravec, F., Nebesarova, J., Kalina, M., Marova, I., Krzyzanek, V., & Obruca, S. (2018). Characterization of the promising poly (3-hydroxybutyrate) producing halophilic bacterium Halomonas halophila. *Bioresource Technology*, *256*, 552–556. https://doi.org/10.1016/j.biortech.2018.02.062

Kushwaha, D., Srivastava, N., Mishra, I., Upadhyay, S. N., & Mishra, P. K. (2019). Recent trends in biobutanol production. *Rev Chem Eng*, *35*(4), 475–504. https://doi.org/10.1515/revce-2017-0041

Lagoa-Costa, B., Kennes, C., & Veiga, M. C. (2020). Cheese whey fermentation into volatile fatty acids in an anaerobic sequencing batch reactor. *Bioresource Technology*, *308*. https://doi.org/10.1016/j.biortech.2020.123226

Lammifyad, C. (2020). Review on impacts of COVID-19 pandemic on life animals and dairy product processing industries of the world. *Insights in Veterinary Science*, *4*(1), 018–024. https://doi.org/10.29328/journal.ivs.1001022

Lappa, I., Papadaki, A., Kachrimanidou, V., Terpou, A., Koulougliotis, D., Eriotou, E., & Kopsahelis, N. (2019). Cheese whey processing: Integrated biorefinery concepts and emerging food applications. *Foods*, *8*(8), 347. https://doi.org/10.3390/foods8080347

Lee, K., Eisterhold, M. L., Rindi, F., Palanisami, S., & Nam, P. K. (2014). Isolation and screening of microalgae from natural habitats in the midwestern United States of America for biomass and biodiesel sources. *Journal of Natural Science, Biology and Medicine*, *5*(2), 333–339. https://doi.org/10.4103/0976-9668.136178

Li, H., Li, C., Liu, W., & Zou, S. (2012). Optimized alkaline pretreatment of sludge before anaerobic digestion. *Bioresource Technology*, *123*, 189–194. https://doi.org/10.1016/j.biortech.2012.08.017

López-Torres, M., & Llórens, Ma. del C. E. (2016). Effect of alkaline pretreatment on anaerobic digestion of olive mill solid waste. *Waste Management*, *58*, 160–168. https://doi.org/10.1016/j.wasman.2016.08.008

Mas, J. (1995). Storage Products in Purple and Green Sulfur Bacteria. In M. T. M. and C. E. B. R. E. Blankenship (Ed.), *Anoxygenic Photosynthetic Bacteria* (1st ed., pp. 973–990). Kluwer Academic Publishers. https://doi.org/10.1007/0-306-47954-0

Mockaitis, G., Bruant, G., Guiot, S. R., Peixoto, G., Foresti, E., & Zaiat, M.

(2020). Acidic and thermal pre-treatments for anaerobic digestion inoculum to improve hydrogen and volatile fatty acid production using xylose as the substrate. *Renewable Energy*, *145*, 1388–1398. https://doi.org/10.1016/j.renene.2019.06.134

Nam, H., Conrad, T. M., & Lewis, N. E. (2011). The role of cellular objectives and selective pressures in metabolic pathway evolution. *Current Opinion in Biotechnology*, *22*, 595–600. https://doi.org/10.1016/j.copbio.2011.03.006

Navia, R., & Vidal, G. (2002). Alkaline pretreatment of kraft mill sludge to improve its anaerobic digestion alkaline pretreatment of kraft mill sludge to improve its anaerobic digestion. *Bull. Environ. Contam. Toxicol.*, *69*, 869–876. https://doi.org/10.1007/s00128-002-0140-4

Onwulata, C., & Huth, P. J. (2008). *Whey processing, functionality and health benefits*. Wiley-Blackwell.

Pais-Chanfrau, J. M., Núñez-Pérez, J., Espin-Valladares, R. del C., Lara-Fiallos, M. V., & Trujillo-Toledo, L. E. (2020). Bioconversion of lactose from cheese whey to organic acids. In N. Gutiérrez-Méndez (Ed.), *Lactose and lactose derivatives* (1st ed., p. 22). IntechOpen. https://doi.org/10.5772/intechopen.87477

Rabaey, K., & Rozendal, R. A. (2010). Microbial electrosynthesis — revisiting the electrical route for microbial production. *Nature Reviews Microbiology*, *8*, 706–716. https://doi.org/10.1038/nrmicro2422

Riaño, B., Blanco, S., Becares, E., & García-González, M. C. (2016). Bioremediation and biomass harvesting of anaerobic digested cheese whey in microalgal-based systems for lipid production. *Ecological Engineering*, *97*, 40–45. https://doi.org/10.1016/j.ecoleng.2016.08.002

Rizwan, M., Mujtaba, G., Memon, S. A., Lee, K., & Rashid, N. (2018). Exploring the potential of microalgae for new biotechnology applications and beyond: A review. *Renewable and Sustainable Energy Reviews*, *92*, 394–404. https://doi.org/10.1016/j.rser.2018.04.034

Saddoud, A., Hassaïri, I., & Sayadi, S. (2007). Anaerobic membrane reactor with phase separation for the treatment of cheese whey. *Bioresource Technology*, *98*(11), 2102–2108. https://doi.org/10.1016/j.biortech.2006.08.013

Smithers, G. W. (2008). Whey and whey proteins-From "Gutter-to-Gold." *International Dairy Journal*, *18*(7), 695–704. https://doi.org/10.1016/j.idairyj.2008.03.008

Tsakali, E., Petrotos, K., D'Allessandro, A., & Goulas, P. (2010). A review on whey composition and the methods used for its utilization for food and pharmaceutical products. In C. R. Centre (Ed.), *6th International Conference on Simulation and Modelling in the Food and Bio-Industry* (pp. 195–201).

USDA. (2022). *Dairy: World markets and trade*. https://apps.fas.usda.gov/psdonline/circulars/dairy.pdf

Uvarova, I., Atstaja, D., Grinbergs, U., Petersons, J., Gegere-Zetterstroma, A., & Kraze, S. (2020). Transition to the

circular economy and new circular business models – an in-depth study of the whey recycling. *IOP Conference Series: Earth and Environmental Science*, *578*(1), 012019. https://doi.org/10.1088/1755-1315/578/1/012019

van Lier, J. B., Tilche, A., Ahring, B. K., Macarie, H., Moletta, R., Dohanyos, M., Pol, L. W. H., Lens, P., & Verstraete, W. (2001). New perspectives in anaerobic digestion. *Water Science and Technology*, *43*(1), 1–18.

Wonglertarak, W., & Wichitsathian, B. (2014). Alkaline Pretreatment of Waste Activated Sludge in Anaerobic Digestion. *Journal of Clean Energy Technologies*, *January 2014*, 118–121. https://doi.org/10.7763/jocet.2014.v2.104

Wurtsbaugh, W. A., Paerl, H. W., & Dodds, W. K. (2019). Nutrients, eutrophication and harmful algal blooms along the freshwater to marine continuum. *WIREs Water*, *6*(5). https://doi.org/10.1002/wat2.1373

Yadav, B., Pandey, A., Kumar, L. R., & Tyagi, R. D. (2020). Bioconversion of waste (water)/residues to bioplastics- A circular bioeconomy approach. *Bioresource Technology*, *298*, 122584. https://doi.org/10.1016/j.biortech.2019.122584

Yun, J. H., & Cho, K. S. (2017). Effect of hydraulic retention time on suppression of methanogens during a continuous biohydrogen production process using molasses wastewater. *Journal of Environmental Science and Health - Part A Toxic/Hazardous Substances and Environmental Engineering*, *52*(1), 37–44. https://doi.org/10.1080/10934529.2016.1221221

Zheng, Z., Xie, J., Liu, P., Li, X., & Ouyang, J. (2019). Elegant and efficient biotransformation for dual production of d -tagatose and bioethanol from cheese whey powder. *Journal of Agricultural and Food Chemistry*, *67*(3), 829–835. https://doi.org/10.1021/acs.jafc.8b05150

9. Annex

Ministério do Meio Ambiente
CONSELHO DE GESTÃO DO PATRIMÔNIO GENÉTICO

SISTEMA NACIONAL DE GESTÃO DO PATRIMÔNIO GENÉTICO E DO CONHECIMENTO TRADICIONAL ASSOCIADO

Cadastro de Acesso Nº AE43468

Tipo de Usuário:	**UNICAMP**
Responsável pelo cadastro:	**28313083808**
Objeto do Acesso:	**Patrimônio Genético**
O acesso foi realizado antes de 17/11/2015 ou obteve autorização de acesso antes de 17/11/2015?	**Não, sem solicitação de autorização em tramitação**
Finalidade do Acesso:	**Pesquisa**
Estas atividades são baseadas em acesso realizado anteriormente?	**Não**
Este cadastro está vinculado a cadastro anterior de remessa?	**Não**

Patrimônio Genético

Título da Atividade:	**Produção de bioenergia a partir de resíduos agroindustriais**
Título da Atividade em inglês:	**Bioenergy production from agro-industrial residues**
Resumo da atividade (incluindo objetivos e resultados esperados ou obtidos, conforme o caso)	**Microalgas são organismos que apresentam um excelente potencial na produção de biodiesel e outros tipos de biocombustíveis renováveis. O seu cultivo não compete com o uso de terra para a produção de alimentos e ela ainda pode crescer em águas inicialmente contaminadas, retirando carbono para seu metabolismo e liberando oxigênio para a atmosfera. O soro de queijo é um co-produto da produção de queijo que apesar de gerar vários outros co-produtos com valores agregados, ainda tem um volume significantemente grande descartado em rios e consequentemente, causando a eutrofização dos mesmos. O tema central desse projeto é o estabelecimento do cultivo de um consórcio de microalgas em soro de queijo para a futura produção de biocombustíveis.**
Resumo não sigiloso da Atividade em inglês	**Microalgae are microorganisms with great potential for the production of biodiesel and other biofuels. Their cultivation does not compete with land and freshwater use, as microalgae can be grown in brackish water, metabolizing the carbon in the substrate and releasing oxygen into the atmosphere. Cheese**

	whey is a dairy by-product that despite having various industrial uses still presents a large fraction of its production discarded in water bodies leading to eutrophication. The main goal of this Project is the establishment of a microalgae consortium to be cultivated in cheese whey for future biofuel production.
Palavra(s)-chave:	**Soro de queijo, digestão anaeróbia, co-digestão, microalgas, biocombustíveis**
Palavra(s)-chave em inglês:	**Cheese whey, anaerobic digestion, co-digestion, microalgae, biofuels**
Período das Atividades:	**01/08/2018 Ainda não iniciado ou em execução**

Equipe

Nome Completo	Documento	Instituição	Nacionalidade
Gustavo Mockaitis	***.130.838-**	UNICAMP	Brasil
Maria Paula Giulianetti de Almeida	***.893.966-**	UNICAMP	Brasil
Vitor Augusto Oliveira Silva	***.961.048-**	UNICAMP	Brasil

Sobre o componente do Patrimônio Genético Acessado (I)

Tipo de Componente:	
Reino	
Filo/Divisão	
Classe	
Ordem	
Família	
Impossibilidade de identificação	**Microalgas de água doce extraídas e cultivadas de um reservatório de água da Faculdade de Engenharia Agrícola – FEAGRI/UNICAMP.**
Trata-se de variedade tradicional local ou crioula ou raça localmente adaptada ou crioula?	**Não**

Sobre a procedência do Patrimônio Genético (I)

Procedência da amostra	***In situ***
UF	**SP**
Município	**Campinas**
Latitude	**22° 49" 6.72' S**
Longitude	**47° 3" 39.68' W**
Bioma	**Mata Atlântica**
Data da Coleta	**01/06/2018**
O acesso ao patrimônio genético será realizado em área indispensável à segurança nacional ou águas jurisdicionais brasileiras, plataforma continental e zona econômica exclusiva:	**Não**
Tipo de componente	**Impossibilidade de identificação**
O acesso ao patrimônio genético será realizado em área indispensável à segurança nacional ou águas jurisdicionais brasileiras, plataforma	**Não**

continental e zona econômica exclusiva:	
Trata-se de variedade tradicional local ou crioula ou raça localmente adaptada ou crioula?	**Não**

Sobre o componente do Patrimônio Genético Acessado (II)

Tipo de componente	**Impossibilidade de identificação**
Reino	
Filo/Divisão	
Classe	
Ordem	
Família	
Impossibilidade de Identificação	**Lodo de biorreator anaeróbio de estação de tratamento de efluentes oriundos de abatedouro de aves**
Trata-se de variedade tradicional local ou crioula ou raça localmente adaptada ou crioula?	**Não**

Sobre a procedência do Patrimônio Genético (II)

Procedência da amostra	***Ex situ***
UF	**SP**
Município	**Pedreiras**
Nome do estabelecimento comercial de Aquisição	
Data de obtenção	**16/03/2018**
Tipo de componente	**Impossibilidade de identificação**

Data do Cadastro	**22/03/2018 15:57:59**
Situação do Cadastro	**Concluído**

Conselho de Gestão do Patrimônio Genético

Situação cadastral conforme consulta ao SisGen em **11:57** de **01/11/2018**

SISTEMA NACIONAL DE GESTÃO DO PATRIMÔNIO GENÉTICO E DO CONHECIMENTO TRADICIONAL ASSOCIADO - SISGEN